

ORGANICALLY MODIFIED SILICATES AS STATIONARY PHASES FOR CAPILLARY ELECTROCHROMATOGRAPHY

THÈSE N° 2385 (2001)

PRÉSENTÉE AU DÉPARTEMENT DE CHIMIE

ÉCOLE POLYTECHNIQUE FÉDÉRALE DE LAUSANNE

POUR L'OBTENTION DU GRADE DE DOCTEUR ÈS SCIENCES

PAR

Stéphane CONSTANTIN

chimiste diplômé de l'Université de Genève
de nationalité française

acceptée sur proposition du jury:

Prof. R. Freitag, directrice de thèse

Prof. M. Gijs, rapporteur

Prof. W. Lindner, rapporteur

Prof. J.-L. Veuthey, rapporteur

Lausanne, EPFL
2001

Abstract

Capillary electrochromatography (CEC) is a microfluidic separation technique where the liquid flow is powered by an electric field instead of a pressure gradient. This mode of propulsion, reducing the dispersion of the analytes and leading to the absence of pressure drops, contributes to an increasing interest for CEC compared to pressure driven liquid chromatography.

Efficient stationary phases need to be developed to promote a widespread use of CEC. Toward this goal, the present work describes the synthesis and the use of organically modified silicates (ormosils) as stationary phases for capillary electrochromatography.

Ormosils, made by the sol-gel technique, consist of a silica framework containing organic materials. The chemistry of the sol-gel technique was studied in this work to control the resolutions, the efficiencies and the morphologies of the ormosil stationary phases. The factors affecting these parameters were defined and independently studied by electrochromatography and by electronic and optic microscopy. n-octyl modified silicates were chosen as stationary phases in the investigations and mixtures of polycyclic aromatic hydrocarbons (PAHs) were used as the test sample. Based on these results, methods were proposed for the formation of coatings and monoliths inside fused silica capillaries. The corresponding open tubular columns (OTCs) and monolithic columns (MCs) were studied with regard to their applications in CEC. Separations of PAHs, achieved with OTCs, were used to optimize the parameters acting during an electrochromatographic separation. Capillaries coated with ormosils containing different organic moieties were tested to separate several types of analytes. To miniaturize the CEC format, glass chips containing a capillary channel coated with ormosil stationary phases were used in electrochromatographic experiments. The difficulties of injection and detection systems were overcome by using commercial electrophoretic equipment.

Keywords: Capillary electrochromatography (CEC); sol-gel technique; organically modified silicates (ormosils); open tubular columns (OTCs); monolithic columns (MCs); polycyclic aromatic hydrocarbons (PAHs).

Résumé

L'électrochromatographie capillaire (CEC) est une technique de separation microfluidique où le flux liquide est généré par un champ électrique à la place d'un gradient de pression. Ce mode de propulsion, réduisant la dispersion des analytes et conduisant à une absence de pertes de charge, contribue à l'intérêt grandissant de la CEC par rapport à la chromatographie liquide conduite par la pression.

Des phases stationnaires efficaces doivent être développées pour promouvoir un large emploi de la CEC. Pour atteindre cet objectif le travail présenté décrit la synthèse et l'emploi de silicates organiquement modifiés (ormosils) comme phases stationnaires pour l'électrochromatographie capillaire.

Les ormosils, fabriqués par la technique sol-gel, consistent en un réseau de silice contenant des matériaux organiques. La chimie liée à la technique sol-gel a été étudiée dans ce travail pour contrôler les résolutions, les efficacités et les morphologies des phases stationnaires d'ormosils. Les facteurs affectant ces paramètres ont été définis et étudiés séparément par électrochromatographie et par microscopie optique et électronique. Les silicates modifiés par du n-octyl ont été choisis comme phases stationnaires dans cette étude et des mélanges d'hydrocarbures polycycliques aromatiques (PAHs) ont été utilisés comme échantillons test. Basés sur ces résultats, des méthodes ont été proposées pour la formation de revêtements et de monolithes dans des capillaires de silice fondue. Les colonnes correspondantes, respectivement les colonnes tubulaires ouvertes (OTCs) et les colonnes monolithiques (MCs), ont été étudiées par rapport à leur applications en CEC. Les séparations de PAHs, accomplies avec les OTCs, ont été utilisées pour optimiser les paramètres agissant lors d'une separation électrochromatographique. Les capillaires, revêtus avec des ormosils contenant différent substituants organiques ont été testés pour séparer plusieurs classes d'analytes. Pour miniaturiser le format de la CEC, des chips en verre, contenant un canal capillaire revêtu d'ormosil comme phase stationnaire, ont été utilisés dans des expériences électrochromatographiques. Les problèmes de l'injection et de la détection ont été surmontés par l'emploi d'un appareil électrophorétique commercial.

Mots clefs: Electrochromatographie capillaire (CEC); technique sol-gel; silicates organiquement modifiés (ormosils); colonnes tubulaires ouvertes (OTCs); colonnes monolithiques (MCs); hydrocarbures polycycliques aromatiques (PAHs).

Merci à Frédéric Garret-Flaudy pour avoir été durant ces quatre dernières années un collègue formidable et un ami toujours présent, dans les moments agréables et les autres....

Un immense merci à Lisa Hunt pour son amitié et pour avoir corrigé la langue de Shakespeare que contient cette thèse.

Merci à mes parents pour m'avoir permis d'effectuer des études et pour m'avoir toujours soutenu dans mes choix.

Merci à Arnaud Desponds et Philippe Girard pour leur compétence en informatique et leur constante disponibilité dans ce domaine.

Merci à Mme le Prof. Ruth Freitag pour avoir été ma directrice de thèse et pour m'avoir permis de participer à différents congrès internationaux.

Merci aux Profs. J.L. Veuthey, W. Lindner, M. Gijs pour avoir accepté de juger le contenu scientifique de ce travail.

Merci à Daniela Hoegger pour nos interminables discussions sur la nature du flux électroosmotique et sur le concept de la CEC.

Merci à Laure, Roberto, Steph, Françoise, Matteo, Igor et Kevin pour leur bonne humeur jamais démentie...

Merci à tous les membres de ma famille et mes amis.

Merci à Madgalena Jozwick pour nos nombreuses discussions sur la chromatographie en face d'un café.

Merci à l'école polytechnique fédérale de Lausanne et au fond de la recherche scientifique suisse pour le financement de ce travail.

Enfin merci à tous ceux qui de près ou de loin ont contribué à la réussite de cette thèse.....

TABLE OF CONTENT

1- Introduction.	p. 9
1.1- Capillary Electrochromatography (CEC).....	p. 9
1.2- Instrumentation for CEC.	p. 10
1.3- Objective of the Present Work.	p. 11
2- Theoretical Aspects of Capillary Electrochromatography.	p. 13
2.1- Electrophoresis.	p. 13
2.2- Electroosmosis.	p. 16
2.3- Electrodriven Liquid Chromatography.	p. 22
2.3.1- Retention and Migration.	p. 23
2.3.2- Efficiency and Resolution Factor in Open Tubular Columns.	p. 25
2.4- Chromatographic Phases.	p. 30
2.4.1- Monomeric Stationary Phases.	p. 31
2.4.2- Polymeric Stationary Phases.	p. 36
2.4.3- Mobile Phases.	p. 39
3- Investigation of Monomeric Stationary Phases for CEC	p. 41
3.1- Conditioning of the Capillary Walls.	p. 41
3.2- Synthesis of Monomeric Stationary Phases.	p. 44
3.3- Experimental.	p. 45
3.4- Results and Discussion.	p. 56
4- The Sol-Gel Technique.	p. 59
4.1- The Nature of the Catalysts.	p. 59
4.2- Effect of the Catalyst on the Hydrolysis and Condensation Mechanisms.	p. 61
4.3- Parameters Describing the Initial Constituents of the Sol.	p. 65
4.4- The Mutual Solvent.	p. 66
4.5- Drying of the Gel.	p. 67
4.6- The Particulate Theory.	p. 68
5- Investigation of Ormosils Coatings in CEC.	p. 71
5.1- Thickness of the Stationary Phase.	p. 71
5.2- Stabilization of the Stationary Phase.	p. 72
5.3- Influence of the Organic Content in the Sol Synthesis.	p. 83
5.4- Influence of the Water Content in the Sol Synthesis.	p. 85
5.5- Influence of the Mutual Solvent in the Sol Synthesis.	p. 88
5.6- Influence of the Reaction Time in the Sol Synthesis.	p. 91
5.7- Influence of the Catalyst in the Sol Synthesis.	p. 94
5.8- Influence of the Temperature in the Sol Synthesis.	p. 97
5.9- Conclusions and Perspectives.	p. 101

6- Silicates Modified with Different Organic Moieties: Evaluation as Coatings in OTCs-CEC.	p. 103
6.1- Alkylsilicates.	p. 103
6.2 - Polar Organosilicates and Organosilicates with Ionic Exchangers.	p. 113
6.3- Conclusion and Perspectives.	p. 116
7- Ormosils monoliths for CEC.	p. 117
7.1- Chemical Induction of the Gelation.	p. 117
7.2- pH Gradient.	p. 120
7.3- Factors Influencing the Formation of a Monolith.	p. 123
7.4- Factors Influencing the Porosity of the Monoliths.	p. 125
7.5- Reduction of the Volume Shrinkage.	p. 131
7.6- Conclusions and Perspectives.	p. 144
8- Factors Influencing the Electrochromatographic Resolution.	p. 145
8.1- Mobile Phases.	p. 145
8.1.1- Organic Solvents.	p. 146
8.1.2- Electrolytes.	p. 151
8.2- Applied Voltage.	p. 156
8.3- Temperature.	p. 159
8.4- Length of the Columns.	p. 163
8.5- Column Inner Diameter.	p. 164
8.6- Thickness of the Coating.	p. 169
8.7- Conclusions.	p. 171
9- CEC Micro Chips.	p. 173
9.1- Introduction.	p. 173
9.2- Making of the Chips.	p. 173
9.3- Stationary Phases.	p. 174
9.4- Electrochromatographic Separations.	p. 175
10- Conclusions and Perspectives.	p. 179
12- Appendix.	p. 191
13- Curriculum Vitae.	p. 199

1- Introduction.

1.1- Capillary Electrochromatography (CEC).

Capillary electrochromatography (CEC) is a liquid microseparation technique in which the flow of the mobile phase is powered by electroosmosis. Separations in CEC result from the differential motion of the analytes that arise from two distinct mechanisms. The first mechanism, the electrophoresis, affects the charged analytes. The second mechanism, the chromatography, is based on interaction of the analytes with a so-called stationary phase present in the capillary.

Several features make CEC an attractive separation technique. CEC combines some interesting features of capillary electrophoresis (CE) with features of high performance liquid chromatography (HPLC). In principle, charged and uncharged species contained in a sample mixture can be separated with this technique [1].

As in HPLC, the stationary phases for CEC can be tailored to offer a wide range of retention mechanisms and selectivities. This interesting characteristic is to be combined with the advantages of using an electroosmotic flow (EOF) to drive the solution and the analytes through the capillary. The flat flow velocity profile of this liquid flow improves the separation efficiency by reducing the band broadening. Since no back pressure is needed with this mode of liquid phase propelling, no pressure drop can occur in the separation channels. The thickness of the separation channel can be then reduced in CEC with regards to HPLC. Since the diameter of the channels is theoretically known to affect the efficiency, separation in CEC ought to be improved by reducing this diameter. Further advantages arise from the fact that CEC is a micro analytical technique, which requires only minute amounts of sample (in the nanoliter range).

Depending on their physical nature, stationary phases for CEC can be classified into four different types. They can be present inside capillaries as

pseudo stationary phases like micelles, as coatings, as packings (made of particulate material), or as porous rods. The last three types of capillary columns will be called thereafter open tubular columns (OTCs), packed columns (PCs) and monolithic columns (MCs). In CEC, mobile phases are typically organic-aqueous solutions [2] that can contain some electrolytes.

Historically, the term electrochromatography appeared first in 1943 to describe a form of paper electrophoresis [3]. Pretorius and co-workers were the first to demonstrate in the mid 70's the use of electroosmosis to drive a solvent through an analytical packed column [4]. Later, in the early 80's, Jorgenson and Lukacs extended the use of electroosmotic flows as an alternative to pressure driven flows for chromatographic separations [5]. Despite these works, CEC only gained popularity at the beginning of the 90's. At that time, Knox and Grant [6] demonstrated that packed analytical columns driven by electroosmosis showed higher plate numbers than identical columns driven by pressure.

1.2- Instrumentation for CEC.

So far no commercial instrument is available for CEC. A system initially designed for CE (from BeckmanTM), whose instrumentation is basically the same, was used in this work (Fig. 1.1).

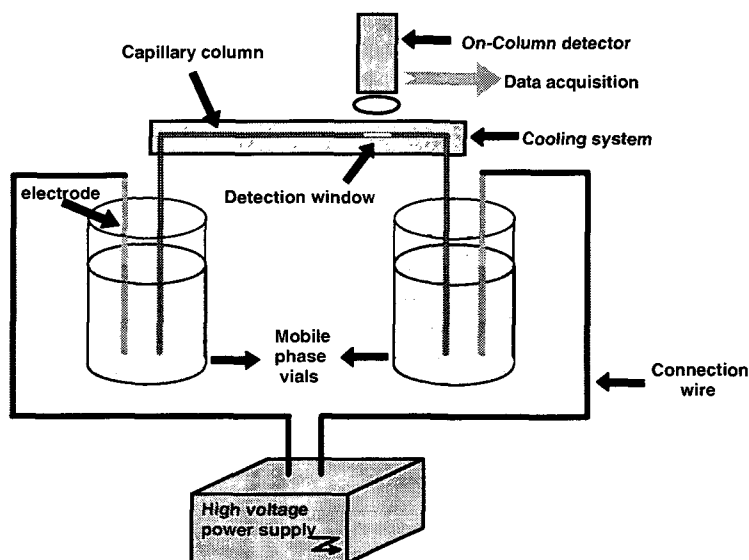


Fig. 1.1: Instrumentation used for CEC in the present work.

The instrumentation includes two electrodes made of a metal with a high oxidation-reduction potential, typically platinum, which are connected to a power supply able to generate high voltages (generally up to 30 kV for most of the commercially available systems). Both electrodes and the extremities of the capillary are immersed in mobile phase vials (Fig. 1.1). The capillary can be maintained at a constant temperature by a cooling system. Detection, used to monitor the separations, can be performed on-column with a spectrophotometric, an electrochemical or a NMR detector. This detection can also be realized with a mass spectrometer connected to the outlet extremity of the capillary.

1.3- Objective of the present work.

Most work in the CEC field till now has focused on packed columns. This trend can be largely explained by the availability of particulate HPLC material suitable for PCs. The second explanation arises from the fact that both MCs and OTCs are difficult to prepare. Monoliths can be inhomogeneous and may cause problems. OTCs, especially columns having inner diameter smaller than 10 μm , known to yield the best electrochromatographic separations according to mass transport limitation, are known to be particularly difficult to coat [7].

Despite their wide use, packed columns have several drawbacks. The packing process of PCs is cumbersome and hard to reproduce, and the choice of the packing material is limited to the commercially available particles with specific stationary phases of specific sizes. Moreover, frits, needed to keep columns packed, distort the liquid flow and induce the formation of bubbles; this is known to strongly influence the EOF. This discontinuity of the liquid in the capillary prevents the electric current from circulating in the CEC set-up and causes an electric breakdown that stops the progression of the electrochromatographic separations. The mechanical fragility of the column at the frits is also a frequently reported problem. This weakness is due to the removal of a strengthening polymer layer at the surface of the capillaries

during the fabrication of the frits. The presence of frits is clearly the major limitation of PCs that has to be overcome to allow the routine use of CEC as an analytical technique.

The objective of the present work was the production of both open tubular columns and monolithic columns for CEC using organically modified silicates (ormosils) as stationary phases. With such columns, this approach aims to solve the problems encountered with PCs. Ormosils were chosen for their dual ability to act as a stationary phase and to generate an electroosmotic flow. Ormosils offer a wide range of physical structures with many different chemical compositions. These unique features confer a particular interest to the ormosils, especially because these characteristics can be tailored during their synthesis.

In this work, the synthesis of ormosils as stationary phases for CEC were first studied in regard to their applications as coating material for open tubular columns. In a second step, synthesis of ormosils containing different organic moieties as interactive sites were carried out and these materials were studied as stationary phases in CEC with regard to their selectivities. In a third step, research aiming to speed up the ormosils synthesis was done. In a fourth step, the production of porous ormosils monoliths was investigated and their application as stationary phases for CEC was studied. In a fifth step, electrochromatographic separations were developed and studied / optimised using a mixture of polycyclic aromatic hydrocarbons (PAHs) as an example. Finally, electrochromatographic experiments were performed on a chip.

2- Theoretical Aspects of Capillary Electrochromatography.

2.1- Electrophoresis.

Electrophoresis is the electrophoretic migration of ions or charged particles in an electrical field. Depending on the pH, analytes having acid-base properties can acquire a net positive or negative charge and then become ionized. These substances, when placed in a uniform electric field, move towards electrodes of the opposite electrical sign.

When two electrodes at different electric potential ϕ are separated by a distance d , ions in the solution between them experience a uniform electric field E of magnitude:

$$E = \frac{\Delta\phi}{d} \quad (2.1)$$

With $\Delta\phi$ = potential difference [V]

d = distance between the electrodes [m]

In such a field, an ion of charge ze experiences a force F_e of magnitude:

$$F_e = \frac{ze\Delta\phi}{d} = zeE \quad (2.2)$$

With z = charge number of the ion

e = elemental charge = 1.602×10^{-19} [C]

An anion responds by accelerating towards the positive electrode, whereas a cation responds by accelerating towards the negative electrode. This acceleration is counterbalanced by a frictional retarding force F_r that is proportional to the speed of the ion. Its electrophoretic migration at infinite dilution u_{ep}^0 is linked to the retarding force through the frictional constant f . If

we consider that the molecules are not small relative to the solvent molecules and that the solutes are identified as spherical particles, the Stokes' relation applies and the frictional retarding force is given by:

$$F_r = fu_{ep}^0 = 6\pi r_h \eta u_{ep}^0 \quad (2.3)$$

For non spherical species and small ions, the numerical value of f is lower than 6 [8].

With r_h = hydrodynamic radius of the ion [cm].

η = newtonian viscosity of the mobile phase [$\text{N} \times \text{s} \times \text{m}^2$].

u_{ep}^0 = electrophoretic migration velocity at infinite dilution [$\text{cm} \times \text{s}^{-1}$].

In equilibrium conditions, the acceleration is zero:

$$F_{ep} = F_r \quad (2.4)$$

Therefore:

$$u_{ep}^0 = \frac{ze}{6\pi r_h \eta} E = \mu_{ep}^0 E \quad (2.5)$$

The absolute electrophoretic mobility μ_{ep}^0 [$\text{cm}^2 \times \text{V}^{-1} \times \text{s}^{-1}$] represents the average velocity of a charged species per unit of electric field strength, in close proximity of the zero concentration.

Separations in CEC are not performed at infinite dilution. When an electrolyte solution is used, the presence of ionic species affects the electrophoretic mobility. The phenomenon of electrostatic interactions in electrolyte solutions, treated extensively by Debye, Hückel and Onsager, is based on the fact that an ion is always surrounded by oppositely charged counterions. When placed in an external electric field, the spherical distribution of counterions around a central ion is distorted (Fig. 2.1), which slows down the migration of the ionic species.

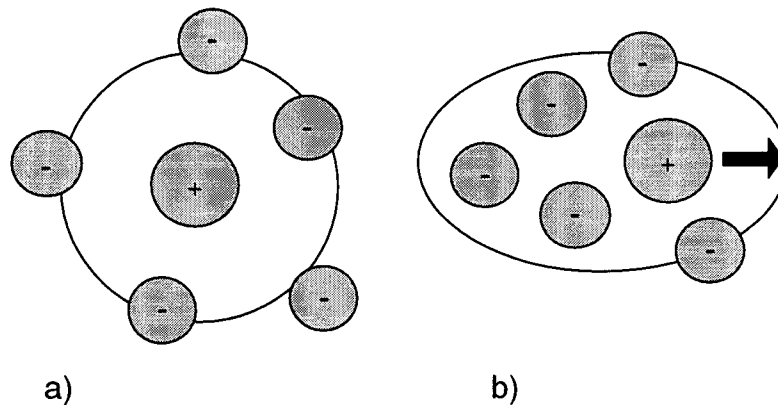


Fig. 2.1: Counterionic atmosphere

- a) In the absence of an applied field, the ionic atmosphere is spherically symmetric.
- b) When an electric field is present the ionic atmosphere is distorted and the centers of positive and negative charge no longer coincide. This charge separation retards the motion of the central ion.

The forces affecting the velocity of the migration are named electrophoretic retardation f_{ret} and relaxation effect f_{rel} . Electrophoretic retardation is caused by the fact that the central ion does not migrate in a stationary environment as is assumed by Stokes' law. The counterions move in the opposite direction of the central ion, causing a friction force that results in a decrease of the mobility. Electrophoretic relaxation is caused by the dissymmetric distribution of the counterionic atmosphere. The shift of the central ion permanently deforms the ionic atmosphere, which now has a lower charge density in the direction of the shift and a higher one at its back. Coulomb forces tend to rebuild the initial spherical structure, which takes a finite time. During this relaxation time the central ion is slowed down by the electric force f_{rel} acting in the opposite direction to its migration.

As a consequence of ionic interactions, the effective electrophoretic mobility μ_{ep} will always be lower than the absolute electrophoretic mobility μ_{ep}^0 . The easiest way to consider the influence of ionic atmosphere on the mobility is to replace the theoretical charge with the smaller effective charge Q_{eff} and the

hydrodynamic radius with the effective radius of the ion including its atmosphere of counterions r_e .

Thus:
$$\mu_{ep} = \frac{Q_{eff}}{6\pi \eta r_e} \quad (2.6)$$

With Q_{eff} = effective charge [C].

r_e = effective radius [cm].

One can assess experimentally the effective electrophoretic mobility by measuring the specific conductance k of a solution of a known concentration C :

$$k = F \sum_{i=1}^n C_i \mu_{ep_i} \quad (2.7)$$

With k = specific conductance [$S \times cm^{-1}$].

C = molar concentration [$mol \times L^{-1}$].

F = Faraday constant = 96485 [$C \times mol^{-1}$].

2.2- Electroosmosis.

Electroosmosis is the motion of a liquid relative to an electrically charged solid surface under the influence of an electric field. This electrokinetically driven flow, called the electroosmotic flow (EOF), is used in CEC to propel the mobile phase through the capillary column. Electroosmosis is an interfacial solid-liquid process, which takes place in CEC-columns at the contact surface between the stationary and the mobile phases. In the case of monolithic columns or packed columns for CEC, it has been proven that the contribution of the capillary wall to the EOF is negligible [9].

The EOF arises from the presence of an electrical double layer located at the interface of all solid surfaces immersed in a liquid [10,11]. In the case of silica-based stationary surfaces, these charges arise from partially ionized acidic

silanol groups ($-\text{Si-O}^-$) [7] and from dissociative and non-dissociative adsorption of ions in solutions [12]. When such surfaces are in contact with a solution, the electroneutrality of the system is maintained by the formation of a counterionic structure containing a slight excess of opposite charges in the solution (electrolyte). The solid surface charge is then counterbalanced by charges having the opposite electric sign. These charges are located very close to the solid surface and form what amounts to a charged sheath around a core of uncharged liquid. The double layer system between the solid surface and the sheath generates an electric potential ψ at the interface between the solid and the electrolyte (Fig. 2.2).

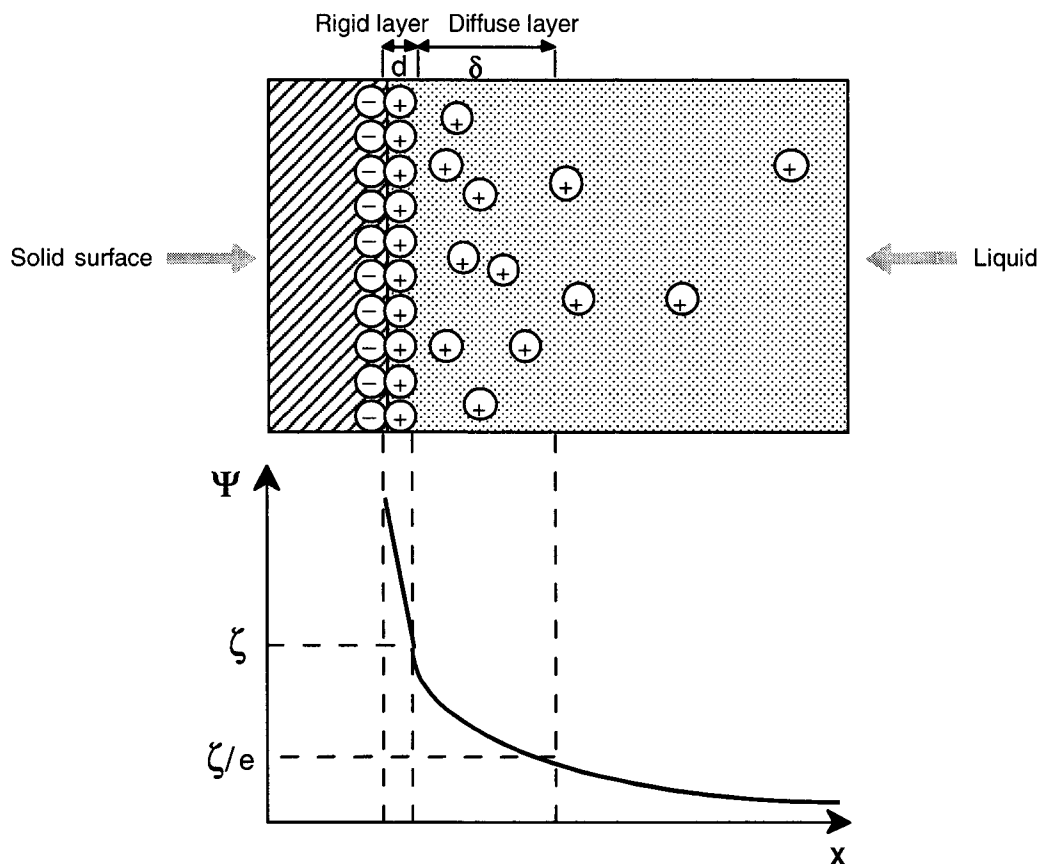


Fig. 2.2: Constitution of the electrical double layer.

Top: distribution of the counterions in proximity to the charged solid surface.

Bottom: decay of the electrical potential as the distance from the solid surface increases.

The thin excess charge area in the solution can be separated into two layers. A rigid layer of counterions fixed to the solid surface does not contribute to the EOF. This layer is called the Helmholtz [13] or Stern Layer. The remainder of the excess charge is distributed among ions that freely exchange with those of the bulk solution. This zone of the double layer structure is called the diffuse part or the Gouy-Chapman layer [14, 15]. The density of charges associated with the counterions decreases rapidly with the distance from the charged solid surface. The electric potential associated with the counterions also decreases with the distance from the wall. In the rigid layer, ψ decreases linearly until it reaches the external limit of the Stern layer. At this point, the electric potential is known as the zeta potential ζ (Fig. 2.2). In the diffuse layer, the electric potential drops exponentially with the distance x from the surface. The thickness d of the rigid layer lies in the molecular range, assuming that a molecular layer of counterions is adsorbed. The thickness of the diffuse layer δ [m] is the distance over which ζ decays by a factor e ($\approx 2,718$). By analogy, δ is often denoted by k^{-1} where k is the Debye-Hückel parameter [16]. For a strong monovalent electrolyte:

$$\delta = \sqrt{\frac{\epsilon_0 \epsilon_r RT}{2CF^2}} \quad (2.8)$$

Where ϵ_0 = permittivity of the vacuum ($88.85 \times 10^{-12} [\text{C}^2 \times \text{N}^{-1} \times \text{m}^{-2}]$).

ϵ_r = permittivity or dielectric constant of the mobile phase.

R = universal gas constant ($8.314 [\text{J} \times \text{K}^{-1} \times \text{mol}^{-1}]$).

T = absolute temperature [K].

C = molar concentration of the electrolyte [$\text{mol} \times \text{L}^{-1}$].

Two other models [12] have been proposed for the interface with an oxide-based stationary phase like silica: the surface complex model and the porous surface model where the silica surface is a gel layer.

When an axial electric field is applied across the length of the capillary column, the ions in the diffuse layer migrate towards an electrode by coulombic interactions. These ions carry the enclosed liquid along with them by viscous forces (Fig. 2.3). This generates a flat liquid flow profile or “plug-like” flow [13, 17]: the electroosmotic flow.

Deviation from the flat shape occurs in the diffuse electric double layer, which is assumed to be between 1-100 nm from the capillary wall [18]. The flat velocity profile of the flow may no longer be valid if any double layer overlapping occurs. This happens when $d_c / \delta \leq 10$, where d_c represents the inner diameter of the separation channel and δ the thickness of the diffuse double layer [13, 19]. Double layer overlapping is also increased in the case of a low concentration of ions in the diffuse layer (mobile phase).

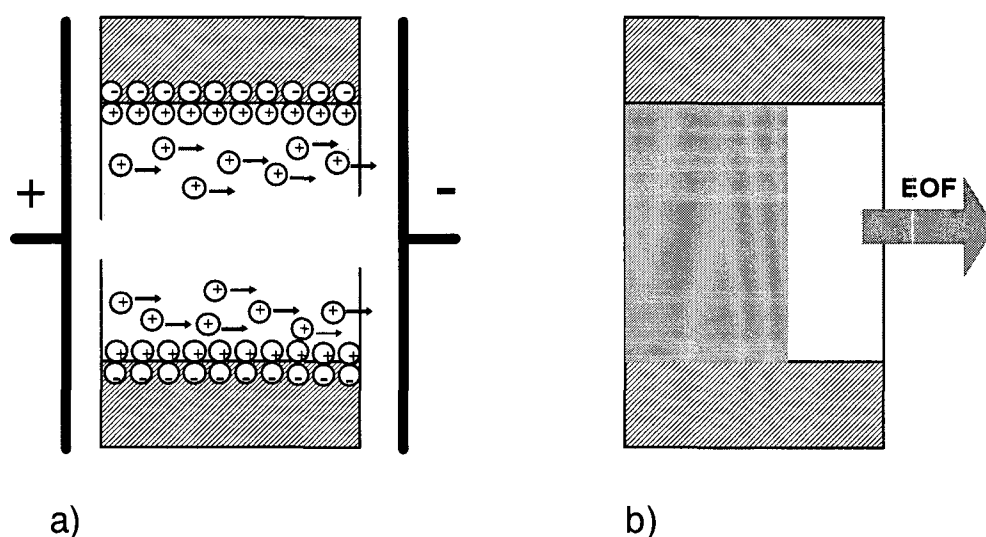


Fig 2.3. Flow velocity profile of a liquid driven by electroosmosis in a longitudinal section of a capillary.

a) Microscopic scale.

b) Macroscopic scale. A flat flow velocity profile is seen.

The velocity u_{eo} of the mobile phase is given by the Von Smoluchowski equation:

$$u_{eo} = \frac{\epsilon_0 \epsilon_r \zeta}{\eta} E = \mu_{eo} E \quad (2.9)$$

With
$$\zeta = \frac{\sigma\delta}{\varepsilon_0\varepsilon_r} \quad (2.10)$$

Where u_{eo} = electroosmotic velocity [$\text{cm} \times \text{s}^{-1}$].

ζ = electrical potential at the external boundary of the compact layer.

σ = charge density of the excess ions in the Gouy-Chapman layer [20].

μ_{eo} = electroosmotic mobility [$\text{cm}^2 \times \text{V}^{-1} \times \text{s}^{-1}$].

μ_{eo} represents the average velocity of the mobile phase flow per unit of electric field strength.

Equation 2.9 has limitations caused by the fact that the values ε_r and η change significantly in a strong electric field [12]. Further limitations arise from the differences in the values ε_r and η in close proximity to the capillary wall and in the bulk of the mobile phase. However, for lack of accurate data, the bulk values are generally employed.

By replacing the value of ζ from eq. 2.10 in eq. 2.9, we obtain:

$$u_{eo} = \frac{\sigma\delta}{\eta} E \quad (2.11)$$

By replacing the value of δ from eq. 2.8 in eq. 2.11, we obtain:

$$u_{eo} = \frac{\sigma}{\eta} \sqrt{\frac{T\varepsilon_r}{C}} \sqrt{\frac{\varepsilon_0 R}{2F^2}} E \Leftrightarrow u_{eo} = \frac{\sigma}{\eta} \sqrt{\frac{T\varepsilon_r}{C}} AE \quad (2.12)$$

With A = constant.

From the eq. 2.12, we see that physical parameters (T and E) as well as parameters dependent on characteristics of the mobile phase (C , η and ε_r) and of the surface of the stationary phase (σ), contribute to the electro-

velocity control. The choice of the mobile phase is then of paramount importance since its constitution affects the viscosity, the dielectric constant, the pH (through the charge density), and the ionic strength (through the electrolyte concentration).

The temperature has a marked effect in CEC. It affects the viscosity of the mobile phase, the thickness of the double layer, the chemical equilibrium as well as molecular diffusion. As a result, the temperature affects the resolutions and the efficiencies in CEC. During electrochromatographic separations, the content of capillary columns for CEC is submitted to Joule heating, the extent of which depends on the conductance of the mobile phase as well as on the capillary diameter. As a result, a temperature gradient [21] from the middle of the capillary to the capillary wall is established:

$$T = T_1 + \frac{Gr_c^2}{4k_c} \left(1 - \frac{r^2}{r_p^2} \right) \quad (2.13)$$

With T_1 = capillary wall temperature [K].

G = heat generation rate [$K \times S \times cm^{-3}$].

r_p = radial position [cm].

k_c = specific conductance of the mobile phase [$S \times cm^{-1}$].

It has to be noted that the development of a temperature gradient only occurs if the heat dissipation between the core of the capillary and its surrounding is low. Along this gradient, the magnitude of both the electroosmotic flow and the electrophoretic flow differ. Indeed, the temperature affects directly δ (eq. 2.8) and η from which depend u_{ep} (eq. 2.5) and u_{eo} (eq. 2.11). The temperature dependence of the viscosity can be expressed as:

$$\eta = be^{\frac{E_a}{RT}} \quad (2.14)$$

With b = constant [$Pa \times s$].

E_a = activity energy for the viscous flow [$J \times mol^{-1}$].

To avoid the establishment of a temperature gradient, and therefore to keep a flat flow profile, the inner diameter of the capillary columns is limited to 200 μm [16, 19]. For capillaries having an inner diameter smaller than 100 μm , the thermal band broadening caused by heating effects can be neglected [7].

Several chemical equilibrium constants, determining both the pH and the capacity factors, are involved in CEC. Through the equilibrium constants, the temperature affects the charge surface density of the stationary phase, therefore the magnitude of the EOF and the selectivity of the separation. The temperature dependence of the chemical equilibrium is described by the Van't Hoff equation:

$$K = e^{\left(\frac{-\Delta H^0}{RT} + \frac{\Delta S^0}{R}\right)} \quad (2.15)$$

Where K = equilibrium constant [dimensionless].

ΔH^0 = enthalpy change associated with the equilibrium [$\text{J} \times \text{mol}^{-1}$].

ΔS^0 = entropy change associated with the equilibrium [$\text{J} \times \text{mol}^{-1}$].

Diffusion, another process involved in CEC, is also dependent on the temperature. The corresponding relation is given by the Stokes-Einstein equation:

$$D_i = \frac{kT}{6\pi\eta r_h} \quad (2.16)$$

2.3- Electrodriven Liquid Chromatography.

CEC is an electrodriven mode of liquid chromatography which uses the electroosmotic flow to propel the mobile phase. Separations of complex mixtures of components can be achieved by the differential migration of the analytes that result from both electrophoresis and interactions with the

stationary phase. The latter principle encountered in CEC is a common feature of liquid chromatography, which implies a partitioning of the analytes between a stationary and a mobile phase. Whereas electrophoresis is a pure electroseparation process, chromatographic processes also rely on physico-chemical interactions with the stationary phase. Two modes of chromatography were investigated in the present work, reversed phase chromatography and ion exchange chromatography.

In reversed phase chromatography, hydrophobic interactions and short range interactions, such as Van der Waals and hydrogen bonding, are at work. Van der Waals forces denote the interactions between molecules with a dipole moment. These forces combine the interactions between molecules of the stationary phase and molecules of the analyte that can be of three kinds: dipole/dipole, dipole/induced-dipole and induced-dipole/induced-dipole. In the case of ion exchange chromatography, coulombic interactions take place between ions contained both in the sample and in the stationary phase.

2.3.1- Retention and Migration.

In pure chromatography, the partitioning of a substance between the stationary and the mobile phases is represented by the chromatographic capacity factor (or retention factor) k' :

$$k' = \frac{n_{sp}}{n_{mp}} \quad (2.17)$$

With n_{sp} = amount of analyte in the stationary phase [mol].

n_{mp} = amount of analyte in the mobile phase [mol].

However, since in CEC the electrophoretic migration has to be taken into account, the characteristic chromatographic capacity factor is no longer valid for describing the migration process [1]. Furthermore, the electric field that drives the mobile phase can influence the retention behavior [23]. The

capacity factor in CEC, k_{cec} , must include effects arising from both chromatography and electrophoresis [24]:

$$k_{cec} = k' + k' \frac{\mu_{ep}}{\mu_{eo}} + \frac{\mu_{ep}}{\mu_{eo}} \quad (2.18)$$

Where k' = pure chromatographic capacity factor.

$k' \frac{\mu_{ep}}{\mu_{eo}}$ = electrophoretic component.

$\frac{\mu_{ep}}{\mu_{eo}}$ = electrophoretic velocity factor.

A more practical expression for eq. 2.18, considering the velocity of the analytes in CEC is:

$$k_{cec} = \frac{(u_{ep} + u_{eo})}{u_{eo} u_{migr.}} - 1 \quad (2.19)$$

For a neutral compound $\mu_{ep} = 0$. According to eq. 2.18, $k_{cec} = k'$, which reflects a pure chromatographic process. For a charged, unretained compound, $k' = 0$ and $k_{cec} = \frac{\mu_{ep}}{\mu_{eo}}$.

The migration of a neutral, chromatographically retained compound in CEC is characterized by the linear velocity of the EOF and the extent of partitioning between the two phases:

$$u_{migr} = \frac{u_{eo}}{1 + k'} \quad (2.20)$$

With $u_{eo} = \mu_{eo} \frac{\Delta\phi}{d}$, eq. 2.20 becomes:

$$u_{migr} = \frac{\mu_{eo}}{1 + k'} \frac{\Delta\phi}{d} \quad (2.21)$$

The detection time t_r , which is the time taken by a neutral analyte to be detected, can be calculated by introducing both its migration velocity u_{migr} and the length from the capillary inlet to the detector d_{id} . By comparison with 2.21:

$$t_r = \frac{d_{id}}{u_{migr}} \Leftrightarrow t_r = \frac{d_{id} \times d(1+k')}{\mu_{eo} \Delta\phi} \quad (2.22)$$

Where t_r = detection time of a neutral compound [min].

d_{id} = length from the capillary inlet to the detector [cm].

The electroosmotic mobility is related to the detection time of an unretained neutral marker t_{eo} (the electroosmotic flow marker) by the equation:

$$t_{eo} = \frac{d_{id}d}{\mu_{eo} \Delta\phi} \quad (2.23)$$

By combining eq. 2.22 and eq. 2.23, we obtain:

$$t_r = t_{eo}(1+k') \Leftrightarrow k' = \frac{t_r - t_{eo}}{t_{eo}} \quad (2.24)$$

For neutral analytes, the capacity factor can easily be determined from electrochromatograms (see appendix C). This can be done by measuring the detection time of an unretained neutral solute t_{eo} and of each neutral analyte t_r .

2.3.2- Efficiency and Resolution Factor in Open Tubular Columns.

Chromatographic retention is frequently described in analogy to solvent extraction by the cascade model. A succession of equilibrated separations is assumed in the separation column. This idea has led to the development of the plate theory that describes the dynamic process of chromatography

with a static model. In this model, the column is sliced theoretically into plates. The knowledge of the height equivalent to a theoretical plate (HETP), which relates to the number of theoretical plates per unit of length, translates the efficiency of the columns.

The overall plate height equation in an open tubular column for a retained analyte, in both pressure driven and electrodriven system, is given by [25]:

$$HETP = \frac{2D_m}{u} + C(k^*)_m \frac{d_c^2 u}{D_m} + C(k^*)_s \frac{d_f^2 u}{D_s} \quad (2.25)$$

- With D_m = diffusion coefficient of the solute in the mobile phase
[cm² × s⁻¹].
- D_s = diffusion coefficient of the solute in the stationary phase
[cm² × s⁻¹].
- $C(k^*)_m$ = dimensionless coefficient for resistance to mass transfer in the mobile phase [dimensionless]. This coefficient is dependent on the form of the velocity profile of the eluent.
- $C(k^*)_s$ = dimensionless coefficient for resistance to mass transfer in the stationary phase [dimensionless].
- d_c = diameter of the column [cm].
- d_f = thickness of the stationary phase [cm].
- u = linear velocity of the analyte in the axial direction [cm × s⁻¹].
- k^* = k' or k_{ccc} depending on the mode of propelling of the mobile phase: pressure driven or electrodriven, respectively.

For retained compounds mass transfer between the mobile and the stationary phases necessitate transcolumn equilibration. Therefore, the theoretical plate height equation for OTC possesses a parameter d_c , linked to the internal diameter of the capillary column.

From the three contribution terms in eq. 2.25, only the resistance to mass transfer in the mobile phase is affected by the shape of the velocity profile. It

is generally assumed that with OTC, the resistance to mass transfer when thin films of stationary phase are used, is negligible [26]. Therefore eq. 2.25 can be written:

$$HETP = \frac{2D_m}{u} + C(k^*)_m \frac{d_c^2 u}{D_m} \quad (2.26)$$

For pressure driven liquid chromatography, $C(k^*)_m$ was defined by Golay [27]:

$$C(k^*)_m^{PD} = \frac{1 + 6k' + 11k'^2}{96(1 + k')^2} \quad (2.27)$$

For electrically driven liquid chromatography (CEC), $C(k^*)_m$ was defined by Bruin et al. [25] by evaluating the general dispersion theory of Aris [28], assuming that the velocity flow profile of the mobile phase is flat:

$$C(k_{cec}^*)_m^{ED} = \frac{k_{cec}^2}{16(1 + k_{cec})^2} \quad (2.28)$$

Since the velocity flow profile is not completely flat in close proximity to the stationary phase, eq. 2.25 constitutes an approximation of $C(k^*)_m$. The complete mathematical treatment of the real velocity flow profile complicates the description of $C(k^*)_m$ and involves Bessel functions [29, 30, 31]. Therefore, despite complex equations, this treatment cannot lead to an analytical calculation for $C(k^*)_m$. Approximations also have to be made to consider the flow profile.

If $k_{cec} = k'$, as already mentioned, electro-driven chromatography exhibits better separation in electrodriven instead of pressure-driven condition, the mass transfer parameter for the mobile phase being smaller for CEC (Fig. 2.4). This feature characterizes the flat flow velocity profile of the mobile phase in CEC where the axial dispersion of the analytes in the capillary is reduced.

This reduced dispersion constitutes a major advantage of the CEC over the pressure driven chromatography where the parabolic flow profile tends to disperse the analytes.

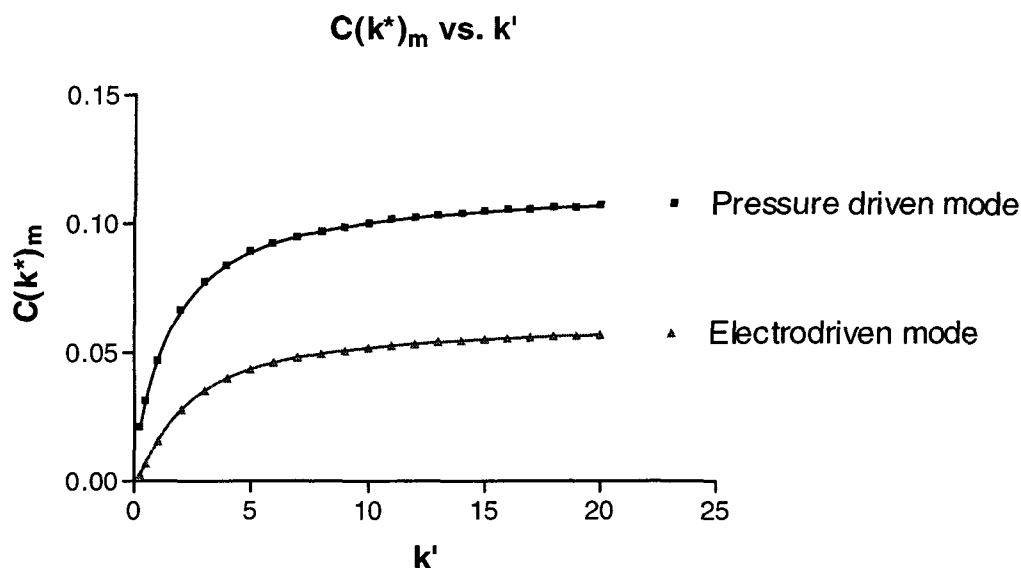


Fig. 2.4: Resistance to mass transfer coefficient for the mobile phase versus k' for electro-driven and pressure-driven chromatography in open tubular columns with the same linear velocity of the mobile phase and with $k_{cec} = k'$.

As seen in Fig. 2.4, the C_m term increases rapidly when retention occurs and $C(k^*)_m^{PD} > C(k^*)_m^{ED}$. Therefore, electrodriven instead of a pressure driven system improves the efficiencies by a factor of 3, as pointed out by Bruin et al. [25]. This phenomenon opens up the possibility of performing OTC-CEC in wider columns than the ones theoretically required for OTC-HPLC, i.e. having an optimal diameter in the range between 1-3 μm [32]. The advantage of using capillaries with larger diameter is obvious since there are fewer practical problems with regard to the capillary preparation.

The presence of diffusion, Brownian motion and extracolumn effects contribute to the decrease of the efficiencies expected from eq. 2.25. In the capillaries, the difference of the chemical potentials between the sample and the mobile phase contributes to a broadening of the analyte bands. This phenomenon arises from the diffusion of molecules aiming to equalize the chemical potentials between zones of different concentrations. This process

counteracts the chromatographic separations. Macroscopically, directed diffusion takes place along a concentration gradient and can be observed as a flux of mass J_i , described by Fick's first law:

$$J_i = -D_i \left(\frac{dC_i}{dx} \right) \quad (2.29)$$

Where: J_i = flux of matter [$\text{mol} \times \text{cm}^{-2} \times \text{s}^{-1}$].

D_i = diffusion coefficient [$\text{cm}^2 \times \text{s}^{-1}$].

x = direction of the concentration gradient.

The self-diffusion of the molecules by Brownian motion, arising from local fluctuations of the thermal energy, also contributes to band broadening but only to a minor extent. Diffusions issued from concentration gradients or from Brownian motions are both entropic processes that counteract the mechanisms that drive the electrochromatographic separations. Finally, extracolumn effects, like those encountered during injection and detection, also contribute to decrease the efficiency of a column. As already mentioned temperature affects the efficiencies obtained in CEC by changing the thickness of the double layer, the chemical equilibria and the molecular diffusion coefficients.

The overall HETP, taking into consideration all the parameters affecting the efficiencies, can be accessed by the trace of an electrochromatogram peak. If we consider that the peaks of neutral compounds in CEC are gaussian peaks, the number of theoretical plates can be calculated from the electrochromatograms by:

$$N = 5.54 \frac{t_r^2}{\delta^2} \quad (2.30)$$

Where t_r = detection time of the analyte [min].

δ = width of the gaussian peak at 50% of its height [min].

Depending on the electroosmotic velocity, the detection time of an analyte can vary largely. To minimize this effect, the detection time of an analyte should be referred to the detection time of a chromatographically un-retained compound, the electroosmotic flow marker detected at t_{eo} . Referring the detection time of an analyte to t_{eo} give the effective number of plate:

$$N_e = 5.54 \frac{(t_r - t_{eo})^2}{\delta^2} \quad (2.31)$$

From the N_e value, and the knowledge of the columns length (L), one can calculate the effective plate height:

$$HETP_e = \frac{L}{N_e} \quad (2.32)$$

The knowledge of the effective number of plate does not give any information about the quality of an electrochromatographic separation. For this reason, the resolution factor R is used to define the quality of the separation between two peaks 1 and 2:

$$R = 2 \frac{t_2 - t_1}{\omega_1 + \omega_2} = 1.175 \frac{t_2 - t_1}{\delta_1 + \delta_2} \quad (2.33)$$

Where $\omega = 4\sigma$ and $\delta = 2.35\sigma$. Therefore $\omega = 1.702\delta$.

ω and σ , correspond respectively to the width at 13.5% and to 60.6% of the height of a gaussian curve.

2.4- Chromatographic phases.

In chromatography, the separations arise from the differential motion of the analytes, which exhibit different affinities for the chromatographic phases, the so-called stationary phase and the mobile phase. The stationary phase is linked to the column whereas the mobile phase moves in the column under the influence of a driving force, i.e. by pressure or by an electric gradient.

The stationary phases, at the “heart” of the CEC technique, are designed to address interactions and stability issues and to promote the electroosmotic flow. So far, most of the research has been carried out with packed CEC columns using particulate, silica-based materials initially designed for applications in HPLC [33]. These materials are mostly functionalized with C₁₈ alkyl moieties chemically bonded to the surface of porous silica beads having a diameter in the range of 1.5-10 μm. However, as already mentioned, packed columns suffer from the necessity of frits and from the limitations concerning the nature and size of commercially available packing material. To overcome these drawbacks custom monolithic or coated stationary phases were synthesized for CEC. These phases were based on organic polymers, ion exchange material or silica [33, 34].

In the present work, silica-based stationary phases were mainly developed. Silica was chosen because its chemistry is well known [35, 36], and for its intrinsic ability to generate a strong EOF due to the silanol groups at its surface. This is of particular interest since no ionic groups are required during the synthesis of the silica stationary phases unlike in the case of organic stationary phases. Indeed, when organic stationary phases are used, no EOF is generated unless ionizable groups are bonded to them. One further advantage of using a silica based material is the fact that CEC uses mostly silica capillaries. The chemistry involved at the surface of the capillary when an attachment to the stationary phase is needed is hence common to both the surface and the stationary phase.

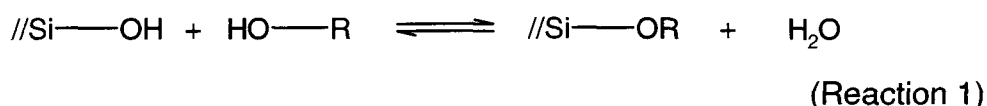
Stationary phases for CEC can be classified into monomeric or polymeric types depending on the functionality of the chemicals involved in their synthesis.

2.4.1- Monomeric Stationary Phases.

These phases are made with monofunctional chemicals to prevent any polymerisation, and therefore any three dimensional extension. Such phases, anchored to the stationary wall after reaction with the silanol groups [37],

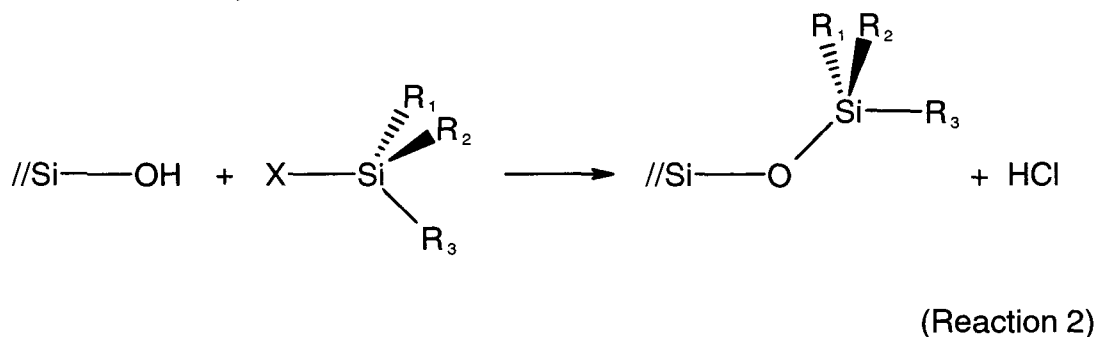
consist of monolayers of grafted molecules containing moieties responsible for the chromatographic activity.

Addition to the silanol groups of the silica wall can be performed by the formation of an ether bond:



With R = organic moiety.

This involves a water condensation reaction that can either be catalysed by an acid or a base. Alcohols are not recommended for this reaction because the corresponding ether bond formed (Si-O-C) is highly reactive toward hydrolysis and therefore cannot be used with aqueous mobile phases [37]. This reactivity can be lowered by the formation of a Si-O-Si-C link, involving a siloxane bond (Si-O-Si). The corresponding synthesis, organosilanization, is carried out with monofunctional organosilanes containing a single reactive group, generally a chlorine or an alkoxy group:

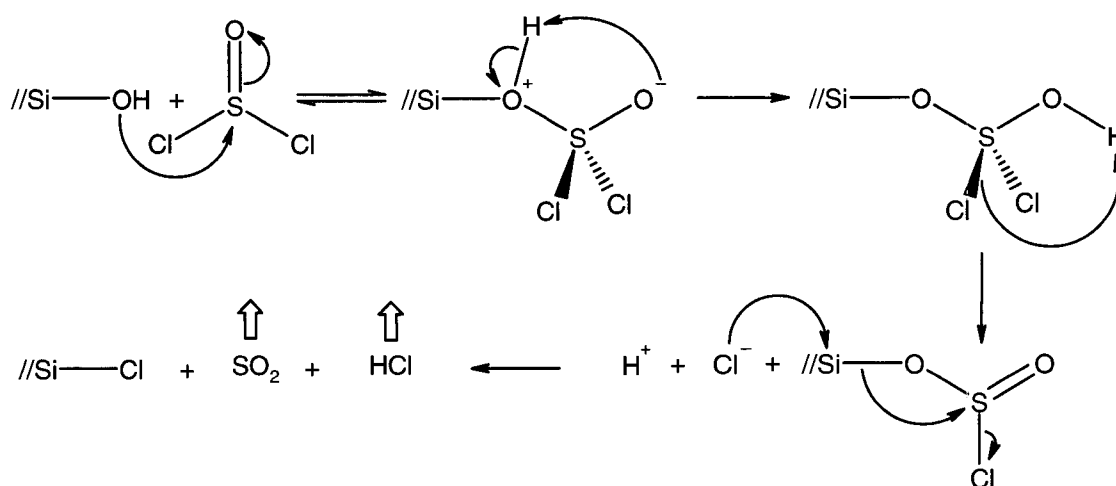


With //Si = Silicon atoms borne on the inner surface of a capillary.

X = easily hydrolysable group (i.e. halide, alkoxy, acyloxy) and Y = //Si or OH.

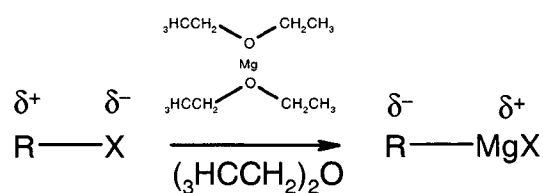
The Si-O-Si bonds obtained via organosilanization have been recognized as the major source of hydrolytic instability of silica based stationary phases [38]. To overcome this problem, the more hydrolytically stable bonds Si-C, are used to link organic moieties to the fused silica surface.

The second approach to monomeric stationary phase consists a nucleophilic addition forming Si-C bonds that are particularly resistant toward temperature and hydrolysis. To perform this reaction, the silanol groups of the fused silica surface are first halogenated. Chlorination is the most frequently reported process. The chlorination of silanols can be done by using SOCl_2 , SiCl_4 or TiCl_4 . Despite the fact that SiCl_4 or TiCl_4 are more effective for the chlorination of the silica surface [39], SOCl_2 is mostly used due to the gaseous nature of the reaction by-products (SO_2 and HCl):



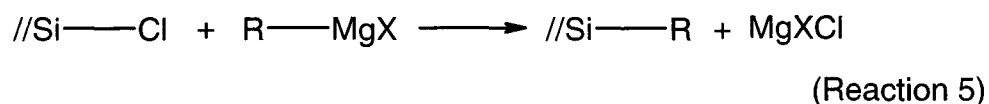
(Reaction 3)

It known that the use of pure SOCl_2 leads to a partial replacement of hydroxyl groups whereas dissolved SOCl_2 gives a complete reaction [36]. In a second step, the halogenosilanes are submitted to a nucleophilic attack either with a Grignard reagent or an organolithium compound:



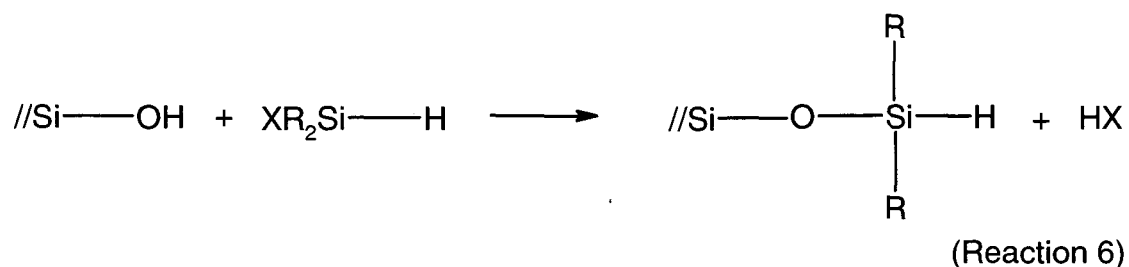
(Reaction 4)

This attack permits the nucleophilic substitution of the halogen by an organic moiety.

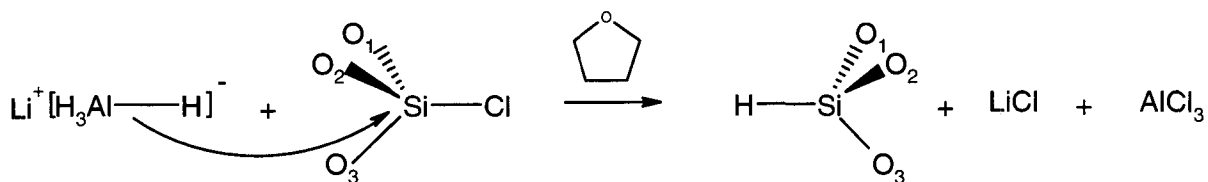


Since the reactions 4 and 5 are very sensitive to moisture, extremely dry conditions have to be maintained during the synthesis. If water is not completely removed, the hydrolysis of the chlorinated surface would give back silanols, whereas the hydrolysis of the nucleophilic compounds would give alcohols.

The third approach known to give monomeric phases is a silanization/hydrosilylation procedure consisting of the formation of Si-C bonds. This procedure involves the preparation of silica hydride surfaces followed by a catalytic addition of these latter to organic compounds containing a terminal alkene. The silanols of the capillary wall are first converted into silicon hydrides by silanization. This step can be done by reacting these groups with hydrosilane (Si-H) containing at least one reactive group via a $S_N2\text{-Si}$ mechanism.



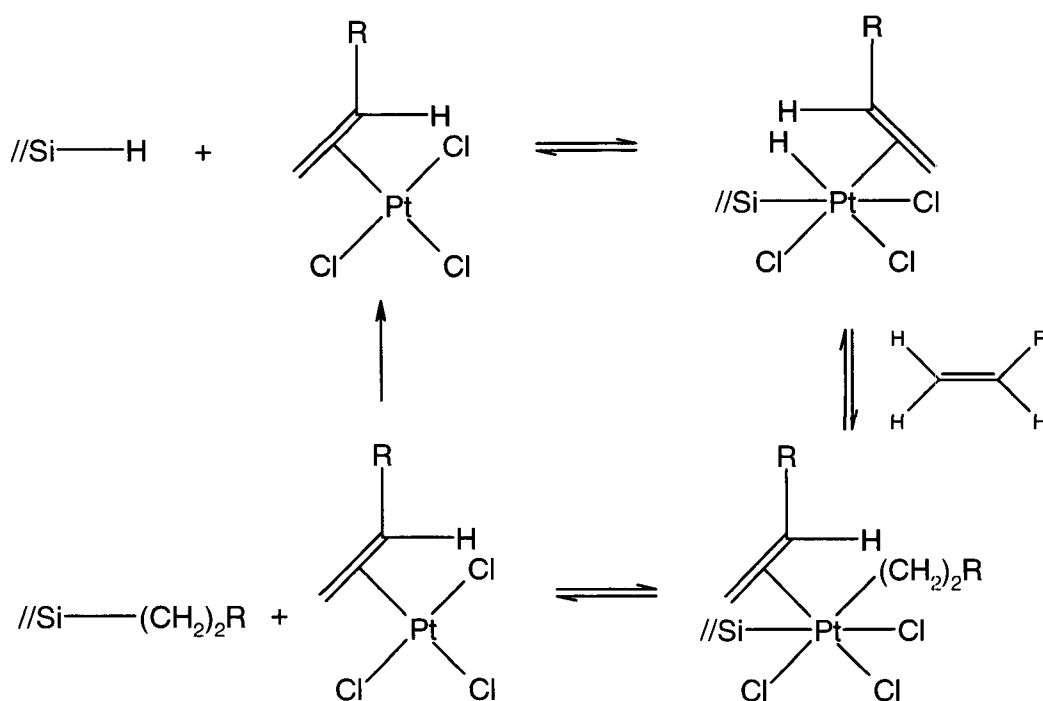
An alternative approach to silanization consists in a reduction of halogenosilanes with highly polarised hydrides like LiAlH_4 . A pentacoordinated intermediate [40] is obtained, and an inversion of the tetrahedron structure of the silicate is observed.



(Reaction 7)

This reduction with hydrides is reported to give higher amounts of silanes than silanization with monofunctional silanes [41]. In a second step, chemicals containing a terminal olefin are grafted to the silanes by hydrosilylation. This reaction is performed in the presence of a group VIII transition metal complex as catalyst. The most commonly used catalyst is hexachloroplatinic acid ($\text{H}_2\text{PtCl}_6 \cdot 6\text{H}_2\text{O}$) in 2-propanol, a solution known as Spier's catalyst.

The hydrosilylation reaction is known to give very high yields, typically >90% [42]. This reaction interferes only minimally with other reactive functionalities and permits the grafting of molecules which otherwise cannot be introduced by regular organometallic reagents [43]. The proposed mechanism for the hydrosilylation reaction, namely the Chalk-Harrod mechanism [44], results in the formation of an anti-Markovnikov adduct at the silica surface:



(Reaction 8)

2.4.2- Polymeric Stationary Phases.

These phases are made with polyfunctional molecules that allow polymerisation. The resulting three-dimensional networks give rise to thicker coatings than with monomeric phases, and permit access to the monoliths. The polymerisation processes to make stationary phases for CEC can be either performed on organic monomers or on organosilanes. Organosilane polymers were studied extensively in the present work.

Organic polymers are attached to the inner wall of the fused silica capillaries through different linking agents. A common approach involves the bonding of methacryl groups ($\text{CH}_2\text{C}(\text{CH}_3)\text{CO}$) to silanol groups of the capillary wall by silanization. Thereafter, another organic species is bonded to this linker inside the capillary, by a double bond reaction and polymerisation [45], to form coatings or monoliths. Coatings made of organic polymers for OTCs can be used in CEC [46], but most of the time they are employed in CE to modify the EOF or to diminish the interaction of solutes with the capillary wall [45]. Organic monoliths, also known as continuous beds, were first prepared by Hjerten et al. for use in HPLC [46]. To assure a certain degree of porosity allowing a flow of the mobile phase, polymers for monoliths are synthesized in the presence of a porogenic agent. EOF through organic polymers is promoted by incorporating ionizable functional groups such as acrylic acid or sulfonic acid monomers into the polymerized mixture. A review of the continuous beds can be found in an article from Pursch and Sanders [33].

Organosilane polymers are fabricated by the sol-gel process [47, 48], a technique in which oxide-based materials can be synthesized without any melting step at elevated temperatures. This technique is based on the simultaneous hydrolysis and condensation of metal alkoxide precursors. It consists in the formation of a sol constituted of metallic oxo based particles (Si-O-Si) dissolved in a solvent [48, 49]. The structure of the sols can differ widely, from low viscosity solutions (spinnable sols) to discrete particle suspensions, depending on the respective rates of hydrolysis and condensation. These rates can be controlled by the nature and the amount of

chemicals being involved in the synthesis of the sol: the silicate precursors, the catalysts, the solvent, and the water. After gelation, an irreversible mechanism involving the connection of clusters of particles, and aging, a phenomenon describing the hydrolysis/condensation occurring after the gelation point, the removal of the solvent gives rise to a dried gel (xerogel). The physical nature of the xerogels being directly related to the structure of the sols [48], xerogels can exhibit a variety of forms ranging from monoliths to particulate powders. Since sols can be tailored by an appropriate choice of reagents and can contain different organic moieties, the sol-gel process becomes a particularly interesting flexible technique to be used in CEC to form coatings or monoliths (Fig. 2.5)

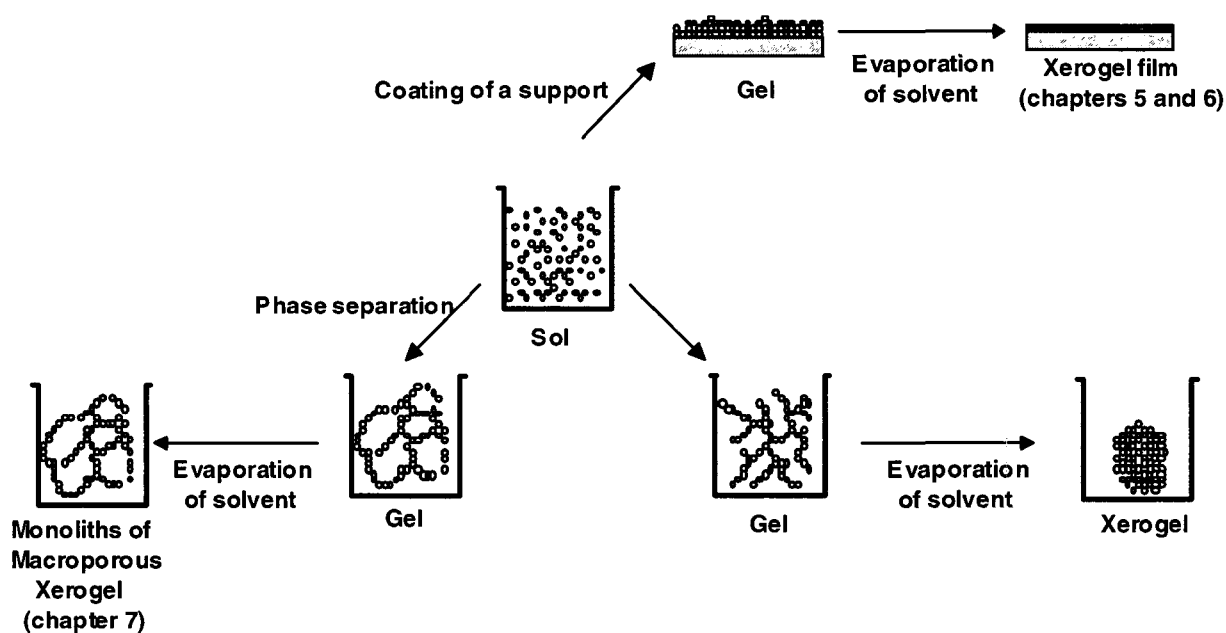


Fig. 2.5: The sol-gel process.

At the functional group level, three reactions are generally used to describe the sol-gel process: hydrolysis, alcohol condensation and water condensation. The general condensation scheme is seen in Fig. 2.6, taking as example tetraethoxysilane (TEOS), the most frequently reported metallorganic precursor.

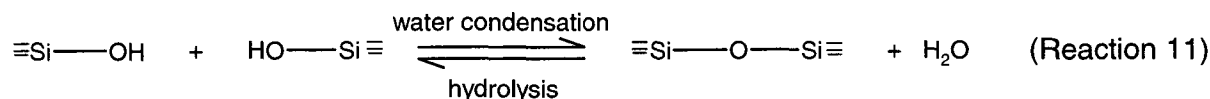
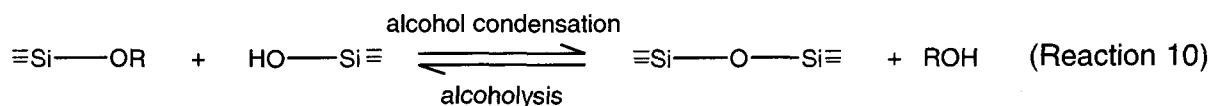
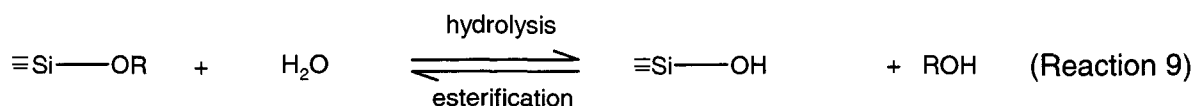


Fig. 2.6: Reactions involved in the sol-gel process with TEOS as metallo-organic precursor. Since the sol-gel process involves numerous reacting species, which differ from their extent of the hydrolysis/condensation, only the basic mechanisms are shown.

The silica organic/inorganic nanocomposites made by the sol-gel process, are becoming particularly interesting selective materials for chemical analysis [50]. Amongst them, the xerogels made from organically modified silicates (ormosils) fulfil the requirements for stationary phases in CEC. These materials are able to generate an EOF due to the acid/base properties of their silanol groups, and are also able to perform chromatographic separations due to their selective interactions with the components of a complex mixture.

Ormosils can be divided into two general classes [51]. In class A, organic molecules are impregnated or entrapped in an inorganic gel matrix. This class of ormosils has been extensively used for the incorporation of proteins for immunoaffinity chromatography [i.g. 52, 53, 54], for chemical sensing properties [i.e. 55], and for the incorporation of dyes in a silica matrix. In class B, organic molecules are covalently linked to the inorganic silica matrix through covalent chemical bonds. In the present work, only class B ormosils were investigated as stationary phases for CEC. Class B ormosils, thereafter simply called ormosils, are made by the polycondensation of TEOS with organosilane precursors carrying the desired organic moieties. With the aim of producing stationary phases for CEC, the effect of the following variables on ormosil synthesis was studied: hydrolysis and condensation, pH, organic solvent, temperature and drying chemical control additive. Both optic and electronic microscopy, as well as resolutions and efficiencies of electrochromatographic separations, were used for the characterization of the

resulting stationary phases.

2.4.3- Mobile Phases.

Most of the mobile phases used in CEC consist of hydroorganic solutions [7] containing an organic modifier and an electrolyte, frequently a buffer. Organic solvents are used in mobile phases to enhance the solubility of apolar analytes and to adjust the capacity factors of the sample constituents, which in turn sets the distribution isotherms. The presence of organic solvents in the mobile phases also affects the dissociation constant of the silanol groups when silica-based stationary phases are used. Theoretically, an increased concentration of organic solvent in the mobile phase shifts the pK_a of the silanols toward higher values [12]. The EOF is thus affected by the organic content of the mobile phase, which can be used to control the Joule heating inside the capillary. Appropriate mobile phases for CEC should exhibit high dielectric constants and low viscosities (ratio ϵ_r/η in eq. 2.9) to get the highest EOF for a given voltage. Since the surface charges and the thickness of the double layer is affected by the presence of an organic solvent [12], the zeta potential should also be taken into account in the choice of the organic modifier, as suggested by eq. 2.9. However, the value for the zeta potential cannot be predicted simply from the binary structure of the mobile phase [56]. Complications arise from microscopic liquid-liquid phases separations between the different components of a hydroorganic mobile phase [56].

Buffers play an important role when electrophoresis is involved in CEC. When analytes with acid-basic properties are to be analysed, it becomes possible to charge them by adjusting the pH with regard to their pK_a values. Being electrically charged, the analytes are separated by electrophoresis in addition to chromatography. Buffers also limit the pH instabilities in close proximity of the electrodes where acid-base reactions are known to occur due to electrolysis of the water [57]. Since the resolution is reduced steadily in OTC-CEC when the buffer concentration is increased [58], it is recommended to

work at low buffer concentration. Crego et al. [58] recommend to use a 1 mM buffer, which provides the highest resolutions with the smallest separation times. However, attention has to be paid to the buffer capacity of the mobile phase, which should not be too low, especially in the case of charged analytes.

Hydroorganic solutions and pure solvents, both without any supporting electrolyte, are also used as mobile phases for CEC. Because the conductance of the mobile phase is low, the heat production by the Joule effect is almost negligible [56]. No viscosity gradient can develop in the capillary, which helps to reduce the band broadening of the analyte bands. This is particularly interesting when high voltages have to be used, generally 30 kV for commercially available CE systems. The use of such high voltage is limited by Joule heating with mobile phases containing an electrolyte.

The nature of the stationary phase chemistry and the double layer formation in hydroorganic solutions or pure solvent without any supporting electrolyte remains elusive [56]. Nevertheless, it is thought that the generation of an EOF without any background electrolyte arises from acid/base reactions at the interface between the mobile phase and the stationary phase. For a silica-based stationary surface, a solvent with basic properties will impose a negative charge by a three step process. The basic group will first adsorb onto the solid surface at an acidic functional group. Proton transfer then takes place from the acid to the base, after which the base partially desorbs into the bulk solution leaving a negative potential at the solid surface [59]. Although aprotic solvents like acetonitrile have both acidic and basic functionalities, they generate negative charges on stationary phases with acidic character. It has to be noted that the highest EOF is obtained by using pure acetonitrile as a mobile phase [56, 60].

3- Investigation of Monomeric Stationary Phases for CEC.

Functionalisation of the capillary wall with monomeric stationary phases was the first attempt in this work to get efficient OTCs for CEC. The traditional approaches to modify silanols for HPLC were adapted to CEC. Experimental details are given at the end of this chapter.

3.1- Conditioning of the Capillary Walls.

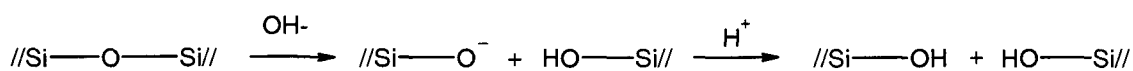
The only active sites to bond stationary phases to the silica surfaces are the silanol groups [61]. Throughout this work, fused silica capillaries were used as physical supports for CEC. Capillaries made of fused silica, instead of borosilicates glass or soda lime glass, were chosen for their better mechanical and optical properties [34] despite the low surface density of their silanol groups (maximum 8-9 groups/nm² [62]). This low surface coverage can be explained by the condensation occurring between silanol groups in close proximity at the high temperatures ($\approx 2000^{\circ}\text{C}$) required during the drawing process of the fused silica capillaries. The low silanol group density confers a chemical inertness to any fused silica surface [62]. To overcome this drawback, two methods are traditionally used to increase the number of silanol groups on the silica surface. The first approach consists of either an acid or an alkaline hydrolysis to increase the number of active sites available for subsequent chemical reactions. When hydrolysis is performed above pH 9, the solubility of silica is greatly enhanced and hydrolysis occurs with a partial dissolution of the silica surface by formation of soluble silicates. The second approach consists of a hydrothermal hydrolysis using water vapor at high temperature [62]. In this case, hydrolysis also occurs with the partial dissolution of the silica surface.

The hydroxylated silica surface, due to its ability to form hydrogen bonds, firmly retains a thick layer of physically adsorbed water [63]. This layer shields the surface of the silica and lowers the reactivity of the silanol groups. To increase the number of reactive silanol groups, and thus the efficiency of a

derivatization step, this adsorbed water must be removed. This process is performed by a thermal treatment. The majority of adsorbed water can be easily removed from a silica surface at 25°C in a vacuum [63], but a monolayer of water, which bridges the gap between the silanol groups at the silica surface, is retained up to 190°C. This usually presents no problem; on the contrary, the hydration water seems to be necessary for a successful surface modification [63].

The silanols on a silica surface can be differentiated into isolated, geminal and vicinal silanols. Silanetriols on a silica surface have also been postulated, but they seem to be highly improbable [36]. The classification depends on the ability of two neighboring silanol groups to interact via hydrogen bonding. This interaction occurs between silanol groups separated by no more than 0.31 nm [35]. Silanols involved in a hydrogen bond have a reduced chemical reactivity, while isolated silanols, which do not take part in hydrogen bonding with other silanol groups, are the most reactive [64] for covalent bonding with stationary phases. However, isolated silanol groups represent the lowest population of silanol groups present on a silica surface. Therefore, the aim of any successful hydrolysis is to increase their number with regard to the population of geminal and vicinal silanol groups.

So far, no general approach to increase the number of isolated silanol groups has been reported, each research group having its own method (Table 1). The most commonly reported approach consists of an alkaline hydrolysis of the silica surface followed by protonation of the silicate groups ($-\text{Si-O}^-$) and then by a thermal treatment:



(Reaction 12)

It has to be noted that the group of Malik et al. does not carry out any hydrolysis but simply washes the silica surface with an organic solvent [65, 66] (see Table 1).

Hydrolysis			Wash	Drying step		Ref.
Catalyst/ Concentration [M]	Time [h]	Temp [°C]		Temp [°C]	Gas flow	
KOH / 1	3	25	1- H ₂ O, 1h 2- HCl, 2h 3- H ₂ O, 3h	125	He / 4h	[67]
NaOH / 1	1	25	1- H ₂ O 2- Ac. ac. 1% (w/v), 2.00h.	Not given	Not given	[68]
NaOH / 1	2	100	1- H ₂ O 2- ACE, 10 min.	120	N ₂ / 1h	[69]
NaOH / 1	3	25	1- H ₂ O, 1h 2- HCl 0.03M, 1h 3- H ₂ O, 1h	120	He / 12h	[70]
NaOH / 1	0.5	25	H ₂ O, 0.5h	110	N ₂ / 12h	[71]
KOH / 1	1	25	H ₂ O, 1h	180	N ₂ / 12h	[72]
No hydrolysis			CH ₂ Cl ₂ in pentane (1:1 v/v)	25	N ₂ / 0.5h	[65, 66]
KOH / 1	2	25	HCl 0.01M / 0.5 h	200-250	He / 2h	[73]
NaOH, 1	0.5	25	H ₂ O / 12h	180	N ₂ / 1h	[74]
NH ₄ OH, pH9	12	25	MeOH / 2h	200	N ₂ / 12h	[62]
water vapor 300°C, no catalyst	12	300	MeOH / 2h	200	N ₂ / 12h	[62]
HCl 10% (v/v)	1.5	120	1- H ₂ O 2- MeOH	140	He / 1h	[75]
HCl Concentrated	12	80	1- H ₂ O 2- ACE 3- Diethyl Ether	Not given	N ₂ / 1H	[76]
NaOH, 1	2	100	1- HCl, 0.1M, 5 min. 2- H ₂ O, 10 min 3- ACE, 15 min.	120	N ₂ / 1h	[46]

Table 1: Overview of some of the reported processes performed to activate fused silica surfaces prior to chemical modification. In most of the cases, hydrolysis is followed by a flush with a liquid and a thermal treatment. (ACE = acetone).

The low capacities factor of fused silica capillaries are a frequently reported drawback [34, 62, 77]. To get efficient separations, the capacity of the stationary phases must be increased. This task can be achieved by increasing the contact surface between the two chromatographic phases, i.e. by using a

porous support or by etching the silica wall of the capillary and then grafting on the stationary phases.

The etching of the silica wall must consist then in a chemical attack of the capillary walls to get a rough surface giving only slight modifications of the volume of the enclosed liquid. This anisotropic etching can be carried out with gaseous hydrogen fluoride (HF), which is known to be the most effective roughening agent of silica surfaces able to form even silica whiskers [78]. For the convenience of the work and for safety reasons, ammonium hydrogen difluoride (NH_5F_2) was used instead of HF. At elevated temperatures, NH_5F_2 dissociates to give gaseous HF and NH_3 [78]. The etching process used for the preparation of OTC-CEC [76, 79] was adapted from the procedure suggested by Onuska and co-workers [78], which involves the deposition of a NH_5F_2 layer from a saturated methanol solution (5% w/v) onto the capillary inner wall.

An alternative method aiming to increase the surface of the stationary phase support consists of the deposition of a porous silica layer on the inner wall of the fused silica capillaries. This enhancement step may be performed by precipitation of silica from a solution of polyethoxysiloxane (PES). PES can be prepared by a hydrolytic polycondensation of tetraethoxysilane (based on the work performed by Tock et al. and by Unger and co-workers [73, 80]). The deposition of a porous silica layer on the capillary wall is reported to be more efficient than the etching of the same wall [81]. Therefore the porous adsorbent layer in capillaries is expected to offer better prospects [73]. Once the surface has been increased, a stationary phase (retentive layer) has to be added.

3.2- Synthesis of Monomeric Stationary Phases.

Since the silica-based stationary phase are popular for both HPLC and CEC, the reactions aiming to functionalize the silanol groups for HPLC were easily transferred to CEC. Three synthetic procedures commonly used in HPLC aiming to produce reversed phases, the organosilanization, the nucleophilic

substitution and the silanization/hydrosilylation, were tested. These reactions were carried out on three kinds of support: naked capillaries, capillaries with an etched inner surface and capillaries coated with a porous silica layer. In all cases, octyl groups (C_8) were grafted on the different silica surfaces.

3.3- Experimental.

The derivatization of silanol group to give octyl phases via organosilanization, silanization/ hydrosilylation and nucleophilic attack were carried on capillaries with an inner diameter of 50 μm and a length of 47 cm (40 from the injection point to the detection point).

Unless stated otherwise in this work, samples under investigations were mixture of polycyclic aromatic hydrocarbons (PAHs). These compounds, namely naphthalene, phenanthrene and pyrene, all absorb above 200 nm and hence were easily detected in our set-up. Moreover, since the chosen analytes were not electrically charged, any separation observed could not be due to electrophoresis and hence proved that a chromatographic separation mechanism was responsible. Test sample was made by mixing 10 mM of naphthalene phenanthrene and pyrene in a mixture acetonitrile / acetone (3:2, v/v). Acetone was used as the EOF marker. The mobile phase was constituted of a mixture ACN / H_2O (1:1, v/v) with NaCl (2 mM). Unless stated otherwise in this work, injection of the sample was performed hydrodynamically (1 s, 1.36 b) and separations were performed at 30 kV (corresponding to an electric field of $638.3 \text{ V} \times \text{cm}^{-1}$ for a column length of 47 cm). The temperature during the electrochromatographic separation was set at 25°C.

Conditioning of the Capillary Walls:

Increase of the silanol concentration in capillaries.

Unless otherwise mentioned in this work, the silanol density was increased by washing the fused silica capillaries with an aqueous NaOH solution (1 M, 60 in, 5 b), then with aqueous HCl solution (10^{-1} M, 15 min, 5 b) and then with distilled water (15 min, 5 b) to remove any trace of NaCl. Both the acid and

water flushing steps were performed for 10 min. The prepared capillaries were then flushed with argon and with anhydrous hexane for 10 min (the latter was dried over Na with benzophenone as a wetness indicator, then distilled under an inert atmosphere) and again flushed with argon (each flush 10 min). Capillaries were allowed to dry in a vacuum oven (12 h, 35°C, 20 mb). Afterwards, the oven was filled with argon and the extremities of the capillaries were plugged with silicon septa for storage.

All the flows in this conditioning step were generated in a custom system for filling the capillaries (Fig. 3.1). The pressures used to generate the liquid or gas flows were a function of the capillary inner diameter (which influences strongly the pressure drop). With capillary with an inner diameter of 25 μm or more, a pressure of 5 b was employed. For capillaries having a diameter below this limit, a pressure of 10 b was used.

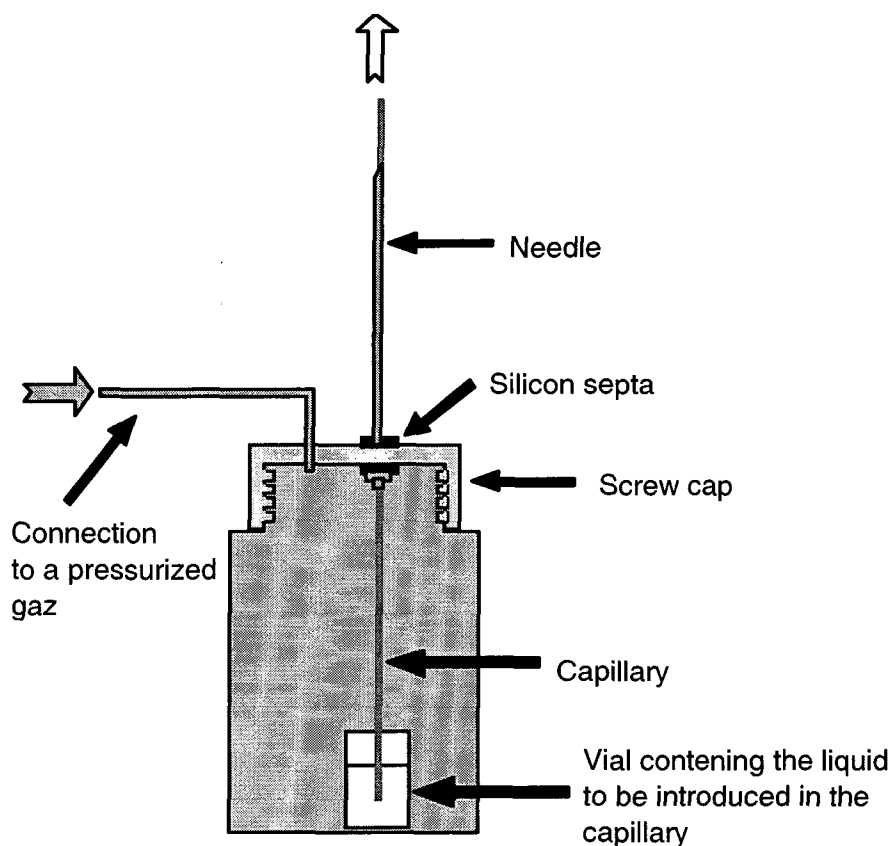


Fig. 3.1: Custom set-up to fill the capillaries with liquids or gas.

Etching of the silica wall surface.

Etching was primarily carried out according to the procedure suggested by Onuska and co-workers [78]. Before the etching step, the etching reagent was deposited into the capillaries. This deposition was performed by the injection of a saturated methanol solution of NH_5F_2 into the capillaries, which was allowed to stand for 1 h. Afterwards the liquid contained in capillaries was sucked out and capillaries were left to dry until a milky film appeared on the capillary wall.

The silanol density was observed to have a marked effect on the deposition of the NH_5F_2 . The growth of a NH_5F_2 layer is not observed in untreated capillaries (Fig. 3.2) while it occurs in capillaries submitted to a conditioning aimed at increasing the silanol group density. An interaction might occur between the silanol groups and NH_5F_2 .

It was observed that the coating obtained by Onuska's approach gives NH_5F_2 layers having a heterogeneous distribution inside the capillaries (Fig. 3.3). The thickness of NH_5F_2 layers decreases from the inlet to the outlet of the capillary, and almost no coating can be seen at the outlet if the capillary length exceeds 100 cm. The coated area of such capillaries exhibit large structures made of NH_5F_2 (Fig. 3.4).

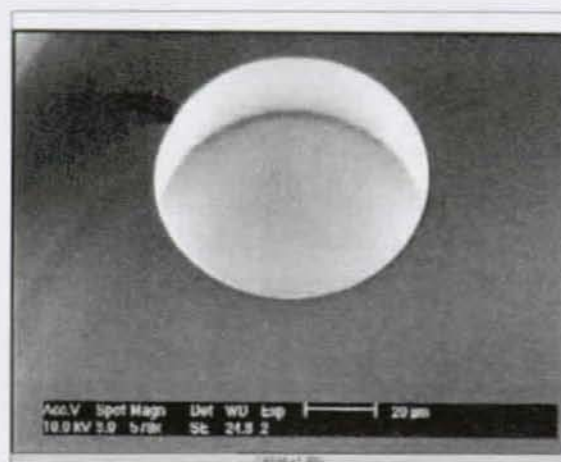


Fig. 3.2: Capillary wall after the NH_5F_2 coating procedure on a naked capillary. (Scanning electronic microphotograph (SEM). Magnification $\times 579$, bar scale: 20 μm)

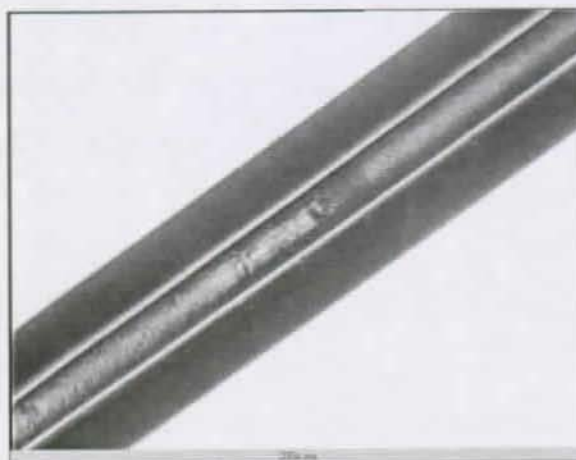


Fig. 3.3: Inhomogeneous layer of NH_5F_2 in a capillary.
(Optical microscopy $\times 100$, partial dark field)

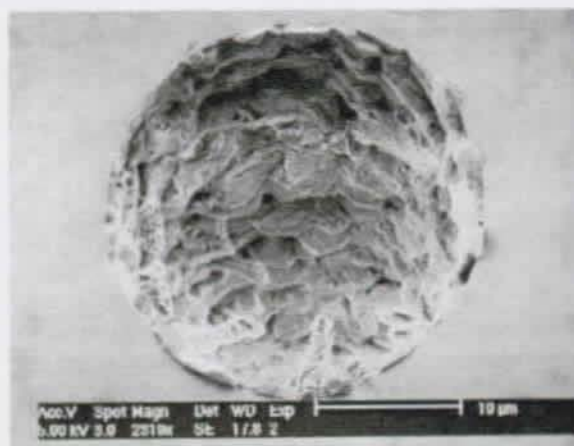


Fig. 3.4: Layer of NH_5F_2 .
(SEM picture $\times 2919$, bar scale: 10 μm)

Another drawback of the coating with methanol as a solvent is the frequent plugging of the capillaries observed when the liquid is aspirated out. During this step, the flow within capillaries breaks the thick layer of NH_5F_2 . The resulting fragments give rise to a plug (Fig. 3.5), especially when capillaries with a small I.D. are used ($< 50 \mu\text{m}$).

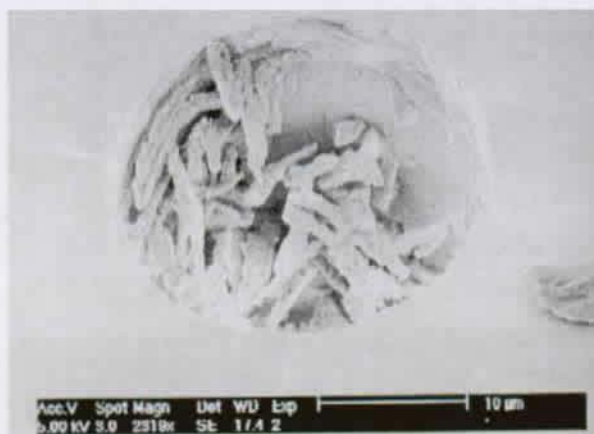


Fig. 3.5: Plug formed by the agglomeration of NH_5F_2 whiskers in a capillary.
(SEM picture $\times 2919$, Bar scale: $10\ \mu\text{m}$)

To improve the homogeneity of the NH_5F_2 layer, different solvents were saturated with NH_5F_2 and their effect on the coating were monitored by SEM. To limit the hydrogen bonding, some aprotic polar organic solvent such as ACN, THF and dioxane were also tested. None of them dissolved NH_5F_2 , or to such a low extent that no coating could be seen. Therefore, protic polar solvents (ethanol, propanol, 2-propanol, butanol and 2-butanol) were tested, even if they were supposed to hydrogen bond with the silanol groups. Ethanol (Fig. 3.6) and 2-propanol (Fig. 3.7) were able to dissolve NH_5F_2 , but the amount of NH_5F_2 deposited on the silica wall was too low to etch the walls.

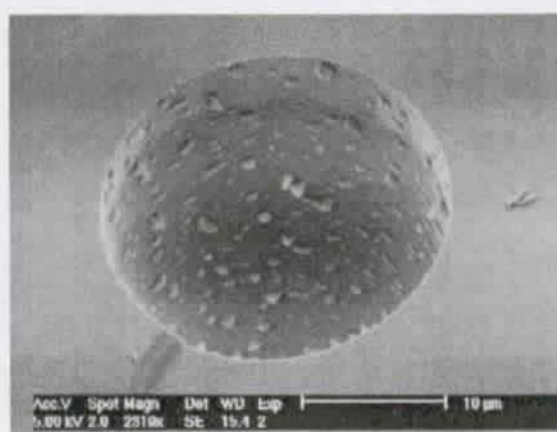


Fig. 3.6: Capillary wall after the NH_5F_2 coating procedure with EtOH as a solvent.
(SEM picture $\times 2919$, bar scale: $10\ \mu\text{m}$)

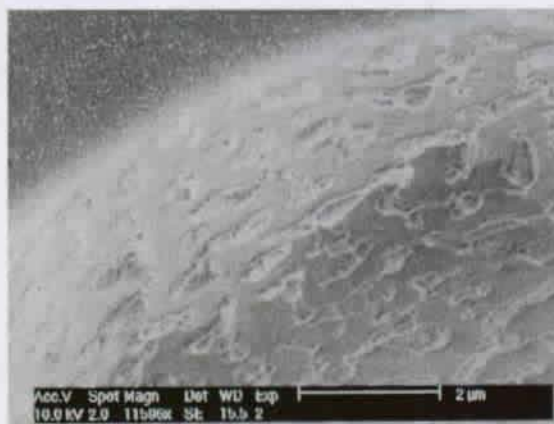


Fig. 3.7: Coverage of NH_5F_2 onto the inner capillary wall using 2-propanol as a solvent.
(SEM picture $\times 11596$. Bar scale: $2 \mu\text{m}$)

To overcome the problems encountered with the deposition method proposed by Onuska, a method aiming to get a thin and uniform coating of NH_5F_2 was developed. This task was achieved by using different mixtures of solvent for NH_5F_2 and a permanent flow for the NH_5F_2 solution.

A solution of MeOH/2-propanol (4:1, v/v) was aspirated with a syringe through capillaries having a maximum length limited to 57 cm for capillaries with an I.D. of $10 \mu\text{m}$. When the liquid reached the other extremity of the capillaries, the aspirating process was reversed (Fig. 3.8). The coating solution was allowed to stay in the capillary for 10 additional min, then argon was aspirated for 10 min. Capillaries were then dried in the vacuum oven (15 min, 35°C , 20 mb) (Fig. 3.9), and their extremities were plugged with silicon septa (used in gas chromatography). Capillaries were then heated (4h, 350°C).

This new method of deposition allows the formation of a homogeneous NH_5F_2 layer within the capillaries by the use of a solution with a reduced concentration of NH_5F_2 and the use of a dynamic flow to deposit the salt.

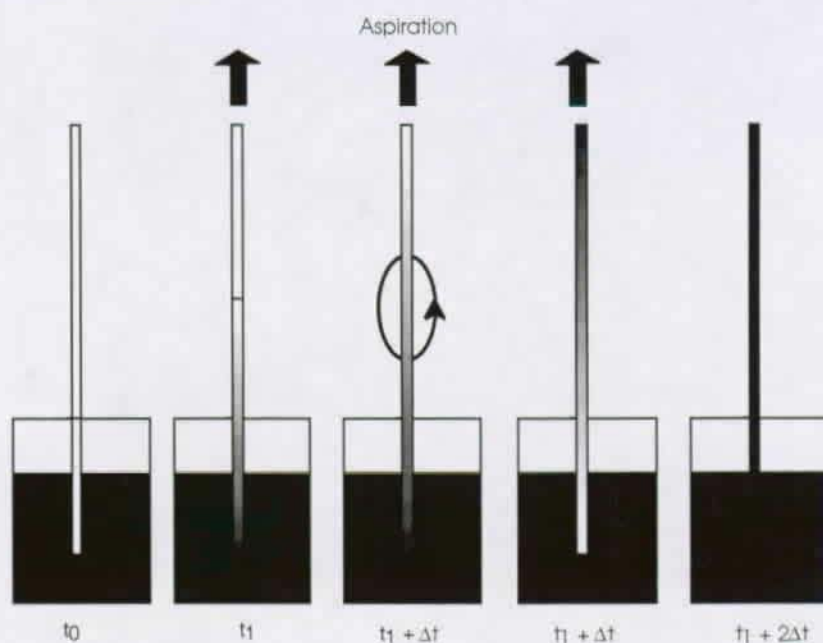


Fig. 3.8: Filling procedure for the NH_5F_2 solution.

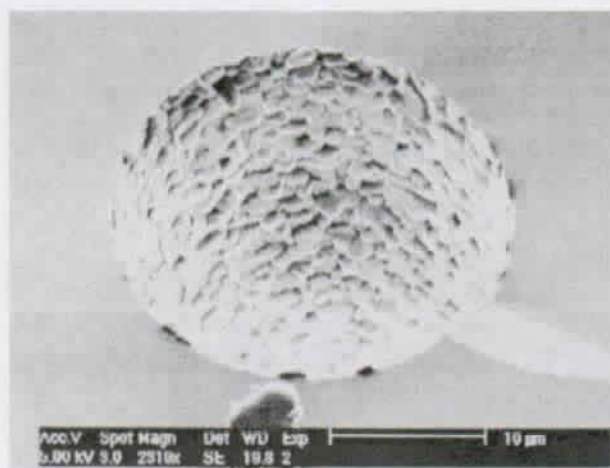


Fig.3.9: Layer of NH_5F_2 after deposition from a saturated 4:1 (v/v) MeOH/Isopropanol solution.
(SEM picture $\times 2919$, bar scale: 10 μm)

It was observed that the roughness of the etched fused silica wall (Fig. 3.10 and 3.11) could be tailored by adjusting the temperature above the temperature where gaseous HF begins to form from the thermal decomposition of NH_5F_2 (230°C) (Fig. 3.12).

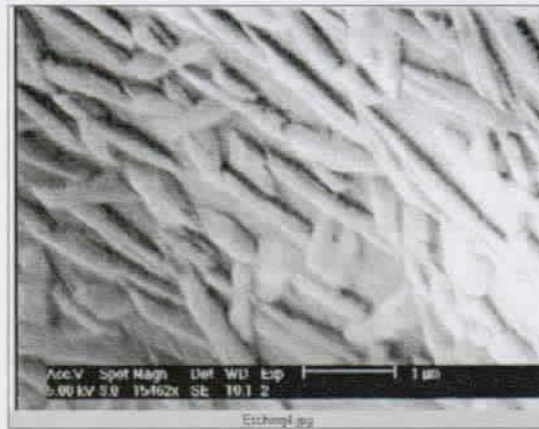


Fig. 3.10: Structure of the silica whiskers after a thermal treatment at 250°C.
(SEM picture $\times 15462$, bar scale: 1 μm)

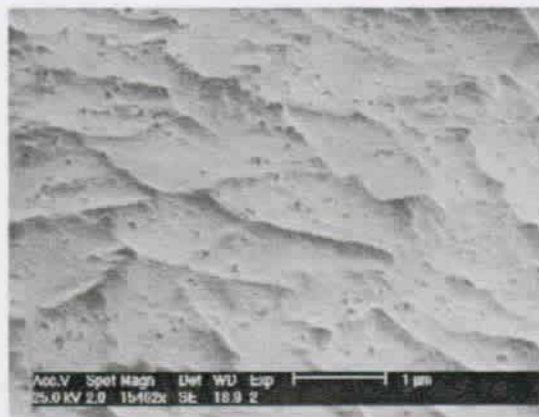


Fig. 3.11: Structure of the silica whiskers after a thermal treatment at 350°C.
(SEM picture $\times 15462$, bar scale: 1 μm)

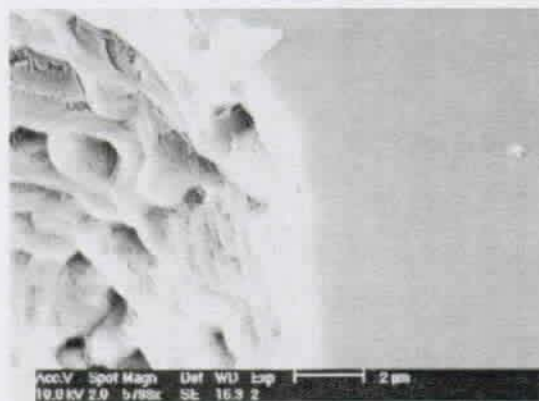


Fig. 3.12: Layer of NH_5F_2 after a thermal treatment during 4 h at 200°C. No vaporisation of NH_5F_2 occurred.
(SEM picture $\times 2919$, bar scale: 10 μm)

To increase the fused silica surface, the highest possible temperature had to be used. 350°C was the upper limit imposed by the necessity to avoid the melting of the silicon septa. After the thermal treatment, the capillaries were unplugged under a chemical hood, and were flushed first with air (15 min, 5 b), then with a solution H₂O/MeOH (2:1, v/v) (15 min, 5 b). Since the etching process reduces the surface density of the silanol groups on the fused silica surface, a hydrolysis step to increase their density was performed afterwards as described previously.

Deposition of a porous layer of silica.

565 µL of EtOH were added in an Eppendorf to 1000 µL of tetraethoxysilane (TEOS). The solution was vortexed for 30 s, then 112 µL of distilled water and 17 µL of an aqueous solution of HCl (10⁻¹ M) were added. The solution was vortexed for 6 h (900 RPM), then EtOH and HCl were evaporated in a vacuum (2h, 25°C, 600 mb). 1 mL of dichloromethane (CH₂Cl₂) was added to the polysiloxane solution. Drops of hexane were added while the solution was kept under constant agitation (50 RPM) until the polysiloxane started to precipitate from the solution. The precipitate was then dissolved by adding a few more drops of CH₂Cl₂. Capillaries were flushed with the solution (10 min, 5 b), then with argon (10 min, 1b). Capillaries were dried in the vacuum oven (35°C, 5h, 20 mb). Capillaries were then filled with an aqueous solution of NH₄OH (0,2 M) and their extremities were plugged. The solution was allowed to react for 1h. Then the solution was flushed out of the capillaries with distilled water (15 min, 5 b), and with argon (10 min, 5 b). Capillaries were then dried in the vacuum oven (12h, 35°C, 20 mb) prior to the preparation of the stationary phase. As a result a porous layer of silica was obtained (Fig. 3.13).



*Fig. 3.13: Porous silica layer at the surface of the inner capillary wall.
(SEM picture $\times 5798$, bar scale: $2 \mu\text{m}$)*

Organosilanization:

The most common approach involves dimethylalkylchlorosilanes, as pointed out by Montes et al. [38]. According to their procedure, dimethyloctylchlorosilane was thus employed as a monofunctional organosilane. Dimethyloctyl-chlorosilane was flushed through the capillaries for 10 min, then the extremities of the capillaries were plugged with silicon septa, and capillaries were heated for 1h at 100°C . A flush with toluene, then with THF (each 10 min, 5 b) was performed afterwards.

Nucleophilic substitution:

Chlorination of the capillary surface. 250 μL of SOCl_2 were dissolved in 2000 μL of toluene. This solution was flushed through the capillaries for 30 min, then their extremities were sealed with silicon septa and heated to 100°C for 16 h [82]. Capillaries were then flushed with argon (10 min, 5 b) and placed in a vacuum oven (4h, 100°C , 20 mb) to completely remove SO_2 and HCl . The oven was then filled with argon and capillaries were plugged at their extremities when not immediately used.

Synthesis of the Grignard reagent. One neck of a 250 mL round-bottomed flask was equipped with a septum, another neck with a West condenser and the third neck with a 100 mL separation funnel. To this flask were added 3 g

of magnesium powder and a magnetic bar. Before initiating the Grignard reaction, the flask was flamed with a burner. During flaming, the flask was purged with argon through the septum port via a syringe needle connected to the end of the argon line. The argon purging was continued throughout the reaction. After cooling the round-bottomed flask, 20 mL of freshly distilled, dry diethyl ether was added. A mixture of 15 mL of 1-chlorooctane in 40 mL of freshly distilled dry diethyl ether was added and incubated for the next 45 min. The temperature of the reaction was kept at 0°C with a water/ice bath. After the complete addition of the alkylbromide ether, the content of the reaction vessel was allowed to mix for an additional 16 h. The condenser and the funnel were removed and replaced with septa. When the last septum was in place, the argon line was removed.

The supernatant of the Grignard reagent was aspirated into a syringe fitted with a 0.22 µm nylon filter. The liquid was injected in the capillaries for the next 10 min, then the capillaries were plugged and allowed to rest for 1 h. The capillaries were then flushed with diethyl ether, followed by EtOH and finally argon (each 10 min). Capillaries were then placed in a vacuum oven and allowed to dry (12 h, 35°C, 20 mb). Grignard reactions were also performed using iodochlorooctane, a more reactive reagent than chlorooctane.

Silylation/Hydrosilylation:

Silylation of the capillary wall. Dimethylchlorosilane was injected into capillaries for 10 min. The capillaries were plugged and allowed to rest for 1 h. Capillaries were then flushed with toluene, THF, and argon (each 10 min, 5 min). Capillaries were then dried in a vacuum oven (12 h, 40°C, 20 mb). A 10⁻² M solution of LiAlH₄ in THF was prepared under dry conditions. This solution was flushed through the chlorinated capillaries for 10 min, then the capillaries were plugged and heated to 60°C for 2 h, and flushed with THF for 15 min. In order to remove the chemisorbed alanes, capillaries were washed 10 min with an aqueous 0.1M HCl solution [41]. Capillaries were flushed with argon for 10 min and dried in the vacuum oven (2 h, 40°C, 20 mb). Capillaries were then filled with argon and stored plugged for hydrosilylation.

Hydrosilylation of the hydrosilanes. A solution of 10 mM hexachloroplatinic acid in 2-propanol was prepared. $\text{H}_2\text{PtCl}_6 \cdot \text{H}_2\text{O}$ being extremely hydrophilic, this catalyst solution was prepared under dry conditions. 2 mL of 1-octadecene were mixed with 70 μL of a 10 mM Spier's catalyst in a micro reaction vial. This solution was heated to 70°C for 1 h, and used to flush the capillary capillaries for 15 min. The extremities of the capillaries were plugged and capillaries were heated to 100°C for 48 h. A flush was then performed, first with hexane, then with THF (both steps 10 min, 5 b). The capillaries were then partially dried with Argon (10 min, 5 b) and further dried in the vacuum oven (12 h, 40°C, 20 mb).

3.4- Results and Discussion.

The observed decreasing thickness in the NH_5F_2 coating with distance can be explained by the chemical reactivity of the silanol groups. As the coating solution migrates into the column, NH_5F_2 is adsorbed onto the capillary wall and the front of the liquid is characterized by an increased alcohol concentration. The silanol groups in this zone can hydrogen bond with MeOH and are thus shielded from any further interaction with the etching reagent. One proof of this shielding effect occurring most probably by hydrogen bonding is the fact that no layer of NH_5F_2 develops in the capillaries when water is used as a solvent, despite the fact that H_2O has a higher solvating power for NH_5F_2 than methanol.

None of the three synthetic procedures used to produce monomeric reversed phases on naked capillaries, on capillaries with an etched inner surface and on capillaries coated with a porous silica layer, gave a useful stationary phase under CEC conditions. If the extremely low amount of the stationary phase is responsible, the retention of the analytes should have been improved by using capillaries with an increased surface. This was not the case, since stationary phases produced after surface enhancement were also unable to separate the PAH mixture. The derivatization of the silanol groups by nucleophilic addition and silanization/organosilanization involve several steps and are cumbersome processes to carry out. The procedures aiming to increase the

contact surface between the two chromatographic phases, the deposition of a porous inert silica layer and the etching of the fused silica surface, are also time consuming steps and require, in the case of the etching procedure, rather drastic conditions. Therefore, an alternative method for stationary phase synthesis had to be found.

4-. The Sol-Gel Technique.

The aim of the work presented in this chapter was to study organosilicate polymers as basis for stationary phases in CEC. The synthesis of such materials is based on the sol-gel technique. The individual influence of the most important factors or chemicals involved in the sol-gel process were studied.

4.1- The Nature of the Catalyst.

Amongst the different reagents involved in the sol synthesis, catalysts are used to overcome the relative chemical inertness of the silicate precursors, which are poorly reactive chemicals in comparison to most other metallo-organic precursors of the early transition metals [48]. Every chemically bonded silicon possesses a partial positive electrical charge due to the polarization of the bonds with its ligands. The chemical reactivity of the silica precursors and silica oligomers can be enhanced by the use of two types of catalysts: electrophilic catalysts and nucleophilic catalysts. These catalysts act in different ways. The first kind of catalyst is able to perform an electrophilic attack on the silicon ligands, whereas the second kind is able to perform a nucleophilic attack on the silicon atoms. Nucleophilic catalysts extend the coordination of the silicon whereas electrophilic catalysts render these atoms more susceptible to a nucleophilic attack by reducing their electron density.

The presence of a catalyst plays a crucial role in the sol-gel process since it allows experimental control over the rate and the extent of both the hydrolysis and the condensation reactions. This determines the concentration and the structure of the interacting silica precursors and oligomers. The effect of the catalysts is complex, depending not only on their concentration, but also on their reaction mechanisms. The most frequently used catalysts are compounds exhibiting acid or base character, but salts and metal alkoxides such as $\text{Ti}(\text{OEt})_4$ have also been used. Mineral acids, ammonia, alkali metal hydroxides and fluoride anions are the most extensively used catalysts. At the

beginning of the sol-gel process, the rates of hydrolysis and condensation are known to be linearly proportional to the concentration of hydronium or hydroxyl ions present in solution when mineral acids or ammonia are used [36, 83]. These reactions are then acid and base specific and their kinetics are enhanced by increasing the concentration of these catalysts [83]. Since only sols with low viscosities are useful for coating OTC for CEC, mineral acid catalysts were mainly studied.

The chemical reactivity of the silicon atoms depends on the inductive effect of their ligands (the electron donating ability of the silicon ligands increases as follows: $\text{SiO} < \text{HO} < \text{RO} < \text{R}$). The ligands, by their electron donating or withdrawing capacities, affect the electronic distribution of the molecule, which in turn enhances the chemical reactivity of molecular regions. As the sol-gel reaction proceeds, silicon atoms experience different ligands that influence their reactivity. At this point, the outcome of the reaction is determined by the nature of the catalyst. Electrophilic catalysts attack preferentially ligands with a high electronic density. This translates by a preferential hydrolysis of monomers and low branched polymers, while condensation occurs mainly between long linear polymers and the monomers.

Nucleophilic catalysts, such as hydroxide ions, attack preferentially silicon atoms with a low electron density. This corresponds to a hydrolysis on highly branched polycondensates. The hydroxide ion abstracts a proton from a silanol group (Si-OH) producing a silicate (Si-O^-) which in turn attacks another silicon atom. This translates by a preferential condensation of monomers and highly branched polymers having the most acidic silanol groups. By this process, particles grow by a constant condensation of monomers on silica nuclei until equilibrium is reached. This equilibrium depends on the amount of catalyst. At low catalyst concentrations, the negative charges on the particles stabilize the sol by electrostatic repulsions once a certain radius is reached. At high concentration, the repulsion between the particles is overcome and the growth continues by a mechanism of mass transfer appearing between particles with different curvatures (so-called Ostwald ripening [35]).

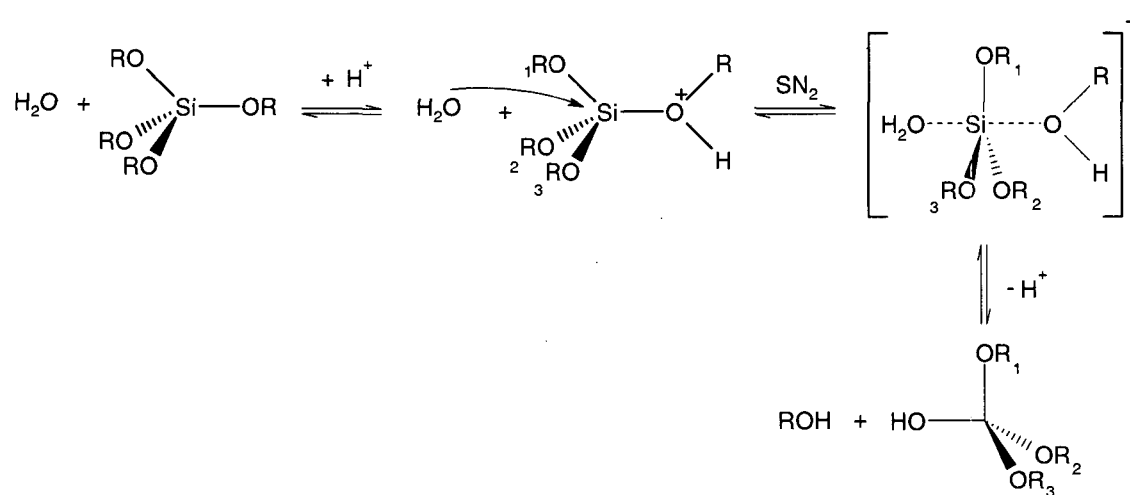
According to these mechanisms, electrophilic catalysts have a hydrolysis rate that is higher than the condensation rate, while the opposite is true for

nucleophilic catalysts. It follows that acid catalysts promote hydrolysis instead of condensation with regards to the condensation while the opposite happens with basic catalysts [62]. As a result, acid catalysts give entangled linear polymers with a less branched structure and a low porosity, while the use of basic catalysts results in highly branched polymers with a high porosity [50]. In the existing literature, the expected properties of the gel are related to both the pH of the sol and to the isoelectric point of the silica. Nevertheless, this simplified approach does not take into account the evolution of the pH with the extent of the condensation [35], and the shift of the silica isoelectric point to higher values in the presence of organosilanes [48 p. 122, 123, 142; 84].

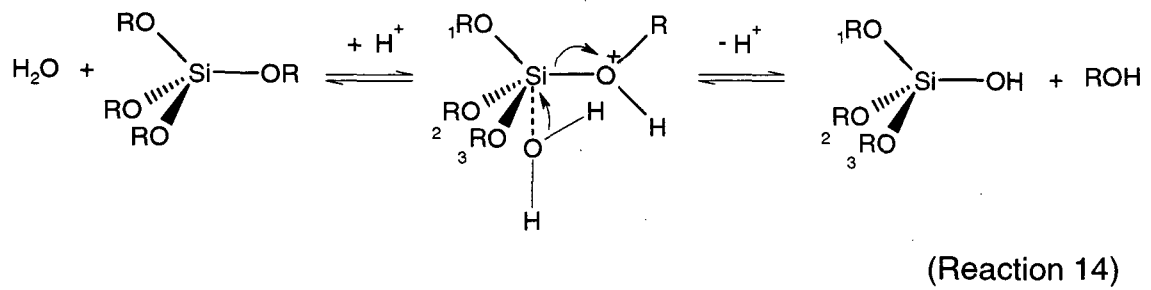
4.2- Effect of the catalyst on the Hydrolysis and Condensation Mechanisms.

Hydrolysis with electrophilic catalysts:

The hydronium ion of mineral acids is the most frequently reported electrophilic catalyst in the sol-gel process. The hydrolysis mechanism with H^+ has been proposed to be either a S_N2 -Si mechanism (reaction 13) or a flank attack of the silicon tetrahedron (reaction 14) [48].

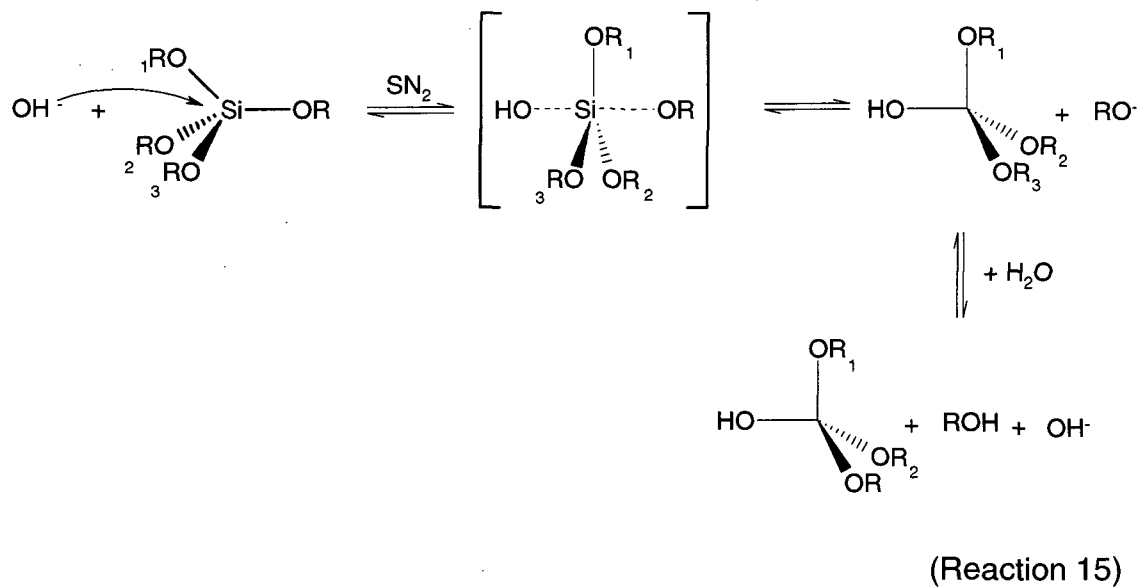


(Reaction 13)

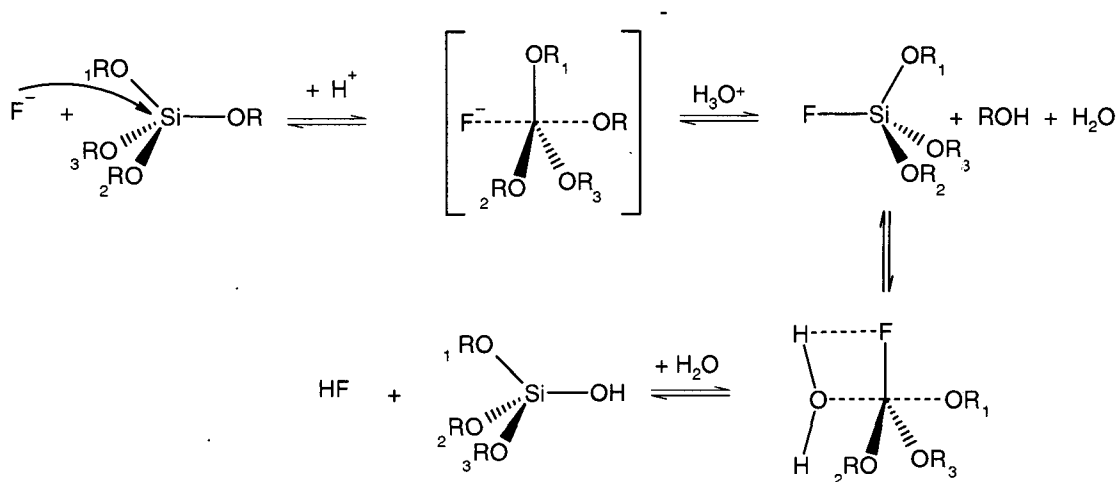


Hydrolysis with nucleophilic catalysts:

The hydroxide ion of NH_4OH is the most frequently reported nucleophilic catalyst in the sol-gel process. A $\text{S}_{\text{N}}2\text{-Si}$ mechanism has been proposed for hydrolysis catalysed by a base, in which -OH displaces -OR with inversion of the silicon tetrahedron (reaction 15) [48].



The fluoride ion is also used as a nucleophilic catalyst in the sol-gel process. The effectiveness of fluoride in the condensation reaction is due to its small ionic radius relative to that of the hydroxyl ion. F^- temporarily increases the coordination of silicon up to 5 or 6 (reaction 16).

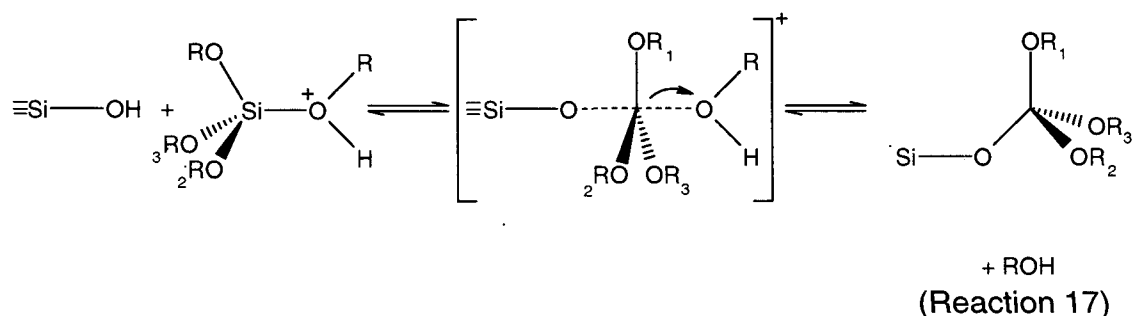


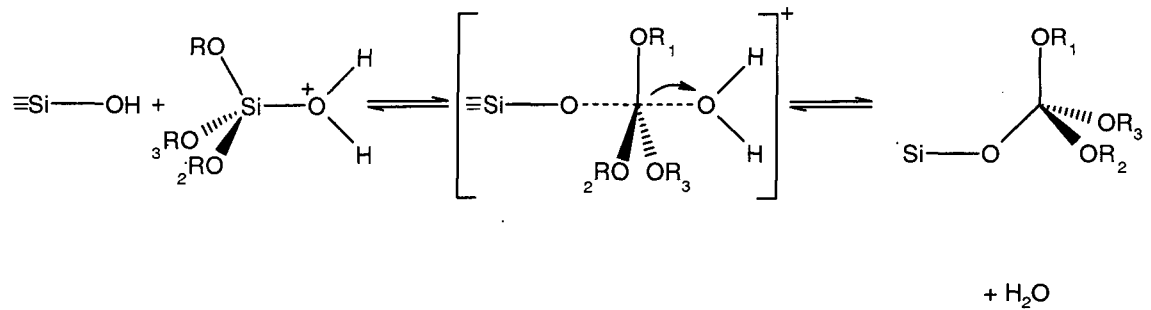
(Reaction 16)

Condensation (oxolation) in the sol-gel process is driven by the formation of an oxo bridge (-O-) between two silicon atoms. This reaction is accompanied by a release of alcohol or water (see reactions 10 and 11). Water produced by condensation is able to react in the hydrolysis of the silicate precursors, and therefore cannot be neglected in the calculations. The amount of water used for sol synthesis affects the degree of condensation. Taking into consideration the by-product water, more linear oligomers are present in the case of $H_r < 100\%$ than in the case of $H_r > 100\%$ (see definition of H_r in paragraph 4.3).

Condensation with electrophilic catalysts:

A S_N2 -Si mechanism has been proposed for condensation catalysed by an acid, in which -OH displaces -OR with inversion of the silicon tetrahedron [48]. This reaction can either produce alcohols (reaction 17) or water (reaction 18).





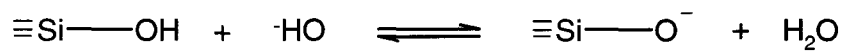
(Reaction 18)

Since reaction 17 is an equilibrium, one has to carefully control the amount of alcohol which cleaves the polysiloxane bonds in the sol.

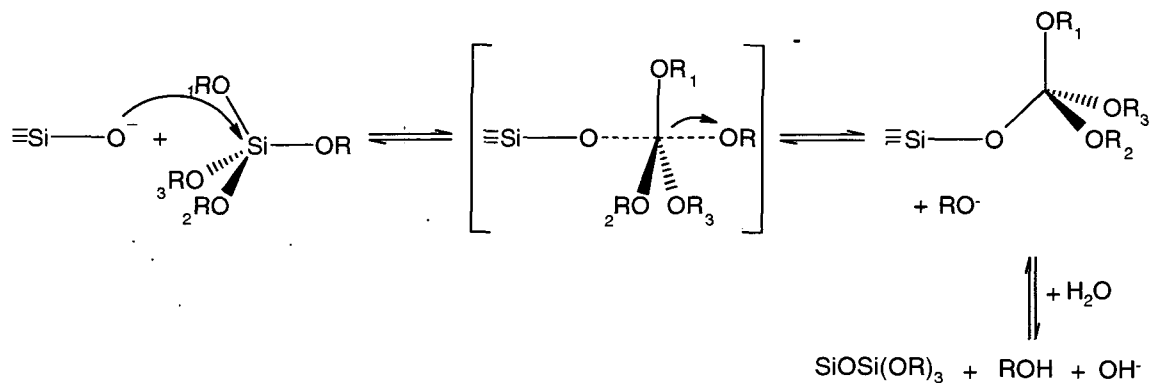
Condensation with nucleophilic catalysts.

A $\text{S}_{\text{N}}2\text{-Si}$ mechanism has been proposed for condensation catalyzed by a base, in which $-\text{OSi}$ displaces $-\text{OR}$ with inversion of the silicon tetrahedron (reaction 19 b) [48].

With NH_4OH as catalyst, this reaction occurs first by a deprotonation of the silanol groups (reaction 19 a).

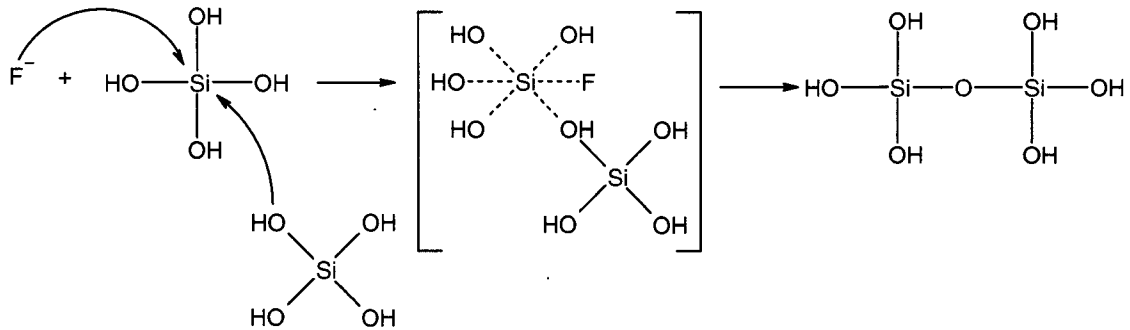


(Reaction 19 a)



(Reaction 19 b)

With fluorine ion as catalyst, an increased valency of the silicon atom to 6 has been proposed (reaction 20):



(Reaction 20)

4.3- Parameters describing the initial constituents of the sol.

Assuming that the water produced by condensation (Reaction 11) can be used for further hydrolysis (Reaction 13, 14 or 15), the quantity of water theoretically needed to achieve total hydrolysis can be calculated by the following relation:

$$n_{\text{H}_2\text{O}} = \frac{1}{2}n_1 + \frac{f_{op}}{2}n_2 \quad (\text{Eq. 4.1})$$

Where $n_{\text{H}_2\text{O}}$ = theoretical quantity of water required to perform the hydrolysis [mol].

n_1 = quantity of TEOS [mol].

n_2 = quantity of organosilicate co-precursor [mol].

f_{op} = functionality of the organosilicate precursor [mol].

In the present work, the volume of water used in the sol-gel process is related to H_r (hydrolysis rate). H_r corresponds to the percentage of the theoretical amount of water needed to perform a complete hydrolysis.

$$V_{\text{H}_2\text{O}} = 18H_r n_{\text{H}_2\text{O}} \quad (\text{Eq. 4.2})$$

Where H_r = molar percentage [%].

$V_{\text{H}_2\text{O}}$ = volume of water.

To define mixtures of silicates precursors for the synthesis of ormosils, the quantity of organosilane is related to the quantity of the TEOS with the ratio R:

$$n_2 = Rn_1 \quad (\text{Eq. 4.3})$$

With R = molar percentage of organosilane [%].

To define the volume of the of co-solvent used in the sol syntheses, a value R_s is defined as follows:

$$V_s = R_s (V_{\text{H}_2\text{O}} + V_{\text{TEOS}} + V_{\text{organo silane}}) \quad (\text{Eq. 4.4})$$

Where R_s = volume percentage of the organic solvent [%].

V_{TEOS} = volume of the tetraalkoxysilane [mL].

$V_{\text{organosilane}}$ = volume of the organosilane [mL].

Throughout this work, "pH" is given as $-\log[\text{HCl}]$ at the beginning of the sol-gel process. Indeed the measured pH, as frequently reported, is ill defined in a non aqueous solution, and the pH changes during the polycondensation reaction [48, p.212]. For all calculations performed, it is supposed that the volume of dissolved catalyst does not change the volume of its solvent.

4.4- The Mutual Solvent.

Silicate and organosilicate precursors are not soluble in water. A mutual solvent, generally an organic solvent, is therefore needed as a reagent in the sol-synthesis to enhance the mutual dissolution of the silicate precursors and

water. To obtain a homogeneous liquid at the beginning of the sol synthesis, it is generally assumed that equal volumes of mutual solvent and polysiloxane precursors permit the dissolution of the water for hydrolysis [85]. In our case, to limit the dilution of the reacting species, only small amounts of mutual solvent were added. As a consequence, two phases were observed at the beginning of the sol synthesis. Since homogeneous liquids were obtained after different period of mixing, the disappearance of the interface between the two phases was used to monitor the extent of the sol-gel process. Indeed, the disappearance of this interface gives an indirect indication of the extent of hydrolysis. It has to be noted that the presence of an interface is also responsible for the observed light scattering effect. This effect results from the light diffraction of soluble entities bigger than the visible light, and can be used in the sol-gel process to monitor the growth of the particles.

The addition of a mutual solvent plays a dual role. It affects the kinetics of hydrolysis by enhancing the probability of contact of the silicate precursors and water, but it also changes the concentration of the reagents involved in the sol synthesis. If alcohols are used as mutual solvents, the amount of siloxane bonds formed is reduced by alcoholysis, the reverse of reaction 10. It is known [86] that the use of alcohol causes incomplete hydrolysis and leads to an equilibrium with remarkable amounts of unhydrolyzed groups.

4.5- Drying of the gel.

After completion of the sol-gel process, solvents have to be removed from the porous polycondensates to obtain a xerogel. During this evaporation step, the volume of the gel shrinks. In the most dramatic cases, the volume can be reduced by a factor of 100 [48]. Syneresis is the term used to describe the phenomena occurring during the drying of gels. Syneresis results from capillary forces throughout the developing porous network during drying. These forces expel actively the liquid from the pores, in addition to the evaporation process. The resulting contraction of the pore volume, amongst other things, puts in close proximity still un-condensed silanol groups. These, borne at the inner pore surface, can then react and the condensation process

can proceed further. This process only stops when the solvent is completely removed.

Drying affects the mechanical resistance of the drying gel. The capillary forces create mechanical stress that migrates towards the bulk of the gel at its liquid-gas interface. If the drying step is performed at such a speed that the forces are not released, the polymer may not be able to withstand the stress and cracks will form. To overcome this major problem encountered in the sol-gel technology, three approaches have been suggested. The first one consists in using polycondensates with a high porosity, thus facilitating solvent evaporation. The second possibility is to produce polycondensates with a low degree of branching. Since such structures possess more degrees of freedom, they can dissipate the mechanical stress more easily. The third approach consists in drying the gel extremely slowly (years) or using supercritical evaporation to avoid any motion of liquid within the porous framework of the polycondensates by avoiding the creation of a liquid gas interface.

The presence of a support also has a marked influence on the formation of cracks in films. The substrate constrains the developing forces and cracking does not occur during drying of thin gel films [48].

4.6- The Particulate Theory.

In the sol-gel process, condensation occurs, up to a certain point, by formation of discrete dense particles called the primary particles. These primary particles can further aggregate into a three dimensional network, the gel. The particulate theory of gel formation was described by Iler in 1955 [35], and was monitored by NMR [87] by Engelhardt and co-workers. These researchers have shown that the sequence of condensation products is monomer, dimer, linear trimer, cyclic trimer, and higher order rings. This sequence of condensation requires at some point both depolymerisation (ring opening) and the availability of monomers which are in solution equilibrium with the oligomeric species and/or are generated by polymerization by the reverse of equations 10 and 11.

The nature of the catalyst affects the solubility of the silica. The solubility is higher with nucleophilic than with electrophilic catalysts [35], and this phenomenon affects the size of the primary particles. For electrophilic catalysts, the growth of the primary particles is stopped by the lack of residual monomers when the particles exceed 2 nm in diameter [35]. These particles aggregate into chains by further condensation, giving linear structures with few branches. The example of a bead necklace is frequently used to describe these structures. When nucleophilic catalysts are used, primary particles grow by a mechanism of dissolution/precipitation. Small particles are dissolved into silica monomers that contribute to the growth of bigger particles by condensation at their surface. This mechanism leads to the formation of macroscopic beads (Fig. 4.1).

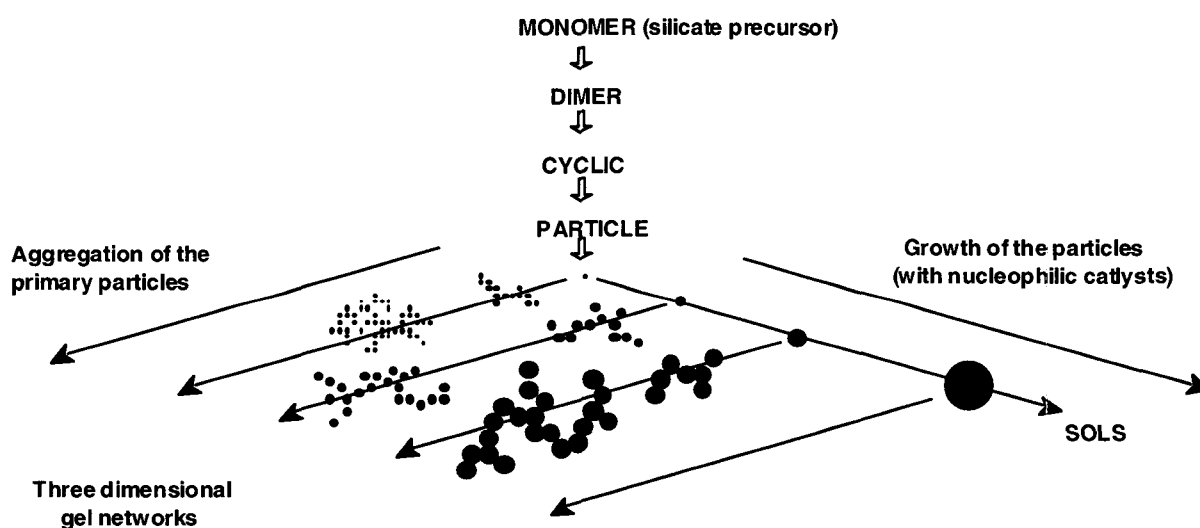


Fig. 4.1: Formation of gels or discrete particles by the sol-gel technique.

5- Investigation of Ormosil Coatings in CEC.

Electrochromatographic separations of PAHs with OTCs, coated with ormosil xerogels containing octyl (C_8) moieties, were achieved in our laboratory. Factors affecting the ormosil coatings were independently studied.

Many of the parameters determining the result of the sol-gel process are interconnected. Variations affecting the amount of a reagent change the concentration of the reactive species, which in turn affects the kinetics of the reactions. Therefore, the studies carried out by varying one extensive parameter independently only indicate some general trends.

5.1- Thickness of the stationary phase.

Two techniques are used to coat capillaries with a sol based material. The techniques differ mainly in the thickness of the resulting coatings. The first technique, called the "static coating" consists in filling first the capillary with the sol. The solvent of the sol is then evaporated under reduced pressure from one extremity of the capillary, the other extremity being plugged [66]. Under these conditions, only the solvent is removed from the column, leaving behind the stationary phase, which is deposited on the capillary wall. The second technique, called the "dynamic coating", consists in flushing the capillary first with the sol, then with an inert gas [54, 72, 88, 89, 90]. This gaseous flush removes most of the sol from the capillary leaving just a thin film of sol on the capillary wall. This technique permits the deposition of a thinner layer of stationary phases than with the static coating. Since the use of thin phases should improve efficiencies (parameter d_f in eq. 2.25), dynamic coating was used in this work unless otherwise mentioned.

The viscosity of the sols is also known to affect the thickness of the stationary phase. Thin phases are obtained by using low viscosity sols (spinnable sols). To this end, sols made of linear polymers in solution are preferable [91]. To maintain the low viscosities of the sols, gelation outside the capillary should be avoided. A second requirement concerns the production of chemical bonds during the coating process. It is known from the work of Yamamoto et al. and

of Sakka et al. that coated films are optimal when chemical bonds between the coating and the support form before bonds within the coating [91, 92]. To fulfil all these conditions, spinnable sols must be used. The spinnable sols used for the coatings contain water ($H_r \approx 100\%$), an acid catalyst (HCl) and low quantities of alcohol. These reagents are known to form sols with elevated concentrations of un-reacted silanol groups due to incomplete hydrolysis/condensation reactions [48].

5.2- Stabilisation of the Stationary Phase.

The stationary phase layers obtained via dynamic coating are sensitive to the Rayleigh instability, a phenomenon related to the mechanical instability of liquid films deposited onto the surface of cylindrical tubes [93]. If one considers spinnable sols as liquids, this phenomenon leads to the formation of droplets of ormosil in capillaries that can ultimately result in the plugging of the OTCs. To prevent this phenomenon to occur, the tearing of the ormosil film must be avoided, i.e. by rapid increase of the sol viscosity. This can be done by a quick gelation, induced by rapid evaporation of the solvent contained in the sol. The evaporation of the sol was then carried out in two steps. First, capillaries filled with a spinnable sol were flushed with argon (5 min, 5 b). In a second step gel-coated columns were completely dried in a vacuum oven (12 h, 35°C, 20 mb) to evaporate the remaining solvent. Uniform coatings, as shown by optical microscopy as in Fig. 5.1, were obtained with this approach. Separations of a PAH mixture can be achieved with such columns (Fig. 5.2).

Xerogels obtained from the deposition, and the in-situ drying of ormosil sol layers within capillaries, give stationary phases resistant to the Rayleigh instability. Since these xerogels are obtained from spinnable sols they are able to react with H_2O , which is a frequent component of the mobile phases in CEC. This reactivity can result in irreproducible electrochromatographic separations due to the change in the nature of the stationary phase.

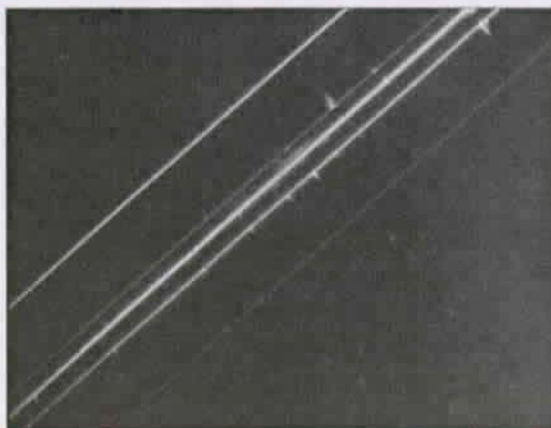


Fig. 5.1: Capillary coated with an ormosil xerogel.
(Optical microscopy $\times 50$, partial black field, visible light)

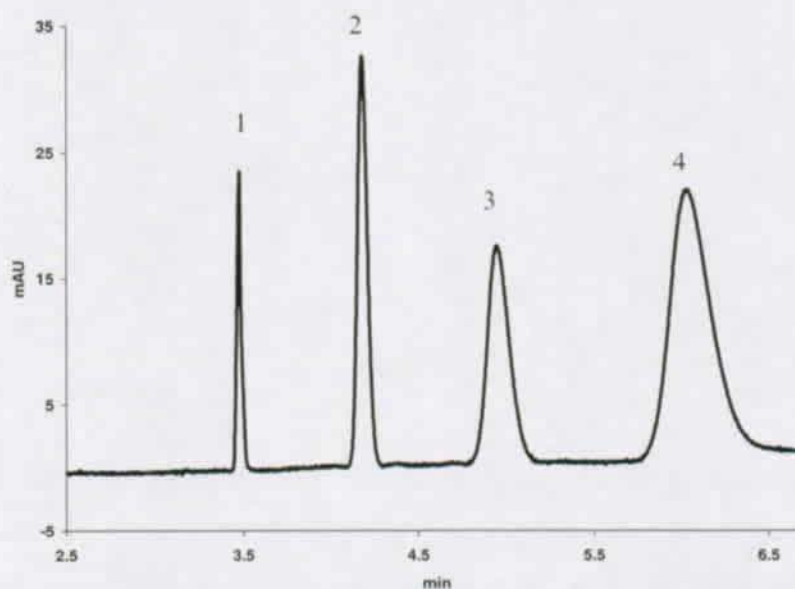


Fig. 5.2: Electrochromatogram showing the separation of the test sample. (1) Acetone, (2) naphthalene, (3) phenanthrene (4) pyrene. Sol made with TEOS, octyltriethoxysilane ($R=40\%$), EtOH ($R_s=30\%$), H_2O ($H_t=100\%$) and HCl (final concentration 10^{-3} M). Capillary 47 cm (40 cm from the injection point to the detection point), I.D. $50 \mu\text{m}$. Mobile phase AACN/ H_2O (1:1, v/v), containing NaCl (2 mM). $E=638$ [V \times cm].

To make the ormosil xerogels less sensitive to the contact with water, hydrolysis/condensation mechanisms must be driven to completion. A chemical stabilisation the stationary phase, obtained by pushing hydrolysis and condensation to completion, is needed. Xerogel coated capillaries were therefore flushed with H_2O (10 min, 3 b) before their first use.

Since these treated columns showed electrochromatograms analogous to the one presented in Fig. 5.2, no modification of the ormosil xerogel structure was evidenced.

The H₂O flush was repeated with sol-coated columns or partially dried gel-columns instead of xerogel coated columns. In this case, the columns were unable to effectuate any electrochromatographic separation of PAHs, as seen in Fig.5.3.

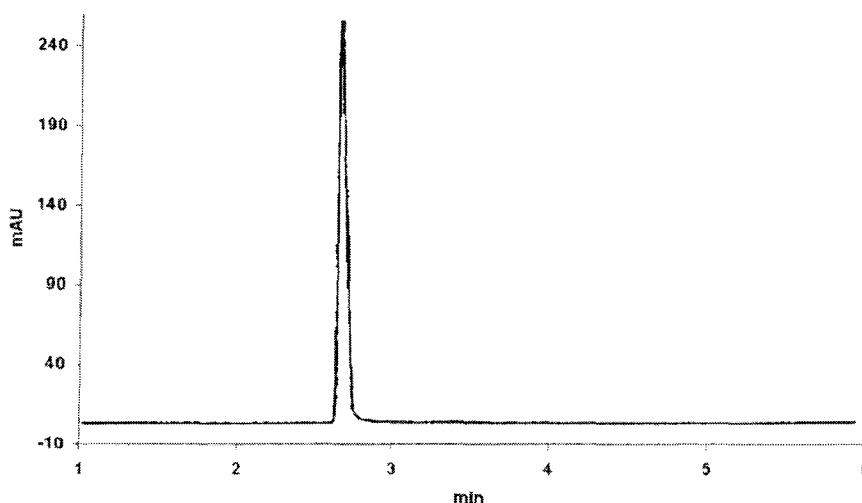
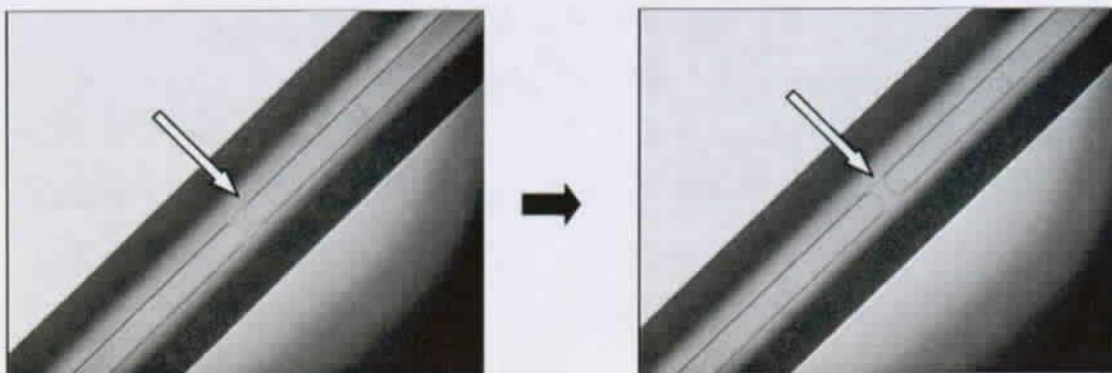


Fig. 5.3: Electrochromatogram of the test sample.

The absence of retention in sol-coated and partially dried gel-coated columns is explained by a removal of the stationary phase from the capillaries during their flushing (Fig. 5.4). Further evidence for this removal is obtained by using sols doped with a fluorescent dye. When liquids are injected into sol-coated or partially dried gel-coated columns, the droplets coming out of the capillaries are fluorescent. Since gelation is theoretically an irreversible process [48], the solubility of the partially dried gels is surprising. The velocity of the gelation process on thin layers can explain this solubility. In this case the linear low-branched chains forming the sol are brought together by the rapid evaporation of the solvent, and there is little time for the formation of crosslinks between the chains. This low degree of crosslinkage may be the cause of the polysilicate redissolution [94].



*Fig. 5.4: Capillary coated with a partially dried gel and filled with ACN/H₂O (1:1, v/v). Droplets of ormosils are formed within the capillaries by Rayleigh instability. This effect is less pronounced when the column is filled with H₂O only.
(Optical microscopy $\times 50$, partial black field, visible light)*

To increase the mechanical resistance of the gel-coated columns to the removal of the stationary phase during the flushing of the capillaries with H₂O, the columns were further dried after the gelation of the sol in a vacuum oven (2 h, 35°C, 20 mb) to obtain a partially dried gel. To further limit the occurrence of the Rayleigh process (Fig. 5.4), a quick crosslinkage of the chain of primary particles still present in the partially dried gel was needed during the H₂O flush. This task was completed by using a catalyst added to H₂O. The nature and the concentration of the catalyst were found to have a marked effect on the structure of the gel surface. To study this influence, drops of spinnable ormosil sols were placed on a microscope slide and then dried, partially (2 h, 35°C, 20 mb), or completely (12 h, 35°C, 20 mb). The layers obtained were thin, the low viscosity of the sol resulting in a good spreading over the flat surface. The effects of different aqueous solutions containing mineral acids and bases were tested on these layers. Their hardness, in particular, was monitored by scratching their surface with a needle. It was observed that basic solutions wrinkled the gel surface whereas acid solutions did not. Aqueous alkaline washes gave densely wrinkled stationary phases on low viscosity gels, but not on dense gels or xerogels, as monitored by the scratching technique. If wrinkling is desired, the alkaline treatment must be performed on a soft gel made from a spinnable sol originally catalysed with a HCl concentration in the range 10^{-2} to $10^{-3.5}$ M. Gels

made with a pH below 2 did not wrinkle. Since these particularly acids gels are known to possess a structure made of highly entangled chains of primary particles [48], their porosity should be low. The low concentration of interconnected pores may limit the diffusion of water and its further use in hydrolysis/condensation processes, and can explain the absence of wrinkling. Aqueous solutions of $\text{OH}^- 10^{-2} \text{ M}$ were found to be the best solutions to harden the gels and to wrinkle their surfaces (Figs. 5.5 and 5.6). NaOH concentrations above 10^{-2} M should not be used in alkaline treatment because they lead to cracking or removal of the stationary phase layer, as observed in Fig. 5.7. The wrinkling of the gel is probably the result of a differential diffusion of OH^- . At the surface of the stationary phase, water and hydroxide ions increase the hardness of the viscous ormosil gel by forming a highly branched and compact polycondensate. The surface is made harder by the formation of a dense network of polysiloxane. The diffusion in this dense network should be reduced, and a gradient of water and the alkaline is formed in the stationary phase [95]. This leads to the development of distortive forces between the hard and shrunken surface and the inner part of the gel, which at that time is still soft. This phenomena gives rise to a wrinkled surface.

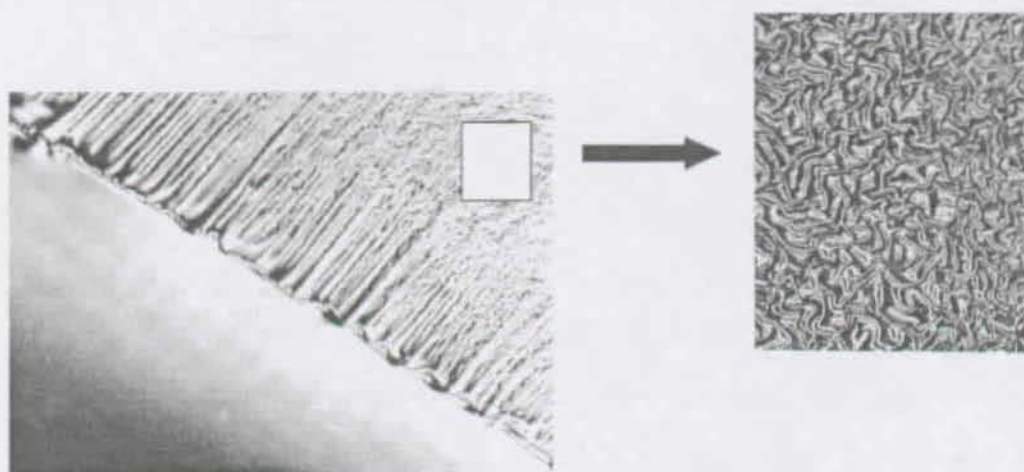


Fig. 5.5: Picture of a partially dried gel where only the upper right half has been treated with a basic wash (10^{-2} M , NaOH, 5 min). Gel: TEOS, octyltriethoxysilane ($R=30\%$), Ethanol ($R_s= 30\%$) H_2O ($H_r=100\%$), HCl (final concentration 10^{-3} M). Alkaline wash NaOH 10^{-2} M 5 min. (Optical microscopy, transmittance mode, partial black field, visible light, magnification: big picture $\times 50$, small picture $\times 100$)

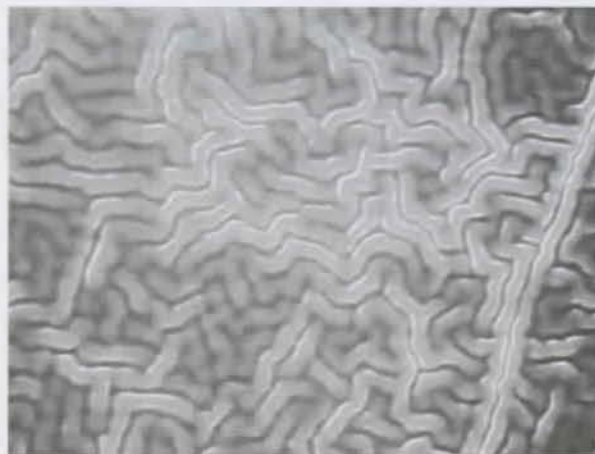


Fig. 5.6: Picture of a partially dried gel made fluorescent by doping the polysiloxane with fluorescein. Gel: TEOS, octyltriethoxysilane ($R=30\%$), ethanol ($R_s=30\%$), H_2O ($H_r=100\%$), HCl (final concentration 10^{-3} M). Alkaline wash NaOH 10^{-2} M 5 min. (Optical microscopy $\times 50$, transmittance mode, UV light)

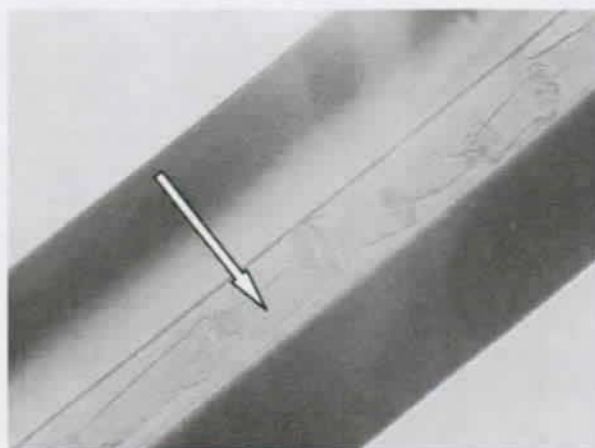


Fig. 5.7: Removal of the stationary phase layer with concentrated hydroxide solution. The tube seen inside the capillary corresponds to the shrunken ormosil coating. (Optical microscopy $\times 100$, transmittance mode, visible light)

The thickness of the stationary phase in a capillary could not be accessed experimentally, because the determination of this value by ellipsometry cannot be done on the convex surface. It is important to note that the thickness of the gels is an important factor in the wrinkling of the gel and may be not the same on the surface of a microscope slide and in a capillary.

While this wrinkling effect is still visible in capillaries (Fig. 5.8), it is less apparent inside the capillary than on a microscope slide.

The Rayleigh instability remains in capillaries as seen in Figs. 5.8 and 5.9 where the coating is not homogeneous, even if the alkaline wash was experimentally shown to limit this phenomenon.

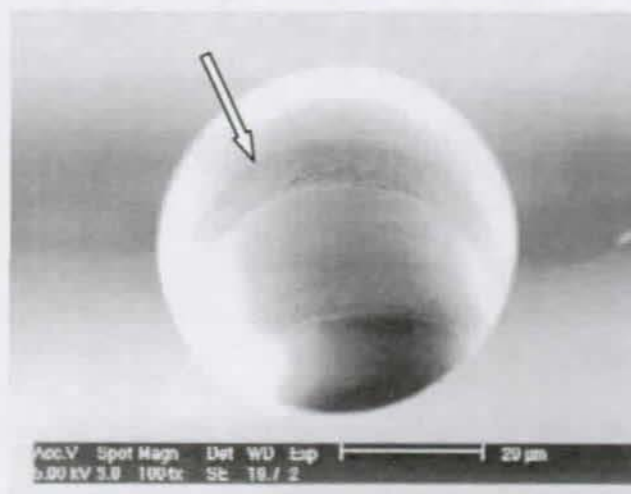


Fig. 5.8: Picture of capillary coated with a xerogel ormosil layer. Gel: TEOS, R=30% octyltriethoxysilane, Ethanol ($R_s=30\%$), H_2O ($H_r=100\%$), HCl (final concentration 10^{-3} M). Alkaline wash NaOH 10^{-2} M 5 min, followed by a drying step (12 h, 35°C , 20 mb) (SEM picture $\times 1004$, bar scale $20\ \mu\text{m}$)

To improve the uniformity of the stationary phase layer inside the capillary, it was found that rough capillary surfaces give a better result than smooth ones. These rough capillary walls are obtained through an etching of the silica with NH_5F_2 (see chapter 3.3). This procedure also reduces the tendency of the stationary phase film to tear as a consequence of the Rayleigh instability; hence a more uniform coating is obtained (Fig. 5.10).

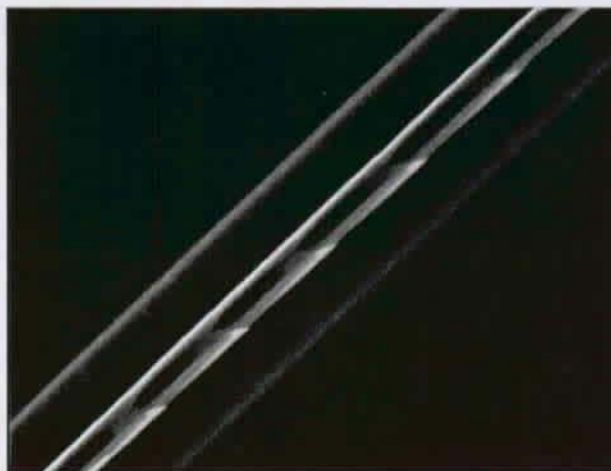


Fig. 5.9: A capillary coated with a xerogel ormosil layer. The layer has been made visible by doping the coating with fluorescein.

Gel: TEOS, octyltriethoxysilane ($R=30\%$), ethanol ($R_s=30\%$), H_2O ($H_r=100\%$), HCl (final concentration 10^{-3} M). Alkaline wash NaOH (10^{-2} M, 5 min), followed by a drying step (12h, 35°C , 20 mb). Wash of the capillary with NaOH (10^{-3} M) to reinforce the fluorescence of the dye.

(Optical microscopy $\times 50$, UV light by transmittance)

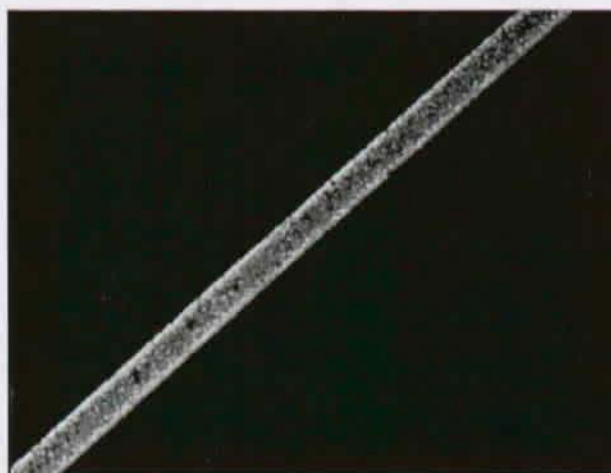


Fig. 5.10: Picture of an etched capillary coated with a xerogel ormosil layer.

The layer has been made visible by doping the coating with fluorescein. Gel: TEOS, octyltriethoxysilane ($R=30\%$), ethanol ($R_s=30\%$), H_2O ($H_r=100\%$), HCl (final concentration 10^{-3} M). Alkaline wash NaOH (10^{-2} M, 5 min), followed by a drying step (12h, 35°C , 20 mb). Wash of the capillary with NaOH (10^{-3} M) to reinforce the fluorescence of the dye.

(Optical microscopy $\times 50$, UV light by transmittance)

Since the alkaline wash was observed to increase the surface of the stationary phase, the chemical stabilization of the gel was carried out by flushing a capillary coated with a partially dried gel (as describe before) with water containing NaOH (10^{-2} M, 5 min, 3 b). The alkaline solution was allowed to stay in the columns for 5 min. The columns were afterwards flushed with argon (10 min, 5 b), then the capillaries were completely dried in a vacuum oven (12 h, 35 °C, 20 mb). This alkaline wash step was found to be mandatory to shorten the time needed to achieve the separation of the component of the test mixture (Fig. 5.11). The reduction of the time needed to achieve the separation of the test sample is clearly evidenced if one compares Figs. 5.11 and 5.2.

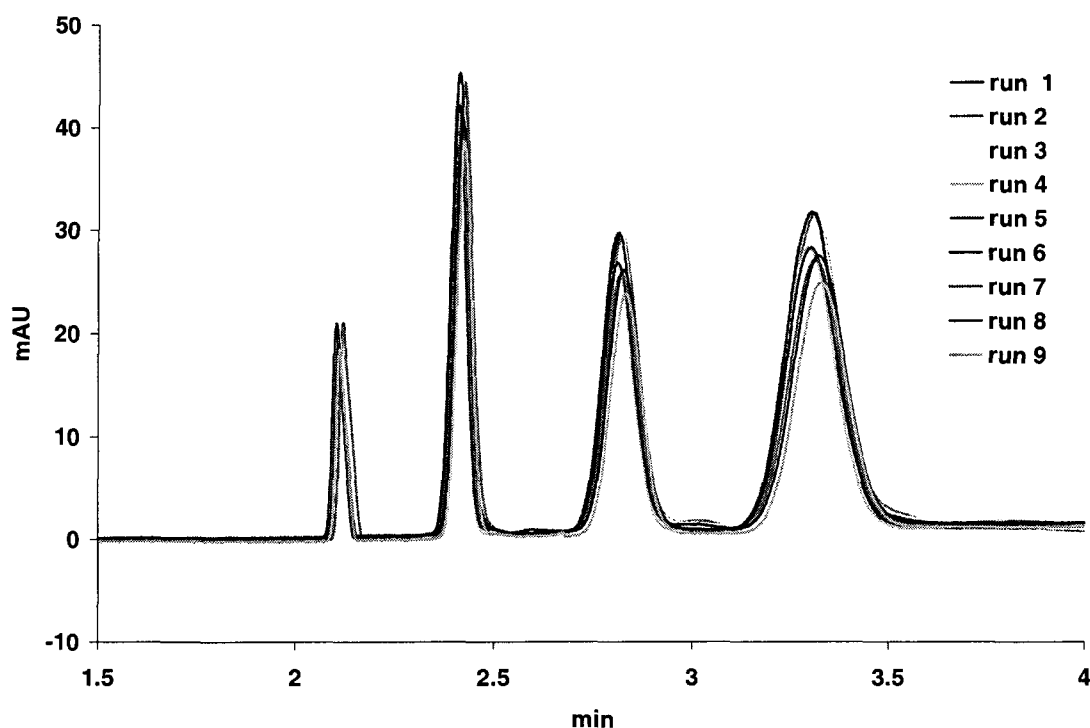


Fig. 5.11: 9 successive electrochromatographic separations of the PAHs mixture. Octyl based stationary phase. Mobile phase ACN/H₂O (1:1, v/v) with NaCl (2 mM).

After the completion of the coating process, it was observed that during the first electroseparation of the PAH mixture, the less retained analytes tended to co-elute. This translated i.e. into an overlapping of the EOF marker and the naphthalene peak. This phenomenon could be avoided by applying a voltage gradient before the first electrochromatographic separation. In addition,

electrochromatograms exhibited peaks for every successive separation with detection times shifted toward higher values. An equilibrium was reached after several separations, but the detection times still tended to fluctuate greatly. To assure reproducible electrochromatograms we found that a conditioning of the OTCs for CEC was mandatory prior to the first separation [95]. This conditioning was performed by flushing the columns coated with the wrinkled ormosil xerogel with an aqueous NaOH solution (10^{-2} M). This step slightly reduce the detection time and ensure reproducibility. Subsequently, throughout this work, OTCs were conditioned prior to their first use or after storage in dry conditions as follows: capillaries were flushed with 10 volumes of an aqueous NaOH solution (10^{-2} M). A flush with the mobile phase was then done (5 min, 1.32 b). A blank run was then performed (10 min, highest voltage bearable for the capillary), followed by another flush with mobile phase (5 min, 1.32 b). The column was equilibrated for 15 min with the mobile phase.

The reproducibility of the separation with the alkaline treatment (see Fig. 5.11) is excellent for the detection times of the analytes ($CV < 0.4\%$, see Table 2). The reproducibility concerning the area of the peaks is less good ($CV > 10\%$, see Table 3), even if the surface of the analytes peaks are normalized by the surface corresponding to the acetone peaks, a chemical used as an internal standard in our case.

	t_r (acetone)	t_r (naphthalene)	t_r (phenanthrene)	t_r (pyrene)
Run 1	2.119	2.421	2.819	3.304
Run 2	2.119	2.423	2.821	3.308
Run 3	2.104	2.410	2.810	3.300
Run 4	2.100	2.408	2.808	3.294
Run 5	2.100	2.406	2.810	3.298
Run 6	2.100	2.408	2.810	3.302
Run 7	2.104	2.416	2.819	3.313
Run 8	2.108	2.417	2.827	3.319
Run 9	2.110	2.421	2.829	3.325
average=	2.107	2.414	2.817	3.307
SD	0.008	0.007	0.008	0.010
CV	0.361%	0.271%	0.280%	0.309%

Table 2: Reproducibility of the electrochromatographic separation of the test sample (after the alkaline wash and the conditioning step, from Fig. 5.5). Parameter studied: detection time of the analytes. SD= Standard deviation; CV= coefficient of variation (see appendix C).

	S (naphthalene)	S (phenanthrene)	S (pyrene)
Run 1	4.537	5.698	10.691
Run 2	4.592	5.798	11.467
Run 3	4.746	5.829	11.187
Run 4	4.310	5.345	10.078
Run 5	4.796	5.959	11.077
Run 6	2.827	3.628	7.577
Run 7	4.499	5.654	10.802
Run 8	4.700	5.900	10.900
Run 9	4.352	5.457	10.042
average=	4.373	5.474	10.425
SD	0.603	0.721	1.168
CV	13.790%	13.166%	11.200%

Table 3: Reproducibility of the electrochromatographic separation of the test sample (after the alkaline wash and the conditioning step, from Fig. 5.5). Parameter studied: area of peaks. The areas have been normalized by the surface of the EOF marker.

Unless otherwise mentioned, the protocol used in this work for the optimization of OTCs for CEC was designed on a two step approach. The aim of the first step was to anchor the stationary phase to the capillary wall. During the second step of the coating process, columns coated with partially dried gels were flushed with an alkaline aqueous solution. This flush, bringing high amounts of water in contact with the stationary phase, should drive both the hydrolysis and the condensation reactions to completion.

5.3- Influence of the Organic Content in the Sol-Synthesis.

To study the effect of the concentration of an organosilane on the feasibility of electrochromatographic separations, ormosil solutions containing different ratios R (TEOS/n-octyltriethoxysilane) with R ranging from 0 to 100%, were prepared. A protocol from the works of Colón et al. was adapted to our use for the coating of the capillaries [54, 72].

Sol syntheses: TEOS, n-octyltriethoxysilane ($0 < R < 100\%$) and EtOH ($R_s = 25\%$) were placed in an Eppendorf. The solution was vortexed (15 s, 2500 RPM). H_2O ($H_r = 100\%$) and HCl (final concentration 10^{-3} M) were added. A permanent vortexing was carried out during 6 h (6 h being the time after which complete hydrolysis was expected [72]).

Coating process: ormosil sols were injected into the capillaries (1 min, 5 b). After 10 min, capillaries were flushed with argon (5 min, 5 b) and then partially dried (2h, 35°C , 20 mb). Afterwards, the coated capillaries were flushed with an aqueous NaOH solution (10^{-2} M, 5 min, 3 b) and then dried overnight (35°C , 20 mb).

Electrochromatography. Coated capillaries were washed with an aqueous NaOH solution 10^{-2} M (5 min, 1.36 b), then with the mobile phase (10 min, 1.36 b). The mobile phase was allowed to stand in the capillary for 1h, then an electric field of 20 kV was applied for 30 min with a initial voltage ramp of $1\text{kV} \times \text{s}^{-1}$. The mobile phase was used to flush the capillary again (5 min, 1.36 b) and a blank run was performed. This last procedure was repeated until flat baseline was obtained. Unless otherwise mentioned in this work, points for the graphs are the average of three experimental results.

Fig. 5.12 shows the influence of the amount of octyltriethoxysilane on the detection time of the test sample components, while Fig. 5.13 shows its influence on the effective plate height, H_e .

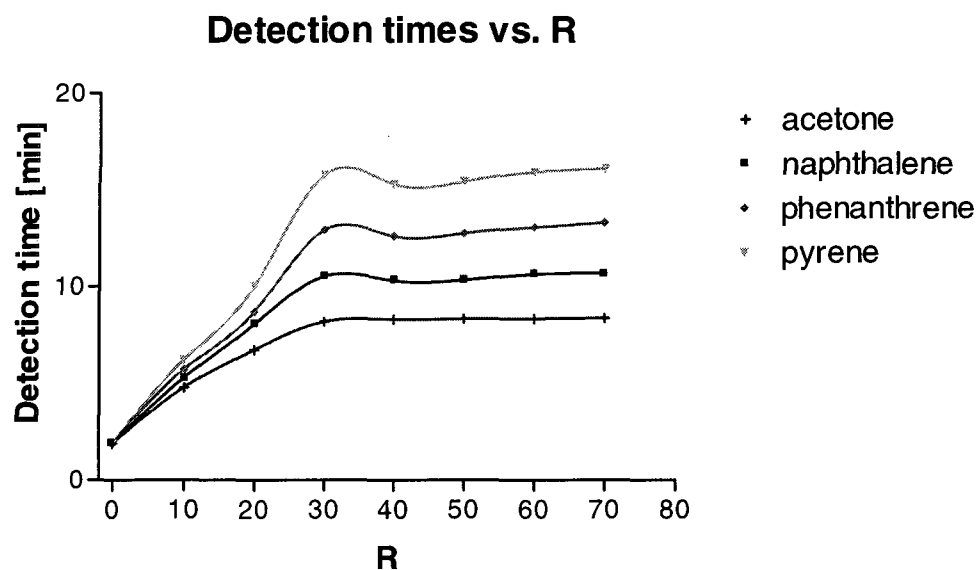


Fig. 5.12: Detection time of the test sample plotted against the amount of organosilane content. Electric field $212.8 \text{ V} \times \text{cm}^{-1}$.

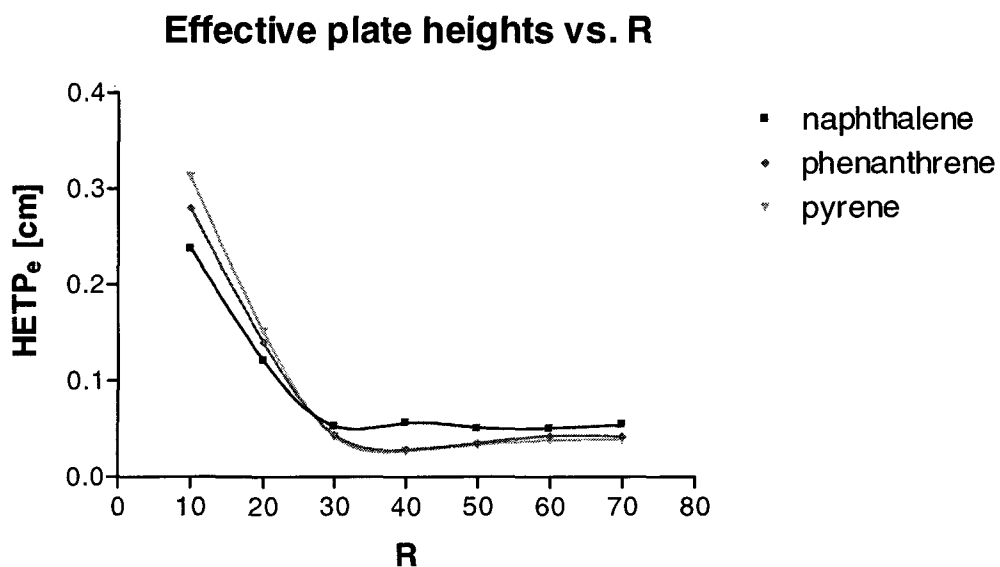


Fig. 5.13: Effective plate height for the three PAHs plotted against the amount of organosilane content. Electric field $212.8 \text{ V} \times \text{cm}^{-1}$.

A coating of pure polysiloxane ($R=0\%$) was shown not to exhibit any selectivity for the components of the test mixture. Coatings containing

between 10 and 70% of n-octyltriethoxysilane allowed electrochromatographic separation of the PAH mixture. In the range $0 < R < 30\%$, the efficiencies of the columns are linearly related to the organic content of the stationary phase while for $30 < R < 70\%$ a plateau is reached. In this last range, surprisingly, a further increase of the n-octyl concentration does not improve the separation. In Fig. 5.12, it is seen that in the range $0 < R < 30\%$ the detection times of the analytes increase as the organic content is increased. If we consider the velocity of the EOF, indicated by the detection time of acetone (the electroosmotic flow marker), the increased detection time may correspond to a decrease in the number of the silanol groups substituted by C_8 groups at the surface of the stationary phase, and hence a corresponding decrease in the EOF.

With $R > 30\%$, the EOF becomes stable. This apparent contradiction of a stable EOF with a presumed further reduction of the silanol groups may arise from a modification of the double layer structure, leading to a more hydrophobic stationary phase. Unless otherwise mentioned in this work an organic content of $R = 40\%$ was subsequently chosen to obtain the highest efficiencies and the highest theoretical amount of silanol groups.

The concentrations of the n-alkyl moieties are limited to $R = 70\%$, by the fact that a phase separation occurs in the sol after 4 h of intensive mixing if higher ratios are used. This prevents the use of such sols as coating solutions. The phase separation may be explained by a non-uniform dispersion of the hydrophobic organosilicates in the hydrophilic silica matrix [51]. This phenomenon may also be invoked to explain the relatively stable efficiencies observed with $30 < R < 70\%$.

5.4- Influence of the Water Content in the Sol Synthesis.

Stationary phases obtained by the two step process should theoretically exhibit the same chromatographic characteristics, regardless of the initial H_r . Nevertheless, as shown below, the water implicated in the sol formation has a marked effect on the chromatographic separation. To study the effect of water on the efficiencies, ormosil solutions containing concentrations of water were prepared with $50 < H_r < 250\%$.

Sol syntheses: TEOS, n-octyltriethoxysilane ($R=40\%$), EtOH ($R_s=25\%$) were vortexed in an Eppendorf (15 s, 2500 RPM). Then H_2O ($50 < H_r < 250\%$) and HCl (final concentration 10^{-3} M) were added. A permanent vortex was carried out during 6 h.

Coating process and electrochromatography: see protocol described in 5.3.

Fig. 5.14 shows the influence of the amount of water on the detection time of the test sample components, while Fig. 5.15 shows its influence on the resolution. Fig. 5.16 exhibits the effective plate height as a function of H_r .

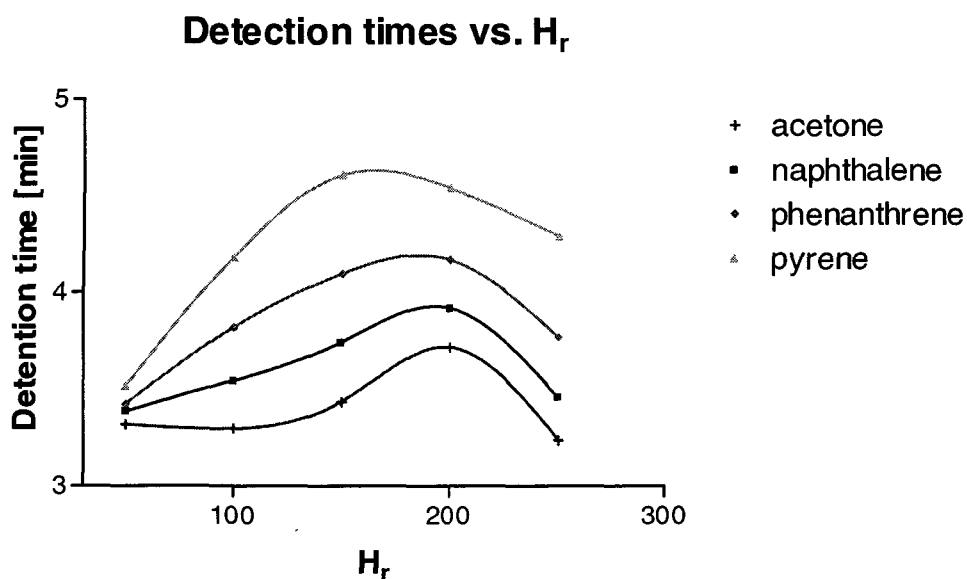


Fig. 5.14: Detection time of the test sample plotted against the amount of water. Applied voltage 425.5 V.cm^{-1} .

From Figs. 5.14, 5.15 and 5.16, it can be deduced that the detection time, the resolution factors and the effective plate heights depend on the quantity of water used. This indicates that the xerogel structure of the stationary phase strongly depends on the sol structure obtained during the first step.

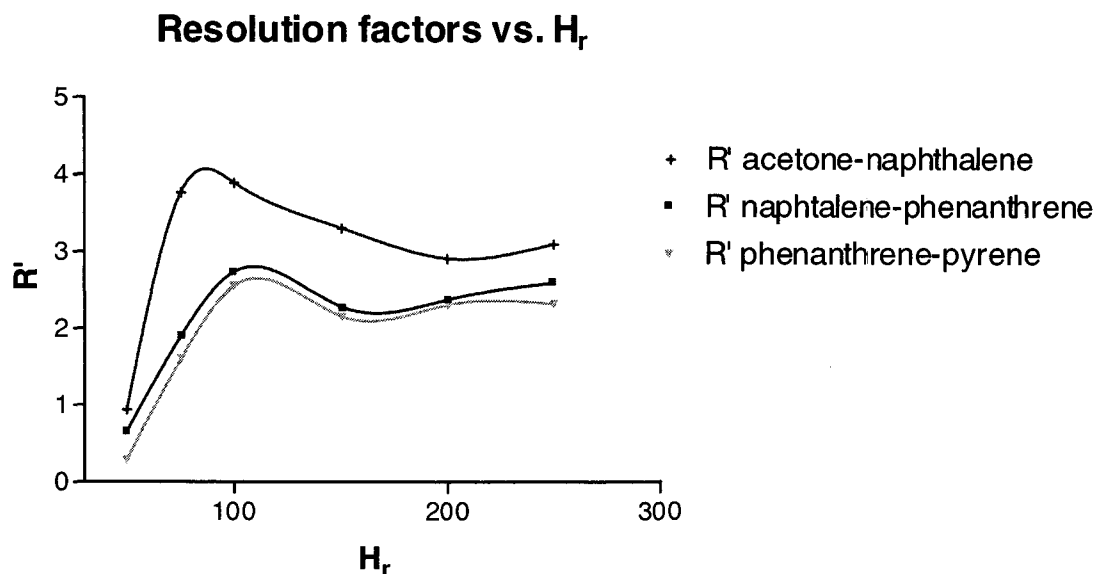


Fig. 5.15: Resolution factor for the three PAHs plotted against the amount of water. Applied voltage $425.5 \text{ V} \times \text{cm}^{-1}$.

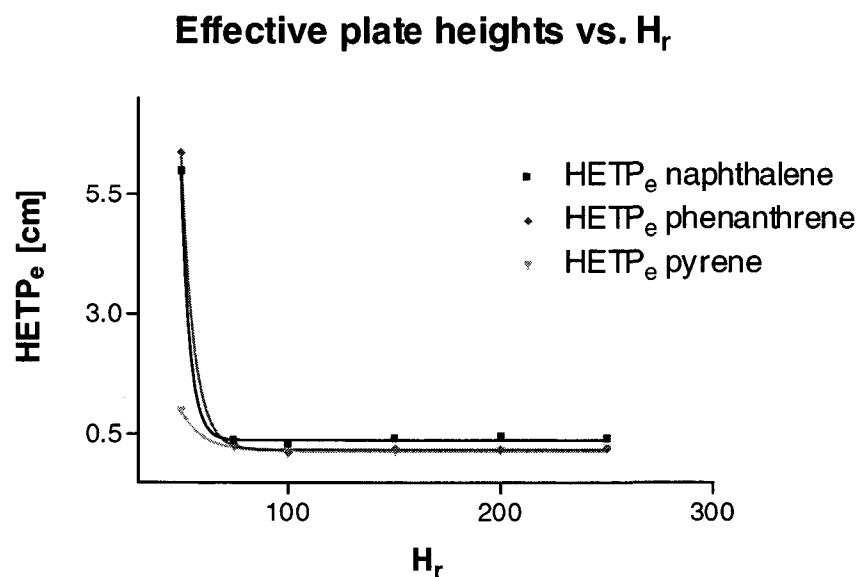


Fig. 5.16: Effective plate height for the three PAHs plotted against the amount of water. Applied voltage $425.5 \text{ V} \times \text{cm}^{-1}$.

In Fig. 5.14, where the detection time is related to the amount of water used in the sol-gel process, one can see that all curves have an optimum. This optimum is shifted towards lower H_r values for analytes with longer detection time. The electroosmotic flow, as shown by the migration time of acetone, is maximal at $H_r = 200\%$. It can be assumed that with this amount of water,

the hydrolysis/condensation process takes place in such a way that the content of silanol groups in the stationary phase is very high. With $H_r=200\%$, the extent of condensation in the sol gel process is then favored.

In Fig. 5.15, it is seen that the resolution factors also show an optimum. The maximum of the curves is obtained for approximately $H_r=100\%$. Higher quantities of water lead to a slight decrease of the resolution. The same effect is seen in Fig.5.16, but to a lesser extent due to the scale of the ordinates. The highest chromatographic efficiencies being obtained with the sols containing amount of water corresponding to $H_r=100\%$, linear low branched particles of sols seem to be required for effective coatings. According to these data, an amount of water corresponding to $H_r=100\%$ is recommended. Unless otherwise mentioned, this ratio was used in this work.

5.5- Influence of the Mutual Solvent in the Sol-Synthesis.

The alcoholic condensation (reaction 10) produces alcohols that affect the mutual solubility of water and alkoxysilicates. Since this reaction occurs during the synthesis of spinnable sols, the initial amount of mutual solvent can be reduced. To initiate this auto production of alcohol, and to limit as much as possible the dilution of the reacting species taking part in the sol formation, small quantities of solvent were added. Methanol, ethanol, 2-propanol, acetonitrile, tetrahydrofuran and dioxane were tested in the synthesis of ormosils, and their efficiencies were monitored via the time required to get a transparent sol.

Sol syntheses: TEOS, n-octyltriethoxysilane ($R=40\%$) and a mutual solvent (methanol, ethanol, 2-propanol, acetonitrile or tetrahydrofuran) ($R_s=25\%$) were vortexed in an Eppendorf (15 s, 2500 RPM). Then H_2O ($H_r=100\%$) and HCl (final concentration 10^{-3} M) were added to the solution. A permanent vortex was carried out during 6 h. The constant solvent volume ($R_s=25\%$) maintains the concentration of reagents constant, regardless of the solvent used.

Coating process and electrochromatography: see protocol described in 5.3.

Alcohols were found to be the best solvents, leading to a transparent sol within 45 min. This observation gives an indirect measurement of the rate of hydrolysis and indicates that this class of compounds is the most effective at enhancing the hydrolysis. One further advantage to use alcohols, is the formation of azeotropes with water. This permits an easy removal of any unreacted water during the drying step.

To study the effect of ethanol on the efficiencies of the separations, coatings were made from sols containing this alcohol at different concentrations ($50 < R_s < 250\%$).

Sol syntheses: TEOS, n-octyltriethoxysilane ($R=40\%$), EtOH ($10 < R_s < 40\%$) were vortexed in an Eppendorf (15 s, 2500 RPM). H_2O ($H_r = 100\%$) and HCl (final concentration 10^{-3} M) were then added to the solution. A permanent vortex was carried out during 6 h.

Coating process and electrochromatography: see protocol described in 5.3.

Fig. 5.17 shows the influence of the amount of alcohol on the detection time of the PAHs while Fig. 5.18 shows its influence on the effective plate height.

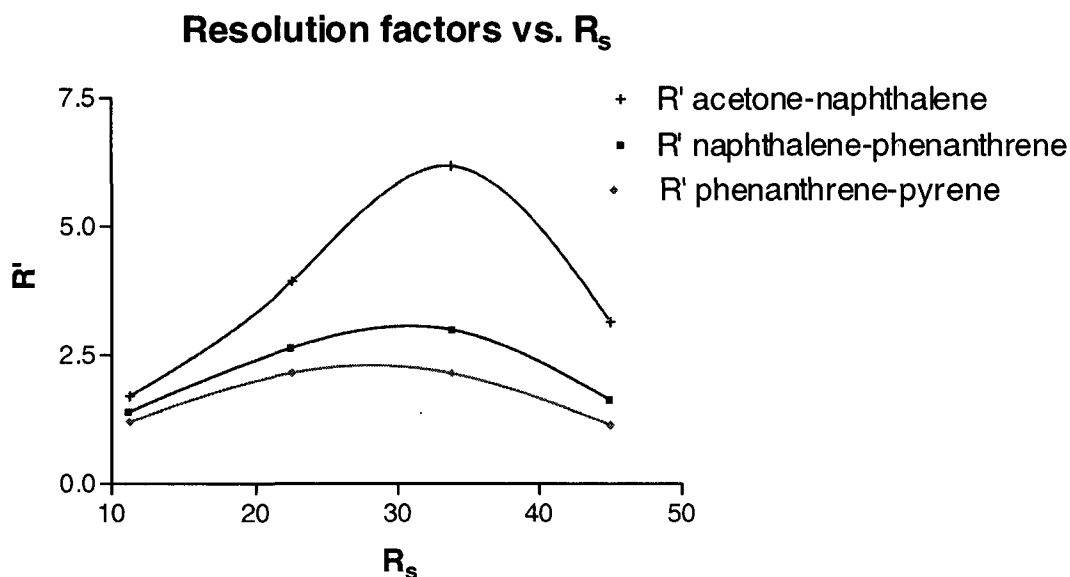


Fig. 5.17: Resolution factor for the test compounds plotted against the amount of ethanol. Applied voltage 638.3 V.cm^{-1} .

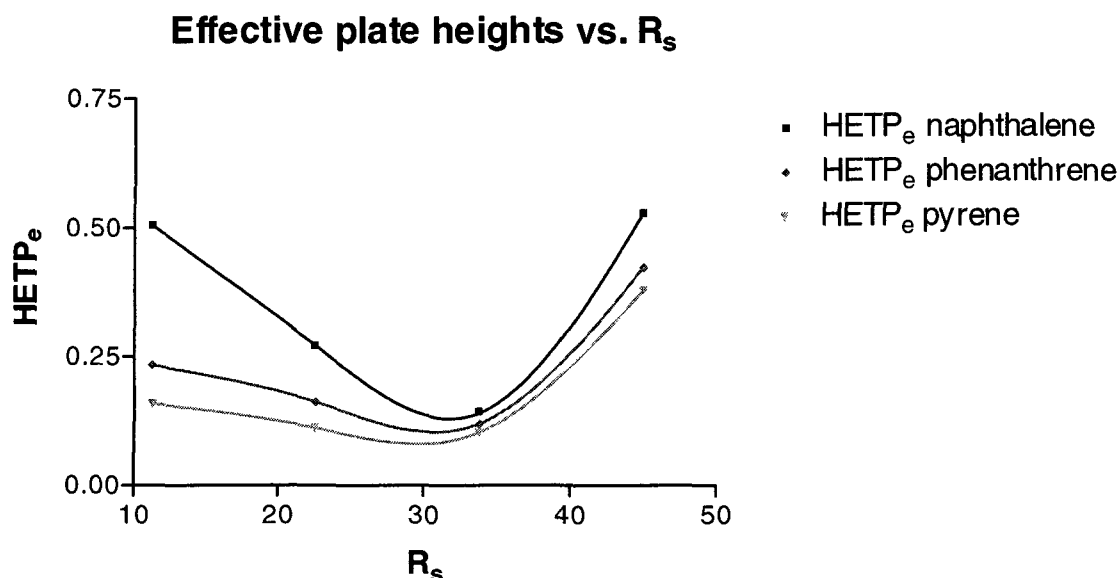


Fig.5.18: Effective plate height for the test compounds plotted against the amount of ethanol. Applied voltage $638.3 \text{ V} \times \text{cm}^{-1}$.

According to Figs. 5.17 and 5.18, the highest efficiency given by the test stationary phase is approximately found at $R_s=30\%$. Therefore, unless otherwise mentioned, this amount of solvent was subsequently used in this work. It has to be noted that the disappearance of the liquid-liquid interface in the first stage of the sol synthesis only occurs when a mutual solvent is used. Without such an addition, a homogeneous liquid is only obtained after days of mixing for the experimental conditions used. Increasing R_s in the range $0 < R_s < 30\%$ leads to a improvement of the electrochromatographic separation. This is explained by the increase of the solubility of the silicate precursors and water, and therefore by an increased probability of contact between these molecules during hydrolysis. When the amount of EtOH is increased above $R_s=30\%$, the efficiency decreases again. This phenomenon can be explained by re-esterification of the silanol groups. The extent of condensation is then lowered, which translates into shorter chain lengths and lower degrees of branching in the primary structure of the ormosils. The highly entangled linear chains of ormosils at $R_s > 30\%$ keep the porosity of the stationary phase very small. This porosity confers a low capacity to the stationary phase.

Another explanation for the decreased efficiency above $R_s=30\%$ is a more efficient removal of water by the formation of an azeotrope in sols containing high amounts of EtOH ($R_s>30\%$). The stationary phase, after the coating of the capillary and its subsequent drying, might be denser than with low amounts of EtOH ($R_s<30\%$). Since the primary structure of the sol affects the stationary phase, this denser structure might affect the capacity. The retention is then modified and lower efficiencies are obtained than with stationary phases made with $R_s=30\%$.

5.6- Influence of the Reaction Time in the Sol Synthesis.

The extent of hydrolysis and condensation affect the structure of the sol and the xerogels used for coatings in OTC-CEC. To study the effect of the sol reaction time on electrochromatographic separations, capillaries were coated with sols reacted for different times.

Sol syntheses: TEOS, n-octyltriethoxysilane ($R=40\%$) and EtOH ($R_s=25\%$) were vortexed in an Eppendorf (15 s, 2500 RPM). Water ($H_r=100\%$) and HCl (final concentration 10^{-3} M) were then added to the solution. A permanent vortex was carried out during period of time ranging from 45 to 420 min.

Coating process and electrochromatography: see protocol described in 5.3.

Columns coated with sols obtained in the range 45-70 min were not capable of separating the sample mixture. Coatings were then performed with sols taken at different reaction times from 90 to 420 min.

Fig. 5.19 shows the influence of the sol reaction time on the resolution factors of the test sample components. Fig. 5.20 shows its influence on the capacity factor.

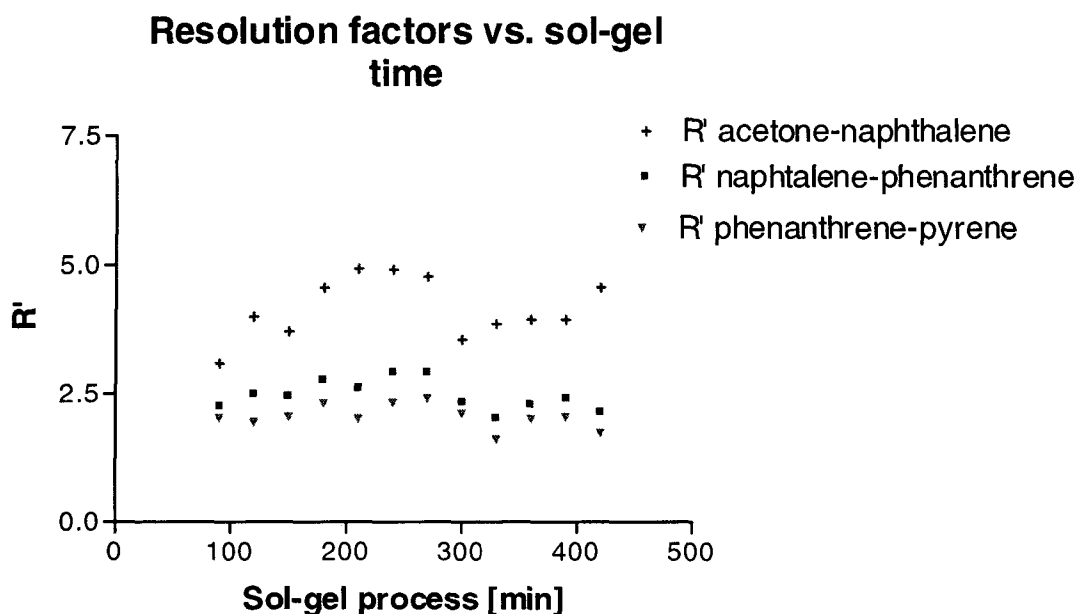


Fig.5.19: Resolution factors for the test compounds plotted against the sol synthesis time. Applied voltage $319.2 \text{ V} \times \text{cm}^{-1}$.

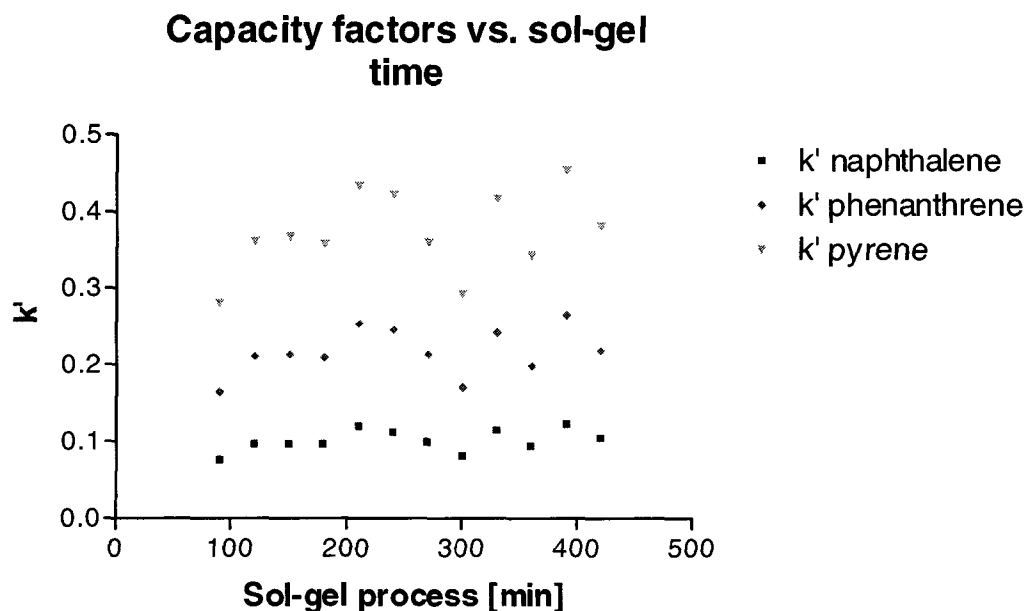


Fig. 5.20: Capacity factors for the test compounds plotted against the sol synthesis time. Applied voltage $319.2 \text{ V} \times \text{cm}^{-1}$.

The relatively constant quality of the stationary phases, observed by us, regardless of the time allowed for the sol reaction, can be explained by the fact that a two step process was applied in this work to coat the capillaries. The partial drying step before the alkaline wash concentrates the unreacted

groups and improves the extent of condensation by syneresis. The completion of the sol-gel reaction should then be quicker in porous, partially dried gels or xerogels than in bulky sols where the reacting compounds are diluted by the presence of the solvents.

In Fig. 5.19, it can be seen that the resolution factors for the analytes are more or less constant over the range of time studied. Fig. 5.20 also shows similar capacity factors for all sample components, even though a large distribution of the points around the average value can be observed. Judging from these results, it can be concluded that a prolonged sol reaction time does not improve the performance of the stationary phase. These results contradict results obtained by Colón et al. who recommended the use of sols reacted for 6 h in a single-step procedure [89]. This group proved, mostly by NMR investigations, that 6 h is mandatory to complete the hydrolysis/condensation scheme of the metalloorganic precursors when $H_r > 100\%$ was used. According to their results, the best resolution factors should be observed for coatings reacted for this amount of time.

In our laboratory, spinnable sols were observed to be stable toward gelation for over two years in absence of evaporation. However, with EtOH and $R_s < 35\%$, the growth of a single silicate monofilament could be observed in the storage vials. This did not affect the separation behaviour of the stationary phases made with the remaining stored ormosil sols (Fig. 5.21).

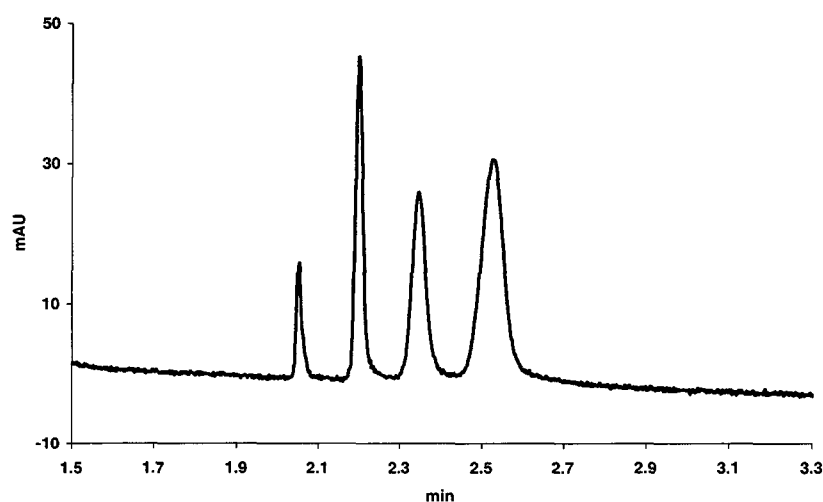


Fig. 5.21: Electrochromatogram of the test sample obtained with a column coated with a one-year-old solution of ormosil. EOF marker thiourea 5 mM. Mobile phase ACN/H₂O (1:1, v/v) containing NaCl (2 mM). Electric field = $638.3 \text{ V} \times \text{cm}^{-1}$.

5.7- Influence of the Catalyst in the Sol Synthesis.

To study the effect of the catalyst on the formation of sols, these latter were synthesised with catalysts of different natures and concentrations.

The use of basic catalysts in the sol-gel technique results, as already mentioned, in the formation of discrete particles (Fig. 5.22). These catalysts do not fulfil the required task proposed in this work and were therefore not investigated.

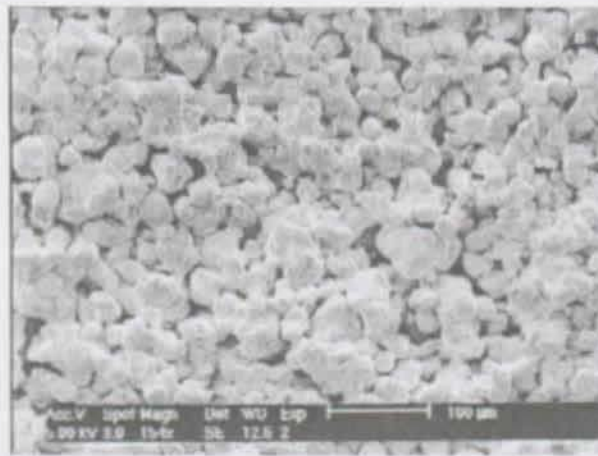


Fig. 5.22: Example of particulate xerogel made with an ormosil sol catalysed with a base. Sol made with TEOS, tetraethoxysilane ($R=40\%$), EtOH ($R_s=40\%$), H_2O ($H_f=200\%$), NH_4OH ($10^{-1}M$). (SEM picture $\times 154$, bar scale $100 \mu m$)

Studies using HCl demonstrate a working range for this catalyst. The lowest concentration limit to get spinnable sols was found to correspond to $pH=4.2$. Below this concentration, no transparent sols are obtained but a white/opaque solution was seen. This may be the result of light scattering of the colloidal microstructure of the sol (Fig. 5.23). In our experimental conditions no upper concentration limit was found for HCl.



Fig. 5.23: Picture of a typical sol obtained with HCl at $\text{pH} > 4.2$. Picture taken after 4 h of mixing.

With a $\text{pH} < 4.2$, no opaqueness was observed. At a macroscopic scale, the solution appeared homogeneous and could be considered as spinnable. Therefore, the concentrations of HCl must be kept above 10^{-4} M to catalyse sols for coatings in CEC. Increasing the HCl concentration reduced the time required to get a homogeneous liquid within the reaction vial. With $[\text{HCl}] = 10^{-3}$ M, the emulsion present at the beginning of the sol-gel process changed to a homogeneous liquid after 45 min. With $[\text{HCl}] = 10^{-1}$ M, the homogeneous liquid was obtained in less than one minute, in this case accompanied by a noticeable heat production. As a first approximation, a ten-time increase of the HCl concentration reduces the time required to obtain a homogeneous liquid by a factor of 4. The time required for the synthesis of the sol can hence be dramatically reduced by using a high concentration of catalyst.

To monitor the influence of the xerogel structure on the electrochromatographic separation of the test sample (Fig. 5.24), a test xerogel was made with a sol catalysed with $[\text{HCl}] = 10^{-1}$ M and EtOH with $R_s = 15\%$ according to the protocol given in 5.3.

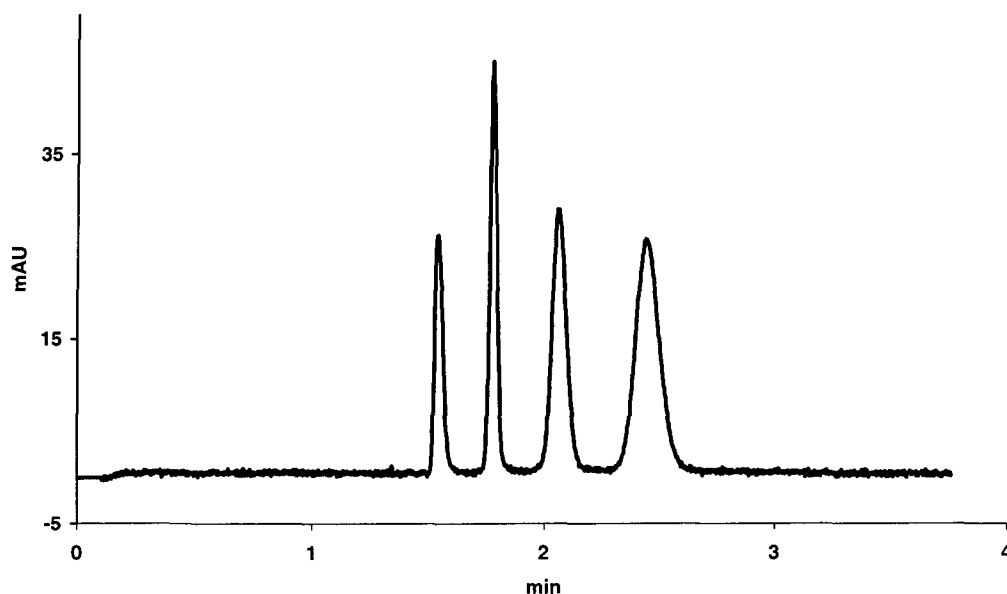


Fig. 5.24: Electrochromatographic separation of the test sample with a sol catalysed with HCl 10^{-1} M. Electric field = $638.3 \text{ V} \times \text{cm}^{-1}$.

The resistance of the ormosil gel surfaces to scratching was more pronounced for gels made from sols containing high concentrations of HCl. The same tendency was observed for the corresponding xerogels. Since an increase in acidity reduces the degree of branching of the polysiloxane, a possible explanation for the improved hardness of the most acid gels could be that the chains made by the condensation of the primary particles are longer. A higher degree of entanglement is then possible, which should strengthen the whole structure of the gel and therefore the structure of the final xerogel.

HCl is used as an electrophilic catalyst in the general protocol proposed here, but the same results were obtained with HNO_3 and H_2SO_4 . These strong mineral acids give spinnable sols when used at concentration above 10^{-4} N. HF at any concentration gave particulate sols as evidenced by measurable opaqueness. This difference can be explained by the presence of the fluoride ion, which catalyses the condensation reaction [83].

Ormosil xerogels made via sols containing high concentration of mineral acid were efficient to separate the test sample. This result is surprising because

the porosity of such phase, therefore its capacity, is theoretically very low. Indeed, it is widely accepted that the acid synthesis of the sols results in the formation of polymers of the short branched linear type, which interpenetrate easily during drying to form dense structures with low surface areas [96]. However, it has been postulated by Menon and co-workers that in a two steps sol-gel synthesis, involving first a highly acid synthesis followed by a basic treatment to complete the hydrolysis, the polymers should be highly branched and not interpenetrate during drying [84]. The gels obtained were proven to possess a colloidal nature and the corresponding particulate xerogels were shown to exhibit a high surface area. This may explain the good resolution obtained in this work.

Increasing the catalyst concentration has a dual effect on the preparation of ormosil sols. The time required for performing the sol-gel process is dramatically reduced and a lower amount of solvent is needed to initiate the process leading to the self-production of co-solvent. $R_s=15\%$ was used for a sol made at pH 1, as shown on Fig. 5.24. The resolution is almost the same as that obtained with the same sol made at pH 3 with $R_s=30\%$, which indicates that the several parameters involved in the sol-gel process are mutually dependent.

5.8- Influence of the Temperature in the Sol Synthesis.

Most chemical reactions are dependent on the temperature. According to the Arrhenius equation, this parameter plays an important role in accelerating the kinetics of chemical reactions. The time taken to complete the sol-gel process should be reduced by increasing the reaction temperature. The effect of temperature on the sol formation was studied in the range of 5 to 200°C.

Sol syntheses: TEOS, n-octyltriethoxysilane ($R=40\%$) and EtOH ($R_s=25\%$) were vortexed in an Eppendorf (15 s, 2500 RPM). Water ($H_r=100\%$) and HCl (final concentration 10^{-3} M) were then added.

Coating process and electrochromatography: see protocol described in 5.3.

Results:

The stationary phases made at temperature in the range 5-40°C showed analogous separations of the test sample shown in Fig. 5.11. Sols prepared at higher temperature (50, 100 and 150°C), were not transparent after 6 h of intensive mixing. At these temperatures, a phase separation was observed with the formation of glassy beads (Fig. 5.25). This phenomenon prevented the use of the sols for coatings, unless one changes the concentration of the mutual solvent (see below).

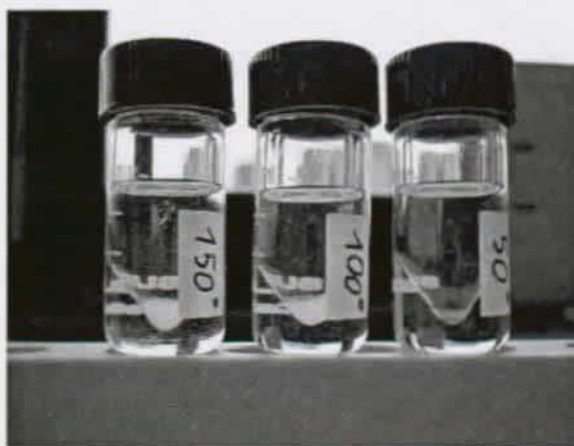
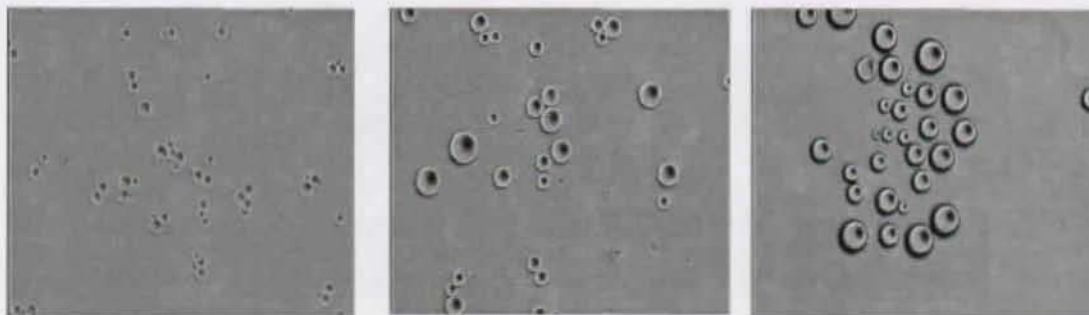


Fig. 5.25: Influence of the temperature on three vials containing the same reagents. The vials were cooled down to room temperature after 6 h. The discrete particles formed precipitated.

Increasing the temperature led to a larger amount of beads, as seen on Fig. 5.25, and to an increased particle size as shown on Fig. 5.26.



*Fig. 5.26: Picture of beads formed at 50, 100 and 150°C.
(Optical microscopy $\times 50$, transmittance mode, partial black field, visible light)*

The formation of beads was only observed with $R_s \leq 23\%$ and with a temperature above 50°C . Since this phenomenon does not occur on sols made at room temperature and reacted over a long period of time (months), it can be thought that the rate of hydrolysis and condensation are differently affected by the temperature. At high temperature, the rate of condensation seems to increase more quickly than the hydrolysis rate.

After a reaction time of 4 h at 50°C , 100°C and 150°C , no further change was seen in the size and the concentration of the beads. Therefore, the mechanism contributing to the growth of the particles should not involve any dissolution/deposition process as observed in Ostwald's ripening. This contradicts the assumption of a mechanism of condensation in acidic medium where condensation occurs between lowly condensed molecules. To explain this phenomenon, one can speculate the role played by pressure in the promotion of the $S_n2\text{-Si}$ transition state. However, even if the pressure is increased above 78°C by a partial vaporisation of EtOH, only the kinetics should be accelerated, giving the same sol regardless of the temperature. It seems, therefore, that the nucleophilic substitution mechanism is replaced by another mechanism at high temperature.

To benefit to the maximum from the accelerated kinetics afforded by an increased temperature, the sol-gel process was performed close to the boiling point of the compound of the initial sol constituents with the highest vapor pressure. The formation of beads was avoided by working with solvent volumes greater than $R_s=23\%$. The sol syntheses were therefore carried out at 80°C and at pH 3 to accelerate sol formation and to obtain a sol without any beads. Heated sols were synthesized as follow: TEOS, octyltriethoxysilane ($R=40\%$) and EtOH ($R_s=30\%$) were placed in a microreaction vial equipped with a magnetic stirrer. The solution was vortexed for 15 s, then H_2O ($H_r=100\%$) and an aqueous HCl solution (final concentration 10^{-3} M) were added. The microreaction vial was capped and heated up to 80°C for 1h with a constant agitation (100 RPM).

The sol obtained was flushed through the capillaries for 10 min (5 b) using the custom-made system. Afterwards, the capillaries were flushed with argon (5 min, 5 b), then the capillaries were dried (30 min, 50°C, 20 mb). Capillaries were then flushed with an aqueous NaOH (10^{-2} M) solution (5 min, 2 b), then capillaries were flushed again with argon (5 min, 3 b). Capillaries were dried in two steps (150°C, 10 min, 500 mb) then (150°C, 20 min, 20 mb). Prior to the first run, coated capillaries were conditioned as follows: capillaries were flushed with a NaOH (10^{-2} M) solution for 3 min, then washed for 10 min with the mobile phase and equilibrated for 30 min. Blank runs were performed until a flat baseline was obtained. A typical electrochromatogram is shown on Fig. 5.27.

Discussion:

Since the stationary phase thickness is related to the original viscosity of the spinnable sol, experiments increasing the viscosity of the sol, were carried out. The sol syntheses were performed in open reaction vials above the boiling point of the co-solvent. The advantages are to kinetically control the reaction, to drive the hydrolysis close to completion, and to control the sol viscosity [97] by an outdistillation of the co-solvent. However, the sols obtained possessed elevated viscosity and their use resulted in the plugging of the capillaries.

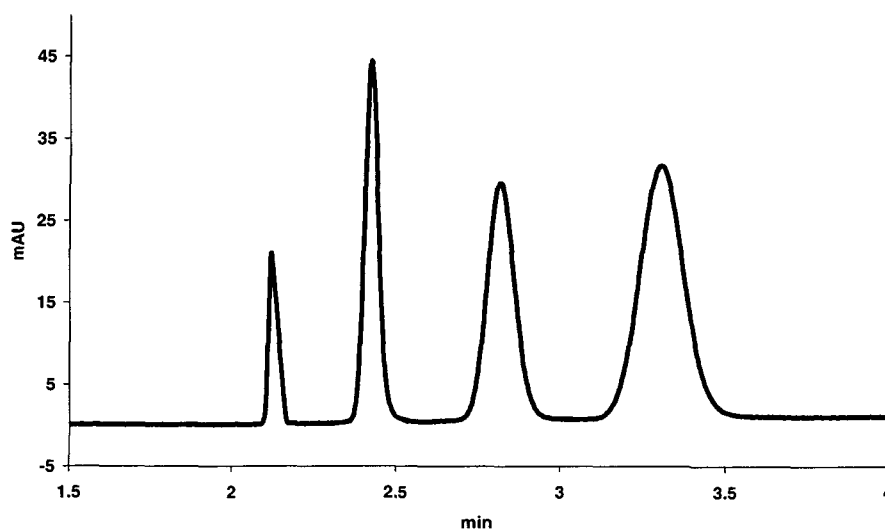


Fig. 5.27: Separation of the test sample. Electric field = $638.3 \text{ V} \times \text{cm}^{-1}$.

Increasing the temperature is an elegant way to reduce the time required for the preparation of sols and gels [98, 99]. This technique is known as the fast sol-gel method [97]. However, special attention has to be paid to the quantity of alcohol used in the sol-gel process to avoid the formation of beads. The temperature and the co-solvent amount are related parameters that both influence the hydrolysis/condensation process.

5.9- Conclusions and Perspectives.

According to the studies described in chapter 5, recommendations can be made for the synthesis of octyl phases for OTCs in CEC. Ethanol should be used as a co-solvent in the sol-gel process. The quantities of the reagents taking part in the sol syntheses should be carefully chosen. Concentrations of octyltriethoxysilane ($R=40\%$), H_2O ($H_r=100\%$), and ethanol ($R_s=30\%$) are recommended.

The process used to make OTCs could be dramatically quickened by increasing the temperature and/or the catalyst concentration in the sols. According to this work, the fabrication of C_8 coated capillary columns for CEC can be done by using one three sol syntheses that differ mostly in their reaction time.

- 10 min. The quickest sol synthesis is obtained with $HCl=10^{-1}$ M. When a dynamic coating is carried out, even the stabilisation of the sols with a basic aqueous solution becomes optional.
- 1 h. The sol synthesis can be performed in 1 h by synthesizing the sol at $80^\circ C$ at pH 3. In this case also, the stabilisation of the sol is optional once the coating is done.
- 6 h. Synthesis of the sols is performed at room temperature at pH 3. An alkaline wash is mandatory to achieve a uniform stationary phase whatever the coating method. In this regard, etched capillaries can be used to obtain more uniform coatings.

The three above approaches to produce OTCs for CEC gave the same separation of a mixture of PAHs. We found that the protocol allowing the synthesis of the sol at pH 1 is then highly recommended in terms of plate height, resolution and retention times [95].

6- Silicates Modified with Different Organic Moieties: Evaluation as Coatings in OTCs - CEC.

In order to increase the number of potential OTC stationary phases for CEC, different silicates modified with different organic moieties were synthesized. The ormosils able to achieve a complete or partial separation of different classes of analytes are presented in this chapter. The precursors of the stationary phase and the analytes can be found in appendix A.

6.1- Alkylsilicates.

Spinnable ormosil sols containing silicates with alkyl chains of different length, ranging from C_6 to C_{16} , were synthesized. The following commercially available metallorganic co-precursors: amytriethoxysilane (C_6), octyltriethoxysilane (C_8), derivatives of octyltriethoxysilane: methyl-octyldimethoxysilane (C_8), dimethyloctylchlorosilane (C_8), and hexadecyl-trimethoxysilane (C_{16}) were used in this context. The non-commercially available alkylsilanes were synthesized in our laboratory by the silanization/hydrosilylation reaction (see chapter 2.4).

The pH plays an important role in the making of alkylsilicates having different alkyl lengths. With alkylsilicates precursors having a linear alkyl chain longer than C_{10} no homogenous sol could be obtained at pH 3 due to a liquid-liquid phase separation occurring during the synthesis of the sol. This phenomenon can be understood by considering a non-homogeneous distribution of the organosilicate precursors in the silica matrix. Due to the difference of polarity between the silicates and the organosilicate precursors, microscopic clusters of molecules sharing the same polarity may be formed. At low pH, the droplets will not have enough time to aggregate by fusion and a rapid condensation will contribute to a uniform grafting of the alkylsilicates on the silica framework. This was indeed observed by synthesizing the sol at pH 1. This low pH circumvents the phase separation and therefore allows the coating of the capillaries. Nevertheless, sols containing alkyl chains longer than C_{10} synthesized at pH 1 turn into a wax after 30 min. The coating

process with such sols should therefore be done before the completion of that time. It was observed that the formation of the wax is a reversible process that is temperature dependent. If the wax is heated to 40°C, a transparent liquid is obtained that can be used again for the coating process.

Amyltriethoxysilane coatings:

Amyltriethoxysilane (C₆) sols were made at pH 1 according to the recommendations given in paragraph 5.9. The coatings were performed with the static method described in paragraph 5.3. Typical electrochromatograms are presented in Figs. 6.1 and 6.2.

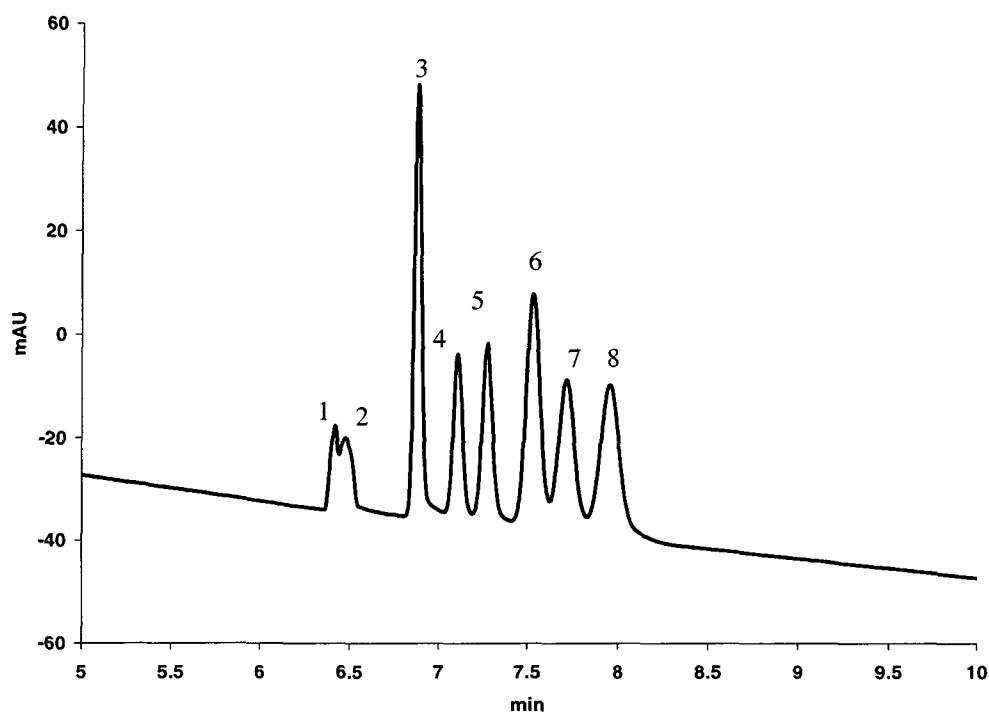


Fig. 6.1: Electrochromatographic separation of a mixture of: (1) DMSO (EOF marker, 30 mM) and resorcinol, (2) acetophenone, (3) naphthalene, (4) fluorene, (5) phenanthrene, (6) pyrene, (7) fluoranthrene, (8) m-terphenyl each 10 mM in ACN. The numbers in brackets correspond to the elution order. Mobile phase ACN/H₂O (1:1, v/v) containing NaCl (2 mM). Capillary 77 cm (70 cm from the injection point to the detection point), I.D. 50 μ m. Hydrodynamic injection 1 s, 1.36 b, applied voltage 30 kV, detection 230 nm.

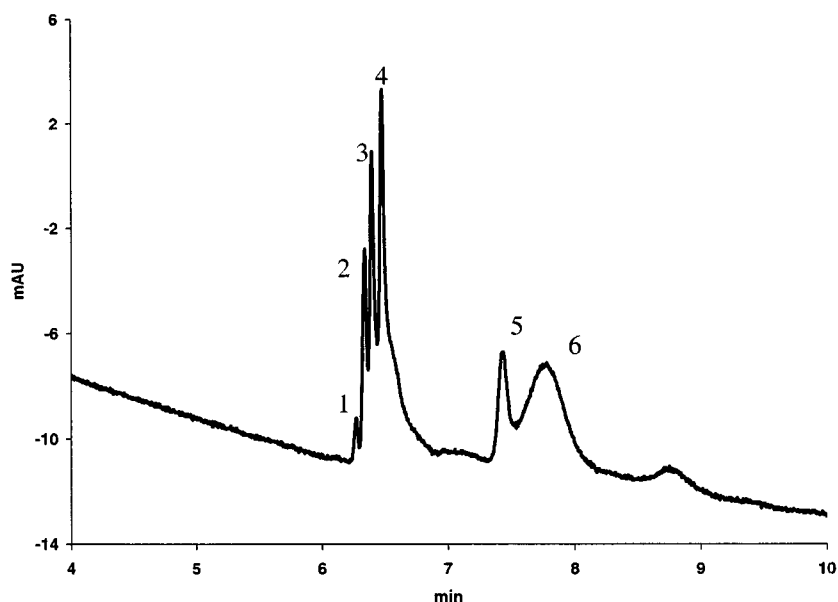


Fig. 6.2: Electrochromatographic separation of a mixture of: (1) DMSO (EOF marker, 30 mM), (2) acetophenone, (3) propiophenone, (4) butyrophenone, (5) n-butylbenzene, (6) 2-acetonaphthone, each 30 mM in ACN. The numbers in brackets correspond to the elution order. Mobile phase ACN/H₂O (1:1, v/v) containing NaCl (2 mM). Capillary 77 cm (70 cm from the injection point to the detection point), I.D. 50 μ m. Hydrodynamic injection 1 s, 1.36 b, applied voltage 30 kV, detection 208 nm.

Octyltriethoxysilane coatings:

Octyltriethoxysilane (C₈) sols were made at pH 1 according to the recommendations given in paragraph 5.9. The coatings were produced with the static method described in paragraph 5.1. Typical electrochromatograms are shown in Figs. 6.3 to 6.6.

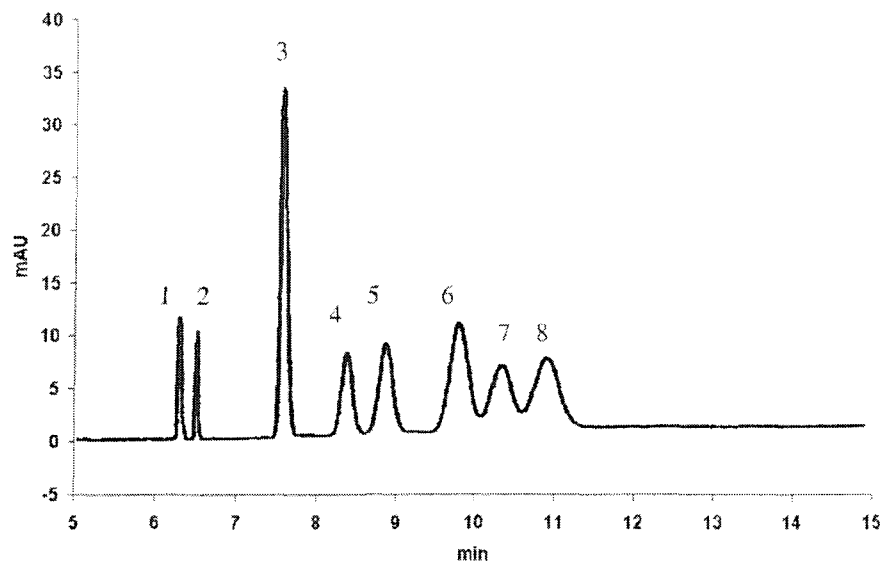


Fig. 6.3: Electrochromatographic separation of a mixture of: (1) DMSO (EOF marker 30 mM) and resorcinol, (2) acetophenone, (3) naphthalene, (4) fluorene, (5) phenanthrene, (6) pyrene, (7) fluoranthrene, (8) *m*-terphenyl each 10 mM in ACN. Mobile phase ACN/H₂O (1:1, v/v) containing NaCl (2 mM). The numbers in brackets correspond to the elution order. Capillary 77 cm (70 cm from the injection point to the detection point), I.D. 50 μ m. Hydrodynamic injection 1 s, 1.36 b, applied voltage 30 kV, detection 230 nm.

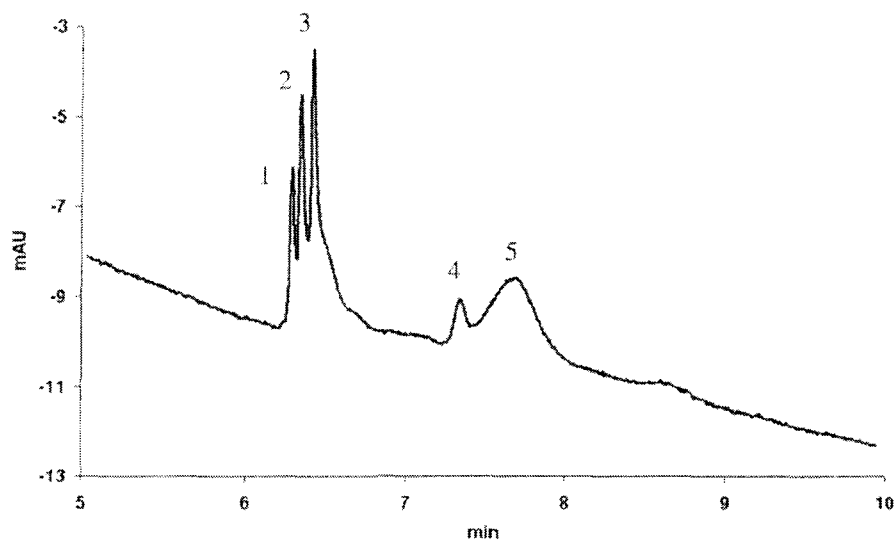


Fig. 6.4: Electrochromatographic separation of a mixture of: (1) acetone (EOF marker) + acetophenone, (2) propiophenone, (3) butyrophenone, (4) *n*-butylbenzene, (5) 2-acetonaphthone, each 30 mM in ACN/acetone (3:2, v/v). Mobile phase ACN/H₂O (1:1, v/v) containing NaCl (2 mM). The numbers in brackets correspond to the elution order. Capillary 77 cm (70 cm from the injection point to the detection point), I.D. 50 μ m. Hydrodynamic injection 1 s, 1.36 b, applied voltage 30 kV, detection 208 nm.

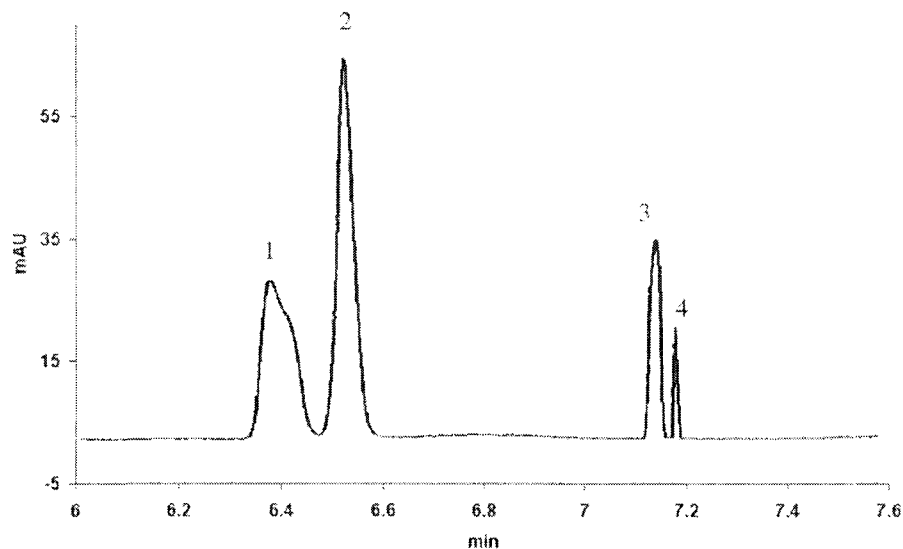


Fig. 6.5: Electrochromatographic separation of a mixture of: (1) DMSO (EOF marker, 30 mM) + hydroquinone + resorcinol + pyrochatechol, (2) 2-naphthol, (3) hydroquinone monomethyl ether, (4) butylbenzene, each 30 mM in ACN. Mobile phase ACN/H₂O (1:1, v/v) containing NaCl (2 mM). The numbers in brackets correspond to the elution order. Capillary 77 cm (70 cm from the injection point to the detection point), I.D. 50 μ m. Hydrodynamic injection 1 s, 1.36 b, applied voltage 30 kV, detection 230 nm.

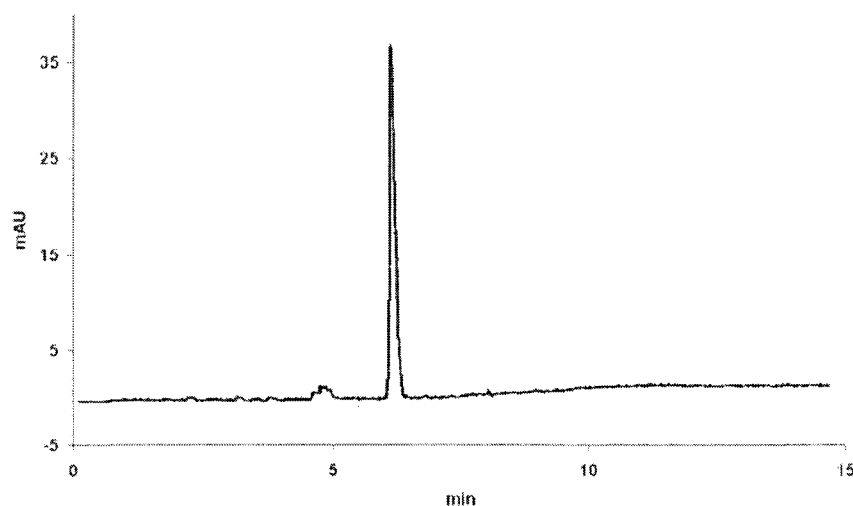


Fig. 6.6: Electrochromatogram of a mixture of tyrosine, phenylalanine and tryptophan 30 mM each in a 20 mM phosphate buffer pH 3. Mobile phase ACN/H₂O (1:1, v/v) containing NaCl (2 mM). Capillary 77 cm (70 cm from the injection point to the detection point), I.D. 50 μ m. Hydrodynamic injection 1 s, 1.36 b, applied voltage 30 kV, detection 208 nm.

Octyltriethoxysilane sols containing KF with an initial concentration of 10^{-3} M were prepared at pH 1 according to the recommendations given in paragraph 5.9. The coatings were produced with the static method described in paragraph 5.1. A typical electrochromatogram is shown in Fig. 6.7.

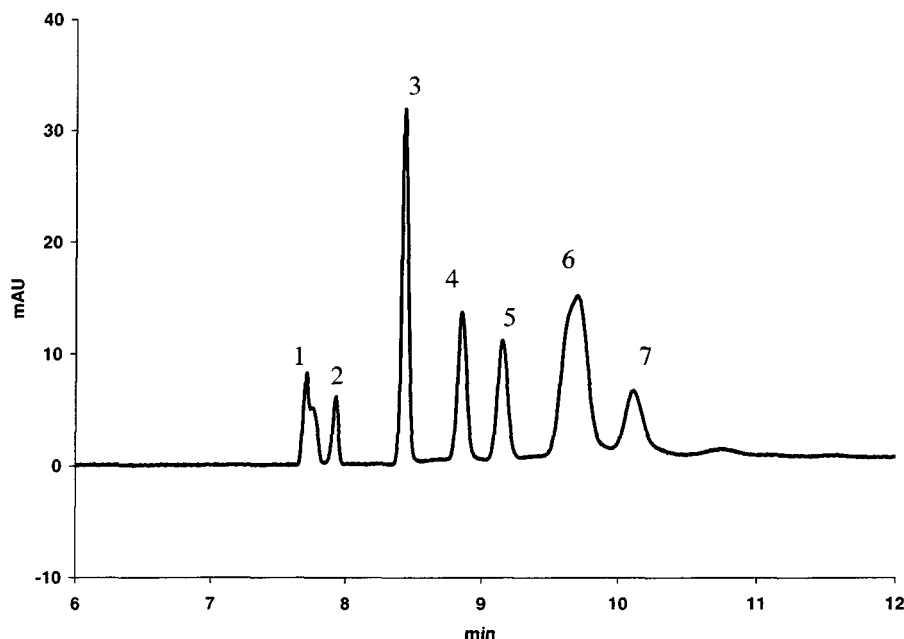


Fig. 6.7: Electrochromatographic separation of a mixture of: (1) DMSO (EOF marker, 30 mM) + resorcinol, (2) acetophenone, (3) naphthalene, (4) fluorene, (5) phenanthrene, (6) pyrene + fluoranthrene, (7) m-terphenyl each 10 mM in ACN. Mobile phase ACN/H₂O (1:1, v/v) containing NaCl (2 mM). The numbers in brackets correspond to the elution order. Capillary 77 cm (70 cm from injection to detection), I.D. 50 μ m. Hydrodynamic injection 1 s, 1.36 b, applied voltage 30 kV, detection 230 nm.

Methyl-octyldimethoxysilane coatings:

Methyloctyldimethoxysilane, like dimethyloctylmethoxysilane, can be connected to the polysiloxane network by two and three bonds respectively. Such organosilicate precursors were employed to study the effect of the degree of bonding on the electrochromatographic separation, as compared to that achieved with n-octyltriethoxysilane.

Methyl-octyldimethoxysilane sols were made at pH 1 according to the recommendations given in paragraph 5.9. The coatings were performed with the static method described in paragraph 5. Typical electrochromatograms are shown in Fig. 6.8 and 6.9.

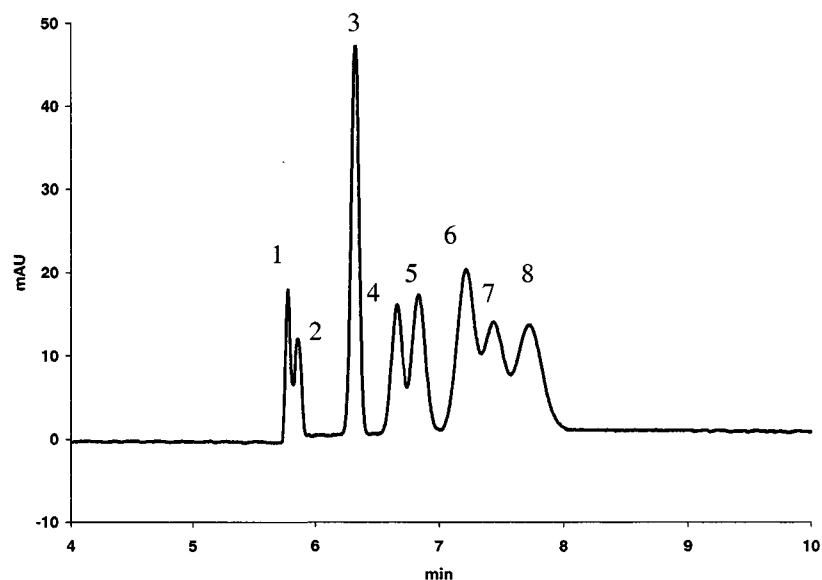


Fig. 6.8: Electrochromatographic separation of a mixture of: (1) DMSO (EOF marker, 30 mM) + resorcinol, (2) acetophenone, (3) naphthalene, (4) fluorene, (5) phenanthrene, (6) pyrene, (7) fluoranthrene, (8) *m*-terphenyl each 10 mM in ACN. Mobile phase ACN/H₂O (1:1, v/v) containing NaCl (2 mM). The numbers in brackets correspond to the elution order. Capillary 77 cm (70 cm from injection to detection), I.D. 50 μ m. Hydrodynamic injection 1 s, 1.36 b, applied voltage 30 kV, detection 230 nm.

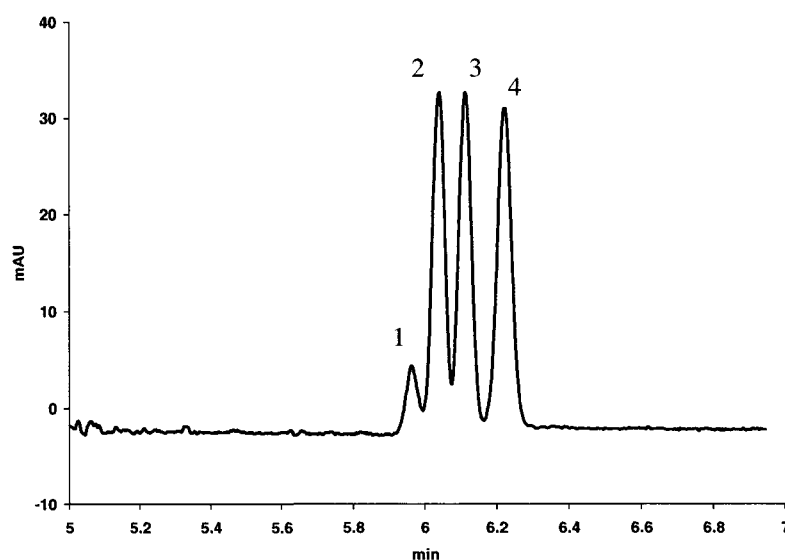


Fig. 6.9: Electrochromatographic separation of a mixture of: (1) acetone (EOF marker), (2) acetophenone, (3) propiophenone, (4) butyrophenone, each 30 mM in ACN/acetone (3:2, v/v). Mobile phase ACN/H₂O (1:1, v/v) containing NaCl (2 mM). The numbers in brackets correspond to the elution order. Capillary 77 cm (70 cm from the injection point to the detection point), I.D. 50 μ m. Hydrodynamic injection 1 s, 1.36 b, applied voltage 30 kV, detection 208 nm.

Dimethyloctylchlorosilane coatings:

All attempts to produce a stationary phase with dimethyloctylchlorosilane failed. Two separated liquid phases formed immediately, which prevented the use of this solution for any coating. This phenomenon might be related to the high reactivity of this precursor, which is activated by the high reactivity of the Si-Cl group and by the electrodonating capacities of the three alkyl groups. Due to the high reactivity of the dimethyloctylchlorosilane, no catalyst was used in the sol synthesis. Since the hydrolysis kinetics for dimethyloctylchlorosilane should be higher than for TEOS, the hydrolysis and condensation should occur almost exclusively between molecules of dimethyloctylchlorosilane. A dimer is the result of the sol-gel process and no further linkage can be formed with TEOS.

Hexadecyltriethoxysilane coatings:

Hexadecyltriethoxysilane sols were made at pH 3 according to the recommendations given in paragraph 5.9. The coatings were performed with the dynamic method described in paragraph 5.3. Typical electrochromatograms are shown in Figs. 6.10 to 6.12.

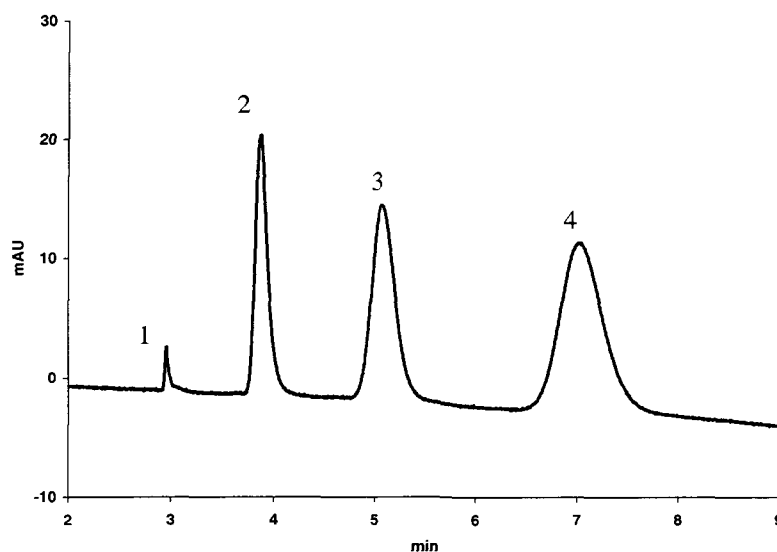


Fig. 6.10: Electrochromatographic separation of the test sample mixture. (1) DMSO (EOF marker, 5 mM), (2) naphthalene, (3) phenanthrene, (4) pyrene. Mobile phase ACN/H₂O (1:1, v/v) containing NaCl (2 mM). Capillary 47 cm (from the injection point to the detection point), I.D. 50 μ m. Hydrodynamic injection 1 s, 1.36 b, applied voltage 15 kV, detection 208 nm.

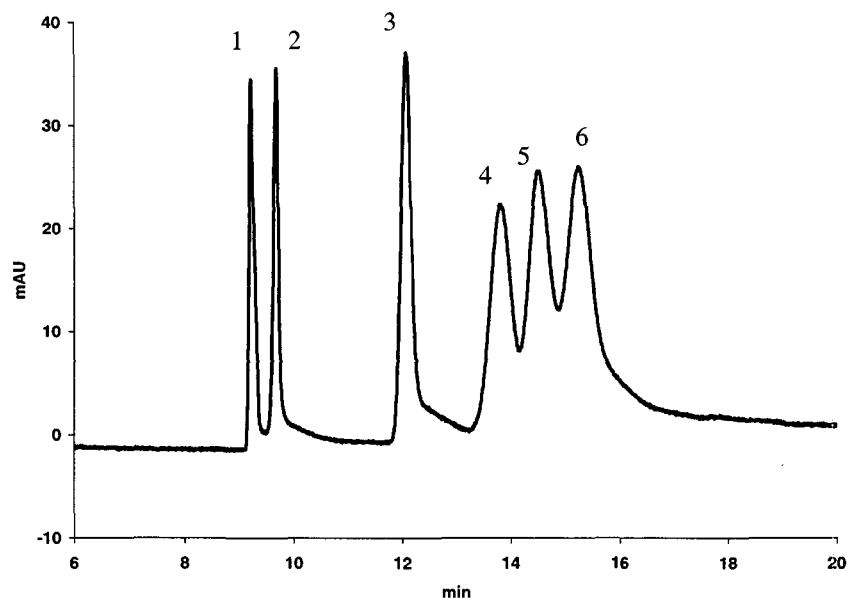


Fig. 6.11: Electrochromatographic separation of a mixture of: (1) pyrochatechol, (2) hydroquinone, (3) butyrophenone, (4) fluorene, (5) fluoranthrene, (6) *O*-terphenyl. Mobile phase ACN/H₂O (1:1, v/v) containing NaCl (2 mM). The numbers in brackets correspond to the elution order. Capillary 47 cm (from the injection point to the detection point), I.D. 50 μ m. hydrodynamic injection 1 s, 1.36 b, applied voltage 15 kV, detection 208 nm.

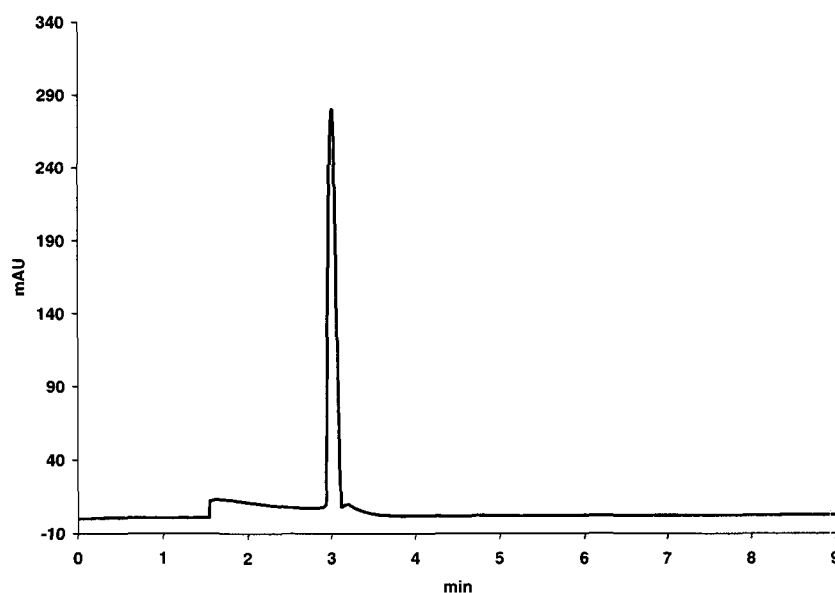


Fig. 6.12. Electrochromatogram of a mixture of amino acids (tyrosine, phenylalanine, tryptophan, histidine, asparagine, glutamine and glutamic acid), 30 mM each in a 20 mM phosphate buffer pH 3. Mobile phase ACN/H₂O (1:1, v/v) containing NaCl (2 mM). Capillary 47 cm (from the injection point to the detection point), I.D. 50 μ m. hydrodynamic injection 1 s, 1.36 b, applied voltage 30 kV, detection 208 nm.

Discussion:

The alkyl chain length affects the selectivity of the separation. From Fig. 6.1 and 6.3, it is seen that C₈ chains give better separations than C₆ chains. The use of the longest possible alkyl chain length is therefore recommended. In this context, it should be noted that the synthesis of ormosils with chains longer than C₁₀ is only possible with a quick sol-gel method done at pH 1.

It can be observed in Fig. 6.5 that alcohols are only weakly retained and that no peak tailing is seen. In this case, the EOF marker, hydroquinone, resorcinol and pyrochatechol are co-eluted. The absence of tailing can indicate the presence of weak interactions between the hydroxyl groups of the analytes and the silanol groups borne on the surface of the stationary phase. Since these interactions are known to occur in pressure driven chromatography with a reversed phase, one can think that different retention mechanisms are at work in HPLC and CEC for the same type of reversed stationary phase.

The extent of bonding of the silicon atom bearing the alkyl moiety to the polysiloxane network have a minor impact on the separations. The resolution of the mixture of DMSO, resorcinol, acetophenone, naphthalene, fluorene, phenanthrene, pyrene, fluoranthrene, and m-terphenyl is better with n-octyl based stationary phases (Fig. 6.3) than with methyl-n-octyl based stationary phases (Fig. 6.8). Since this effect is the contrary for the separation of ketones (Figs. 6.4, 6.9), no clear evidence for the role played by the extent of bonding can be found.

The condensation rate in sols catalysed with both F⁻ and H⁺ should be higher than in sols catalysed only by H⁺. The corresponding xerogels should then exhibit a more porous structure that increases D_s, the diffusion coefficient of the solutes in the stationary phase. According to eq. 2.25, this increase shifts the HETP towards higher values. In addition, a lower resolution should follow. This is indeed seen in Fig. 6.7 where the resolution obtained with a stationary phase catalysed with KF is lower than in Fig. 6.3 where no KF was used.

None of stationary phases containing alkyl chains made with the sol-gel technique were able to separate charged analytes (Fig. 6.12). This failure

seriously impedes the use of CEC for the analysis of compounds of biological interest such as amino acids or polypeptides. The CEC of ionised analytes with OTC coated with stationary containing alkyl moieties seems impossible, as pointed out by Horváth [46]. So far, no clear reason for the lack of retention with reversed stationary phases has been proposed due to the complexity of the CEC mechanism [100].

6.2- Polar Organosilicates and Organosilicates with Ionic Exchangers.

To achieve the separation of charged compounds by OTC-CEC, stationary phases with different polarities or with ion exchange capacities were synthesized.

Dimethyloctadecyl[3-(trimethoxysilyl)propyl]ammonium coatings:

Dimethyloctadecyl[3-(trimethoxysilyl)propyl]ammonium coatings were synthesized to confer anion exchange capacities to the stationary phases in addition to the chromatographic retention arising from the octadecyl moiety. To reinforce the role played by the organic moieties, some octyltriethoxysilane was also grafted to the ormosil.

Syntheses were made with dimethyloctadecyl[3-(trimethoxysilyl)propyl]-ammonium chloride with a ratio $R_1 = 40\%$ or 100% and octyltriethoxysilane with a ratio $R_2 = 0$ or 20% at pH 1 and 3 according to the recommendations given in paragraph 5.9. The coatings were performed with the dynamic method described in paragraph 5.3. None of the electrochromatographic runs gave a baseline separation of charged or neutral analytes (amino acids or PAHs). A typical electrochromatogram is shown in Fig. 6.13.

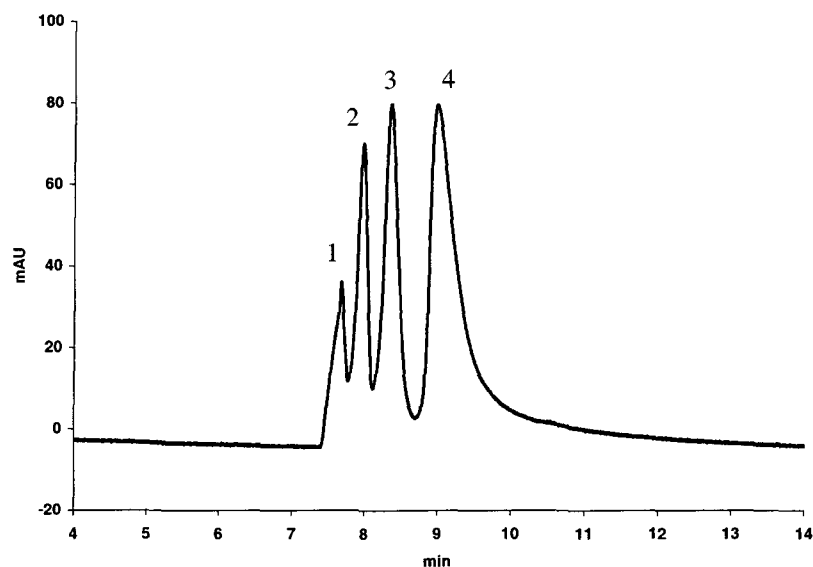


Fig. 6.13: Electrochromatographic separation of the test sample: (1) acetone (EOF marker), (2) naphthalene, (3) phenanthrene, (4) pyrene. Mobile phase ACN/H₂O (1:1, v/v) containing NaCl (2 mM). The numbers in brackets correspond to the elution order. Capillary 47 cm (from the injection point to the detection point), I.D. 50 μ m. hydrodynamic injection 1 s, 1.36 b, applied voltage 15 kV, detection 208 nm.

(Pentafluorophenyl)dimethylchlorosilane coatings:

(Pentafluorophenyl)dimethylchlorosilane sols were made at pH 3 according to the recommendations given in paragraph 5.9. The coatings were produced with the dynamic method described in paragraph 5.3. Typical electrochromatograms are shown in Fig. 6.14 and 6.15. (pentafluorophenyl)-dimethylchlorosilane modified silicates give more efficient stationary phases than hexadecyltriethoxysilane modified silicates (see Figs. 6.11, 6.14). The (pentafluorophenyl)-dimethylchlorosilane coatings were found to be the only stationary phases capable of separating mixtures of charged amino acids (see Figs. 6.12, 6.15). The separation cannot arise from a π - π interaction between the stationary phase and the analytes, because coatings containing aryl groups, like those made with 2-phenylethyl-trimethoxysilane, were unable to perform this separation. A rich electronic density cannot explain the separation either; coatings made with dimethyl(3,3,3-trifluoropropyl)chlorosilane or iodopropyl-triethoxysilane exhibit no separations. It was then thought that the distorted distribution of the benzenic ring engendered by the fluorine atoms is responsible for the separation.

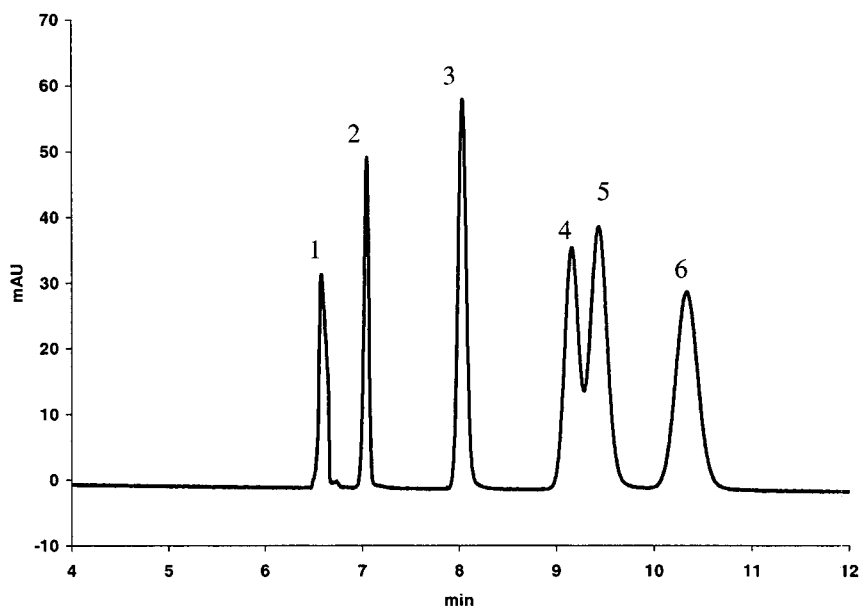


Fig. 6.14: Electrochromatographic separation of a mixture of: (1) pyrochatechol, (2) hydroquinone, (3) butyrophenone, (4) fluorene, (5) fluoranthrene, (6) *O*-terphenyl. Mobile phase ACN/H₂O (1:1, v/v) containing NaCl (2 mM). The numbers in brackets correspond to the elution order. Capillary 47 cm (from the injection point to the detection point), I.D. 50 μ m. hydrodynamic injection 1 s, 1.36 b, applied voltage 15 kV, detection 208 nm.

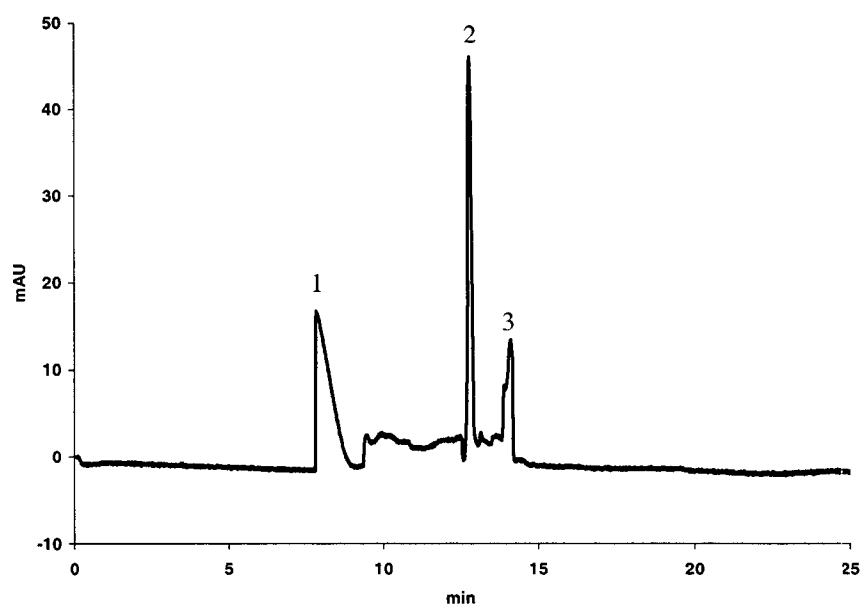


Fig. 6.15: Electrochromatogram of a mixture of amino acids (1) tyrosine, (2) phenylalanine, (3) tryptophan, histidine, asparagine, glutamine and glutamic acid, 30 mM each in a 20 mM phosphate buffer pH 3. Mobile phase ACN/H₂O (1:1, v/v) containing NaCl (2 mM). Capillary 47 cm (from the injection point to the detection point), I.D. 50 μ m. hydrodynamic injection 1 s, 1.36 b, applied voltage 30 kV, detection 208 nm.

6.3- Conclusion and Perspectives.

The alkyl modified silicates used as stationary phases for CEC are not able to separate mixtures of charged analytes. Since these stationary phases can separate these analytes in HPLC, the nature of the chromatographic interactions arising from the use of alkyl moieties should widely differ between HPLC and CEC. Therefore, the use of the reversed phase traditionally employed in pressure driven chromatography cannot be transferred to the OTCs in CEC.

If the separation of charged compounds is envisaged in CEC, stationary phases able to develop further interactions than the ones encountered with the alkyl moieties are required. Since one of the expected fields of application of CEC is the separation of charged peptides and proteins, new stationary phases must be developed. Toward this goal we have synthesized stationary phases made of pentafluoroaryl modified silicates, which were able to achieve the separation of simple mixtures of amino acids. Efforts to tailor the CEC stationary phases for the separation of charged analytes should use the sol-gel technique due to the ease of this approach.

7- Ormosils Monoliths for CEC.

Monolithic columns for CEC putatively have several advantages. Just as CEC, they do not require the presence of frits to retain the packing. Contrarily to the OTC columns, they do not suffer from the low phase ratio that is the main drawback of coated columns.

Sol-gel conditions were investigated to produce efficient stationary phases in monoliths, as an alternative to the packed columns traditionally used for CEC. The task was to inject a homogeneous liquid into the capillary, then to perform an in situ gelation leading to a macroporous structure after a drying step. The spinnable ormosils used so far could not be used for this task because their corresponding xerogels were not macroporous.

7.1- Chemical Induction of the Gelation.

According to the sol-gel theory, nucleophilic catalysts (i.e. OH^-) give higher condensation than hydrolysis rates. Such catalysts were therefore tested as a possible way to obtain xerogels with a macroscopic porous structure.

Experimental:

Sol syntheses with basic catalysts. TEOS, n-octyltriethoxysilane ($R=40\%$) and EtOH ($R_s=30\%$) were vortexed in an Eppendorf. (15 s, 2500 RPM). H_2O (at different concentration $100 < H_r < 400\%$) and the nucleophilic catalysts (NaOH, NH_4OH , amines, final concentration from 1 to 10^{-5} M) were then added to the solution. The syntheses were performed at ambient temperature or at 80°C for 6 h.

Sol syntheses with acid catalysts (spinnable sols). Gelation of spinnable sols can be induced by an evaporation of the solvent (see chapter 5.2). Since this approach is not suited for the formation of a macroporous ormosil structure, a chemically induced gelation had to be found. We found that this gelation was possible upon the addition of 1% (v/v) of N,N-diethylamine to the spinnable sols. Sols were synthesized as follows: TEOS, n-octyltriethoxysilane ($R=100\%$) and EtOH ($R_s=30\%$) were placed in a micro-reaction vial.

The solution was vortexed (15 s, 2500 RPM). Then H₂O (at different concentrations 75<H_r<500%) and HCl (final concentration 10⁻³ M) were added to the solution. A permanent vortex was carried out during 1 h at 80°C.

Results:

Sols synthesized with basic catalysts gave either emulsions or suspensions of particles depending on the nature of the initial reagents. After a certain period of time ranging from 10 min to 1 day, the densest phase of the emulsion, or the discrete particles, tended to settle down. Afterwards, in the case of the emulsion, the two liquid phases gelled. The presence of a solid/liquid or liquid/liquid interface in the sols prevented their use for the making of monolithic columns.

Transparent monolithic gels could be obtained from the spinnable sols. It was found that the water content markedly affected the gelation process. With H_r=100%, transparent gels were obtained within 20 min after the addition of the amine. With H_r≥200%, white monoliths were obtained in less than 10 min (Fig. 7.1). With H_r≥350%, addition of the amine resulted in the formation of two immiscible liquids that gelled afterwards (Fig. 7.2). White monoliths are harder than the transparent ones and do not bend when placed vertically on the microscope slide.

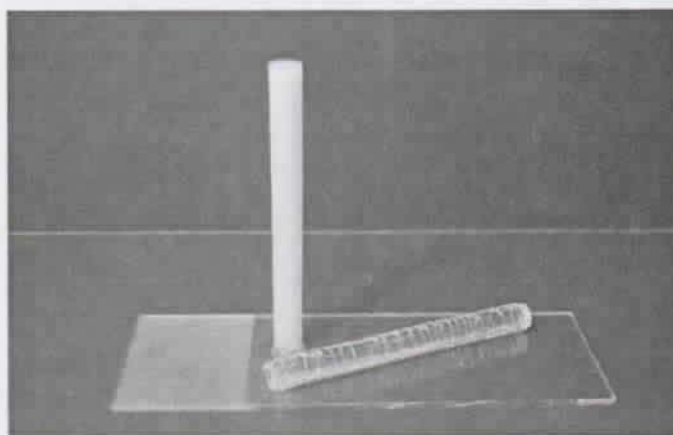


Fig. 7.1: Monoliths obtained after gelation of spinnable sols induced by addition of diethylamine. Gelation was performed in a 1 mL syringe used as a mold. The tip of the syringe was cut off and the gel was pushed out by using the piston. The transparent monolith corresponds to H_r=100%. Cracks appears as soon as the syneresis occurs. The white monolith corresponds to H_r=200%. Light scattering indicates a macroporous gel structure.

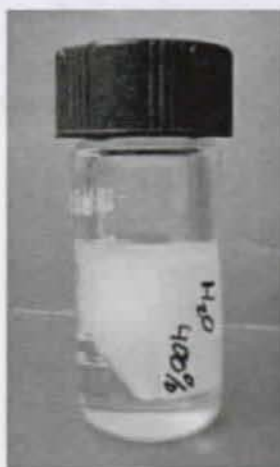


Fig. 7.2: Picture of the sol with $H_r=400\%$ after the addition of diethylamine. The picture was taken before gelation.

Cracking occurred on every monolith, whatever the water concentration. This effect was particularly visible on gels made with $H_r=100\%$ (Fig. 7.3).

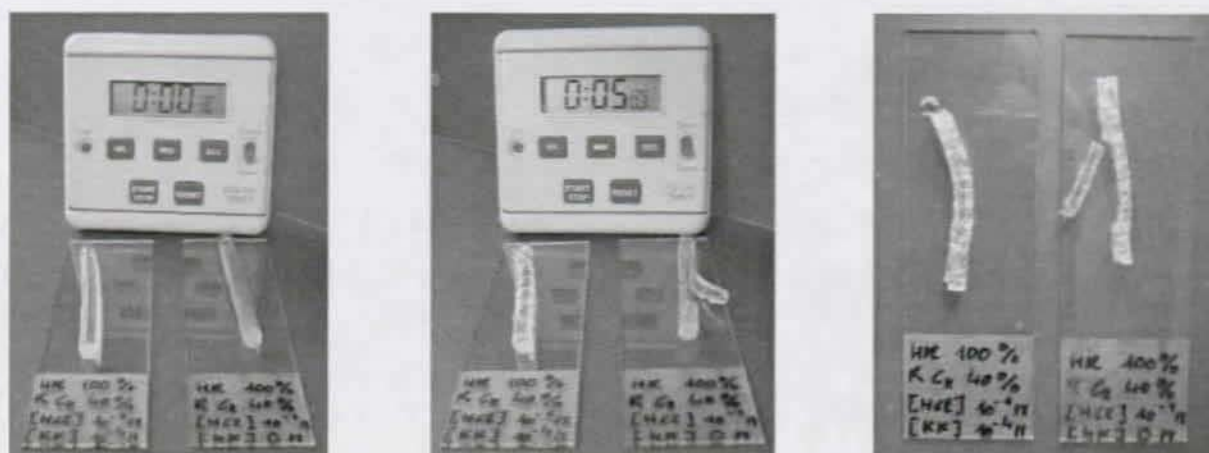


Fig. 7.3: Pictures of the drying process of a gel made with $H_r=100\%$. Cracks appear as soon as the gel is removed from the syringe. Photographs taken at t_0 , 5 min and 1h00.

The amount of N,N-diethylamine added is bigger than the amount of HCl introduced at the beginning of synthesis. Since the spinnable sols were normally stable toward gelation, some explanation for the gelation had to be found. One hypothesis suggests that gelation is caused by a change in the condensation rate. This change cannot arise from an increased concentration of silanol groups since no additional water is added during the induction of

gelation. Since more diethylamine is added than HCl, a neutralisation might occur whereupon the acid catalyst is replaced by an amine. Since this new catalyst is nucleophilic, it can dramatically enhance of the rate of condensation. The second hypothesis involves the formation of salts resulting from the neutralisation of HCl by the amines. It is known that salts affect the double layer structure of repulsive particles, a phenomenon that could prevent chains of primary particles from aggregating [48]. The organic salts made by neutralisation can conceivably reduce the degree of interaction. The Brownian motion of the chains can then possess enough energy to overcome the energetic repulsive barriers.

All gels cracked during the drying process. Transparent gels were especially prone to cracking. Better mechanical resistance was observed for white gels, which exhibit the biggest light scattering effect and therefore the biggest porous structure. To reduce the cracking tendency, drying control chemical additives (DCCAs) were used to enhance the dispersion of capillary forces during syneresis. DCCAs are organic solvents with high boiling points and low vapor pressure [48]. They generally replace half of the mutual solvent used in the sol synthesis. DCCAs are thought to act as plasticizers or affect the sol-gel mechanisms by producing nucleophilic catalysts by hydrolysis. These catalysts enhance the condensation rate, which has a strengthening effect on the gel. The most frequently reported DCCAs are formamide, glycerol and oxalic acid [48, 101].

7.2- pH gradient.

It is known that formamide in acid-catalyzed hydrolysis of metallorganic precursors does not react with TEOS, neither with organosilane nor the mutual solvent, but is hydrolysed to produce NH_3 plus formic acid [48]. NH_3 reacts with water in the sol synthesis, generating hydroxide ions from NH_4OH that increase the degree of condensation. Formamide, and the chemically related amides, N-methylamide and N,N-dimethylamide, were then investigated as modifiers of the condensation rate during the synthesis of sols. In addition to their expected roles as pH shifters, the unreacted amides are also supposed to act as DCCAs.

Experimental:

Syntheses of the sols. TEOS, octyltriethoxysilane ($R=40\%$), a mixture of amide (N,N-dimethylformamide (DMF), N-methylformamide or formamide) and ethanol (1:1, v/v) ($R_s=30\%$) were mixed in a microreaction vial equipped with a magnetic stirrer. The solution was vortexed for 15 s, then the required quantities of H_2O (in the range $100 < H_r < 400\%$) and HCl (final concentration 10^{-1} M) were added. The solution was heated to 80°C for 1h under permanent agitation (800 RPM). Aliquots of the solution were then taken for further gelation with 1% (v/v) N,N-diethylamine or N-methylamine.

Results:

When formamide was used, the sol turned into a white suspension that gelled within 10 min. Therefore, formamide is not suitable to make ormosil monoliths in capillary columns. DMF and N-methylformamide were observed to be efficient DCCAs and good base catalyst generators. Indeed, macroscopically homogeneous gels were obtained with these amides, and cracking was prevented on their corresponding xerogels.

The gelation of the sols was subsequently carried out by adding 1% (v/v) of N,N-diethylamine to the sol made with either DMF or N-methylformamide, followed by a vortexing step at 2500 RPM. The sols were then put in syringes used as a mold, that were capped to prevent evaporation. Gelation was observed within 6 min. With $H_r=100\%$, transparent gels were obtained whereas gels containing higher quantities of water were white. After gelation, gels were allowed to rest for 4 h, then the tips of the syringes were cut off, and their contents were pushed out using the piston. The gels were allowed to dry at ambient temperature and pressure for 1h, then they were further dried in vacuum (12 h, 35°C , 20 mb). Returning the dried monoliths to the mold used during their gelation, it was possible to monitor the volume shrinkage. The extent of volume shrinkage was high for transparent gels, while it was almost negligible for white gels.

To study the impact of heating on N-methylformamide and N,N-dimethylformamide, these DCCAs were added to sols containing EtOH ($R_s=15\%$) as unique mutual solvent. The addition was done on sols cooled at room temperature after an agitation performed for 1h. N,N-Diethylamine was then added to these spinnable sols. Gelation was slower than in the case where the DCCAs were added at the beginning of the sol synthesis. The gelation point was related to the water content and a bilayer structure was observed in capped syringes prior to gelation. Sols with $H_r=100\%$ took 30 min to gel, sols with $H_r=200\%$ took two days, and sols with $H_r>200\%$ took more than one week to gel. To study the catalytic effect of N-methylformamide and N,N-dimethylformamide, sols synthesis was carried out with HCl as the only catalyst. After one hour, the initial emulsion was still present and no sol was formed.

Discussion:

According to our results, an extended rate of condensation occurs when HCl, N,N-DMF or N-methylformamide, and elevated temperature (80°C) are used concomitantly. This association can be explained by an acid hydrolysis of the amides and by the elevated energetic barrier of this mechanism. Heating the reaction to 80°C lowers this barrier and the amide hydrolysis, so the amide hydrolysis is more likely to occur.

It is known that amides in an acid-water medium are in equilibrium with their corresponding amines and carboxylic acids. Entropically, this equilibrium should favor the formation of amines and carboxylic acids but amides possess a good thermodynamic stability [102, p.815]. The OH^- ions from the reaction of the released amine with water can gradually neutralise the hydronium ions of the HCl catalyst. Due to this, the pH increases and the rate of condensation might be increased. This pH shift translates into a sol that should have a hybrid structure between sols obtained with acidic catalysts and sols with basic catalysts. During the first part of sol synthesis, when hydrolysis is favored, long and lowly branched polymers chains are formed. Then, when the rate of condensation increases, condensation may occur between the long chains.

7.3- Factors Influencing the Formation of a Monolith.

Different parameters contributing to the formation of the gel monoliths are investigated in this chapter. The concentration of water in the initial sol and the influence of the mechanical agitation were first studied. The presence of F^- as a catalyst, in addition to H^+ was also investigated. A mechanism is proposed for the formation of the monoliths.

Experimental:

Syntheses of the sols. TEOS, octyltriethoxysilane ($R=40\%$) and a mixture of N-methylformamide and ethanol (1:1, v/v) ($R_s=30\%$) were mixed in a microreaction vial equipped with a magnetic stirrer. H_2O (in the range $100 < H_t < 400\%$) and HCl (final concentration 10^{-1} M) were added. The solution was heated to $80^\circ C$ for periods of time ranging from 15 min to 24 h, and vortexed (800 RPM) for at least 5 min. Aliquots of the sol were then taken for further gelation with 1% (v/v) of N,N-diethylamine.

Results:

It was noticed that the mechanical agitation during the formation of the sol has a marked effect on the formation of monoliths. Vortexed sols, continuously heated, were observed to be transparent until 210 min, then they became opaque. This opacity was quickly followed by gelation, giving rise to white homogeneous monoliths. The situation is different with continuously heated un-vortexed sols, where no loss of transparency occurred after 210 min. At that time, instead of a monolith, these samples gave two transparent immiscible liquids forming two separate layers in the reaction vials. The lower phase consisted of a highly viscous solution while the upper phase was liquid. Both phases gelled after 12 h, indicating that the upper phase was in reality also a dilute sol. This difference in constitution between stirred and un-stirred heated sols before the gelation point can be related to the length of the particles in the spinnable sols. The agitation can mechanically limit the growth of long chains of primary particles. Depending on their lengths, the relatively

small chains are more likely to be dissolved in the solvent, in contrary to the long chains that settle down by gravity. With non-stirred sols, an additional problem arises which can further delay the gelation. This problem is related to the formation of a bilayer structure that limits the diffusion of the reactive molecules between the two immiscible phases. The un-stirred sols therefore are long to gel due to the limited diffusion of water into the phase exhibiting the highest density.

The addition of KF was observed to speed up both the occurrence of white sols and the phase separation. The gelation point of the vortexed sols was reduced to 75 min in the presence of KF (10^{-3} M). The relative high concentration of KF used here is due to the fact that F^- , in presence HCl, can associate with a proton to form HF (pK_a of 3.2 in water [103]). Since HF is a weak acid, the availability of the fluoride ion is limited. Therefore, a high concentration of this acid must be used to benefit from the catalytic activity of F^- .

After 1h vortexed sols are transparent liquids, stable toward gelation for weeks at room temperature. For such sols, close to their gelation points and thereafter called metastable sols, gelation could be achieved in two ways:

- By thermal induction. Sols heated further under permanent agitation finally become macroporous monoliths. If the agitation is not maintained, a monolith exhibiting a non-homogeneous structure is obtained. To make monolithics columns, sols inside the capillaries can be sonicated. According to our results, this kind of mixing is not efficient.
- By chemical induction. This step is done by adding 1-3% (v/v) of N,N-diethylamine to the metastable sols. For a given concentration of the gelation inducer, the quickest gelation times were seen with sols containing the highest concentration of water. Chemical induction does not require elevated temperatures, nor mechanical agitation, except during the mixing step with the amine. This approach is less cumbersome to carry out than thermal induction and should therefore be recommended for making monoliths in capillaries.

Discussion:

The reduced gelation time with KF is due to the catalytic activity of the fluoride ion. It is known that F^- , even in trace amounts, is able to catalyze the condensation [35]. KF has the dual role of strengthening the gel structure and reducing the time needed to get metastable sols. It was subsequently always added to sols used to make monoliths.

Opaqueness indicates the presence of a material in solution having a physical structure larger than the visible wavelengths. This effect, seen with the vortexed ormosils sols, indicates the growth of a macroscopic structure assumed to be droplets. Since this mechanism does not occur with unvortexed solutions, one can think that the formation of the monoliths results from simultaneous phase separation and gelation. In the sol-gel process, this mechanism is known as coacervation [48 p.261].

7.4- Factors Influencing the Porosity of the Monoliths.

Pressure-driven flows in CEC columns are mandatory for many processes like filling the capillaries with the mobile phase or the conditioning process. Therefore, liquid flow through the monolithic column must be possible. Thus, the porosity of the monolith becomes particularly important. In this paragraph, parameters affecting the porosity of the monolith were studied and monitored through microscopy in order to tailor the monolith morphology. H_2O was found to be the most influential parameter affecting the morphology of the ormosils monoliths. Therefore, a study concerning the amount of water was carried out.

Experimental:

Syntheses of the sols: TEOS, octyltriethoxysilane (R=40%) and a mixture of N-Methylformamide-ethanol (1:1, v/v) ($R_s=30\%$) were mixed in a microreaction vial equipped with a magnetic stirrer. The solution was vortexed for 15 s, then suitable quantities of water and of an aqueous HCl/KF solution were added to get final concentrations of $[HCl]=10^{-1}$ M and of $[KF]=10^{-3}$ M with

H_r ranging from 100 to 400%. The solution was heated to 80°C for 1h under permanent agitation (1000 RPM), then cooled down to ambient temperature. 1000 μL of the solution were placed in an Eppendorf to which 10 μl of N-diethylamine were added and the whole solution was vortexed for 15 s. The solution was aspirated in a syringe. The syringe was plugged, the gelation was allowed to occur, and the gel was allowed to age for 2 h. The tip of the syringe was cut off, and the gel was placed on a microscope slide by pushing the piston. The gels were allowed to dry at ambient temperature and pressure for 1h and then were further dried in a vacuum oven (12 h, 35°C, 20 mb). The monoliths were fractured and sputtered with gold prior to SEM observation.

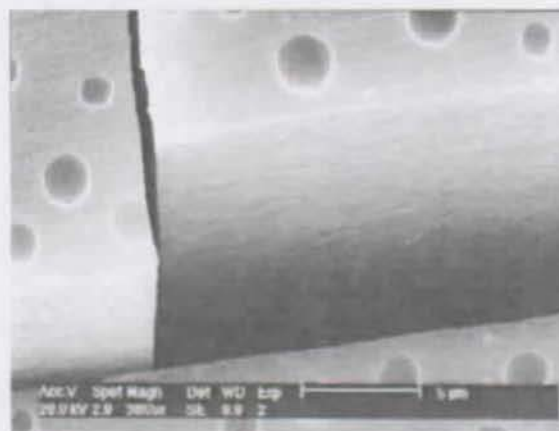
Results and discussion:

Figs. 7.4 to 7.9 show the surface of fractured ormosils monoliths obtained at different H_r .

Fig. 7.4: Monolith made with $H_r=100\%$. (SEM picture $\times 1932$, bar scale 5 μm).



Fig. 7.5: Monolith made with $H_r=150\%$. The holes at the top surface of the gel result from the entrapment of air bubbles between the gel and its mold. (SEM picture $\times 3865$, bar scale 5 μm).



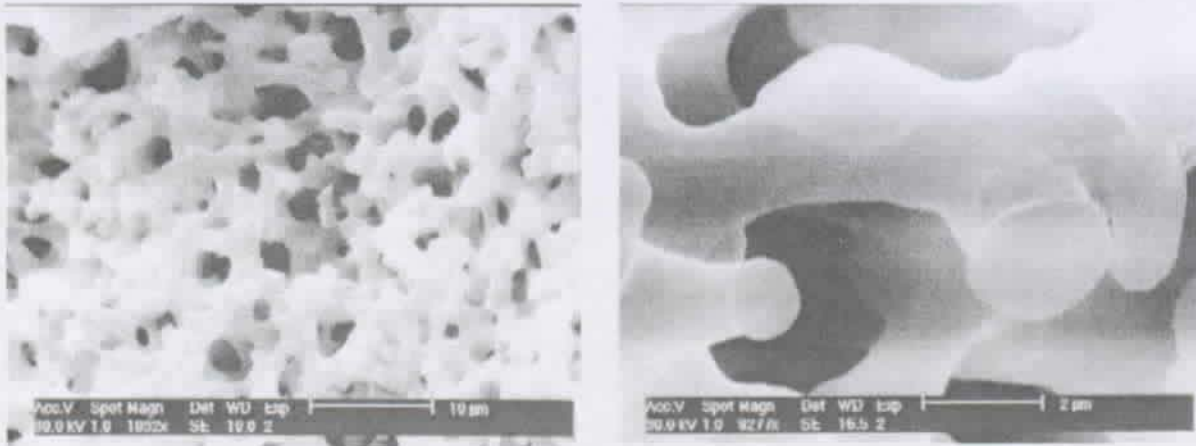


Fig. 7.6: Monolith made with $H_f=200\%$. (Left hand side picture: SEM picture $\times 1932$, bar scale $10\ \mu\text{m}$, right hand side picture: SEM picture $\times 9277$, bar scale $2\ \mu\text{m}$)

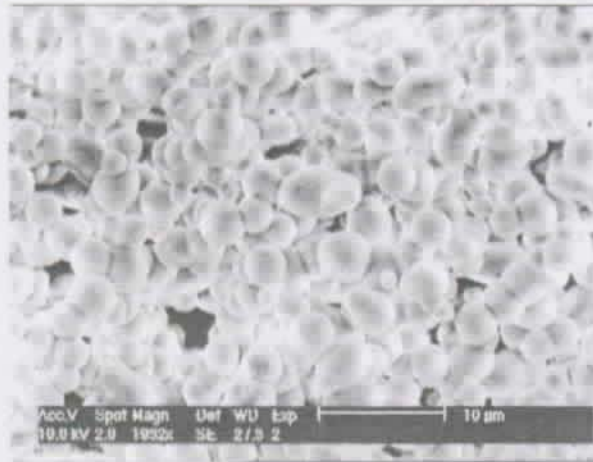


Fig. 7.7: Monolith made with $H_f=250\%$.
(SEM picture $\times 1932$, bar scale $10\ \mu\text{m}$)

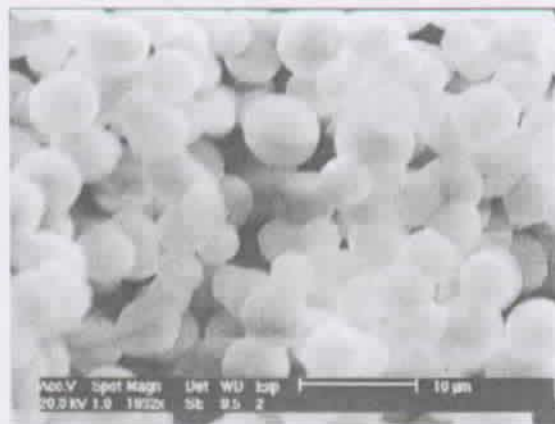


Fig. 7.8: Monolith made with $H_f=300\%$.
(SEM picture $\times 1932$, bar scale $5\ \mu\text{m}$)



Fig. 7.9: Monolith made with $H_r=350\%$. Picture with $H_r>350\%$ show the same structure.
(SEM picture $\times 1159$, bar scale $20 \mu\text{m}$).

The content of water greatly affects the morphology of the ormosil monoliths. Three major types can be observed depending both on the porosity and the homogeneity of the monoliths:

- The first type consists of ormosils xerogels made with $H_r < 200\%$. In this case, no microporous structure can be seen.
- The second type corresponds to xerogels made with H_r in the range 200-300%. In this case, porous monoliths with a homogeneous morphology are seen. The connections between the three-dimensional network of points that forms the porous xerogel, are observed to evolve in parallel with the water concentration. At low concentration, the points exhibit tubular extensions that can be interconnected to form bridges. A mesoporous structure is observed [104]. At high concentration ($H_r > 200\%$), the macroporous xerogel is made of interconnected beads. Increasing the concentration of water in the sol synthesis increases the size and improves the sphericity of the ormosils beads.
- The third type corresponds to $H_r > 300\%$. In this case, a macroporous structure is present, as evidenced by the visible light diffraction. However, the size distribution of the beads becomes broader and blocks of non-macroporous xerogel are formed. No specific structure can be seen. It has to

be noted that with gels produced at $H_r \geq 500\%$, gelation occurs but a bilayer phase is obtained.

The spheroidal shape of the particles observed might be explained by an attempt to reduce the surface tension during the coacervation process. This mechanism forces the gelling clusters of the ormosils beads to adopt the structure with the lowest surface to volume ratio, which is a sphere. This structure has an influence over the mechanical resistance and the breakage of the ormosil monoliths. When H_r allows the formation of a three-dimensional network of ormosil beads, the volume shrinkage of the monoliths is dramatically lowered in parallel with the reduction of the mechanical resistance to breakage. Ormosils monoliths made with $H_r = 200\%$, showing a bone-like structure, are more sensitive to the volume shrinkage, but exhibit a stronger resistance to mechanical breakage.

None of macroporous ormosil monoliths cracked during drying. However, on each of these monolithic xerogels, volume shrinkage was observed, as evidenced by putting back the xerogel monolith into their respective molds (Fig. 7.10).

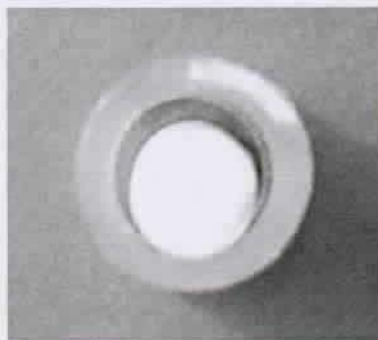


Fig. 7.10: Ormosil monolith with $H_r = 200\%$. Mold: syringe 1 mL.

The specific surface of the ormosil monoliths, as monitored by SEM, is also affected by the content of water. When H_r was in the range 200 to 300%, increasing the water concentration reduces the specific surface. [48].

The size of the gelling mold was also found to influence the morphology of the macroporous ormosil monoliths. When the coacervation process occurs in a

small mold, like the capillaries, the ormosil clusters tend to blend instead of giving beads. The resulting cluster tends to sediment (Figs. 7.11 and 7.12).

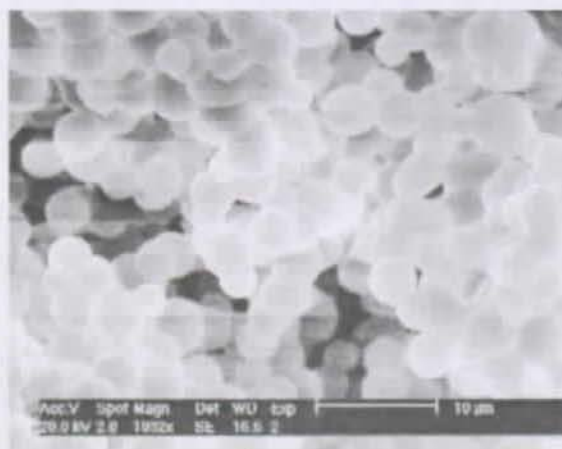


Fig. 7.11: SEM picture of a surface of a fractured ormosil made in a syringe. Metastable sol made with TEOS, octyltriethoxysilane ($R=30\%$), H_2O ($H_f=300\%$), solvents EtOH/*N*-methylformamide (1:1, v/v), HCl (final concentration 10^{-1} M), KF (final concentration 10^{-3} M). Coacervation/gelation inducer 1% (v/v) *N,N*-diethylamine. (SEM picture $\times 1932$, bar scale $10\ \mu\text{m}$)



Fig. 7.12: SEM pictures of a macroporous ormosils monoliths made in a capillary (I.D.= $100\ \mu\text{m}$). The two pictures show two cross-sections of the same capillary. The metastable sol used to make this monolith is analogous to the one used for Fig. 7.11. (SEM pictures $\times 695$, bar scale $20\ \mu\text{m}$)

To avoid the blending of the ormosil clusters within the capillaries, the concentration of the coacervation/gelation inducer must be accurately chosen according to two parameters. The "freezing" of the droplets formed by the liquid-liquid separation must be done quickly to maintain a bead-like structure,

and the gelation time must allow the filling of the capillaries. Depending on the viscosity of the metastable sols and the amount of water, the optimum concentration of N-diethylamine was found to be in the range 1-3% (v/v) (Fig. 7.13).

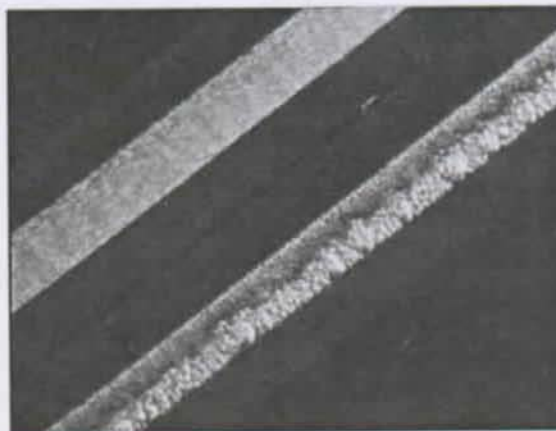


Fig. 7.13: Photographs of two capillaries (I.D.=100 μm). The metastable sol used for the making of the two monoliths is analogous. Left hand corner: 2% of diethylamine added to induced the gelation. Right hand corner: 1% diethylamine added to induced the gelation. The gelation occurs less quickly than with 2% and the wall effect takes place. (Optical microscopy $\times 50$, transmittance mode, partial black field, visible light)

It has to be noted that the coating of CEC capillaries with metastable ormosil sols gives analogous results to the spinnable sols generally used for this purpose. Therefore, the monoliths made with such sols must give efficient stationary phases for the separation of the PAHs.

7.5- Reduction of the Volume Shrinkage.

Macroporous monoliths of ormosil xerogels can be produced with the protocol described in chapter 7.4. Their application as macroporous monolithic stationary phases is prevented by to the volume shrinkage occurring during the drying step, as discussed before (Figs 7.14 and 7.15).



Fig. 7.14: Monolithic columns for CEC according to the protocol in chapter 7.4 with $H_T=200\%$.

Top photograph: naked capillary, I.D. $100\ \mu\text{m}$.

Middle microphotograph: capillary after removal of the macroporous monolith. A layer of macroporous xerogel is still attached to the capillary walls as evidenced from the highlighted channel.

Bottom photograph: macroporous monolith remove from the capillary. The volume has shrunk significantly, leaving voids between the capillary wall and the monolith, which prevents the electrochromatographic use of such a column.

(Optical microscopy $\times 50$, transmittance mode, partial black field, visible light)

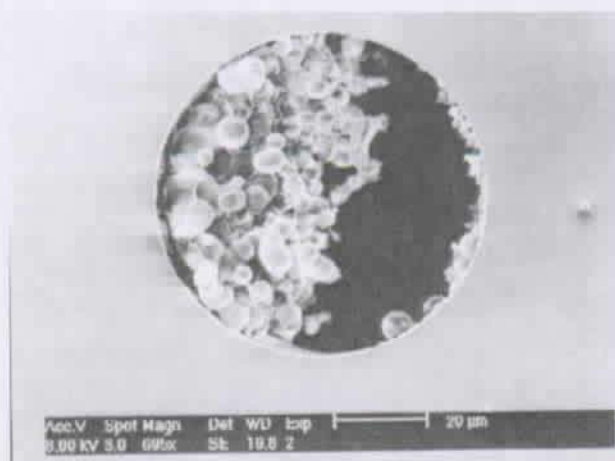


Fig. 7.15: Monolithic columns for CEC according to the protocol given in chapter 7.4 with $H_T=300\%$.

(SEM picture $\times 695$, bar scale $20\ \mu\text{m}$)

To allow the use of macroporous ormosil monoliths in CEC, the volume shrinkage must be reduced. This was attempted in several ways [48]:

- By improving the spherical shape of the ormosil clusters obtained through coacervation.
- By removing the unreacted water from the monoliths.
- By the insertion of an organic polymer bonded to the polysiloxane network.
- By the insertion of an organic polymer non-bonded to the polysiloxane network.
- By the attachment of the macroporous monoliths to the capillary walls.
- By inserting organodialkoxysilanes in the polysiloxane network.

Improvement of the spherical shape:

It was observed that the morphology of the macroporous monoliths could limit the volume shrinkage associated within the drying step, and that this resistance was related to the sphericity of the building units of the monoliths [48]. The sphericity being mainly affected by the surface tension in the coacervation process, the influence of surfactants and of the viscosity of organic solvents was studied.

To study the surfactant effect, 50 μL of an aqueous solution of polyethylene glycol tert-octophenyl ether (Triton X-100) or of sodium dodecyl sulfate (SDS) were added to 1000 μL of metastable ormosils sols made according to the protocol given in chapter 7.4 with $H_r=250\%$. The concentration of the surfactants was chosen to give a final concentration of 1 mM. After mixing the solution at 2500 RPM for 15 s, 11 μL of N,N-diethylamine were added as a gelling agent and coacervation inductor. Fig. 7.16 and 7.17, respectively show the effect of Triton-X and SDS. These figures should be compared with Fig. 7.7.

By comparison with Fig. 7.7, one can see that the surfactants improve the sphericity of the beads. The resistance of the monoliths to mechanical breakage is concomitantly lowered, which indicates weak physical connections between the beads. However, a volume shrinkage during drying is still observed. The second effect of the surfactants is to broaden the size

distribution of the beads. This should complicate the mass transfer in the stationary phase. Both the broad size distribution and the observed volume shrinkage indicate that the use of surfactants is not suited for the production of macroporous monoliths.

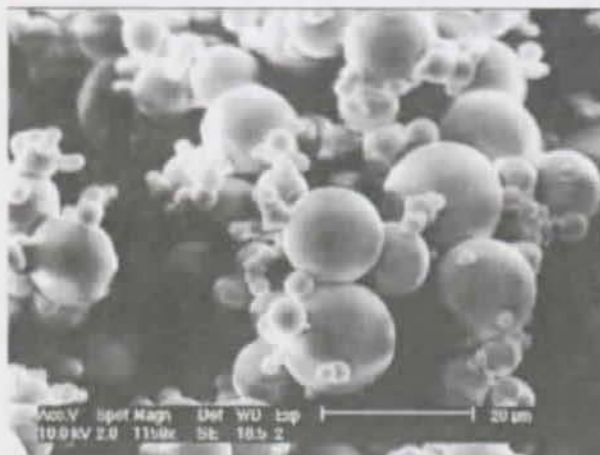


Fig. 7.16: SEM picture of a surface of a fractured ormosils with 1 mM Triton-X. (SEM picture $\times 1159$, bar scale 20 μm)

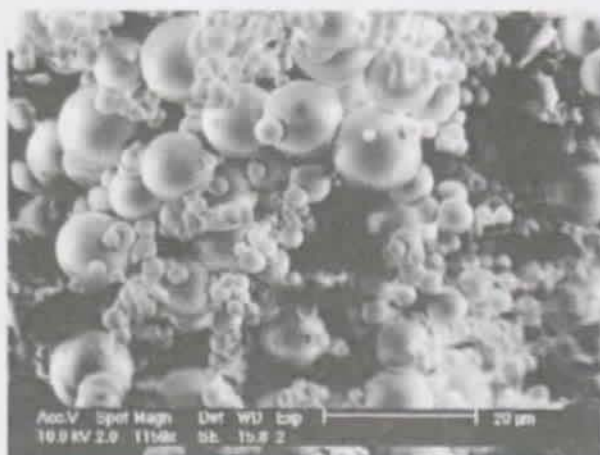
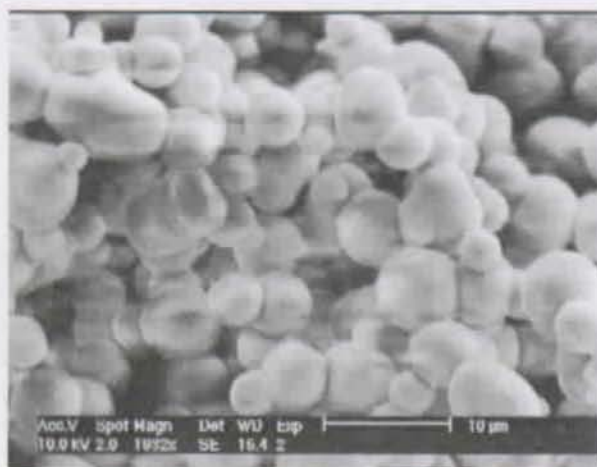


Fig. 7.17: SEM picture of a surface of a ormosil monolith made with 1 mM SDS. (SEM picture $\times 1159$, bar scale 20 μm)

To study the influence of the viscosity of the liquid experiencing the phase separation, organic solvents of different viscosities (EtOH 1.074 cP, ACN 0.369 cP, propionitrile 0.294 cP, glutaronitrile 0.346 cP, THF 0.456, dioxane 1.177 cP, viscosities given at 25°C [103]), were tested in the protocol described in chapter 7.4 with $H_1=250\%$. Using these experimental conditions, the smallest bead sizes were obtained with EtOH (Fig. 7.7), while the biggest bead sizes were seen for THF and dioxane (Fig. 7.18). Solvent exhibiting the lowest viscosities (ACN, propionitrile, glutaronitrile) give ormosil clusters

entrapped in a xerogel matrix (Fig. 7.19) and could therefore not be used. It has to be noticed that acetone could be an appropriate solvent due to its low viscosity (0.306 cP at 25°C [103]). However, this solvent was not used due to its low boiling point (56.5 °C [103]). This also applies for THF (66 °C [103]).



*Fig. 7.18: SEM picture of a fracture surface of an ormosil monolith made with dioxane.
(SEM picture $\times 1932$, bar scale 10 μm)*



*Fig. 7.19: SEM picture of a fracture surface of an ormosil monolith made with glutaronitrile.
(SEM picture $\times 1932$, bar scale 10 μm)*

Despite their reactivity in the sol synthesis, the influence of ACN, propionitrile and glutaronitrile on bead formation was studied. These metastable sols were made with EtOH ($R_s=30\%$) as solvent.

After induction of both the phase separation and the gelation, it was seen that a slight decrease of the sol viscosity by the additions of ACN, propionitrile and

glutaronitrile (20% of solvent per volume of sol) did not improve the sphericity of the beads (Fig. 7.20). More than 20% caused the formation of macroscopical bead clusters, but a longer time is required to dry these gels.

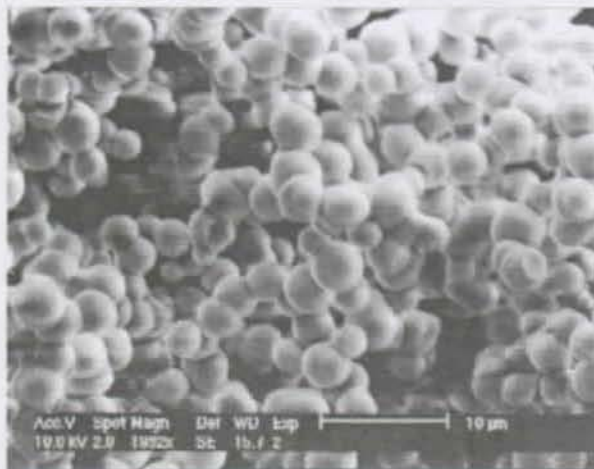


Fig. 7.20: SEM picture of a fracture surface of an ormosil monolith made according to the protocol 3.5.3 with $H_r=250\%$. 20% ACN per volume of sol.
(SEM picture $\times 1932$, bar scale 10 μm)

Removal of the unreacted water contained in the monolith:

During drying, the un-reacted water contained in the ormosil gel is removed. This step is especially important for $H_r > 100\%$. This removal is also important with $H_r \leq 100\%$, but to a lesser extent, because water is never fully reacted [85]. It was thought that reacting the metastable sol with a dehydrating compound before coacervation/gelation should lower the volume shrinkage. Ethylene oxide was chosen as a dehydrating compound for several reasons. First, this chemical is water-soluble. Second, it is gaseous at room temperature, therefore, any unreacted ethylene oxide can be easily removed from the metastable sol. Finally, its addition product with water, the 1,2-dihydroxyethane, can act as a DCCA.

A metastable gel was made with TEOS, octyltriethoxysilane ($R=40\%$), H_2O ($H_r=250\%$), EtOH/N-methylformamide (1:1, v/v, $R_s=30\%$), HCl (final concentration 10^{-1} M) and KF (final concentration 10^{-3} M). Ethylene oxide corresponding to the amount of water added in excess ($H_r=250\%$) was added to 1 mL aliquots of the vortexed metastable sol at 0°C . After the addition, the

capped vials containing the sols were heated up to room temperature and the solution was stirred for 1 h. Then, 1% (v/v) of N,N-dimethylamine was added. The solution was stirred at the highest rotation speed for 15 s and injected into capillaries or allowed to stay in the reaction vial.

Monoliths made of spherical beads were obtained, as monitored by SEM on Fig. 7.21 and 7.22.

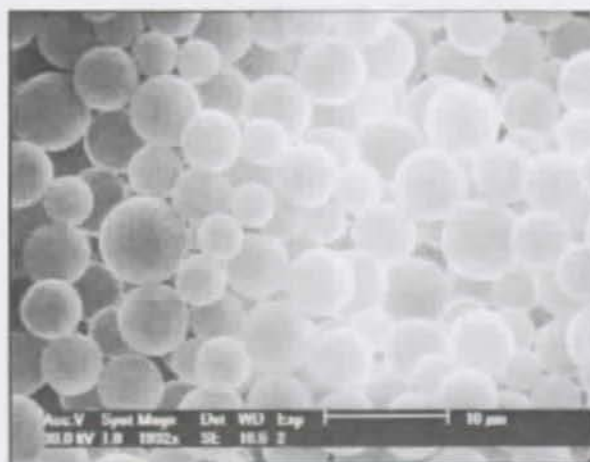


Fig. 7.21: SEM picture of a fracture surface of an ormosil monolith made with ethylene oxide with $H_f=250\%$.
(SEM picture $\times 1932$, bar scale $10\ \mu\text{m}$)

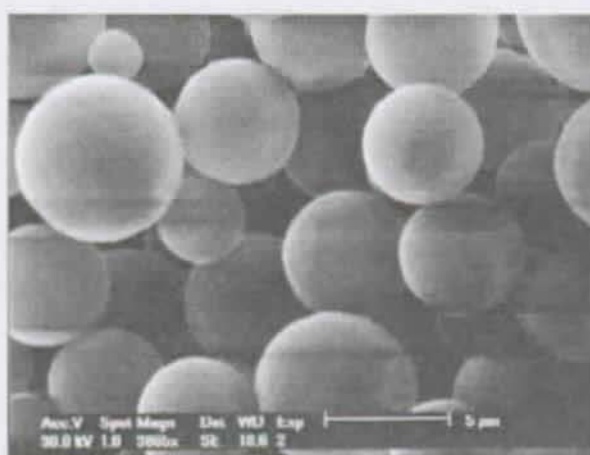


Fig. 7.22: SEM picture of a fracture surface of an ormosil monolith made with ethylene oxide with $H_f=250\%$. The rough surface of the beads is seen.
(SEM picture $\times 3865$, bar scale $5\ \mu\text{m}$)

The porous ormosil monoliths were very fragile and broke into a powder when touched. This poor mechanical resistance indicates weak physical connections between the beads. The goal of having spherical beads and a good size distribution was achieved. However, a marked volume shrinkage occurred with these bead-based monoliths. This prevents their use as stationary phases for CEC.

Insertion of an organic polymer bonded to the polysiloxane network:

Since the drying of the gel removes by evaporation the alcohol or the water produced during the formation of polysiloxane bonds (reactions 10 and 11), a volume shrinkage of the gel is likely. To reduce this shrinkage, one can limit the extent of the condensation by reducing the concentration of the molecules participating in the condensation. This can be achieved by using organosilicate precursors with large organic moieties. Towards this goal, efforts were made to synthesize such precursors [105] for use in a further sol-gel process to make macroporous ormosil monoliths.

Organosilicate precursors were made via a radical polymerisation as follows: methylvinyl-diethoxysilane was added to 5 molar equivalent vinyl benzene in a microreaction vial. Then, a 4 molar equivalent of dioxane containing radical initiator α, α' -azoisobutyronitrile (AIBN) was added to a final concentration of AIBN equal to 1 mM. The solution was vortexed, then heated to 70°C for 30 min in an uncapped vial (N_2 formation). The vial was then capped and allowed to react for 30 min. A transparent liquid was obtained. In an attempt to perform a sol-gel process, 0.5 mL of the polymeric organosilicate precursor solution was added to a solution containing TEOS (3 mL), octyltriethoxysilane ($R=40\%$) and EtOH ($R_s=30\%$). The solution was homogenized (vortex, 30s, 2500 RPM). The synthesis of the sol was not possible since a white precipitate appears as soon as water was added.

The precipitate, due to the hydrophobicity of the polymer made, prevented the use of the organosilicate precursors in the making of monolithic columns for CEC.

Insertion of an organic polymer non-bonded to the polysiloxane network:

In a further attempt to reduce the volume shrinkage, organic, water soluble-polymers were added to the metastable ormosil sol. These polymers decrease the vapor pressure of the liquid contained in the gels. Furthermore, their three dimensional structure, which extends through the polysiloxane network, can reinforce the mechanical structure of the gels.

Polyethylene glycol (PEG) and polyethylene oxide (PEO) were used as water soluble polymers. PEG (average molecular mass = $10000 \text{ g} \times \text{mol}^{-1}$) was purchased and used as received. PEO oxide was synthesised as follows: in a micro reaction vial, placed in a water/ice bath equipped with a magnetic stirrer, 2 mL of ethylene oxide were added under permanent agitation (500 RPM) to 1 mL of 2-nitropropane containing 50 mM of AlCl_3 . The reaction vial was capped, then the solution was heated at 60°C and continuously stirred for 2 h. The vial was then cooled down to room temperature and uncapped for 15 min. Syntheses of metastable sols were made using TEOS, octyltriethoxysilane ($R=40\%$), H_2O ($H_r=250\%$), EtOH/N-methylformamide (1:1, v/v) ($R_s=30\%$), HCl (final concentration 10^{-1} M) and KF (final concentration 10^{-3} M). PEG or PEO were added at the beginning of the synthesis to give final concentrations of 10, 20, 30 and 50 mM. Gelling was induced by adding 1% (v/v) of N-diethylamine to the metastable sols.

In the presence of PEG or PEO, beads with a uniform distribution were obtained. However, the mechanical breakage of the macroporous monolith indicated weak physical bonds between the beads. Every monolith exhibited a tendency to shrink during the drying process and therefore none of the syntheses performed gave successful monolithic stationary phases.

Attachment of the macroporous monoliths to the capillary walls:

Attachment of the monoliths to the capillary walls is a crucial parameter in suppressing the volume shrinkage during the drying of the gel inside the capillary [106]. Since the only anchoring points for the stationary phase are the silanol groups, all the capillaries used were treated with an alkaline wash to increase the surface density of these groups (see chapter 3.3).

Unfortunately this treatment was inefficient in ensuring a good linkage of the macroporous ormosil monoliths, as described before. This indicates a low extent of condensation between the silanol groups at the inner surface of the capillary and those of the macroporous xerogel. Since coacervation takes place shortly after the introduction of the metastable sols, it is possible that the poor attachment results from a slow condensation with the silanol groups of capillary wall, or from their low surface density. To circumvent these drawbacks, different approaches were tested to either speed up the condensation or to increase the chemical reactivity of the capillary walls.

It is known that sonification accelerates the condensation process [107]. Since the linkage of the monolith to the capillary wall should benefit from such treatment, capillaries containing metastable ormosils sols were placed in an ultrasonic bath during the coacervation/gelation process. As seen on a microphotograph (Fig. 7.23), such monoliths do not show any improvement of the anchoring.

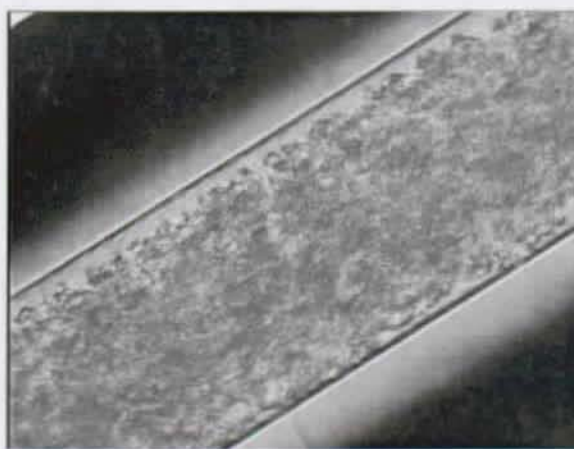


*Fig. 7.23: Photograph of a monolith by sonification. Capillary I.D. 100 μm .
(Optical microscopy $\times 200$, transmittance mode, visible light, partial black field)*

In the second approach, a coating with the metastable sol was first carried out. The metastable sols without any addition of N-diethylamine were injected for 5 min into the capillaries (5 b), afterwards, capillaries were flushed with argon (5 b). Next, the coacervation/gelation process was performed as usual

in the capillaries. This approach did not succeed in increasing the anchoring of the monoliths to the capillary walls (Fig. 7.24).

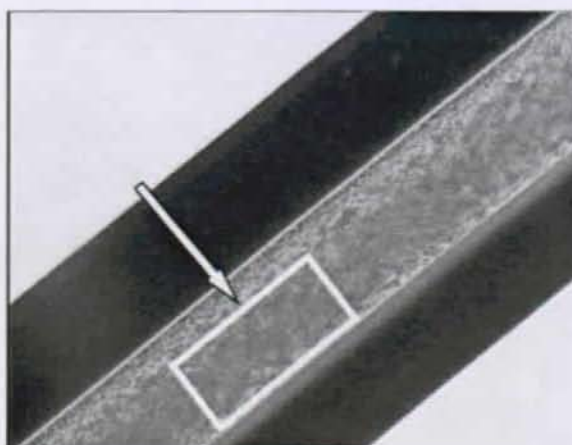


Fig. 7.24: Microphotograph of a monolith obtained with a coated capillary. The darkest zone of the monolith corresponds to a more dense concentration of the stationary phase. The coating gives a rough appearance to the capillary inner wall.

(Optical microscopy $\times 100$, transmittance mode, visible light, partial black field)

Insertion of organodialkoxysilanes in the polysiloxane network:

Reducing the concentration of the silanol groups should limit the condensation process and should increase the flexibility to the polysiloxane network [48]. If the extent of the syneresis is lowered, the volume shrinkage of the ormosils monoliths should also be lowered. Dimethyldiethoxysilane was therefore added as a precursor during ormosil production.

A metastable ormosil sol was prepared with TEOS, octyltriethoxysilane $R_{(1)}=40\%$. Dimethyldiethoxysilane was introduced in the reaction mixture at different ratios $R_{(2)}$ ($25 < R_{(2)} < 100\%$) with regards to the TEOS. A binary solvent EtOH/N-methylamide made with different volume ratios was used with several R_s . The synthesis was catalysed by HCl and KF with respective final concentrations of 10^{-1} M and 10^{-3} M.

It was found that almost no volume shrinkage occurred with gels made from the following sol: $R_{(1)}=50\%$, $R_{(2)}=70\%$, solvent: $R_s=20\%$ with EtOH/N-

methylformamide (3:7, v/v), water: $H_r=200\%$ (Fig. 7.25, 7.26). The induction of the gelation was carried out by adding 40 μL of a mixture diethylamine/ACN (1:3, v/v) to 1000 μL of the sol.

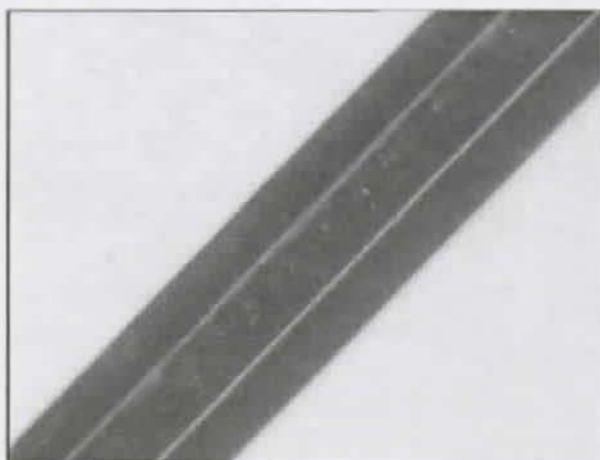


Fig. 7.25: Photograph of a monolithic porous xerogel containing dimethyldiethoxysilane. Capillary I.D. 100 μm . No clear area appeared in the close proximity of the capillary wall, indicating no volume shrinkage.
(Optical microscopy $\times 50$, transmittance mode, visible light)

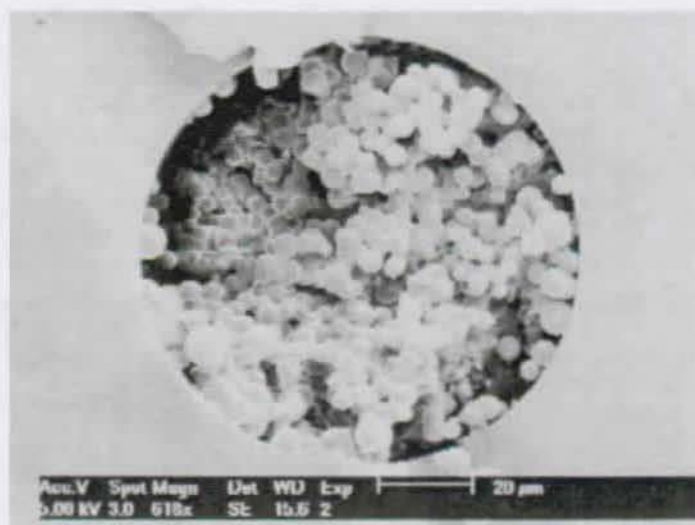


Fig. 7.26: SEM picture of a monolithic porous xerogel containing dimethyldiethoxysilane. Capillary I.D. 100 μm .
(SEM picture $\times 618$, bar scale 20 μm)

While the monolith showed little to no volume shrinkage, it was also unfortunately found to be only loosely attached to the capillary wall (Fig. 7.27). Furthermore, the addition of dimethyldiethoxysilane was observed to dramatically reduce the EOF. This phenomenon was evidenced by coating capillaries with sols generally used to produce the monoliths (Fig. 7.28). These two phenomena prevented the use of monolithic columns made with diethoxysilane in CEC.

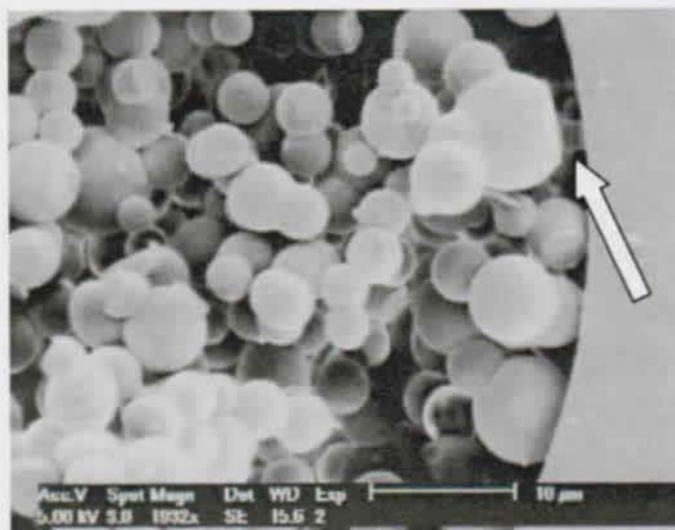


Fig. 7.27: Detail of a monolithic column. The anchoring of the monolithic phase to the capillary wall is weak. Capillary I.D. 100 μm . (SEM picture $\times 1932$, bar scale 10 μm)

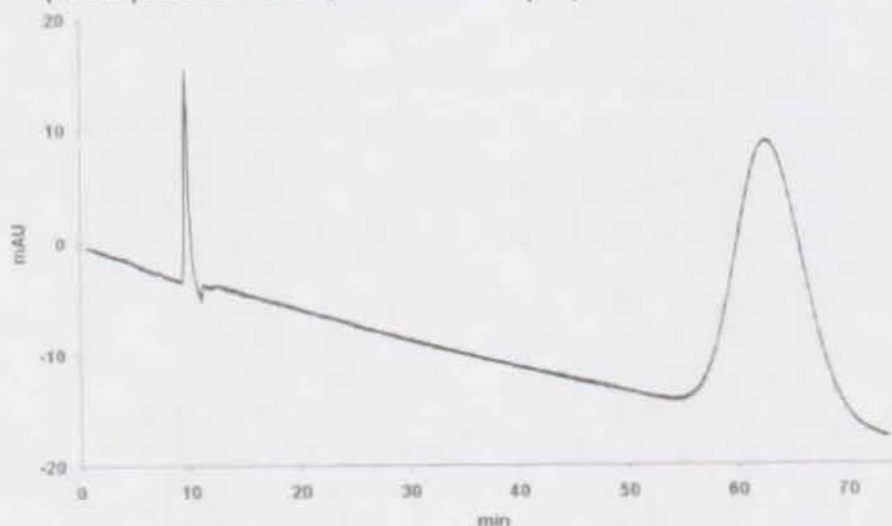


Fig. 7.28: Electrochromatogram (stopped after 75 min) of the test sample with OTCs. Coating with a sol made of TEOS, *n*-octyltriethoxysilane $R_{(1)}=50\%$, dimethyldiethoxysilane $R_{(2)}=70\%$ water ($H_r=200\%$), HCl (10^{-1} M), KF (10^{-3} M). Solvent mixture EtOH/*N*-methylformamide (3:7, v/v) with $R_s=20\%$

7.6- Conclusions and Perspectives.

In this work, efforts were made to make monolithic macroporous stationary phases of ormosils by a direct in-situ formation in the capillaries. This approach could shorten the time to get monolithic columns for CEC since no further modifications (i.e. grafting organic moities to a macroporous framework of silica) are required. This is a distinct advantage over the monolithic silica columns which have been proposed in CEC [104, 106, 108, 109].

The main challenges were reducing of the volume shrinkage and morphological homogeneity of the macroporous polymer inside the capillaries. So far, obtaining a quick coacervation/gelation of metastable ormosil sols by a chemical induction of the gelation/phase separation solved the problems linked to the homogeneity. The volume shrinkage problem was partially resolved by strengthening the macroporous structure. This reinforcement was possible by giving a spherical shape to the building units of the macroporous monolith and by reducing the extent of condensation with the use of dialkyldialkoxysilane. Unfortunately, having a homogeneous morphology and no volume shrinkage by the new coacervation/gelation process in the capillaries is not consistent with the attachment of the stationary phase to the capillary walls. This lack of linkage is due to the rapidity of the gelation, which prevents the condensation mechanism between the silanol groups of the stationary phase and those on the capillary wall. This linkage being a key parameter to obtain usable stable stationary phases [104], the proposed coacervation/gelation approach does not seem applicable for the production of monolithic CEC columns.

8- Factors Influencing the Electrochromatographic Efficiency.

The influence of the mobile phase constitution, of the voltage applied, and of the temperature on the electrochromatographic separation is studied in this chapter. The length of the column, its inner diameter and the thickness of the coating were also investigated.

The stationary phases used in this investigation were prepared as follows (unless otherwise mentioned): TEOS, octyltriethoxysilane ($R=40\%$) and EtOH ($R_s=30\%$) were vortexed in an Eppendorf (15 s, 2500 RPM). H_2O ($H_r=100\%$) and HCl (final concentration 10^{-1} M) were then added. After 6 h of permanent agitation, the sol was used to coat (10 min, 5 b) a capillary ($L=67$ cm, I.D.= 50 μ m) with the dynamic coating method. To ensure good stability of the stationary phase over long periods of time, this capillary was formerly etched with NH_5F_2 then treated with NaOH (see chapter 3.3). The capillary was afterwards partially dried (2 h, 20 mb, $35^\circ C$) and flushed with an aqueous NaOH solution (10^{-2} M, 10 min) (see chapter 5.2). The alkaline solution was removed with argon (5 min, 5 b) and the capillary was subsequently dried (2 h, 20 mb, $35^\circ C$).

8.1- Mobile Phases.

The traditional buffers used in CE are generally not suitable for chromatographic separations in the reversed phase mode. Mobile phases for CEC are generally hydroorganic solutions containing a dilute supporting electrolyte [110]. The electrolyte in the mobile phases provides a conductive medium [111] able to produce a current in the microampere range [56]. This small current is needed to avoid electric shut down of the CEC operating system. To maintain both the silanol groups and the ionisable analytes at a constant degree of ionization, the electrolytes used in CEC are frequently a pH buffer. If mobile phases containing water are used in CEC, this buffer also limits the pH gradient across the capillary resulting from water electrolysis close to the electrodes [112].

8.1.1- Organic Solvents.

Organic solvents, either pure or mixed with water, are used as mobile phases in CEC. Organic solvents are of particular interest in CEC because they enhance the solubility of the analytes. Depending on their nature or their concentration, they adjust the selectivities of the reversed stationary phases. Pure organic solvents can influence the electrokinetic properties of silica through the zeta potential, and therefore can also give rise to an EOF [12]. The use of organic solvents, such as acetonitrile, results in very low currents compared to typical aqueous CE buffers [12, 113]. As a result, the amount of Joule heat produced with non-aqueous or hydroorganic phases in CEC is greatly reduced with respect to CE.

The choice concerning the nature of the organic solvent was governed in this work by several considerations. The organic solvent should be transparent to the optical detection wavelength used (190-600 nm) [114], it should have a high solubility toward the analytes, and it should allow a strong EOF. The potential candidates were the following solvents (Table 4).

Solvent	ϵ_R	η (cP)	ϵ_R/η	ζ (mV) on silica
ACN	37.5	0.34	110	207
Water	80	0.89	90	99
MeOH	32.7	0.54	60	108
DMF	36.7	0.80	46	86
Formamide	111	3.3	34	96
DMSO	46.7	1.96	23.8	23.8

*Table 4: Dielectric constant and viscosities for different CEC.
(Data from Ref. 115, and Ref. 22 for ζ)*

ACN and MeOH are the best candidates for mobile phases in CEC. According to the Von Smoluchowski equation (2.9), the zeta potential and the ratio of the dielectric constant to the viscosity are determining parameters. ACN and MeOH generate the highest EOF, which can even be stronger than when aqueous buffers are used [56]. They are respectively transparent to UV light above 230 nm for EtOH and 180 nm for ACN. They also enhance mass

transfer due to their low viscosity. Additionally, they are miscible in any proportion with water.

No retention of mixtures of PAHs could be obtained on reversed phase columns coated by the sol-gel technique by using ACN or MeOH as unique component of the mobile phase. To increase the affinity of the analytes for the stationary phase, water was added to the pure organic solvents in proportions ranging from 0 to 100% (v/v). This addition strongly influenced the EOF (Figs. 8.1, 8.2).

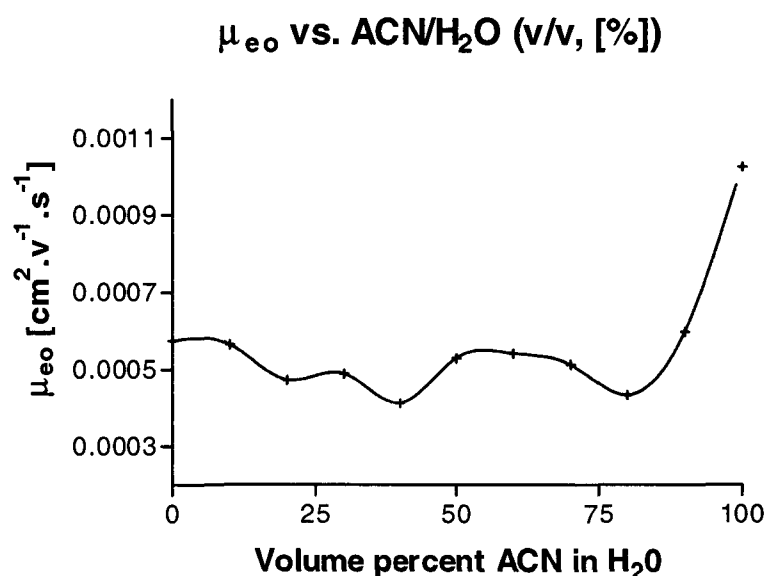


Fig. 8.1: Influence of the mobile phase constitution on the electroosmotic mobility of the EOF with ACN as an organic modifier.

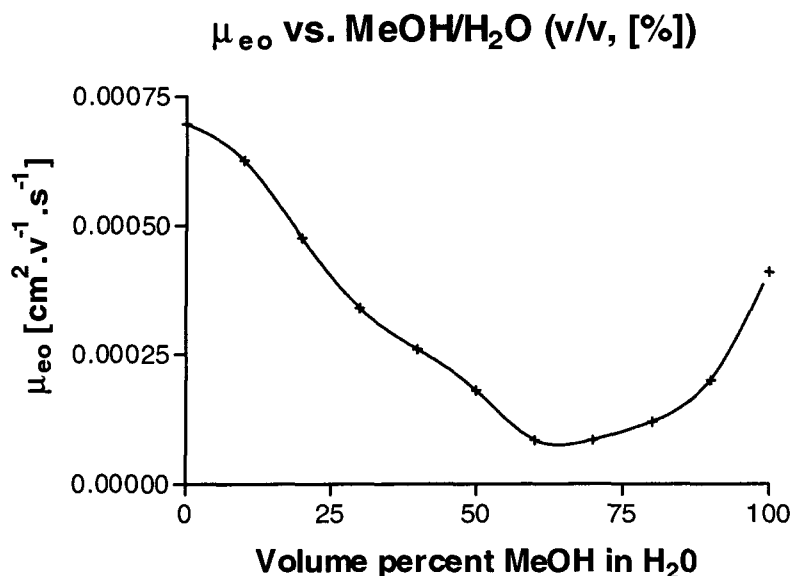


Fig. 8.2: Influence of the mobile phase constitution on the electroosmotic mobility of the EOF with MeOH as an organic modifier.

The electroosmotic mobility does not vary linearly with the amount of water added. This effect cannot be attributed solely to changes in the viscosity, as expected from the bell shaped curves of the viscosity vs. percent of water [12, 56, 116]. The behavior of μ_{eo} can be explained by the modification of the zeta potential and therefore by the modification of the structure of the double layer at the interface between the stationary phase and the mobile phase.

The electroosmotic flow was observed to be higher with ACN than with MeOH. Additionally, ACN is more transparent to UV light. Throughout this work ACN was used as the organic modifier of the mobile phases.

The addition of water to ACN, aiming to improve the electrochromatographic separation of a mixture of PAHs, was only found to be effective in a narrow concentration range (Fig. 8.3). By comparison, EtOH exhibits a broader range of effective concentrations.

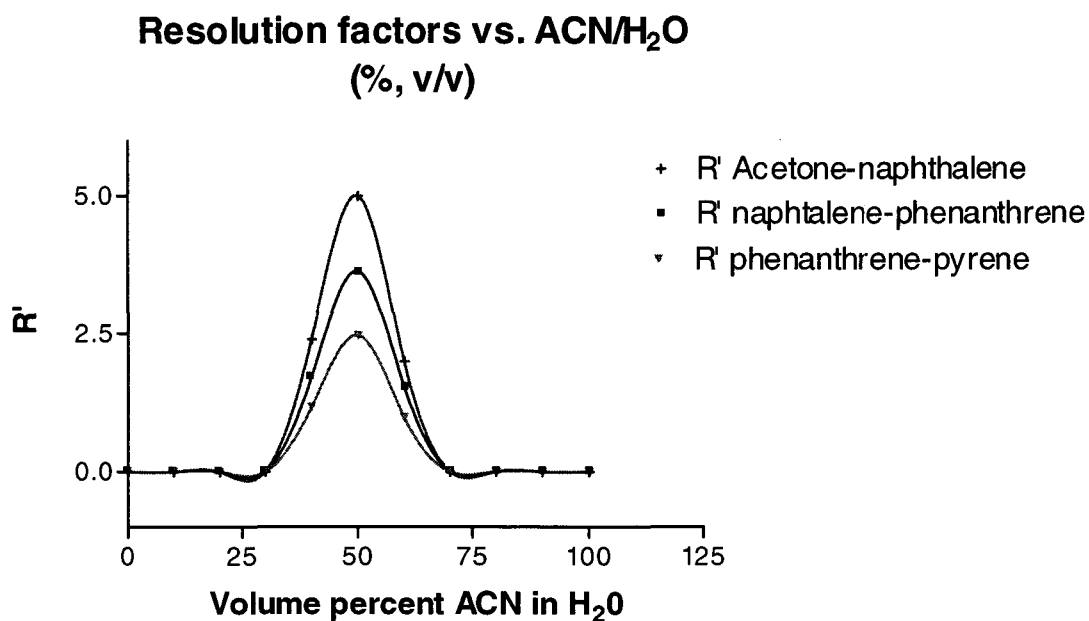


Fig. 8.3: Electrochromatographic separation of the test sample components. Conditions: coated capillary with TEOS, octyltriethoxysilane ($R=40\%$), H₂O ($H_r=100\%$), EtOH ($R_s=40\%$), HCl ($10^{-1}M$). Applied voltage 30 kV.

The PAHs are only separated with the following percentage of solvent/H₂O volume ratios: $40\% < \text{ACN}/\text{H}_2\text{O} < 60\%$ and $40\% < \text{MeOH}/\text{H}_2\text{O} < 70\%$. At higher ACN or MeOH concentration, all analytes co-elute. With 100% ACN or MeOH, a single peak is obtained occurring with the electroosmotic flow marker, indicating a lack of retention and therefore a high affinity of the analytes for the mobile phase. When the concentration of water increases, the mobile phase becomes too polar to afford a good solubility for the PAHs. This can even lead to a lack of dissolution. In such cases, the affinity of the analytes for the stationary phase is tremendously increased and the PAHs are not eluted. Therefore, to achieve good resolution as well as quick runs, a mixture of ACN/H₂O (1:1, v/v) was employed throughout this work to study the electrochromatographic separation of the PAHs.

When biological substances are to be analysed, the control of their charge is a key parameter in CEC, since it influences the electrophoresis. Buffered hydroorganic phases are required. Though, one must pay attention to the nature and the concentration of the buffer. The buffer can experience different

solubilities and not all mobile phases can be used. As an example, the mobile phases made with MeOH or ACN in water at different concentrations were tested with regards to their solvent power for a phosphate buffer. The solubility was indirectly monitored at 208 nm by diffraction using a spectrophotometer (Fig. 8.4).

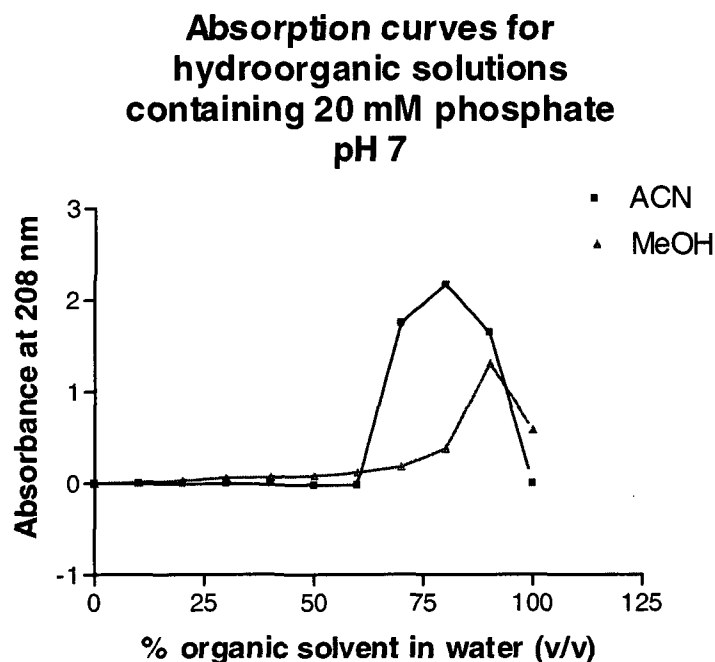


Fig. 8.4: Absorption of UV light at 208 nm in different hydroorganic mobile phases containing a 20 mM phosphate solution pH 7. Pure buffer was used as reference.

The absorption at 208 nm corresponds to light diffraction from the phosphate that precipitates. For the same organic solvent/water ratio, the absorption is only detected at 60% (v/v) for ACN, and at 20% for MeOH. At high ratios in Fig. 8.4, a peak is observed. The apex of these peaks indicates the maximum solubility of the phosphate. The decreasing slope corresponds to the precipitation of the buffer.

Since ACN is a better solvent than MeOH for phosphate, ACN is recommended if buffered mobile phases are to be employed. This difference in solvent power might be explained by the higher dielectric constant of ACN.

8.1.2- Electrolytes.

The ionic strength was observed to strongly affect the electrochromatographic separations. The separations performed with buffered mobile phases were observed to deteriorate with regard to the corresponding separations done without any supporting electrolyte (Fig. 8.5, 8.6). To study the buffer effect on the electrochromatographic separations, buffers with a pH lower than 8 were chosen because they are less aggressive than higher pH values in the case of silica based stationary phases [35, 58].

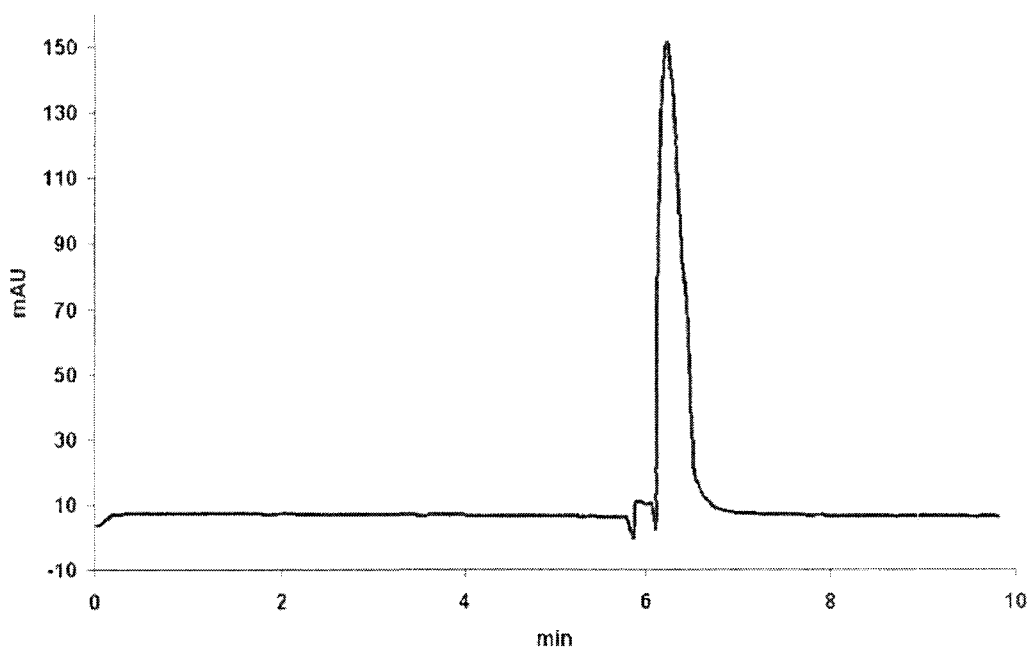


Fig. 8.5: Electrochromatographic separation of the test sample. Mobile phase ACN/H₂O (1:1, v/v) with 20 mM phosphate buffer pH 7. Capillary length 57 cm (50 cm from the injection point to the detection point). Hydrodynamic injection (1s, 1.36 b). Applied voltage 25 kV.

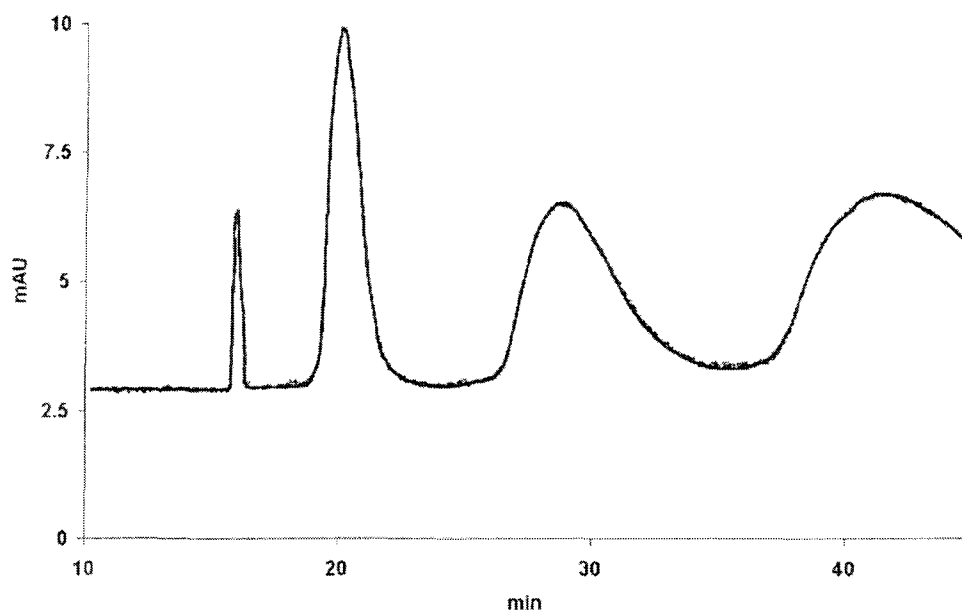


Fig. 8.6: Electrochromatographic separation of the test sample. Mobile phase MeOH/H₂O (1:1, v/v) with 20 mM phosphate buffer pH 7. Capillary length 57 cm (50 cm from the injection point to the detection point). Hydrodynamic injection, (2 s; 1.36 b). Applied voltage 25 kV.

It should be noted that the separation of the PAHs is more affected by the presence of the buffer in the mobile phases containing ACN/H₂O than in MeOH/H₂O. No quantitative result could be obtained due to the impossibility of integrating the overlaid peaks. However, increasing the buffer concentration clearly increases detection time, as expected by the theory, but also severely deteriorates the separation. The efficiency being dramatically lowered by any increase of the buffer concentration, it is therefore recommended to work at the lowest concentration still compatible with the system. Crego and co-workers who also reported this phenomenon, proposed to use a buffer concentration of 1 mM [58]. This assumption is realistic with un-ionisable analytes, but seems out of range with ionisable analytes where the buffer capacity might be quickly exhausted.

To ensure a minimum conductance of the hydroorganic mobile phase, inorganic salts were added at low quantities. This tiny doping was mandatory in order to avoid malfunction of the CEC operating system caused by an electric shut down. Different salts were tested; including: LiCl, NaCl, KCl, and

NaNO_3 . It was observed that for the same salt concentration, an increase in the size of the monovalent cation resulted in a decrease of the EOF [117]. Therefore LiCl would be ideal. However, NaCl was used instead for availability reasons. The use of NaNO_3 as electrolyte in the mobile phase generates a lower electroosmotic flow than with NaCl . Nevertheless, the use of this salt gives an injection double peak which can be helpful for the determination of the electroosmotic flow (Fig. 8.7).

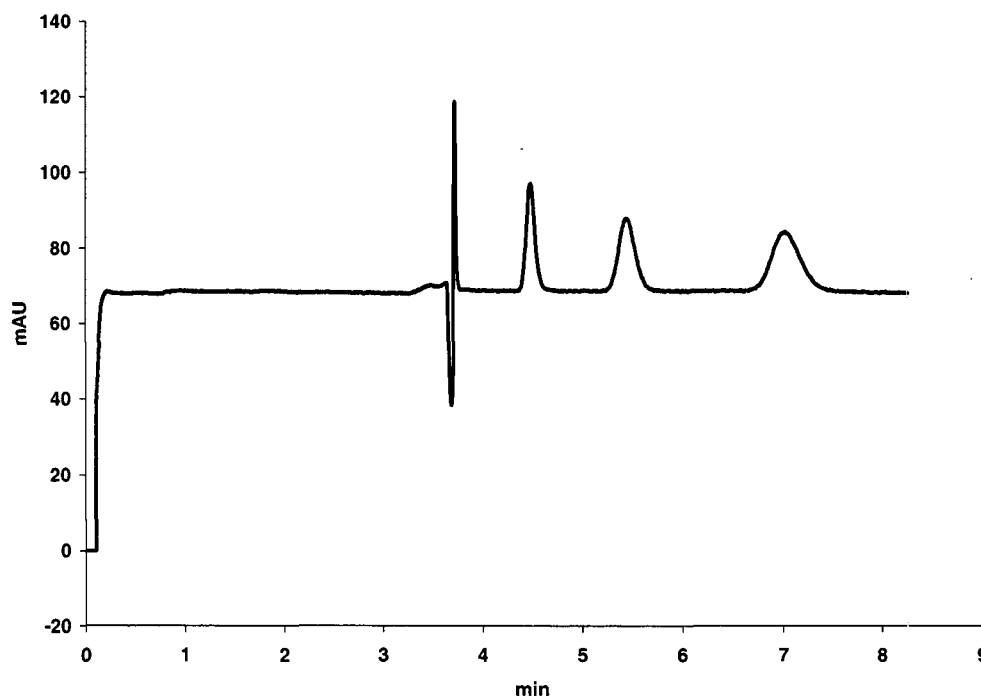


Fig. 8.7: Electrochromatographic separation of the test sample Stationary phase: TEOS, octyltriethoxysilane ($R=40\%$), H_2O ($H_r=100\%$), HCl (final concentration 10^{-1} M). Capillary length 47 cm (40 cm from the injection point to the detection point), I.D. 50 μm . Applied voltage 30 kV.

It was found that a minimum NaCl concentration of 2 mM was mandatory to avoid electric shut down of our CEC system. The conductance of the mobile phase can be further improved by increasing the electrolyte concentration but the reproducibility is simultaneously reduced. In all observed separations, a strong baseline distortion occurred between successive runs with $[\text{NaCl}]=5$ mM, but the detection times remained constant (Fig. 8.8). The resolution of PAHs was also noted to be strongly dependent on the NaCl concentrations. However, no general tendency can be pointed out, since the selectivity varied

markedly with different NaCl concentrations (Figs. 8.9 to 8.12). This effect was seen even with equilibration times of more than 1 h.

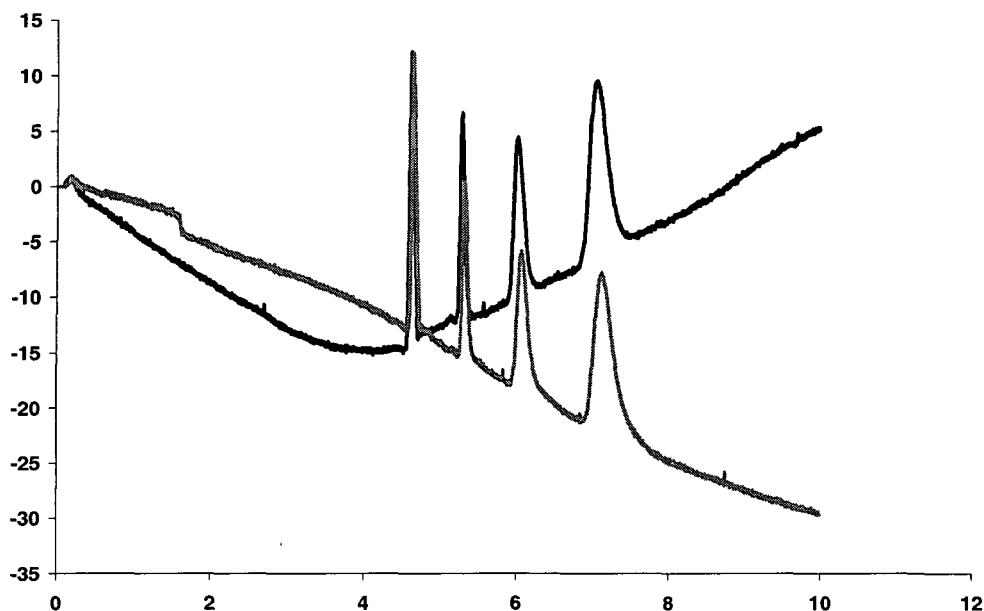


Fig. 8.8: Two successive electrochromatograms of the test sample. Synthesis of the sol: TEOS, octyltriethoxysilane ($R_s=30\%$), H_2O ($H_r=100\%$), HCl (final concentration 10^{-3} M). Mobile phase ACN/ H_2O (1:1, v/v) containing NaCl (5 mM). Electroosmotic flow marker DMSO 5 mM. Capillary length 67 cm (60 cm from the injection point to the detection point). Hydrodynamic injection, 1s. Applied voltage 25 kV. Detection at 208 nm.

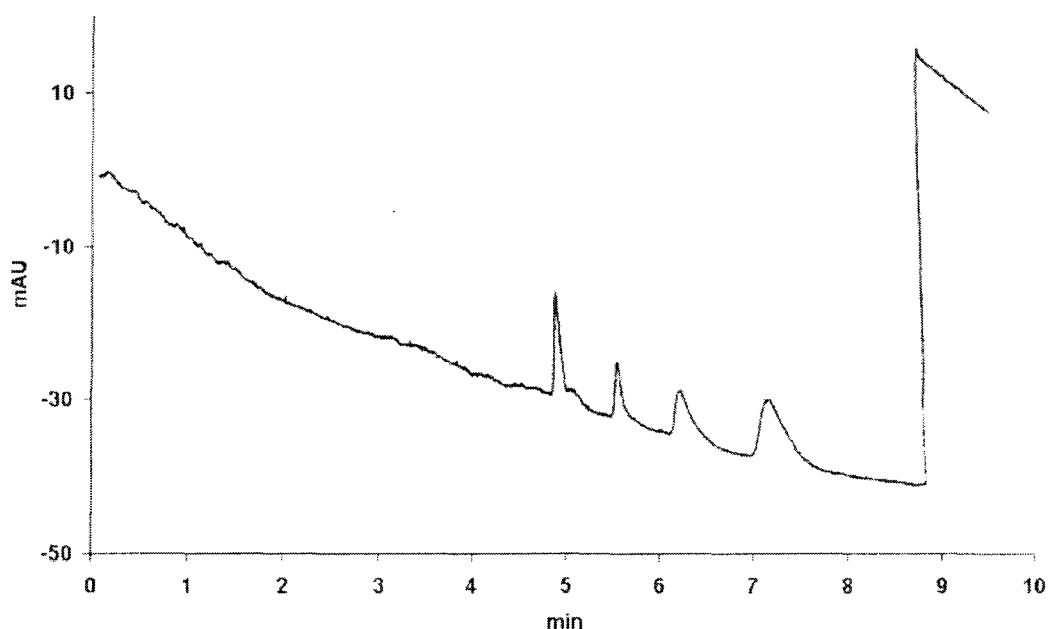


Fig. 8.9: Electrochromatogram performed with the same column and conditions as for Fig. 8.8 except for $[NaCl] = 10$ mM.

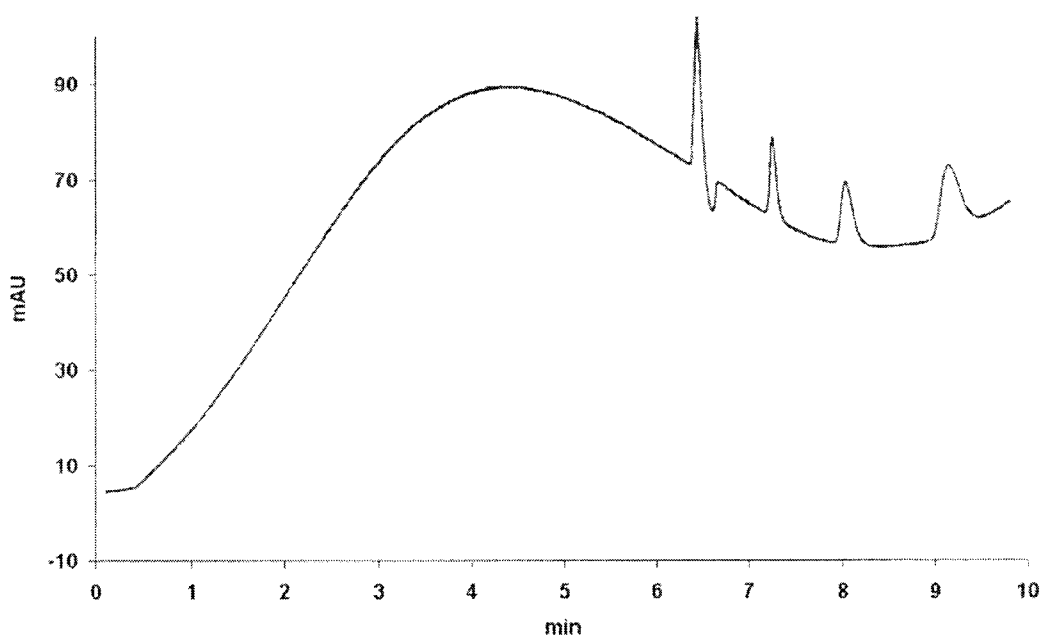


Fig. 8.10: Electrochromatogram performed with the same column and conditions as for Fig. 8.8 except for $[NaCl] = 20\text{ mM}$.

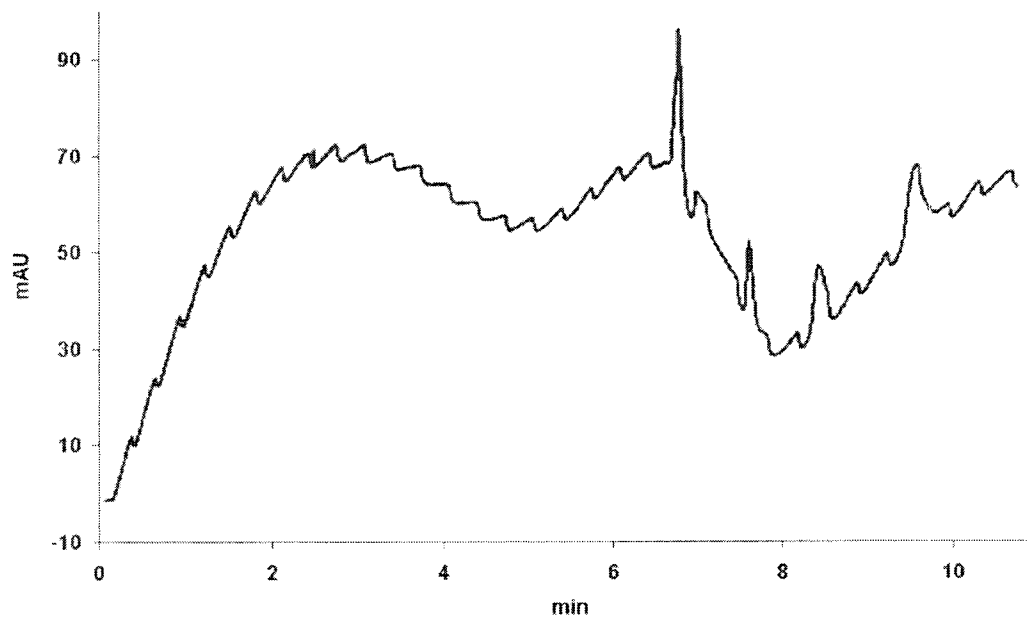


Fig. 8.11: Electrochromatogram performed with the same column and conditions as for Fig. 8.8 except for $[NaCl] = 30\text{ mM}$.

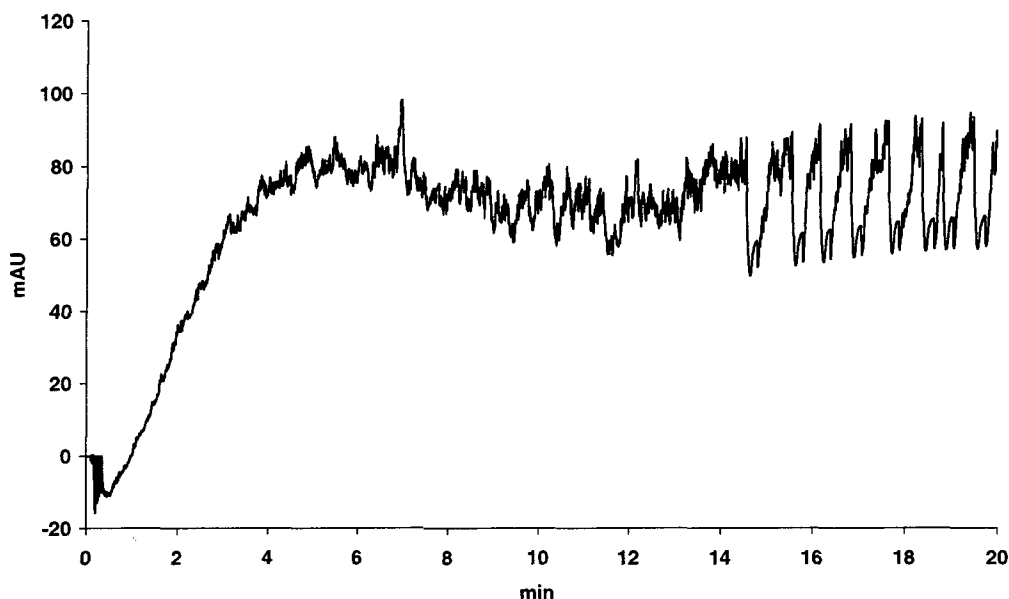


Fig. 8.12: Electrochromatogram performed with the same column and conditions as for Fig. 8.8 except for $[NaCl] = 40$ mM.

8.2- Applied Voltage.

The applied voltage plays a crucial role in CEC since it affects the EOF and therefore the velocity of the mobile phase (Fig. 8.13). The velocity of the mobile phase affects in turn the separation in CEC, as in any chromatographic process. As shown in Fig. 8.14, the resolution is lowered when the mobile flow velocity is increased. To evidence this deterioration of the electrochromatographic separations, efficiencies were plotted against the EOF velocity. A typical graph is presented in Fig. 8.15 for 3 OTCs exhibiting different roughness of the fused capillary wall. OTC₁ (L=90 cm) had a rough surface obtained by an etching with NH_5F_2 (see chapter 3.3) while OTC₂ and OTC₃ (L=47 cm each) had a smooth surface.

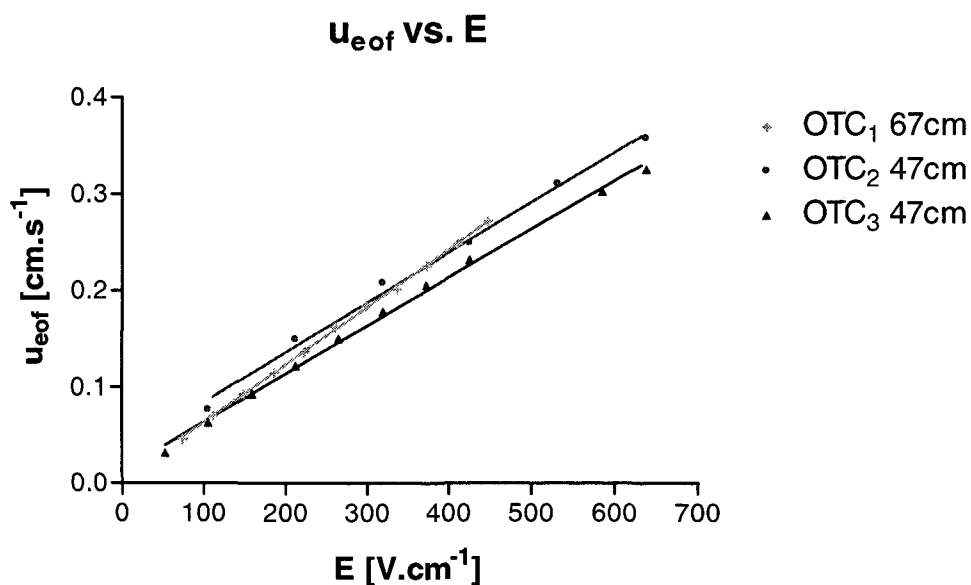


Fig. 8.13: Influence of the applied electric field on the EOF velocity.

$$\text{OTC}_1: u_{eof} = 6.10^{-4} \cdot E + 3.018 \cdot 10^{-3}; \quad r^2 = 0.9995$$

$$\text{OTC}_2: u_{eof} = 5.189 \cdot 10^{-4} \cdot E + 3.23 \cdot 10^{-3}; \quad r^2 = 0.9941$$

$$\text{OTC}_2: u_{eof} = 5.016 \cdot 10^{-4} \cdot E + 1.31 \cdot 10^{-3}; \quad r^2 = 0.9969$$

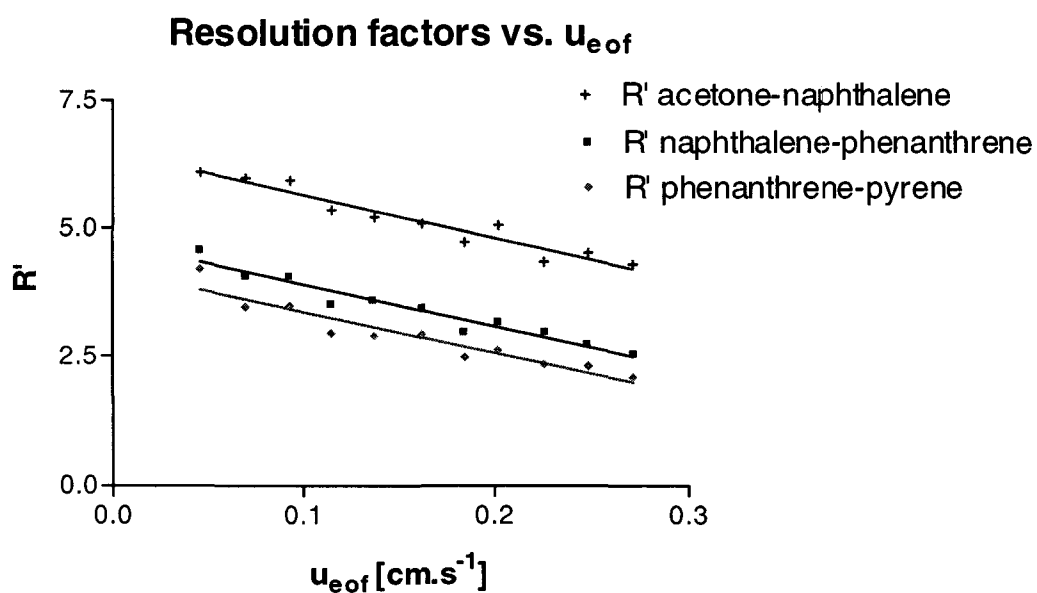


Fig. 8.14: Influence of the EOF velocity on the resolution factors.

$$R'_{\text{acetone-naphthalene}} = -8.42 u_{eof} + 6.49; \quad r^2 = 0.9288$$

$$R'_{\text{naphthalene-phenanthrene}} = -8.24 u_{eof} + 4.73; \quad r^2 = 0.9457$$

$$R'_{\text{phenanthrene-pyrene}} = -8 u_{eof} + 4.165; \quad r^2 = 0.9011$$

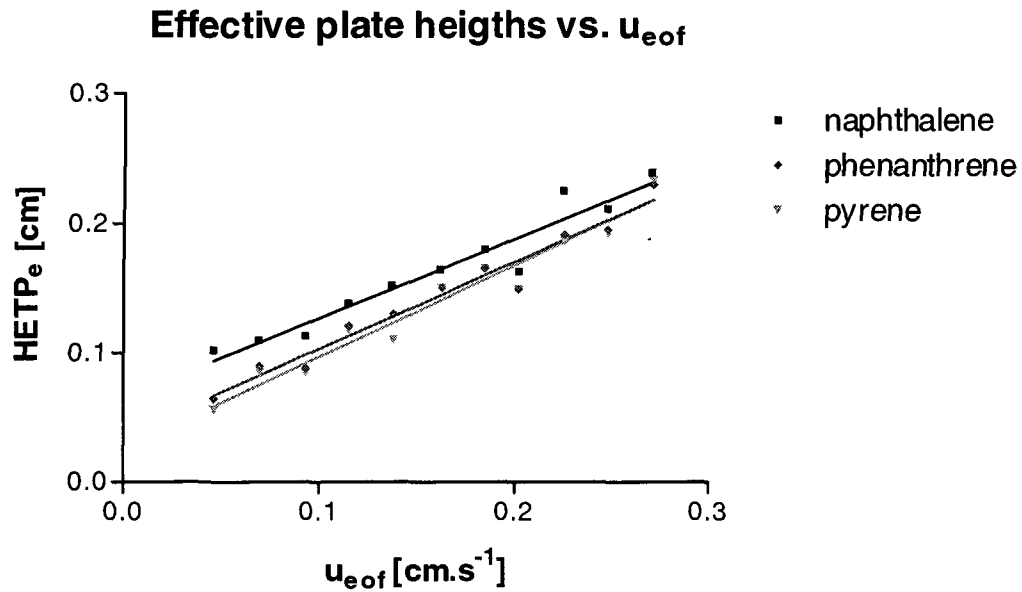


Fig. 8.15: Influence of the EOF velocity on the $HETP_e$.

$$\begin{aligned}
 HETP_{e \text{ naphthalene}} &= 612 \cdot 10^{-3} u_{eof} + 53.2 \cdot 10^{-3}; \quad r^2 = 0.9321 \\
 HETP_{e \text{ phenanthrene}} &= 672.2 \cdot 10^{-3} u_{eof} + 35.59 \cdot 10^{-3}; \quad r^2 = 0.9612 \\
 HETP_{e \text{ pyrene}} &= 706.7 \cdot 10^{-3} u_{eof} + 26.03 \cdot 10^{-3}; \quad r^2 = 0.9544
 \end{aligned}$$

According to Fig. 8.15, a three-fold increase in u_{eof} would lead to a two-fold increase of the $HETP_e$. This result is unexpected with OTCs because small variation of the efficiencies are theoretically obtained when the velocity of the mobile phase is increased. This contradictory result can be explained by the large diameter of the capillaries used in this work. The diameter of a capillary (d_c^2) being a square parameter in the definition of the HETP (eq. 2.25), lower efficiencies are expected for the widest columns. Since the velocity of the EOF is used to multiply the term containing d_c^2 in eq. 2.25, the efficiencies of large columns become particularly low at high velocity of the mobile phase.

The experimental determination of both R' and $HETP_e$ relies on the geometrical characteristics of the electrochromatographic peaks, which are dependent on both the flow rate and the capillary length. To be independent of these characteristics, one can use the capacity factors k' , which are calculated from the detection times (eq. 2.24). The knowledge of k' yields information about the separations. Therefore the capacity factors of the test sample components are shown in Fig. 8.16.

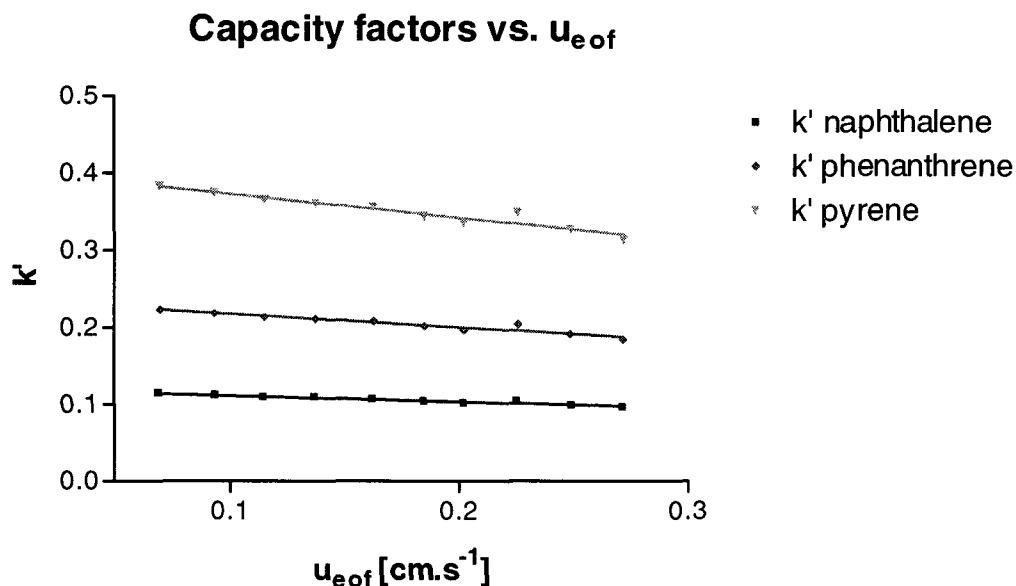


Fig. 8.16: Influence of the EOF velocity on the resolution factors.

$$\begin{aligned}
 k'_{\text{naphthalene}} &= - 74.99 \cdot 10^{-3} u_{eof} + 118.3 \cdot 10^{-3}; & r^2 &= 0.921 \\
 k'_{\text{phenanthrene}} &= - 172.2 \cdot 10^{-3} u_{eof} + 234.6 \cdot 10^{-3}; & r^2 &= 0.9255 \\
 k'_{\text{pyrene}} &= - 497.5 \cdot 10^{-3} u_{eof} + 647.8 \cdot 10^{-3}; & r^2 &= 0.955
 \end{aligned}$$

It is seen that the capacity factors decrease slightly with an increased EOF. According to eq. 2.17, this decrease leads to a diminution of the amount of sample present in the stationary phase to the profit of the amount of sample in the mobile phase.

8.3- Temperature.

The temperature affects the chemical equilibrium involved in the partitioning mechanism of reversed phase chromatography. The influence of the temperature on chromatographic separation in CEC was studied using the Peltier element housed in the P/ACE 5500 set-up. This element is able to produce a temperature between 10°C and 45°C. Therefore, the study was performed in this temperature range.

The electroosmotic mobility (Fig. 8.17), the capacity factors (Fig. 8.18), the separation factors (Fig. 8.19) and the effective plate heights (Fig. 8.20) were found to have different degrees of dependence on the temperature.

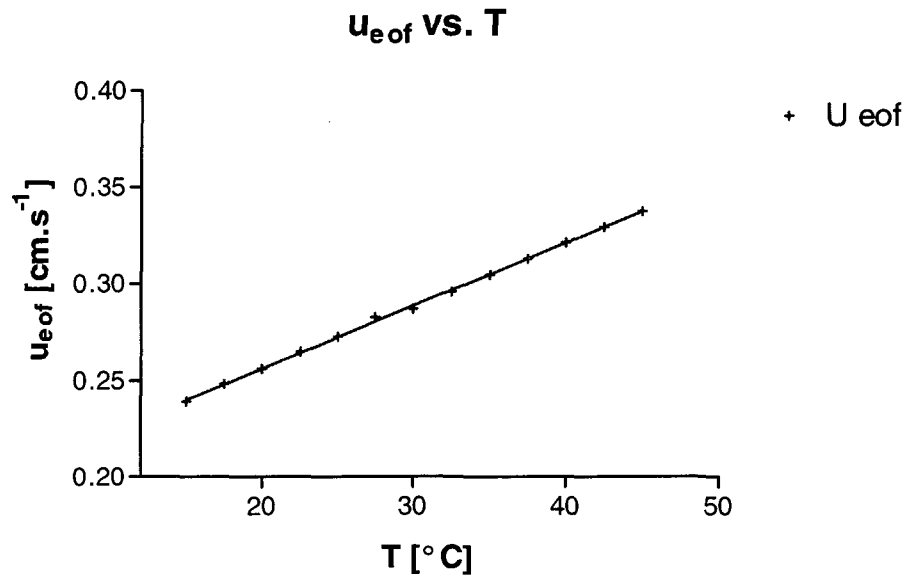


Fig. 8.17: Influence of the temperature on the electroosmotic velocity.

$$U_{eof} = 3.24 \cdot 10^{-4} T + 1.913 \cdot 10^{-1}; r^2 = 0.9992$$

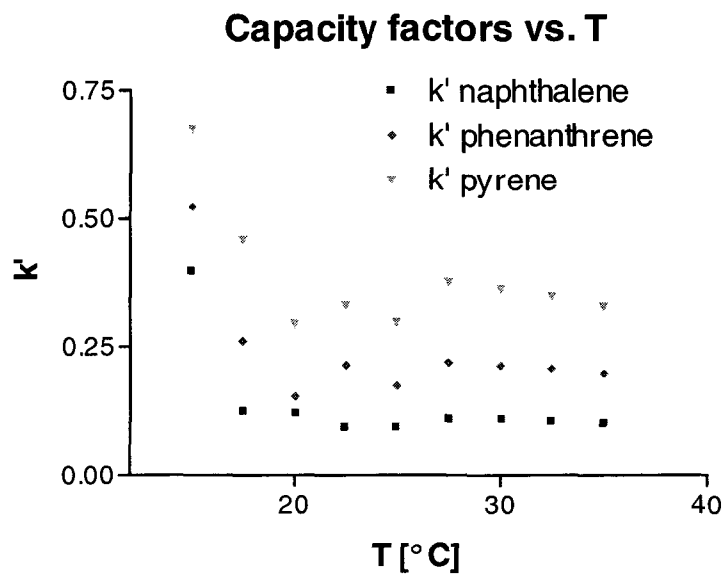


Fig. 8.18: Influence of the temperature on the capacity factors.

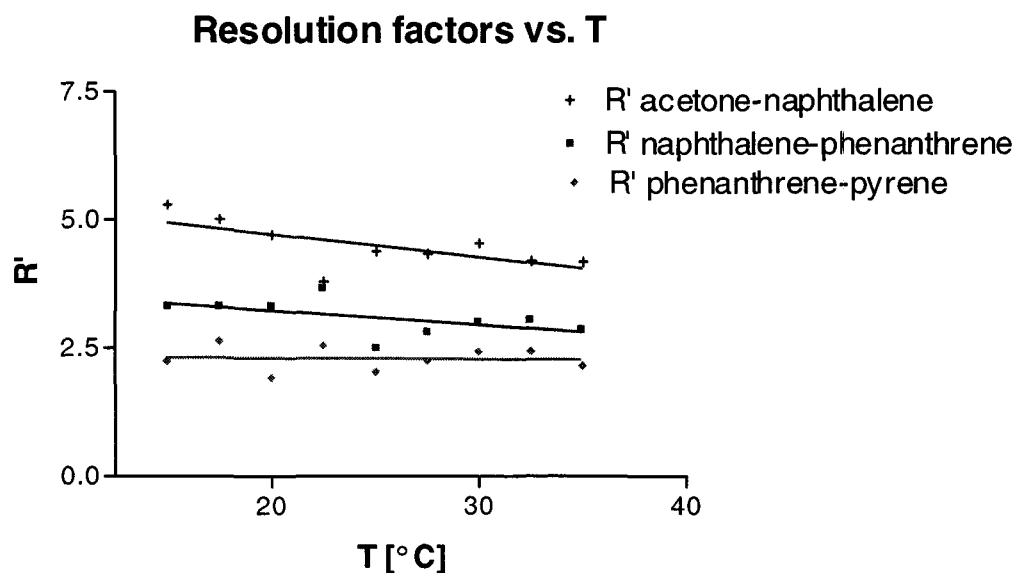


Fig. 8.19: Influence of the temperature on the resolution factor.

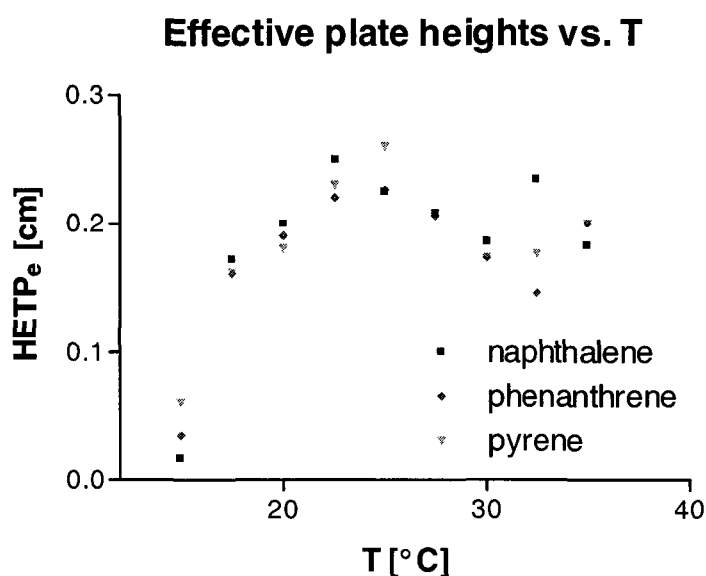
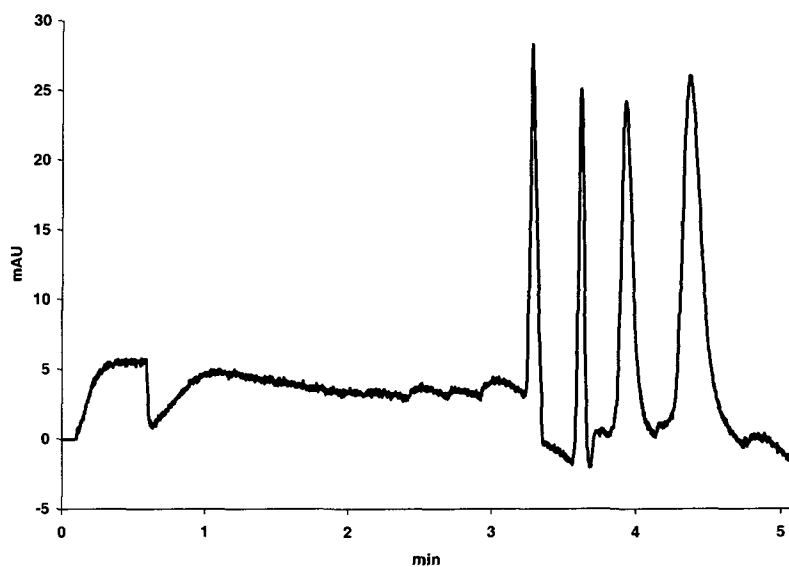


Fig. 8.20: Influence of the temperature on the effective efficiencies.

The best separations of PAHs and the lowest plate heights are obtained at low temperature, even if the EOF is comparatively low. This effect can be explained by a viscosity increase at low temperature, which limits the diffusion rate of the solutes. The longitudinal diffusion, which is a counterproductive phenomenon for the HEPT, is decreased and the dispersion of the solute bands is lowered.

It has to be remarked that the electrochromatographic runs with silica sol-gel based stationary phases should be maintained below 30°C. If this is not the case, the background noise increases dramatically. (Figs. 8.21, 8.22). A flat baseline is recovered when the temperature is lowered again.



8.21: Electrochromatogram at 35°C.

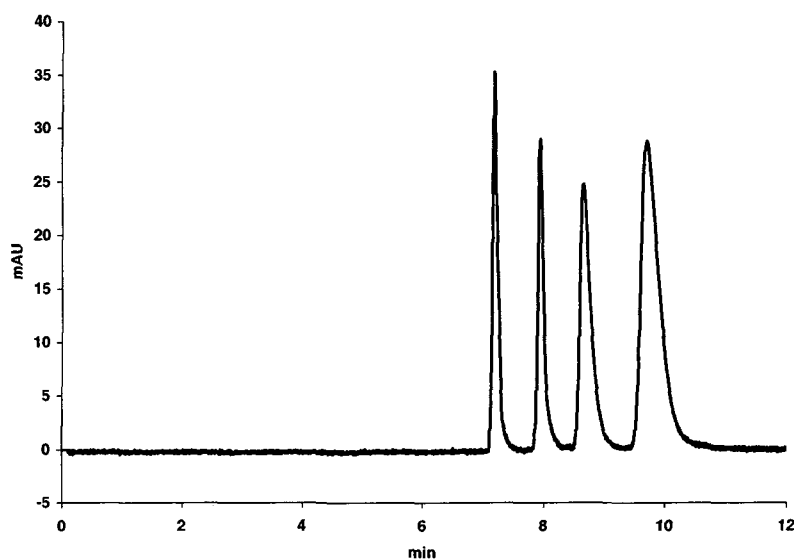


Fig. 8.22: Electrochromatogram taken at 15°C with the column used to make the Fig. 8.21.

8.4- Length of the Column.

Since the separations in CEC with OTCs are based on solute-wall interactions, the length of the capillaries influences the separation. To study this effect, OTCs of 97 cm (90 cm from injection to detection, 50 μm I.D.) were used. Between successive electrochromatographic runs, the lengths of the capillaries were reduced by cutting off 10 cm. OTCs with respective effective lengths ranging from 90 to 20 cm were thus obtained. To maintain a constant linear velocity of the mobile phase, an electric field of $309 \text{ V} \times \text{cm}^{-1}$ was applied to each column (30 kV being the highest voltage available in the electrochromatographic separation of a test mixture of PAHs).

The resolution factors related to the electrochromatographic separation are shown in Fig. 8.23.

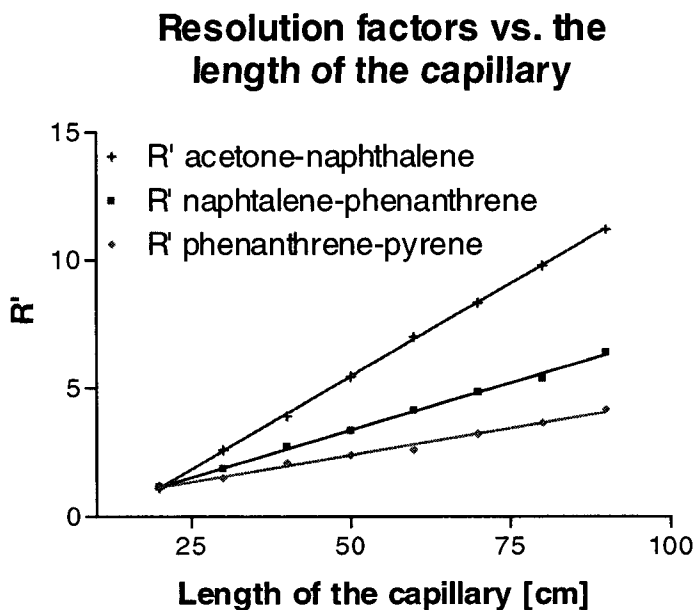


Fig. 8.23: Resolution factors of the constituents of the test mixture plotted versus the length of the capillaries.

$$R_{\text{acetone-naphthalene}} = 14.47 \cdot 10^{-2} \cdot L - 1.78; \quad r^2 = 0.9997$$

$$R_{\text{naphthalene-phenanthrene}} = 73.68 \cdot 10^{-3} \cdot L - 32.11 \cdot 10^{-2}; \quad r^2 = 0.9978$$

$$R_{\text{phenanthrene-pyrene}} = 41.88 \cdot 10^{-3} \cdot L + 30.36 \cdot 10^{-2}; \quad r^2 = 0.9893$$

The resolution factors (Fig. 8.23) are observed to increase linearly with the length of the OTCs in the electrochromatographic separations of the PAH

mixture. This indicates the same retention phenomena over the length of the entire capillary, and therefore a uniform coverage of the stationary phase.

A minimal column length is required to achieve separation of the test sample constituents. This minimal length must afford resolution factors higher than 1.5, assuming this value gives baseline resolution. Nevertheless, this assumption does not apply to our system because the retention factors in this work were calculated from the width of the peaks at half height, a calculation that does not take into account the frequent tailing effect of the PAHs' peaks observed in CEC (see appendix C). To get baseline separated peaks in the minimum analysis time, the resolution factors must be higher than 2. This value corresponds to OTCs with an effective length of at least 40 cm (from the injection point to the detection point) for the separation of PAHs.

8.5- Column Inner Diameter.

The column inner diameter d_c is involved in the calculation of the efficiencies for OTCs in CEC (eq. 2.25). So far, the capillaries were 50 μm wide, which is far bigger than the theoretical optimal value of 10 μm for CEC. However, this diameter was kept because former research [118, 119], based on the work of Schurig et al. [120], has proven the feasibility of working with 50 μm wide capillaries for OTC-CEC. Such capillaries are convenient since low back pressure is required to fill them in a relatively short time.

The capillary inner diameter has been proven to be of paramount importance in the preparation of OTC for CEC. This parameter strongly influences the efficiencies of the column via a square parameter in the Van-Deemter equation (eq. 2.25). Therefore, the efficient separation of PAH mixture are expected to be improved by using capillaries with a diameter smaller than 50 μm .

It was found that none of the techniques suitable for coating 50 μm bore capillaries, including both methods at pH 1 or 3 at room temperature, with the heated sol method, was applicable to smaller bore capillaries. The limitation

arises mainly from a pronounced tendency of the stationary phase to detach from the capillary surface and to form plugs that prevent any further use of the OTCs (Fig. 8.24).

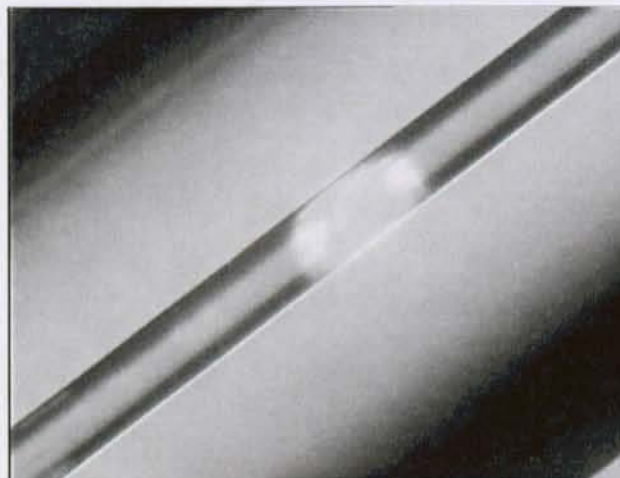


*Fig. 8.24: Plug made by a detached piece of the ormosil stationary phase in a 25 μm I.D. capillary. To make the plug fluorescent, the stationary phase was doped with fluorescein, then a contact with a basic solution was carried out.
(Optical microscopy $\times 100$, transmittance mode, UV light)*

Plugs were mainly formed when high pressure was applied to the capillaries. To prevent this from occurring, a mechanically more stable structure had to be obtained. It was found that etching the capillaries with NH_5F_2 , prior to the coating procedure, made the stationary phases sufficiently resistant to the liquid flows.

To study the influence of the diameter on the separations, capillaries with internal diameters of 10, 25, 50 μm were first etched with NH_5F_2 then treated with an alkaline wash in order to increase the surface density of the silanol groups. The capillaries were subsequently coated with aliquots of sols taken from the same stock solution. It was noticed that due to their reduced diameter, 10 μm capillaries did not withstand voltages higher than 18 kV. To allow the use of higher voltage, the usual NaCl concentration of 2 mM had to be increased. This was not done since the resolution of the PAH is deteriorated by further addition of an electrolyte. A 15 kV applied voltage was therefore used for every run. For all the runs, aliquots of the same PAH test

mixture were injected. The injections were performed hydrodynamically for the 50 μm capillaries and electrokinetically for 10 and 25 μm capillaries. Typical electrochromatograms are shown in Fig. 8.25, 8.26, 8.27. For all capillaries, the length was 47 cm (40 cm from the injection point to the detection point).

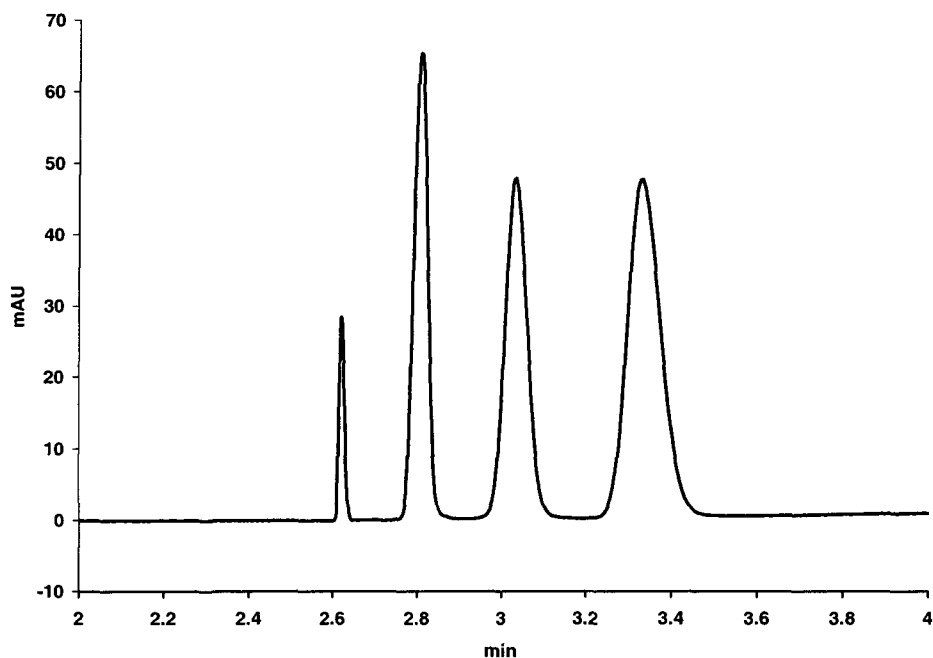


Fig. 8.25: Electrochromatogram of the test mixture. Mobile phase ACN/H₂O (1:1, v/v) containing NaCl (2 mM). Hydrodynamic injection 1 s, 1.36 b. Capillary I.D. 50 μm .

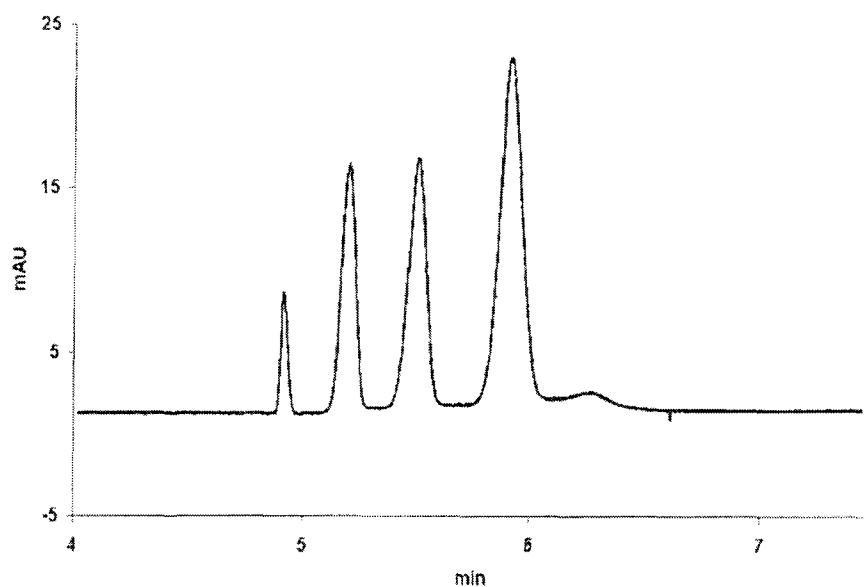


Fig. 8.26: Electrochromatogram of the test mixture Mobile phase ACN/H₂O (1:1, v/v) containing NaCl (2 mM). Electrokinetic injection: 5 s at 10 kV. Capillary I.D. 25 μm .

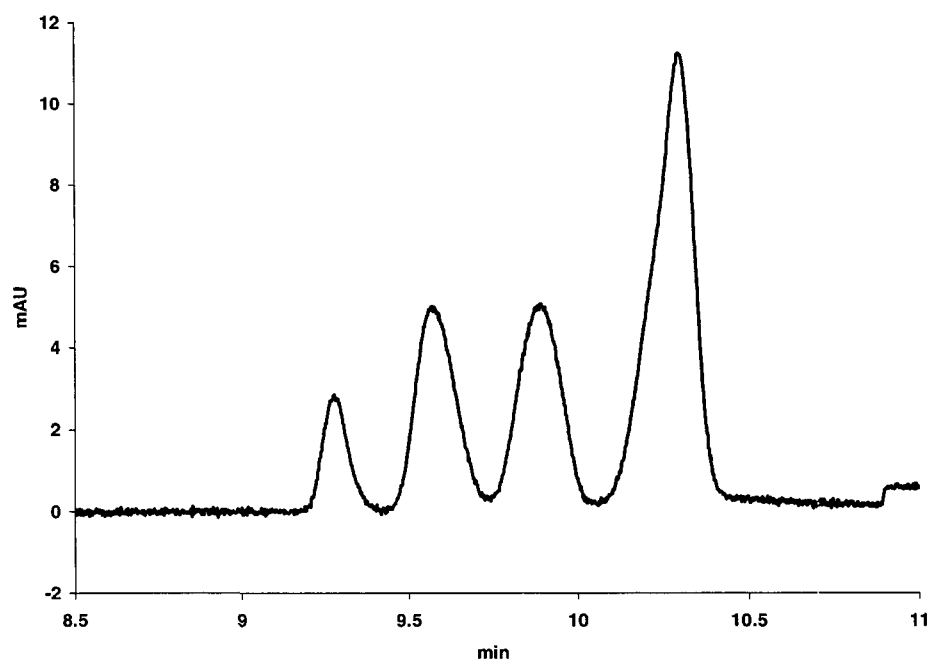


Fig. 8.27: Electrochromatogram of the test mixture Mobile phase ACN/H₂O (1:1, v/v) containing NaCl (2 mM). Electrokinetic injection: 5 s at 10 kV. Capillary I.D. 10 μ m.

Figs. 8.28 to 8.31 summarize the effect of the capillary inner diameter on the EOF (Fig. 8.28), the resolution factors (Fig. 8.29), the capacity factors (Fig. 8.30) and the effective HETP_e (8.31).

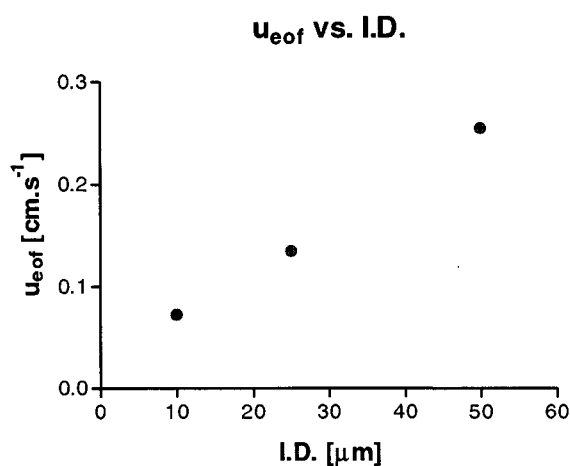


Fig. 8.28

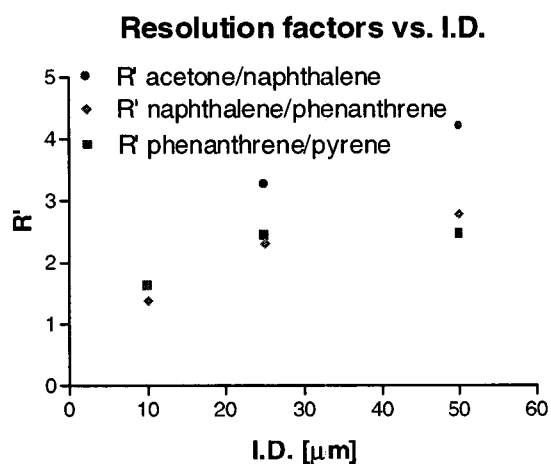


Fig. 8.29

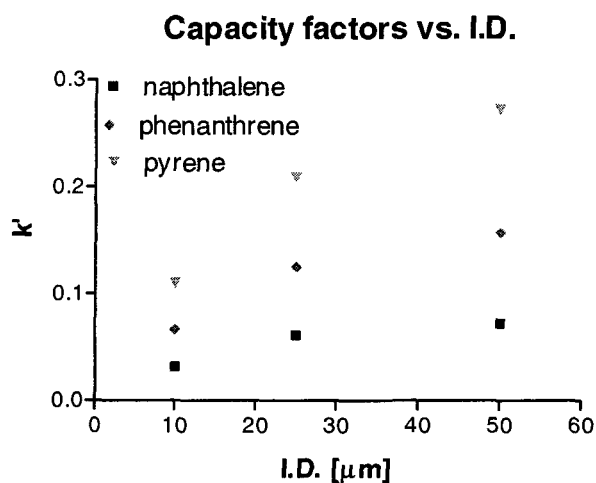


Fig. 8.30

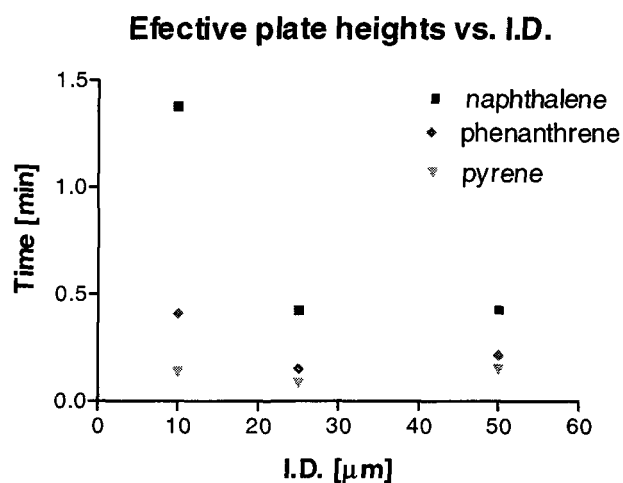


Fig. 8.31

According to the above diagrams, the reduction of the capillary inner diameter does not lead to any improvement in the electrochromatographic separation of a mixture of PAHs. It can be seen in Fig. 8.28 that the EOF is highest in the columns with the largest inner diameter. To obtain an equivalent flow rate of the mobile phase, with small and wide bore capillaries, the electrolyte concentration must be increased for capillaries in smaller inner diameters. However, this is not applicable in the establishment of the differences between the three kinds of capillaries studied, because ionic strength of the mobile phase also affects the electrochromatographic separations.

The separation of neutral compounds by CEC with ormosil xerogel layers is not improved by the use of capillaries with inner diameters below 50 μm . Furthermore, the preparation of OTCs, via the sol-gel approach in small bore capillaries, especially the 10 μm ones, implies several steps (etching with NH_5F_2 , treatment to increase the surface silanol groups, coating, chemical stabilization, drying) that gives a poor yield of success. It is estimated that only 20% of the 10 μm capillaries could be used, versus close to 100% of the 50 μm ones. Plugging was the main problem to overcome.

8.5- Thickness of the Coating.

The analytes in OTC-CEC move by diffusion into or onto the stationary phase. Therefore, the thickness of the stationary phases in OTCs affects the efficiency of the separation (see eq. 2.25). This parameter was studied.

Coatings of two different thickness are possible with the ormosil sols (see chapter 5.1):

- Thin coatings ($< 0.01 \mu\text{m}$, not visible via SEM) are obtained via the dynamic coating process.
- Thick coatings ($\approx 0.1 \mu\text{m}$) are obtained by the static coating method (Fig. 8.32). The solvents are removed by placing the capillaries in a vacuum oven (1h00, 120°C , 20 mB).

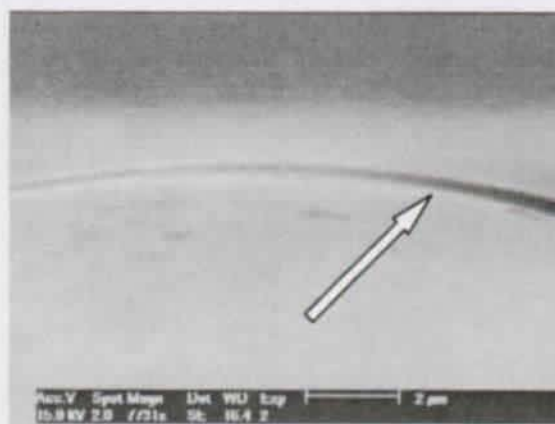


Fig. 8.32: Stationary phase layer made by the static coating method. SEM, magnification $\times 7731$, bar scale $2 \mu\text{m}$.

A spinnable sol made with TEOS, octyltriethoxysilane ($R=40\%$), EtOH ($R_s=30\%$), H_2O ($H_r=100\%$), HCl (final concentration 10^{-1} M), was prepared. Thin and thick coating were made according to the two coating methods in 77 cm columns (70 from the injection point to the detection point, I.D. $50 \mu\text{m}$). Electrochromatographic separations of a PAHs mixture were achieved at 30 kV. Samples: naphthalene, phenanthrene and pyrene 10 mM each in ACN/ H_2O (9:1, v/v). Thiourea (30 mM) was used as an electroosmotic flow marker. Figs. 8.33 to 8.36 show several chromatographic parameters versus the thickness of the stationary phase.

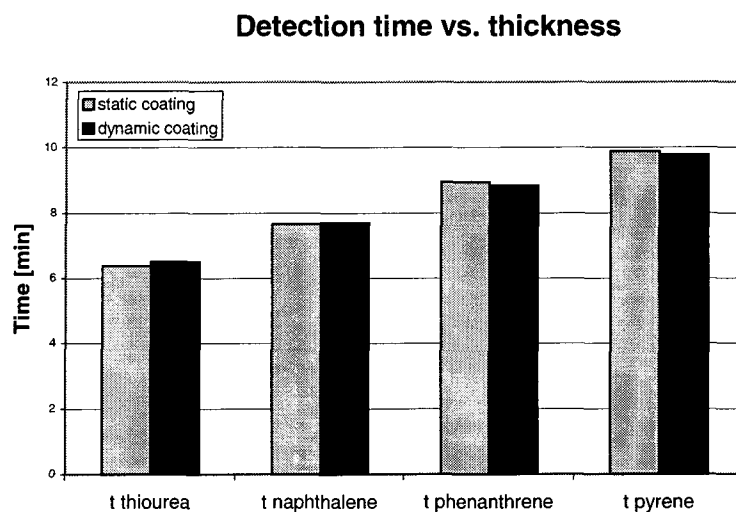


Fig. 8.33: Detection time plotted vs. thickness of the stationary phase.

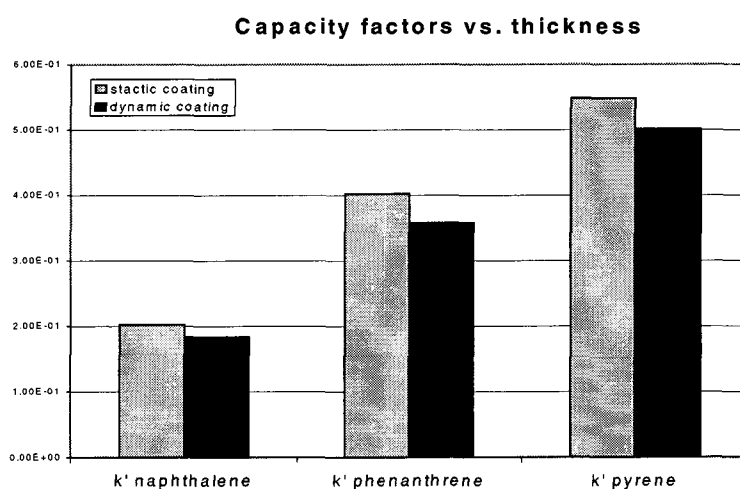


Fig. 8.34: Capacity factors plotted vs. the thickness of the stationary phase.

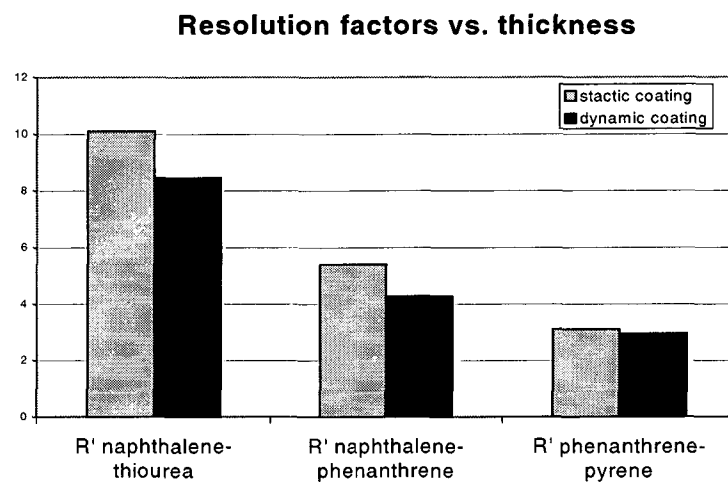


Fig. 8.35: Resolution factors plotted vs. the thickness of the stationary phase.

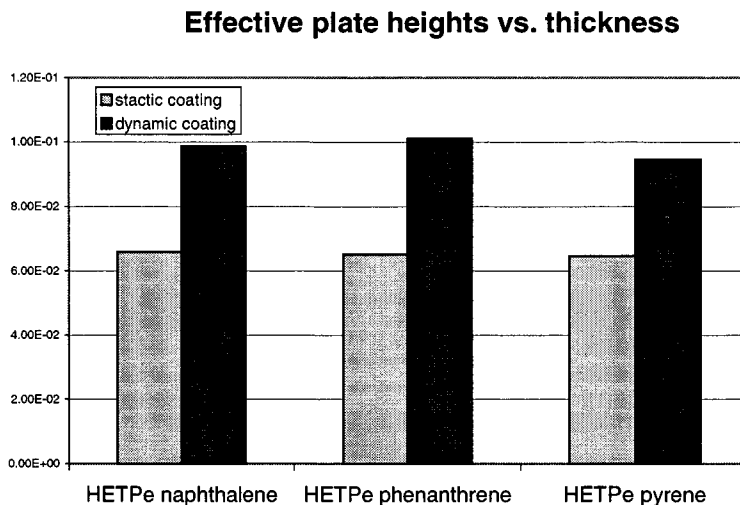


Fig. 8.36: $HETP_e$ plotted vs. the thickness of the stationary phase.

According to Fig. 8.33, the thickness of the stationary phase does not contribute to a major difference in the PAHs' detection time, as the detection times are almost the same between thick and thin stationary phases. The differences observed on Fig. 8.36 for the $HETP_e$ arise from a difference in the peak widths of the two kinds of coatings. Thin stationary phases were observed to give broader peaks than the thick ones.

According to equation 2.25, the use of thick stationary phase layers is not recommended since they increase the height equivalent of a theoretical plate. However, it was observed that the selectivity of the PAHs separation was better with such coating.

8.7- Conclusions.

In this chapter, the optimization of several factors influencing the electrochromatographic separation has been performed. From these results, several recommendations can be proposed for the CEC conditions. The mobile phase should be a hydroorganic solution made of ACN/H₂O containing NaCl in a concentration able to generate the minimum conductivity required to run the electrochromatographic set-up. If this condition is not fulfilled, i.e. in the case of an electrolyte concentration higher than 5 mM, the resolution in the separation of neutral analytes is lowered.

The temperature at which the separation is done should be low, as well as the voltage applied during a run if high resolutions and high efficiencies are needed to achieve a separation. We found the best conditions for the separation of neutral compounds at 15°C. The choice of an applied voltage depends on the residence time of the analytes in the column, a parameter that affects the diffusion. Since the best resolutions are obtained at low voltage, their use is recommended. However, such low voltages translate into long times required to achieve the complete separation. If we take into consideration the diffusion and the time required to achieve a separation, we can recommend, as a compromise, to work at 15°C with an applied voltage of 15 kV. The geometry of the OTCs has a marked effect on the electrochromatographic separation. Since the best resolutions are obtained with long columns having a large I.D., columns longer than 40 cm and with an I.D.=50 μm should be used. This result contradicts the theory that columns of 10 μm or below are best suited for the separations. However, one has to keep in mind the problems arising from the difficulty of making reproducible columns with an I.D. smaller than 50 μm , which can lead to poor interpretation of the diameter effect. According to our results, thick coatings ($\approx 0.1 \mu\text{m}$) produced by the static coating method are recommended for the production of OTCs. Indeed, such columns give the best efficiencies and resolutions, probably due to their enhanced capacities. This result is also surprising because the use of the thinnest stationary phases are generally assumed to give the best electrochromatographic separations.

9- CEC Micro Chips.

9.1- Introduction.

In recent years, microfabricated devices ('microchips') for bio-chemical and bio-analytical applications have been shown to be more than just an alternative to conventional (macroscopic) techniques. In the field of analytical separations, microchips have been successfully employed for free zone electrophoresis [121, 122], gel electrophoresis [123] and open-channel electrochromatography (μ -CEC) [124].

We have recently started a collaboration with the Institute of Microsystems (Swiss Federal Institute of Technology, Lausanne, Switzerland) to do CEC on a chip. The role of our laboratory consists in the developing stationary phases and coating the CEC chips, while the Institute of Microsystems is responsible for making the chips.

The main problem encountered by people who want to do CEC on a chip is the lack of instrumentation to perform both the injection and the detection. To overcome this, our idea was to use both the injection and the detection system of a commercially available set up (system P/ACE 5500 from Beckman) initially designed for capillary electrophoresis [125].

9.2- Making of the Chips.

Microchips (Figs. 9.1 and 9.2) were microfabricated from pyrex wafers by a photolithographic process followed by a HF etching step. The channels were hermetically sealed by a fusion bonding with a pyrex cover plate [126]. Both the inlet and the outlet of the chips were connected to silica capillaries using an in-house technique designed to minimise dead volume.



Fig. 9.1: CEC chip. The separation channel of the chip has been evidenced by a filling with a blue dye.

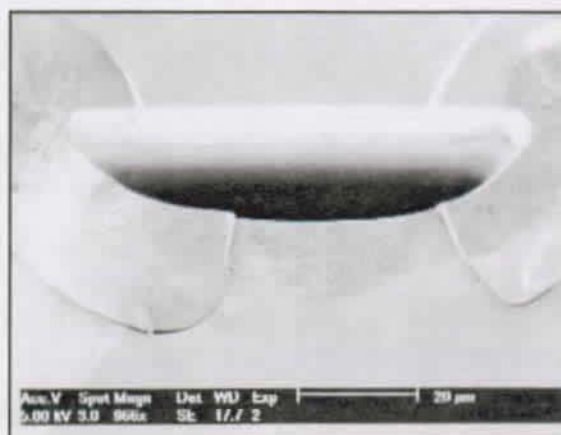


Fig. 9.2: Cross section of the CEC chip.
SEM picture. Magnification $\times 966$, bar scale $20 \mu\text{m}$

9.3- Stationary phases.

Ormosil xerogels were used as stationary phases for the CEC chip. Dynamic coatings of the separation channel were carried out with ormosil sol made with TEOS, octyltriethoxysilane ($R=40\%$), EtOH ($R_s=40\%$), H_2O ($H_r=100\%$), HCl (final concentration 10^{-1} M).

The sol was injected into the separation channel with a syringe connected to the outlet capillary of the chip via plastic tubing. When the sol was almost in

contact with the interface of the chip and its inlet capillary, the syringe was removed. The sol was allowed to stay 10 min, then the unreacted liquid was sucked out with a syringe with a fixed piston. Air was aspirated for at least 30 min to avoid plug formation, then the chip was placed in a vacuum oven (2 h, 30°C, 20 mb). The CEC chip was then mounted in the Beckman's cartridge (Fig. 9.3) and the stationary phase conditioning was performed according to the protocol described in chapter 5.2.



Fig. 9.3: CEC chip housed in the Beckman's cartridge used with the P/ACE 5500 system. The detection slit ($800 \times 100 \mu\text{m}$) of the cartridge was aligned with the outlet of the chip's separation channel to allow for detection. The cooling system of the cartridge adapted to house a chip was short-circuited to avoid leakage of the cooling liquid.

9.4- Electrochromatographic separations.

Special attention during the selection of the mobile phase was paid to the microchip's connections to the inlet and outlet capillaries, since the glue had to be chemically inert towards the mobile phase chosen. In the end, a classical mobile phase for reversed phase chromatography, which consisted of a 1:1 (v/v) mixture of acetonitrile and water, containing in addition 5 mM NaCl to avoid breakdown of the electrical current during the run, was chosen.

Pyrex tends to show a noisy baseline after irradiation with UV light for some time. This limited the detection wavelengths suitable for the CEC-chip experiments to values > 270 nm. This may in the future pose a problem for some analytes. However, for the feasibility study here, a mixture of PAHs was chosen as the standard sample for the CEC-experiments. In order to allow a comparison of the performance, the ormosil stationary phase was prepared in both a standard fused silica CE-capillary and a Pyrex microchip. The results obtained with both column types for the separation of the standard mixture were subsequently compared. Figure 9.4 shows the separation in a capillary and figure 9.5 the one obtained with the chip.

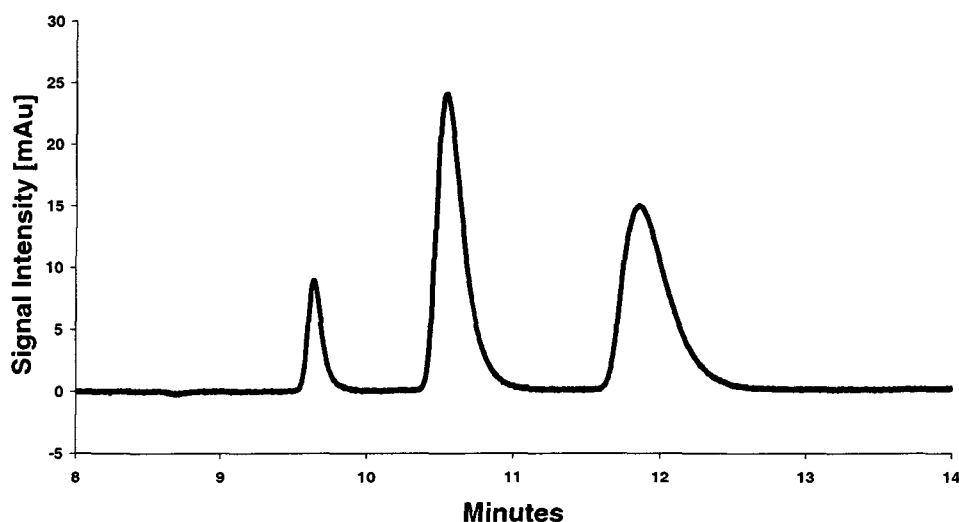


Fig. 9.4: Electrochromatogram obtained with a capillary.

Mobile phase ACN/H₂O (1:1, v/v) containing NaCl (2 mM); $E=186.5$ $V \times cm^{-1}$, hydrodynamic injection: 1 s at 1.36 b, length: 67 cm (60 cm from the injection to the detection point), inner diameter 50 μm . Detection 280 nm.

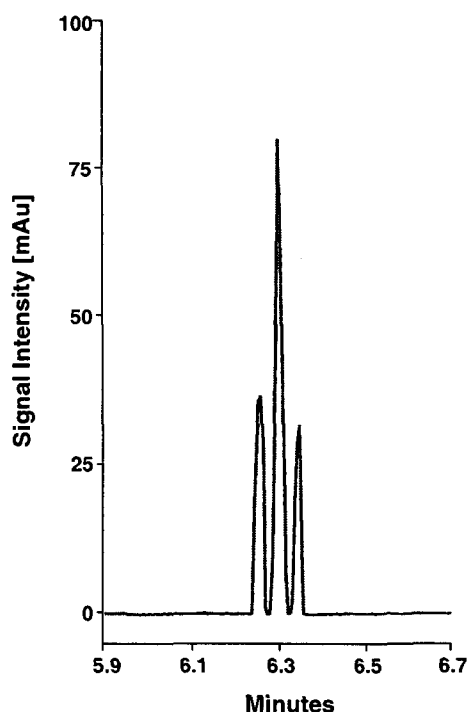


Fig. 9.5: Electrochromatogram obtained with a chip.

Mobile phase ACN/H₂O (1:1, v/v) containing NaCl (5 mM); $E=183 \text{ V} \times \text{cm}^{-1}$; hydrodynamic injection: 3 s at 1.36 b; separation channel: width 90 μm , depth 23 μm , length 60 cm, length of the capillaries: inlet 15 cm, outlet 7 cm. Detection 280 nm.

Naphthalene, phenanthrene and pyrene separated in the fused silica capillary all gave comparatively broad peaks with elution times ranging from 9.5 to 13 min. The same compounds analyzed in chips give somewhat sharper peaks with shorter elution times between 6.0 to 6.5 min. The resolution is better in the case of the capillary. However, since base-line separation is achieved in both cases, this is of no analytical advantage. Plate numbers (chromatographic efficiency) are superior in the case of the chip. But, since the mobile phase composition, the applied electric field and the injection time are slightly different, a direct comparison of these values is not possible. If anything, the separation achieved with the CEC-chip appears to be of equal quality or even slightly superior to the one obtained with the conventional capillary under optimized conditions. This could be due to the diffusion path length confronting the analytes. The fused silica capillary had a constant diameter of 50 μm , which is about twice the depth of the chip channel (23 μm). An analyte in the middle of a given separation channel will be in closer proximity to a wall in a CEC-chip.

A major worry prior to the application of the CEC-chip was the possibility of peak disturbance due to pronounced Joule heating. This could have been a problem for the chip, since the flow of the cooling liquid in the cartridge had to be short-circuited. However, from the results shown in figure 9.5, this seems not to be the case.

10- Conclusions and Perspectives.

In the present work, organically modified silicates made by the sol-gel technique were investigated as stationary phases in capillary electrochromatography. These polymeric stationary phases are recommended since monomeric phases, also investigated, were not able to separate the neutral analytes contained in the test sample.

A judicious choice of the several interconnected parameters involved in the sol-gel technique permits to tailor the ormosils. Amongst them, the choice of the chemicals involved in synthesis of the sol is of paramount importance. Different possibilities were studied. The concentration of the organosilicates, the nature and the concentration of the catalyst and the quantity of water were found to be the most determining parameters in sol synthesis. Depending on these parameters, experimental conditions are defined in this work to produce ormosil coatings or ormosils macroporous monoliths within capillaries.

Coated capillaries :

In this work the open tubular columns coated with ormosils were able to separate neutral analytes. Using a n-octyl modified silicate phase, the factors affecting the separations were identified and optimized. Since an efficient separation requires both a suitable stationary phase and optimized electrochromatographic conditions, both of these aspects were studied. These optimized conditions, used as a standard, were transferred to the production of OTCs containing different organo modified silicates. The ability of these columns to separate a mixture of different classes of analytes was tested. For reversed stationary phases, separations of neutral analytes were achieved. A marked difference is observed for mixtures of charged compounds where the electrochromatographic separations failed. Since the same organic moieties gave a separation in traditional pressure driven systems, the comparison of the chromatographic models in CEC and in HPLC does not seem to apply. Further efforts should be made to investigate the mechanisms contributing to the separations in CEC, which are not yet clearly understood.

Two major contributions of this work concern the limitation of the capillary inner diameters and the time required to produce OTCs for CEC. This work proves the feasibility of electrochromatographic separations with large diameter capillaries (50 μm). Till now the diameter of the column was theoretically limited to less than 50 μm by comparison with pressure driven chromatographic models. The effective separations obtained give further evidence that the chromatographic mechanisms in CEC and HPLC are different. The second advance of this work is the dramatic decrease of the time required to produce coated capillaries. According to similar approaches described in the literature, at least 6h are required to synthesize the sols, to which 12 h are added after the coating to dry the columns. In this work the use of high acidic conditions in the sol synthesis and a vacuum drying can reduce the time of these steps to 10 min and 2 h. respectively.

The reproducibility of the separations obtained, excellent for a single column, can vary between columns made with the same protocol. Effort must be made to improve reproducibility if the columns are to be produced on a large scale.

Monolithic columns :

In the present work, a method for the formation of a macroporous ormosil monolith inside capillaries was developed. This was achieved by rigorous adjustments of the sol synthesis and careful control of a liquid-liquid phase separation process. This technique presents numerous advantages over the traditional approach. The technique proposed consists of a single step low temperature procedure with no need of a further functionalisation of the silica, in contrary to the approaches proposed in the literature. The technique developed is therefore less cumbersome to carry out but does suffer from two important drawbacks. The first is the weak anchoring of the monolith within the capillaries. The second drawback is the extremely low EOF obtained with the ormosils used to make monoliths. These disadvantages limit the use of such monoliths in CEC.

The macroporous ormosil monoliths produced in this work could be used as stationary phases in HPLC. In HPLC columns, the monoliths do not

suffer from the lack of anchoring, and do not have to produce an EOF. In this case, the monolithic stationary phases are particularly interesting because they can be easily tailored for specific interactions with any kind of analyte. Since ideal stationary phases are not always available commercially, the macroporous ormosil monoliths proposed in this work have a great potential in this regard.

Chips :

Electrochromatographic chips were used in an attempt to miniaturize the CEC. The concept of employing a commercial CE system with a custom-made CEC chip to simplify the injection and detection system was shown to be successful. Since it was proven that small separation channels are not mandatory to achieve electrochromatographic separations of neutral compounds, this work permits fabrication of chips with larger channels.

11- Bibliography.

- [1] Colón, L.A., Guo, Y.; Fermier, A.; *Anal. Chem.*, 1997, 461 A.
- [2] Colón, L.A.; Reynolds, K.J.; Alicea-Maldonado, R.; Fermier, A.M.; *Electrophoresis*, 1997, 18, 2162-2174.
- [3] Berraz, G.; *Anales Asoc. Quim. Argentina*, 1943, 31, 96-97.
- [4] Pretorius, V.; Hopkins, B.J.; Schieke, J.D.J.; *J. Chromatogr. A*, 1974, 99, 23-30.
- [5] Jorgenson, J.W.; Lukacs, K.D.; *J. Chromatogr.*, 1981, 218, 209-216.
- [6] Knox, J.H.; Grant, I.H.; *Chromatographia*, 1991, 32, 317-328.
- [7] Crego, A.L.; González A.; Marina, M.L.; *Crit. Rev. Anal. Chem.*, 1996, 26(4), 261- 304.
- [8] Kuhn, R.; Hoffstetter-Kuhn, S.; *Capillary Electrophoresis: Principles and Practise*, Springer-Verlag Eds.; 1993, ISBN: 3-540-56434-9.
- [9] Dittmann, M.M.; Rozing, G.P.; *J. Micro. Sep.*, 1997, 9, 399-408.
- [10] Dittmann, M.; Rozing, G.P.; *J. Chromatogr. A*, 1996, 744, 63-74.
- [11] Cantwell, F.F.; *Anal. Chem.*; 1979, 51, 623-632.
- [12] Schwer, C.; Kenndler, E.; *Anal. Chem.*, 63, 1801-1807.
- [13] Rice, C.L.; Whitehead, R.; *J. Phys. Chem.*, 1965, 69, 4017
- [14] Gouy, G.; *J. Phys.*, 1910, 9, 457-468.
- [15] Chapman, D.L. ; *Phil. Magn.*, 1913, 25, 475-481.
- [16] Debye, P.; Hückel, E.; *Phys. Z.*, 1923, 24, 185-206.
- [17] Van de Goor, A.A.A.M.; Wanders, B.J.; Everaerts, F.M.; *J. Chromatogr*, 1989, 470, 95-104.
- [18] Knox, J.H.; *Chromatographia*, 1988, 26, 329.
- [19] Knox, J.H.; Grant, I.H.; *Chromatographia*, 1987, 24,135-143.
- [20] Helmholtz, H.L.; *Wiedemann's Ann. Phys. Chem.*, 1879, 7, 337-382.
- [21] Grushka, E. ; McCormick, R.M. ; Kirkland J.J. ; *Anal. Chem.*, 1989, 1, 241-246.

- [22] Tsuda, T. ; Anal. Chem. ,1987, 59, 521-523.
- [23] Vissers, J.P.C.; Claessens, H.A.; Coufal, P.; J. High Resolut. Chromatogr., 1995, 18, 540.
- [24] Rathore, A.S.; Horvath, Cs.; J. Chromatogr. A, 1996, 743, 231-246.
- [25] Bruin, G.J.M.; Tock, P.P.H. ; Kraak, J.C. ; Poope, H. ; J. Chromatogr., 1990, 517, 557-572.
- [26] Knox, J.H.; J. Chromatogr. Sci., 1980, 18, 453.
- [27] Golay, M.J.E.; Gas Chromatography; Desty D.H. Ed., Butterworths London, 1958, 36-55.
- [28] Aris, R.; Proc. R. Soc. Lond. [Ser. A], 1959, A252, 538-550.
- [29] Martin, M.; Guiochon, G.; Walbroehl, Y.; Anal. Chem., 1985; 57, 561-563.
- [30] Martin, M.; Guiochon, G.; Anal. Chem., 1984, 56, 614-620.
- [31] McEldoon, J.P.; Datta, R.; Anal. Chem., 1992, 64, 230-233.
- [32] Jorgenson, J.W.; Guthrie, E.J.; J. Chromatogr., 1983, 255, 335-348.
- [33] Pursch, M. ; Sander, L.C. ; J. Chromatogr. A, 2000, 887, 313-326.
- [34] Göhlin, K.; Larson, M.; J. Chromatogr., 1993, 645, 41-56.
- [35] Iler, R.K.; The Chemistry of Silica; John Wiley and Sons eds., 1979, ISBN 0-471-02404-X.
- [36] Unger, K.K.; Porous Silica – Its Properties and Uses as Support in Column Liquid Chromatography (Journal of Chromatography Library, Vol. 16); Elsevier Scientific Publishing Co.; New-York, 1979, ISBN 0-444-41683-8.
- [37] Pesek, J.J.; Matyska, M.T.; Sandoval, J.E.; Williamsen, E.J.; J. Liq. Chrom. and Rel. Technol., 1996, 19(17,18), 2843-2865.
- [38] Montes, M.C. ; Van Amen, C. ; Pesek, J.J. ; Sandoval, J.E. ; J. Chromatogr. A, 1994, 688, 31-45.
- [39] Locke, D.C.; Schmermund, J.T.; Banner, B.; Anal. Chem., 1972, 44(1), 90-92.
- [40] Corriu, R.J.P.; Guerrin, C.J.; J. Organomet. Chem., 1980, 198, 231-320.

-
- [41] Pesek, J.J.; Sandoval, J.E.; Chu, C.H.; Jonsson, E.; Chemically Modified Surfaces, Mottola, H.A. and Steinmetz eds., 1992, Elsevier publishers, p 57-72.
- [42] Chalk, A.J. ; Harrod, J.F. ; J. Am. Chem. Soc., 1965, 87(1), 16-21.
- [43] Sandoval, J.E.; Pesek, J.J., Anal. Chem., 1989, 61, 2067-2075.
- [44] Ojima, I.; The Hydrosilylation reaction; The Chemistry of Organic Silicon Compounds; Patai, S. and Rappoport, 1989, John Wiley and Sons Eds., Ch. 25.
- [45] Pesek, J.J.; Matyska, M.T.; Electrophoresis, 1997, 18, 2228-2238.
- [46] Huang, X. ; Zhang, J.; Horwáth, C.; J. Chromatogr. A, 1999, 858, 91-101.
- [47] Hench, L.L.; West, J.K.; Chem. Rev., 1990, 90, 33-72.
- [48] Brinker, C. ; Scherer, G.W.; Sol-Gel Science, The Physics and Chemistry of Sol-Gel Processing, Academic Press Eds., 1990, ISBN 0-12-134970-5.
- [49] Sanchez, C.; Ribot, F. ; New. J. Chem., 1994, 18, 1007-1047.
- [50] Collinson, M.M.; Crit. Rev. Anal. Chem., 1999, 29(4), 289-311.
- [51] Wen, J. ; Wilkes, G.L.; Chem. Mater., 1996, 8, 1667-1681
- [52] Zühlke, J.; Knopp, D.; Niessner, R.; Fresenius J. Anal. Chem., 1995, 352, 654-659.
- [53] Cichna, M.; Knopp, D.; Niessner, R.; Anal. Chim. Act., 1997, 339, 241-250.
- [54] Guo, Y.; Colón, L.A.; J. Microcolumn Sep., 1995, 7(5), 485-491.
- [55] Lan, H.L.; Dave, B.C.; Fukuto, J.M.; Zink, J.I.; Valentine, J.S.; J. Mater. Chem., 1999, 9, 45-53.
- [56] Wright, P.B.; Lister, A.S.; Dorsey, J.G.; Anal. Chem., 1997, 69, 3251-3259.
- [57] Kelly, M.A.; Altria, K.D.; Clark, B.J.; J. Chromatogr. A, 1997, 768, 73-80.
- [58] Crego, A.L.; Martínez, J.; Marina, M.L.; J. Chromatogr. A, 2000, 869, 329-337.
- [59] Fowkes, F.M.; Advances in Ceramics; Messing, G.L. et al. Eds; The American Ceramic Society, Inc.; Boston, MA, 1987, Vol. 21, 411-421.

- [60] Whitaker, K.W.; Sepaniak, M.J.; *Electrophoresis*, 1994, 15, 1341-1345.
- [61] Vansant, E.F.; Van Der Voort, P.; Vrancken, K.C.; *Characterization and Chemical Modification of the Silica Surface*, Elsevier, Amsterdam, 1995.
- [62] Dorsey, J.G.; Cooper, W.T.; *Anal. Chem.*, 1994, 66, 857 A
- [63] Nawrocki; *J. Chromatogr. A*, 1997, 779, 29-71.
- [64] Mauss, M.; Engelhardt, H. ; *J. Chromatogr.*, 1986, 371, 235-242.
- [65] Hayes, J.D.; Malik, A.; *J. Chromatogr. B*, 1997, 695, 3-13.
- [66] Wang, D.; Chong, S.L.; Malik, A.; *Anal. Chem.*, 1997, 69, 4566-4576.
- [67] Ruan, Y.; Feenstra; Kraak, J.C.; Poppe, H; *Chromatographia*, 1993, 35(9-12), 597-606.
- [68] Srinivasan, K.; Pohl, C.; Avdalovic; *Anal. Chem.*, 1997, 69, 2798-2805.
- [69] Huang, X.; Horwath, Cs ; *J. Chromatogr. A*, 1997, 788, 155-164.
- [70] Swart, R.; Kraak, J.C.; Poppe, H.; *J. Chromatogr. A*, 1994, 670, 25-38.
- [71] Cobb, K.A.; Dolnik, V.; Novotny, M.; *Anal. Hem.*, 1990, 62, 2478-2483.
- [72] Guo, Y.; Colón, L.A.; *Anal. Chem*, 1995, 67(15), 2511-2516.
- [73] Tock, P.P.H.; Boshoven, C.; Poppe, H.; Kraak, J.C.; *J. Chromatogr.*, 1989, 477, 95-106.
- [74] Li, F.; Z. Hanbang, Gao, D. ; Lu, G.; Gu, J.; Fu, R.; *Chin. Sc. Bull.*, 1998, 43(9), 790-791.
- [75] Van Berkel, O.; Poppe, H.; Kraak, J.C.; *Chromatographia*, 1987, 24, 739-744.
- [76] Pesek, J.J.; Matyska, m.; *J. Chromatogr. A*, 1996, 736, 255-264.
- [77] Cheng, W.; McCown, M.; *J. Chromatogr.*, 1985, 318; 73-82.
- [78] Onuska, F.I.; Comba, M.E.; Bistricki, T.; Wilkinson, R.J.; *J. Chromatogr.*, 1977, 142, 117-125.
- [79] Pesek, J.J.; Matyska, M.T.; *J. Chromatogr. A*, 1996, 736, 313-320.
- [80] Unger, K.K.; Schick-Kalb, J.; Krebs, K.F.; *J. Chromatogr.*, 1973, 83, 5-9.

-
- [81] Swart, R.; Kraak, J.C.; Poppe, H.; Trends in Anal. Chem., 1997, 16(6), 332-342.
- [82] Pesek, J.J.; Swedberg, S.A.; J. Chromatogr., 1986, 361, 83-92.
- [83] Pope, E.J.A.; Mackenzie, J.D.; J. Non-Cryst. Sol., 1986, 87, 185-198.
- [84] Menon, V.C.; Komarneni, S.; Park, M.; Schmücker, M.; Schneider, H; J. Sol-Gel Sci. and Tech., 1998, 11, 7-16.
- [85] Klein, L.C.; Ann. Rev. Mater. Sci., 1985, 15, 227-248.
- [86] Schmidt, H.; Scholze, H.; Kaiser, A.; J. Non-Cryst. Sol., 1984, 63, 1-11.
- [87] Engelhardt, V.Q.; Altenburg, W.; Hoebbel, D.; Wiecker, W.Z.; Anorg. Allg. Chem., 1977, 43, 418
- [88] Narang, P.; Colón, L.A.; J. Chromatogr. A, 1997, 773, 65-72.
- [89] Rodríguez, S.A.; Colón, L.A. ; Anal. Chim. Acta, 1999, 397, 207-215.
- [90] Li, F.; Zhang, H. ; Gao, D. ; Lu, G. ; Gu, J. ; Fu, R. ; Chin. Sci. Bull., 1998, 43(9), 790-791.
- [91] Sakka, S. ; Kamiya, K.; Makita, K.; Yamamoto, Y.; J. Non-Cryst. Sol., 1984, 63, 223-235.
- [92] Sakka, S.; J. Sol-Gel Sci. Techn., 1994, 2, 451-455.
- [93] Bartle, K.D.; Wooley, C.L.; Markides, K.E.; Lee, M.L.; Hansen, R.S; J. High Resol. Chromatogr. Chromatogr. Commun., 1987, 10, 128-136.
- [94] Scherer, G.W.; J. Sol-Gel Sci. and Tech., 1997, 8, 353-363.
- [95] Constantin, S.; Freitag, R.; J. Chromatogr. A, 2000, 887, 253-263.
- [96] Nair, B.N.; Elfering, W.J.; Keizer, K.; Verweij, H.; J. Colloid and Interface Sci., 1996, 178, 565-570.
- [97] Bryans, T.R.; Brawner, V.L.; Quitevis, E.L.; J. Sol-Gel Sci. and Tech., 2000, 17, 211-217.
- [98] Colby, M.W.; Osaka, A.; Mackenzie, J.D.; J. Non-Cryst. Sol., 1986, 82, 37-41.
- [99] Huang, H, Orlor, B.; Wilkes, G.L.; Macromolecules, 1987, 20, 1322-1330.
- [100] Stahlberg, J; J. Chromatogr. A, 2000, 892, 291-301.

- [101] Orcel, G.; Hench, L.L.; Artaki, I.; Jonas, J.; Zerda, T.W.; *J. Sol-Gel Sci. and Tech.*, 1988, 105, 223-231.
- [102] Vollhardt, K.P.C.; *Traité de Chimie Organique*, 1987, W.H Freeman and Company Eds., NY. and Oxford, ISBN 2-80041-1312-4
- [103] *The Merck Index, Tenth Edition*, 1983, Merck and Co., ISBN 911910-27-1
- [104] Nakanishi, K.; Shikata, H.; Ishizuka, N.; Koheiga, N.; Soga, J.; *J. High Resol. Chromatogr.*, 2000, 23(1), 106-110.
- [105] Schubert, U.; Hüsing, N.; Lorenz, A.; *Chem. Mater.*, 1995, 7, 2010-2027.
- [106] Ishizuka, N.; Minakuchi, H.; Nakanishi, K.; Soka, N.; Nagayama, H.; Hosoya, K.; Tanaka, N.; *Anal. Chem.*, 2000, 72, 1275-1280.
- [107] Iwamoto, T.; Mackenzie, J.D.; *J. Sol-Gel Sci. and Tech.*, 1995, 4, 141-150.
- [108] Minakuchi, H.; Nakanishi, K.; Soga, N.; Tanaka, N.; *J. Chromatogr. A*, 1997, 762, 135-146.
- [109] Minakuchi, H.; Nakanishi, K.; Soga, N.; Ishizuka, N.; Tanaka, N.; *Anal. Chem.*, 1996, 68, 3498-3501.
- [110] Hjerten, S.; Liao, J.L.; Zhang, R.; *J. Chromatogr.*, 1989, 473, 273-275.
- [111] Crego, A. L.; Martínez, J.; Marina, M.L.; *J. Chromatogr. A*, 2000, 869, 329-337.
- [112] Kelly, M.A.; Altria, K.D.; Clark, B.J.; *J. Chromatogr. A*, 1997, 768, 73-80.
- [113] Sahota, R.S.; Kahledi, *Anal. Chem.*, 1994, 66, 1141-1146.
- [114] Desbène-Monvernay, A., Mofaddel, N.; *Analisis*, 1999, 27(2), 144-150.
- [115] CRC Handbook of Chemistry and Physics:
<http://www.knovel.com/knovel/Databook/default.htm?WCI=ShowTable&WCU=900101&SpaceID=1&BookID=34&NodeID=9007585>
- [116] Melander, W.R.; Horvath, C.; *High Performance Liquid Chromatography*; Academic Press. New-York, 1980.
- [117] Cherkaoui, S.; Veuthey, J.L.; *J. Chromatogr. A*, 2000, 874, 121-129.
- [118] Vindevogel, J.; Sandra, P.; *Electrophoresis*, 1994, 15, 842-847.
- [119] Francotte, E.; Jung, M.; *Chromatographia*, 1996, 42(9-10), 521-527.

-
- [120]Mayer, S.; Schurig, V.; J. Liq. Chromatogr., 1993, 16, 915-931.
- [121]A. Manz, D. J. Harrison, E. Verpoorte, J. C. Fettinger, A. Paulus, H. Lüdi and H. M. Widmer, J. Chromatogr., 1992, 593, 253-258.
- [122]K. Seiler, D. J. Harrison and A. Manz, Analytical Chemistry, 1993, 65, 1481-1488.
- [123]A. T. Woolley, R. A. Mathies, Analytical Chemistry, 1995, 67, 3676-3680.
- [124]S. C. Jacobson, R. Hergenröder, L. B. Koutny, and J. M. Ramsey, Analytical Chemistry, 1994, 66, 2369-70.
- [125]Constantin, S.; Freitag, R.; Solignac, D.; Sayah, A.; Gijs, M.A.M.; Sensors and Actuators, 2000, to be published.
- [126]Sayah, S.; Solignac, D.; Cueni, T.; Gijs, M.A.M.; Sensors and Actuators, to be published.

12- Appendix.

Appendix A: Instruments and Chemicals.

Instrumentation.

All electrochromatography experiments were carried out on a Beckman P/ACE 5500 (Beckman, Fullerton, CA, USA) system using a diode array detection system. Data were processed using the P/ACE software. The optic microscope used was an Axiovert 100 (Carl Zeiss, Oberkochen, Germany). The scanning electron microscope was a XLS-30 (Philipps, The Netherlands). Vacuum drying was performed in vacuum oven, Heraeus vacutherm model VT 6025 (Heraeus, Hanau, Germany). The oven was connected with a vacuum pump, model MD4C, equipped with a pressure digital controller CVC2, all from Vacuubrand (Wertheim, Germany). Microreaction vials of 3 and 5 mL equipped with magnetic stirrer were from Suppelco (Bellefonte, PA, USA).

Chemicals:

All chemicals are from Fluka Chemie AG. (Buchs, Switzerland) except for acetonitrile and methanol (HPLC grade) which were from Biosolve (Valkenswaard, The Netherlands). Water was purified using an Elix-3 system (Millipore, Bedford, MA, USA). Fused silica capillaries (100, 75, 50, 25 and 10 μm) were from Bio-Rad (Hercules, CA, USA) and from Polymicro Technologies (Phoenix, AZ, USA).

Amyltriethoxysilane $\text{CH}_3(\text{CH}_2)_4\text{Si}(\text{OC}_2\text{H}_5)_3$

Dimethyloctadecyl[3-(trimethoxysilyl)propyl]ammonium:
 $\text{CH}_3(\text{CH}_2)_{17}\text{N}^+(\text{CH}_3)_2(\text{CH}_3)_2\text{Si}(\text{OCH}_3)_3$

Dimethyloctyldimethoxysilane $\text{CH}_3(\text{CH}_2)_7\text{Si}(\text{CH}_3)_2\text{Cl}$

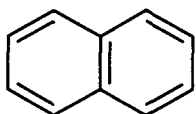
Octyltriethoxysilane $\text{CH}_3(\text{CH}_2)_7\text{Si}(\text{OC}_2\text{H}_5)_3$

Hexadecyltrimethoxysilane $\text{CH}_3(\text{CH}_2)_{15}\text{Si}(\text{OCH}_3)_3$

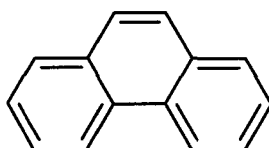
Methyloctyldimethoxysilane $\text{CH}_3(\text{CH}_2)_7\text{SiCH}_3(\text{OCH}_3)_2$

(Pentafluorophenyl)dimethylchlorosilane $(\text{C}_6\text{F}_5)\text{C}(\text{CH}_3)_2\text{Si}(\text{CH}_3)_2\text{Cl}$

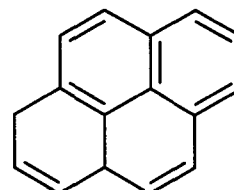
Some of the analytes used in the present work:



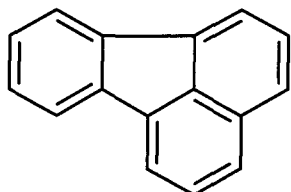
Naphthalene



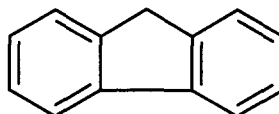
Phenanthrene



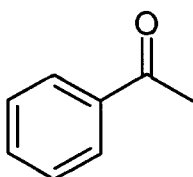
Pyrene



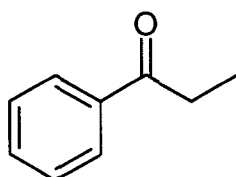
Fluoranthrene



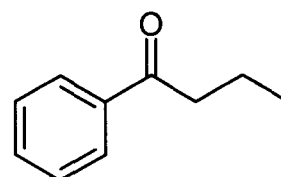
Fluorene



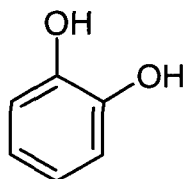
Acetophenone



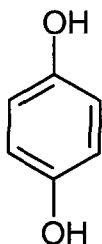
Propiophenone



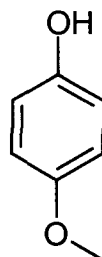
Butyophenone



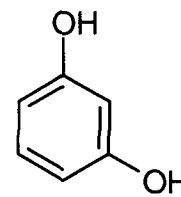
Pyrochatechol



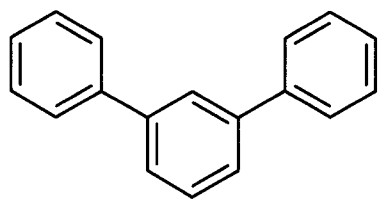
Hydroquinone



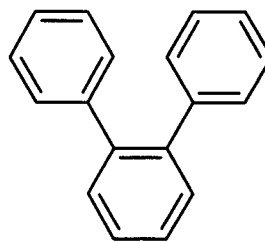
Hydroquinone
monomethyl ether



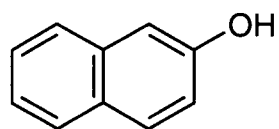
Resorcinol



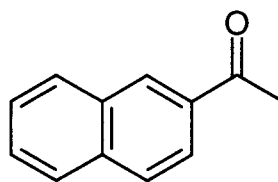
M - Terphenyl



O - Terphenyl



2 - Naphtol

2 - Naphtol monomethyl
ether

Appendix B

List of Symbols and Abbreviations.

b	= constant [Pa \times s]
C	= molar concentration [mol \times L ⁻¹]
$C(k^*)_m$	= dimensionless coefficient for resistance to mass transfer in the mobile phase [dimensionless]
$C(k^*)_s$	= dimensionless coefficient for resistance to mass transfer in the stationary phase [dimensionless]
D	= diffusion coefficient [cm ² \times s]
D_i	= diffusion coefficient [cm ² \times s ⁻¹]
D_m	= diffusion coefficient of the solute in the mobile phase [cm ² \times s ⁻¹]
D_s	= diffusion coefficient of the solute in the stationary phase [cm ² \times s ⁻¹]
d	= distance between the electrodes [m]
d_c	= diameter of the column [cm]
d_f	= thickness of the stationary phase [cm]
d_{id}	= length from the capillary inlet till the detector [cm]
E	= electric field [V \times m ⁻¹]
E_A	= activity energy for the viscous flow [J \times mol ⁻¹]
e	= elemental charge = 1.602 \cdot 10 ⁻¹⁹ [C]
F	= Faraday constant = 96485 [C \times mol ⁻¹]
F_R	= frictional retarding force [N]
f	= frictional constant [N \times s \times cm ⁻¹]
G	= heat generation rate [K \times cm ² \times s ⁻¹]
ΔG	= enthalpy change associated to the equilibrium [J \times mol ⁻¹]
ΔH^0	= standard enthalpy change [J \times mol ⁻¹]
$HETP$	= height equivalent to a theoretical plate [m ⁻¹]
$HETP_e$	= effective height equivalent to a theoretical plate [m ⁻¹]
J_i	= flux of matter [mol \times cm ⁻² \times s ⁻¹]
K	= equilibrium constant [dimensionless] or chromatographic equilibrium constant [dimensionless]

$k = k'$,	= capacity factor [dimensionless]. In paragraph 2.2, k = Debye-Hückel length [m]
k_s	= specific conductance [$S \times cm^{-1}$]
k_c	= specific conductance of the mobile phase [$S \times cm^{-1}$]
k_{cec}	= capacity factor in CEC [dimensionless]
L	= length of the column [cm]
N	= number of theoretical plates [dimensionless]
N_e	= effective number of theoretical plates [dimensionless]
n	= quantity of matter [moles]
Q_{eff}	= effective charge [C]
R	= universal gas constant ($8.314 [J \times K^{-1} \times mol^{-1}]$)
r_c	= radial position
r_e	= effective radius [cm]
r_h	= hydrodynamic radius of the ion [cm]
r_p	= radial position [cm]
ΔS^0	= standard entropy change associated to the equilibrium [$J \times mol^{-1}$]
T	= absolute temperature [K]
T_1	= capillary wall temperature [K]
t, t_r	= detection time of a neutral analyte [min]
t_{eo}	= detection time of an unretained analyte [min]
t_r'	= detention time of a chromatographically unretained ion [s]
u	= linear velocity of the analyte in the axial direction [$cm \times s^{-1}$]
u_{eo}	= electroosmotic velocity [$cm \times s^{-1}$]
u_{ep}^0	= velocity of the electrophoretic migration at infinite dilution [$cm \times s^{-1}$]
u_{ep}	= effective electrophoretic velocity of an unretained ion [$cm \times s^{-1}$]
z	= charge number of the ion
δ	= thickness of the chromatographic peaks at 50 % of its height [min]. In paragraph 2.2, δ = thickness of the diffuse double layer [m]
ϵ_0	= permittivity of the vacuum ($88.85 \times 10^{-12} [C^2 \times N^{-1} \times m^{-2}]$)

ϵ_r	= permittivity or dielectric constant of the mobile phase [$C^2 \times N^{-1} \times m^{-2}$]
ζ	= zeta potential [V]
η	= newtonian viscosity of the mobile phase [Pa \times s]
μ_{eo}	= electroosmotic mobility [$cm^2 \times V^{-1} \times s^{-1}$]
μ_{ep}^0	= electrophoretic mobility at infinite dilution [$cm^2 \times V^{-1} \times s^{-1}$]
μ_{ep}	= electrophoretic mobility [$cm^2 \times V^{-1} \times s^{-1}$]
σ	= thickness of the chromatographic peaks at 60,6 % of its height [min]. In paragraph 2.2, σ = charge density of the excess ions in the Gouy-Chapman layer.
$\Delta\phi$	= difference of potential [V]
ψ	= electric potential [v]
ω	= width of the chromatographic peaks at 13.5 % of its height [min]

Appendix C.

Parameters used to quantify the separations in CEC with uncharged compounds.

The parameters used in this work to quantify the electrochromatographic separations are based on the intrinsic properties of the Gaussian curve.

Capacity factor:

The capacity factor is an experimental parameter that is widely used to describe the migration rates of solutes on columns. For a solute A, the capacity factor k_a' is defined as:

$$k_a' = K_a \frac{V_s}{V_m} = \frac{t_r - t_0}{t_0}$$

with $K_a = \frac{C_s}{C_m}$; s and m being the respective indexes for the stationary and the mobile phase.

Resolution factor:

According to the mathematical properties of the Gauss curve, we have

$$\omega = 4\sigma' \text{ and } \delta = 2.35\sigma'. \text{ Therefore } \omega = 1.702\delta$$

The resolution factor corresponds to:

$$R = 2 \frac{t_2 - t_1}{\omega_1 + \omega_2} = 1.175 \frac{t_2 - t_1}{\delta_1 + \delta_2}$$

Effective efficiencies:

The effective efficiency of an analyte corresponds to:

$$HETP_e = \frac{L}{N_e}$$

Statistics

Mesure of precision by the sample standard deviation:

$$s = \sqrt{\frac{\sum_{i=1}^N (x_i - \bar{x})^2}{N - 1}}$$

With N = number of replicates data making up the population.

\bar{x} = sample mean. It corresponds to the population mean if N is small.

x_i = represents the individual values of x making up a set of N replicate measurements.

In analytical chemistry the standard deviation are frequently quoted in relative rather than absolute terms. Toward this goal the coefficient of variation is used.

$$CV = 100 \frac{s}{\bar{x}}$$

12- Curriculum Vitae.

Education :

- 1997-2001 : Ph.D. at the Swiss Federal Institute of Technology in the laboratory of chemical biotechnology (LBCH).
1995-1996 : Master's degree in chemistry from Geneva University.
1991-1994 : Bachelor's degree in Chemistry from Geneva University.
1990 : High school degree (Baccalauréat D - with honors).

Experience :

- 1997-2001 : EPFL. Techniques studied : CEC / CE / micro HPLC / electronic and optic microscopy / sol-gel technology.
1993-1996 : Diploma work (4 months) (Prof. J.L. Veuthey). Techniques GC-FID / GC-MS / derivatisation chemistry.
3 months of practical training in the department of analytical chemistry of the university of Lausanne : ICP / X-Ray fluorescence / AAS / TOC / electronic microscopy / ultracentrifugation.
2 stages of 1 month each in analytical chemistry : SPE / LLE / HPLC / CZE.
1 stage of 1 month in physical chemistry : EPR, NMR.

Publications :

Constantin, S. ; Freitag, R. ; *Improvement of stationary phase preparation for open-tubular capillary electrochromatography (OT-CEC) by using the sol-gel method.* J. Chromatogr. A ; 2000, 887, 253-263.

Constantin, S. ; Freitag, R. ; Solignac, D. ; Sayah, A. ; Gijs, M.A.M ; *Capillary Electrochromatography chips suitable for integration into conventional CE-systems.* Sensors and Actuators, Accepted.

Solignac, D.; Sayah, A. ; Constantin, S. ; Freitag, R. Gijs, M.A.M ; *Powder blasting as a novel technique for the realisation of capillary electrophoresis chip.* Sensors and Actuators, Accepted.

Oral Presentations :

Capillary electrochromatography chip integrated in a cartridge – Eurosensors XIV, 27-30 August 2000 Copenhagen, Denmark.

Capillary electrochromatography on a chip– International Symposium on the separation and analysis of proteins, peptides and polynucleotides – ISPPP'00- 5-8 November 2000 Ljubljana, Slovenia.

Capillary electrochromatography in analytical biotechnology, SPP'99, Epalinges, Switzerland.

Posters :

Constantin, S. ; Freitag, R. ; Capillary electrochromatography chip integrated in a cartridge, ISPPP'2000.

Constantin, S. ; Freitag, R. ; Capillary electrochromatography chip integrated in a cartridge, Eurosenors'2000.

Constantin, S. ; Freitag, R. ; Organically modified silicates as stationary phase for CEC, HPCE'2000.

Constantin, S. ; Freitag, R. ; Capillary electrochromatography in analytical biotechnology, SPP'99.

Constantin, S. ; Hoegger, D. ; Freitag, R. ; Capillary electrochromatography in analytical biotechnology, ISPPP'99.

Constantin, S. ; Hoegger, D. ; Freitag, R. ; Neuartige, Kontinuierliche Stationäre Phasen für die Elektrochromatographie, DECHEMA'99.

Freitag, R. ; Brüggeman, O. ; Constantin, S. ; Berruex, L, Process monitoring and quality control during production of recombinant anti-rhesus D antibodies, HPLC'98.

Brüggeman, O. ; Constantin, S. ; Berruex, L. ; Kasper, K. ; Freitag, R. ; Quantifizierung und Charakterisierung von rekombinanten Anti rhesus D Antikörpern als Beitrag zur Entwicklung eines biotechnischen, DECHEMA'98.

Freitag, R. ; Constantin, S. ; Brüggeman, O. ; Capillary electrophoresis as a tool for the quantification and characterization of recombinant anti rhesus D IgG, 30th annual meeting of the USGEB/USSBE'98.

Freitag, R. ; Constantin, S. ; Brüggeman, O. ; Quantification and characterization of recombinant anti rhesus D IgG using capillary electrophoresis. HPCE'98.

Freitag, R. ; Abdellali, M. ; Berruex, L. ; Brüggeman, O, Constantin, S. ; IgG characterization of anti rhesus D immunoglobulins, SPP biotech module 1 '97.

Courses and conferences :

ISPPP'00, 5-8 November 2000 Ljubljana, Slovenia.

Eurosenors XIV, 27-30 August 2000 Copenhagen, Denmark.

HPCE'00, 20-24 February 2000, Saarbrücken, Germany.

14^{ième} séminaire du 3^{ième} cycle en sciences pharmaceutiques, 4-8 October 1999, Zermatt, Switzerland.